ASYMMETRIC HOMOGENEOUS HYDROGENATION OF PROCHIRAL SUBSTRATES MEDIATED THROUGH CARBOXYLIC ACID AND CARBAMIC ACID METAL-BINDING FUNCTIONAL GROUPS

By

Tamara M. de Winter

A thesis submitted to the Graduate Program in Chemistry

in conformity with the requirements for the

Degree of Doctor of Philosophy

Queen's University

Kingston, Ontario, Canada

(December, 2015)

Abstract

The need for enantiopure chiral compounds has driven the development of asymmetric synthesis, and more specifically asymmetric catalysis. The ability to selectively produce one enantiomer versus another has been a significant discovery for the production of natural products and pharmaceuticals, as both enantiomers may elicit very different interaction in living animals, either being therapeutic or toxic. This thesis investigates the structure of the substrate and its effect in the homogeneously-catalyzed asymmetric hydrogenation of C=C and C=O double bonds.

In a study of the asymmetric hydrogenation of unsaturated carboxylic acids, the effects of the length of the linker between the unsaturation and the carboxylic acid functional group on the yield and selectivity of the asymmetric hydrogenation reaction were investigated. We selected Noyori's Ru-binap catalysts and their derivatives as they are known to work well, in terms of high conversions and enantioselectivities, for the asymmetric hydrogenation of unsaturated carboxylic acids, such as atropic or tiglic acid. Other catalysts selected were a Rh-catalyst, and two Ir-catalysts reported to hydrogenate unsaturated carboxylic acids.

In the subsequent chapter, this study was extended to ketoacids. The effect of the change in unsaturation, i.e. olefin to ketone, is discussed, as well as the effects of the length of the linker on the asymmetric hydrogenation.

In these two studies, it was found that a *gamma*, *delta*-unsaturated carboxylic acid and a *gamma*-ketoacid could be asymmetrically hydrogenated in medium to high yield and enantioselectivity; however, the asymmetric hydrogenation of substrates with a greater distance between the unsaturation and the acid group had poor yield and selectivity.

In the fifth chapter, a new methodology for the asymmetric hydrogenation of allylamines was developed. This new method takes advantage of a reversible reaction between amines and carbon dioxide (CO_2) to suppress unwanted side reactions. The effects of various parameters on the enantioselectivity and conversion of the reaction were studied. It was found that the homogeneous-catalyzed asymmetric hydrogenation of 2-phenylprop-2-en-1-amine resulted in complete conversion and good enantioselectivity. Also, the presence of $CO_{2(g)}$ impeded the side reactions and the formation of unwanted byproducts. The best results found for 2-phenylprop-2-en-1-amine were implemented in the hydrogenation of its derivatives.

Acknowledgements

During the past five years at Queen's I have been extremely fortunate to work with such wonderful people, gain irreplaceable friendships and grow as a scientist and person. I would first like to thank my supervisor Professor Philip Jessop for the opportunity, his guidance and mentorship. Your patience, knowledge, and excitement about the work done in your group is inspiring and I would not have been successful without your support.

Without the help of the staff, I wouldn't have made it through graduate school. I would like to thank Dr. Sauriol for all her help with the NMR facilities and for allowing me to constantly interrupt with mystery spectra. Kim, you have been an amazing person in my time here. You have always gone above what was expected, whether it was a fun chat or helping with pressing or rushed orders. I would have not finished as quickly as I did without you. Annette and Michelle, thank you so much for your guidance here. You helped to keep me on track and calm my panic, whether it was a late transcript or finishing my thesis on time. Ed and Robin, your help has been amazing during my time here and I appreciate everything you have done for me. I would also like to thank my internal reader Dr. Dave Zechel and my examining committee Dr. Donald Macartney, Dr. Mike Baird, Dr. Brant Peppley and Dr. Steve Bergens.

I would like to thank my peers throughout my time at Queen's. Thank you Sean Mercer, Elize Ceschia, Tobias Robert, Bhanu Mudraboyina and Keith Huynh you have

To my family, you have supported me throughout my life. Thanks to my parents, who have been there regardless of what I needed, whether it was someone to cry to or to remind me to work harder. You have pushed me to achieve and never to settle. To my siblings, Johny, Erika, and Christopher, whether you know it or not, you all have supported and encouraged me to work hard. I appreciate you all. To Oma and Opa, your love and support was remarkable. You have been supportive of my journey here to become a "Dr."; you have taught me to work hard and excel. I am very grateful to both of you, my parents, and the rest of the family for the person I am today. From an early age you all inspired me to exceed expectations and challenge myself. I watched how hard you worked and I have carried that work ethic with me in everything I do.

Finally, I would like to thank Mike King. You have been my biggest supporter and I will never be able to thank you enough for the sacrifices you have made thus far, and most likely will continue to make. You have been kind, generous, and compassionate during our time together and even during the hard times of thesis writing. You have become important to me and my best friend.

Statement of Originality

I hereby certify that all the work described within this thesis is the original work of the author. Any published (or unpublished) ideas and/or techniques from the work of others are fully acknowledged in accordance with the standard referencing practices.

(Tamara Marie de Winter)

(November, 2015)

Table of Contents

List of Figures

List of Tables

List of Schemes

List of Abbreviations and Symbols

(aq)	Aqueous
atm	Atmosphere
(-)-bis-(S)-1-PEA	(-)-Bis[(S)-1-phenylethyl]amine
bipy	2,2'-Bipyridine ligand
Cat.	Catalyst
Cy	Cyclohexane
DBU	1,8-diazabicyclo[5.4.0]undec-7-ene
DIPEA	Diisopropylethylamine
DCM	Dichloromethane
DMCA	Dimethylcyclohexylamine
DMF	Dimethylformamide
ee	Enantiomeric excess
EI	Electron Impact
en	Ethylene diamine ligand
Eq.	Equivalence
ESI	Electrospray Ionization
FID	Flame Ionization Detector
(g)	Gas
g	Gram
GC	Gas Chromatography
h	Hour

HMBC	Heteronuclear Single Quantum Coherence
HPLC	High Pressure Liquid Chromatography
HRMS	High-Resolution Mass Spectrometry
HSQC	Heteronuclear Multiple-bond Correlation
IPA	Isopropanol
***i*-Pr₂NEt**	N,N-Diisopropylethylamine
kg	Kilogram
m	Meta (1,3-aromatic substitution pattern)
MEA	Monoethanolamine
mmol	Millimoles
mol	moles
MS	Mass Spectroscopy
Mes	Mesitylene ligand
NBS	N-Bromosuccinimide
NMR	Nuclear Magnetic Resonance
o	Ortho (1,2-aromatic substitution pattern)
p	Para (1,4-aromatic substitution pattern)
pKₐ	Negative logarithm of the acid dissociation constant
ppm	Parts per Million
py	Pyridine ligand
q	Quartet
RBF	Round Bottom Flask
RT	Room Temperature

T	Temperature
THF	Tetrahydrofuran
TsOH	*p*-Toluenesulfonic acid
Wt %	Weight Percent
α	Bite angle
δ	NMR chemical shift

List of Numbered Compounds
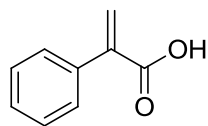
1
atropic acid
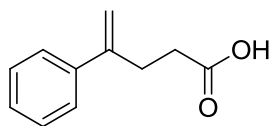
2
4-phenyl-4-pentenoic acid
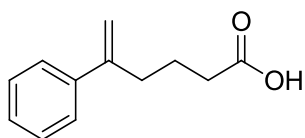
3
5-phenyl-5-hexenoic acid
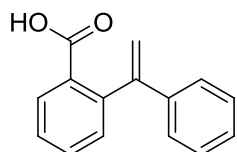
4
2-(1-phenylethenyl)benzoic acid
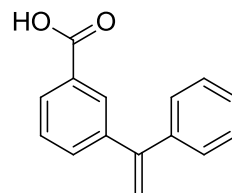
5
3-(1-phenylethenyl)benzoic acid
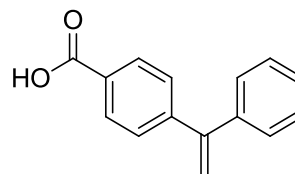
6
4-(1-phenylethenyl)benzoic acid
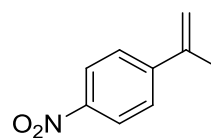
7
4-(propen-2-yl)nitrobenzene
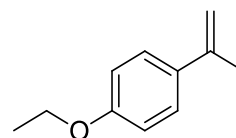
8
1-ethoxy-4-(prop-1-en-2-yl)benzene
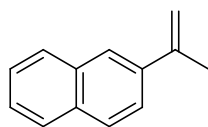
9
4-(propen-2-yl)naphthalene
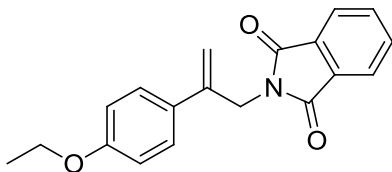
13
2-(3-bromoprop-1-en-2-yl)naphthalene

10
2-[2-(4-ethoxyphenyl)prop-2-en-1-yl]-1*H*-
isoindole-1,3(2*H*)-dione
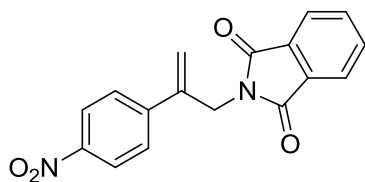
14
1-(3-bromoprop-1-en-2-yl)-4-
ethoxybenzene
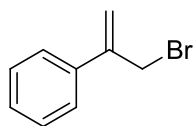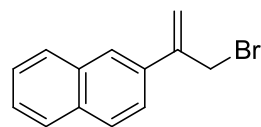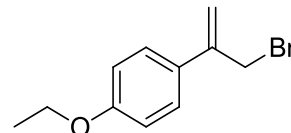
11
2-[2-(4-nitrophenyl)prop-2-en-1-yl]-1*H*-
isoindole-1,3(2*H*)-dione

15
2-[4-(trifluoromethyl)phenyl]prop-2-en-1- ol

12
α-(bromomethyl)styrene
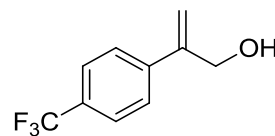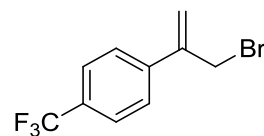
16
1-(3-bromoprop-1-en-2-yl)-4-
(trifluoromethyl)benzene
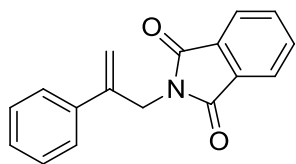
17
2-phenyl-3-phthalimidopropene
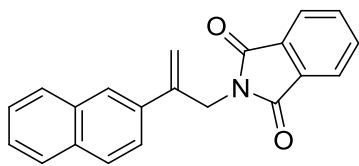
18
2-[2-(napthalen-2-yl)prop-2-en-1-yl]-1*H*-isoindole-1,3(2*H*)-dione
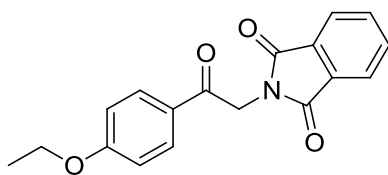
19
2-[2-(4-ethoxyphenyl)-2-oxoethyl]-1*H*-isoindole-1,3(2*H*)-dione
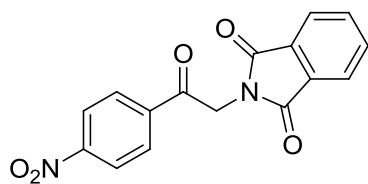
20
2-[2-(4-nitrophenyl)-2-oxoethyl]-1*H*-isoindole-1,3(2*H*)-dione
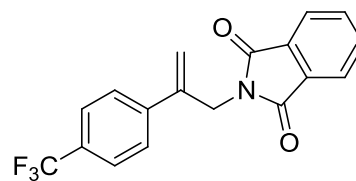
21
2-{2-[2-(trifluoromethyl)phenyl]prop-2-en-1-yl}-1*H*-isoindole-1,3(2*H*)-dione
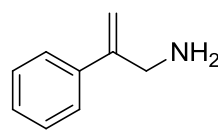
22
2-phenylprop-2-en-1-amine
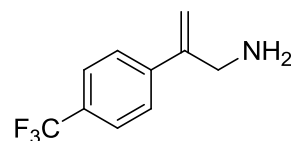
23
2-[4-(trifluoromethyl)phenyl]prop-2-en-1-amine
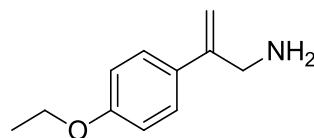
24
2-(4-ethoxyphenyl)prop-2-en-1-amine
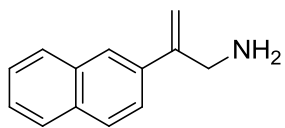
25
2-(naphthalene-2-yl)prop-2-en-1-amine
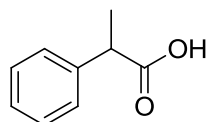
26
2-phenylpropanoic acid
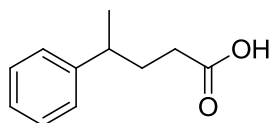
27
4-phenylpentanoic acid
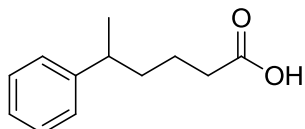
28
5-phenylhexanoic acid
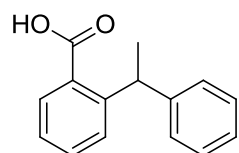
29
2-(1-phenylethyl)benzoic acid
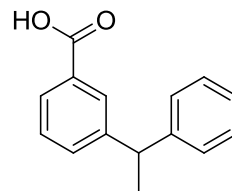
30
3-(1-phenylethyl)benzoic acid
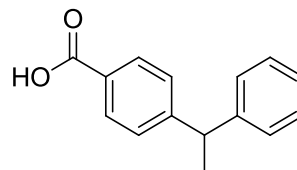
31
4-(1-phenylethyl)benzoic acid
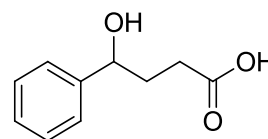
32
4-hydroxy-4-phenylbutanoic acid
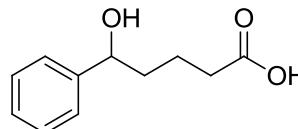
33
5-hydroxy-5-phenylbutanoic acid
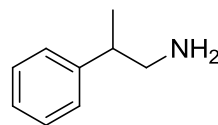
34
2-phenylpropan-1-amine
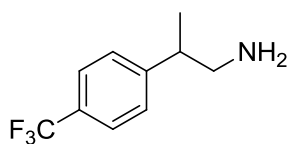
35

2-[4-(trifluoromethyl)phenyl]propan-1-amine
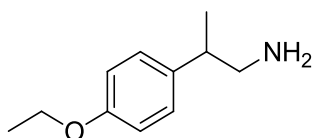
36

2-(4-ethoxyphenyl)propan-1-amine
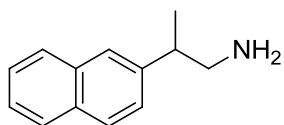
37

2-(naphthalene-2yl)propan-1-amine
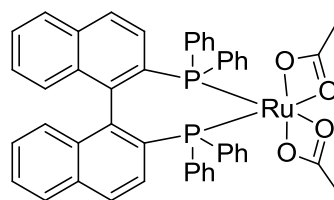
38

diacetato[(R)-(+)-2,2'-bis(diphenyl-phosphino)-1,1'-binaphthyl]ruthenium (II)
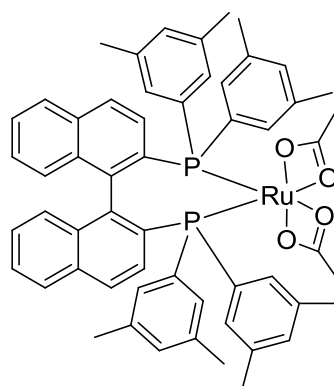
39

diacetato{(R)-(+)-2,2'-bis[di(3,5-xylyl)-phosphino]-1,1'-binaphthyl}ruthenium (II)
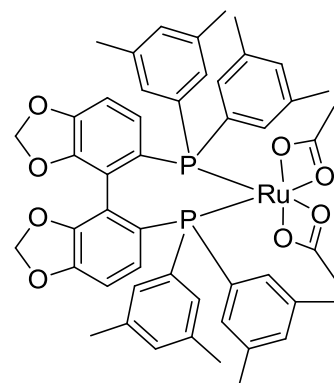
40

diacetato{(R)-(+)-5,5'-bis[di(3,5-xylyl)-phosphino]-4,4'-bi-1,3-benzodioxole}ruthenium (II)
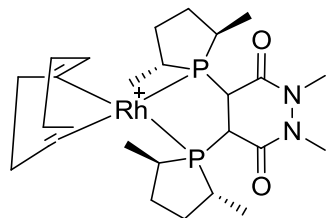
41

(-)-4,5-bis[(2R,5R)-2,5-dimethylphospholanyl](1,2-dimethyl-1,2'-dihydropyridazine-3,6-dione)(1,5-cyclooctadiene)rhodium(I)
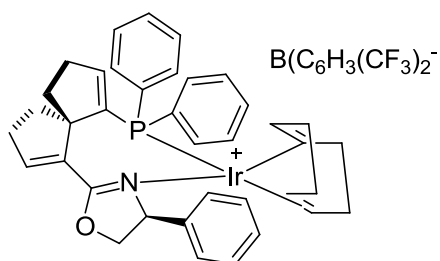
45

Dichloro[(S)-(-)-2,2'-bis(diphenylphosphino)-1,1'binaphthyl]ruthenium

B(C₆H₃(CF₃)₂⁻ → $B(C_6H_3(CF_3)_2)^-$

42
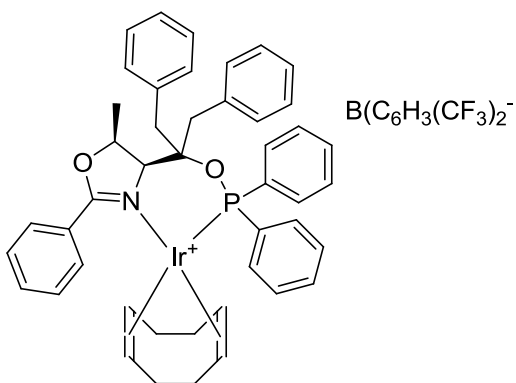
1,5-cyclooctadiene{(4S)-(-)-[(5R)-6-(diphenylphosphino)spiro[4.4]non-1.6-dien-1-yl]4,5-dihydro-4-phenyloxazole}iridium(I) tetrakis(3,5-bistrifluoromethyl)phenylborate
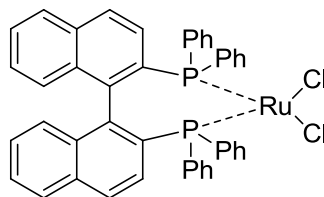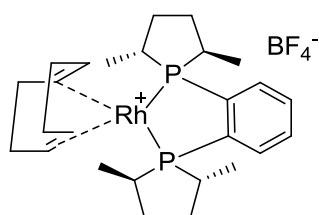
51

(-)-1,2-Bis((2R,5R)-2,5-dimethylphospholano)benzene(1,5-cyclooctadiene)rhodium(I) tetrafluoroborate

$B(C_6H_3(CF_3)_2)^-$

43

((4S,5S)-(-)-O-[1-benzyl-1-(methyl-2-phenyl-4,5-dihydrooxazol-4-yl)-2-phenylethyl]-diphenylphosphinite)(1,5-cyclooctadiene)iridium(I) tetrakis(3,5-bistrifluoromethyl)phenylborate
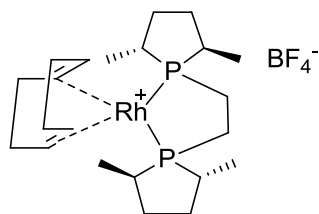
52

(+)-1,2-Bis((2R,5R)-2,5-dimethylphospholano)ethane(1,5-cyclooctadiene)rhodium(I) tetrafluoroborate
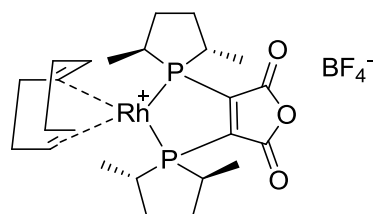
53

(+)-2,3Bis[(2S,5S)-2,5-
dimethylpholanyl]maleic
anhydride(1,5-cyclooctadiene)rhodium(I)
tetrafluoroborate

Chapter 1 - Introduction

1.1 – Hydrogen: industry and utilization

As the most abundant element in the universe, hydrogen has been estimated to make up more than 90 % of all atoms and 75 % of the total mass of the universe.[1] On earth, molecular hydrogen ($H_{2\,(g)}$) exists in very small amounts as a non-toxic gas, approximately 1 ppm by volume in the atmosphere. It can be found primarily bound to other elements to form compounds such as: water (H_2O), methane (CH_4) and other organic matter (living plants, petroleum, coal, etc.), and minerals.[1]

Molecular hydrogen is required in large quantities for many commercial uses, including the fixation of nitrogen in the Haber-Bosch process[2] and the hydrogenation of fats and oils. It is also used in the production of methanol, hydrodealkylation, hydrocracking, and hydrodesulfurization, along with its use as a rocket fuel, in welding, the reduction of metallic ore[1], and replacing helium as the carrier gas in analytical instrumentation.[3]

As a result of the high demand for $H_{2\,(g)}$, an enormous amount is produced in the United States each year, which was estimated to be *ca.* 10.7 million tons of

hydrogen in 2006.[4] A few of the more common methods developed for the synthesis of molecular hydrogen used today consist of steam reforming, charcoal gasification, and water electrolysis.[1]

1.2 – Catalysis

In the past, fine chemicals were traditionally prepared via non-catalytic routes. However, the need for larger-scaled reactions (multiple Kg) emerged and with the rise of awareness in the 20th century towards sustainable development,[5] it became apparent that it was necessary to reduce production costs, minimize waste and consider aspects of safety. These essential changes motivated industry to look towards transition metal-based catalytic processes to meet these goals for the past couple of decades.[6] In 1990, in the US, the production of chemicals that utilized catalysis at least once in their manufacturing processes produced an income of $ 890 billion dollars.[7]

Catalysis has the ability to lower the activation energy of essential reactions, resulting in quicker reaction times; it uses less resources, generates less waste and the catalyst itself is potentially recyclable.[5,8] Major accomplishments that resulted from the use of catalysts were: an increase in synthetic efficiency[9] of opening selective routes to the numerous products[10] required today for pharmaceuticals, material sciences and other chemical

2

industries. Catalysis represented a new way to control reactions in terms of selectivity, including chemoselectivity, regioselectivity, diastereoselectivity and enantioselectivity. [9,10]

1.3 – Types of catalysis

Depending on the reagents involved and the type of phases, catalysis is generally grouped into three main categories: heterogeneous catalysis, homogeneous catalysis and biocatalysis.[10,11] Due to the nature of this thesis a discussion of heterogeneous and homogeneous catalysis will follow.

1.3.1 – Heterogeneous catalysis

Heterogeneous catalysis refers to a reaction where the phase of the catalyst is different than that of the reactants.[8,12] In this case, the phases not only refer to solids, liquids and gases but in catalysis it may also refer to immiscible liquids, where the reaction occurs at the interface.[13] Heterogeneous catalysis exhibits many advantages which include ease of handling, superior stability, and ease of separation.[14] In addition, heterogeneous catalysts demonstrate chemo- and diastereoselective hydrogenation with a broad application for various functional groups (Scheme 1.1).
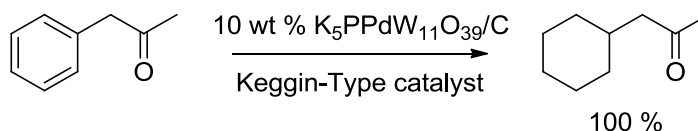
Scheme 1.1. An example of chemoselectivity found in heterogeneous catalysis.[186]

Heterogeneous catalysts work by having the reactants adsorb onto the surface of the catalyst. Once adsorbed, the reactants undergo the catalytic reaction, producing product(s), which is then desorbed from the surface. Two types of adsorption are possible. The first is physisorption, where the reactant is attracted to the surface of the catalyst through weak van der Waals interactions. The other is chemisorption, which is a much stronger interaction between the surface of the catalyst and the reactant. This type of adsorption involves the formation of a covalent bond between the reactant and the surface of the catalyst.[12,13]

1.3.2 – Homogeneous catalysis

Homogeneous catalysis refers to a reaction in which the catalyst and the reactants are in the same phase.[12] Homogeneous catalysis presents many advantages over its heterogeneous counterpart. Homogenous catalysis usually proceeds through relatively mild conditions, demonstrates better selectivity, are generally more adaptable and is inherently simpler to study chemically and

kinetically compared to heterogeneous systems, which has allowed more detailed investigations to transpire.[12,15] One major disadvantage that has restricted the use of homogeneous catalysis in industry is the cost due to the inherently more difficult separation of the catalyst from the product at the end of the reaction.[12] Types of homogeneous catalysts are Bronsted or Lewis acid and base, organocatalysts, and metal complexes.

1.4 – Catalytic hydrogenation

One of the most useful and versatile methods in organic synthesis to reduce a substrate is the catalytic hydrogenation of unsaturated substrates. The merits of this type of reaction are its large reaction scope, selective reduction of most unsaturated functional groups, and high yields, thus making catalytic hydrogenation a valuable synthetic tool.[16] Catalytic hydrogenation has also shown to be industrially relevant for its clean addition of dihydrogen towards sp^2 carbons such as those in C=C, C=O and C=N bonds.[14] These hydrogenation reactions can proceed with the use of either heterogeneous or homogeneous catalysts, yet only recently have these reactions been primarily conducted with homogeneous catalysts for the manufacturing of fine chemicals.[17]

1.5 – Asymmetric catalytic hydrogenation

An important branch of catalysis is one that focuses on the formation of chiral compounds. This type of catalysis is often referred to as asymmetric catalysis, in which a chiral catalyst is used to favour the formation of one stereoisomer over the other during the conversion of an achiral substrate into a chiral product.[18,19] This ability to selectively produce chiral molecules from catalytic hydrogenation was a very significant discovery for the production of natural products and pharmaceuticals.[19–22]

Accordingly, asymmetric hydrogenation became increasingly important in the 1950s, and with that heterogeneous catalysis became the method of choice. In addition to the obvious advantages of heterogeneous systems—its stability, ease of handling and separation—it also demonstrated the propensity to produce chiral products with 10-15% enantioselectivity.[14] However, by the 1960s the disadvantages of heterogeneous catalysis became evident with asymmetric hydrogenations, specifically with regard to poor regio- and stereoselectivity. These catalysts could not provide the enantiomeric excess that was required for the hydrogenation of prochiral molecules and, as a result, the focus transitioned to homogeneous catalysis.[14] Nonetheless, heterogeneous catalysis eventually came back into focus and recent developments have successfully proven the separation advantages and given comparable enantioselectivities to those achieved by homogeneous systems.[23]

As biologically active molecules in living systems only occur as one enantiomeric form, chiral or stereoisomeric discrimination is very important as the two enantiomers of an introduced molecule can interact with the receptor sites in biological systems differently, leading to very different effects. The enzymes and cell surface receptors found in living animals, such as humans, are chiral and the two enantiomers of a racemic drug could interact with different activities, one being therapeutical, but the other being ineffective or even toxic.[20,24–29] An example of one stereoisomer producing a therapeutic effect and the other elucidating a toxic interaction was the thalidomide medication tragedy in the 1960s.[20,30]

The demand for enantiomerically pure products increased and for some applications became a necessity, particularly in the pharmaceutical industries.[19] Several methods were developed to meet this demand and are still used today. These consist of optical resolution via diastereomers, chromatographic separation, enzymatic or chemical resolution and asymmetric synthesis.[19–21] Asymmetric synthesis, specifically in terms of catalysis, became an ideal method for preparing these optically active compounds, i.e. producing a single enantiomer, in large quantities.[19,21,22]

1.6 – Homogeneous asymmetric hydrogenation

A new approach to asymmetric hydrogenation emerged in the late 1960s, and homogeneous catalytic hydrogenation became a topic of increasing interest.[14] This was due to some key advantages of homogeneous catalysis over heterogeneous catalysis including: improved cost effectiveness, lower environmental impact, and ease of tunability.[31] However, the most significant was that homogeneous catalytic hydrogenations are easier to study, specifically with respect to reaction mechanisms. As such, mechanistic information was quickly obtained, which allowed faster development in this area.[32]

The first practical homogeneous hydrogenation catalyst, $RhCl(PPh_3)_3$, was discovered by Sir Geoffrey Wilkinson in 1965. Wilkinson's catalyst was one of the first compounds to show high activity towards the hydrogenation of alkenes under mild conditions (25 °C, 1 atm $H_{2\ (g)}$).[33] The interest in asymmetric homogeneous hydrogenation catalysis flourished and directed the attention to modifying Wilkinson's catalyst by substituting the achiral phosphine ligands with chiral phosphines.[14] This subject of asymmetric homogeneous catalysis quickly grew and garnered interest from leading researchers such as W. S. Knowles,[34,35] R. Noyori,[21] and J. D. Morrison.[36]

Through the incorporation of chiral phosphine ligands onto the metal centre of Wilkinson's Catalyst, they were able to hydrogenate certain olefins with

an optical yield of only 3-15%, which was determined via polarimetry. Although the stereoselective conversions using these new catalysts were not impressive, they created a solid foundation for asymmetric homogeneous hydrogenation.[14,25] These were the first examples of asymmetric homogeneous hydrogenations independently reported by Hörner *et al.*[37] (Scheme 1.2) and Knowles and Sabacky[38] (Scheme 1.3) in 1968. In 2001, W. S. Knowles, R. Noyori, and K. B. Sharpless were awarded the Nobel Prize in chemistry for their contributions to catalytic asymmetric synthesis. Since the first demonstration of asymmetric catalysis in the 1960s, chiral catalysts for the asymmetric catalytic hydrogenation to synthesize enantiomerically pure compounds has been used for the past five decades.[14]

R	% *ee*
Et	7-8
MeO	3-4
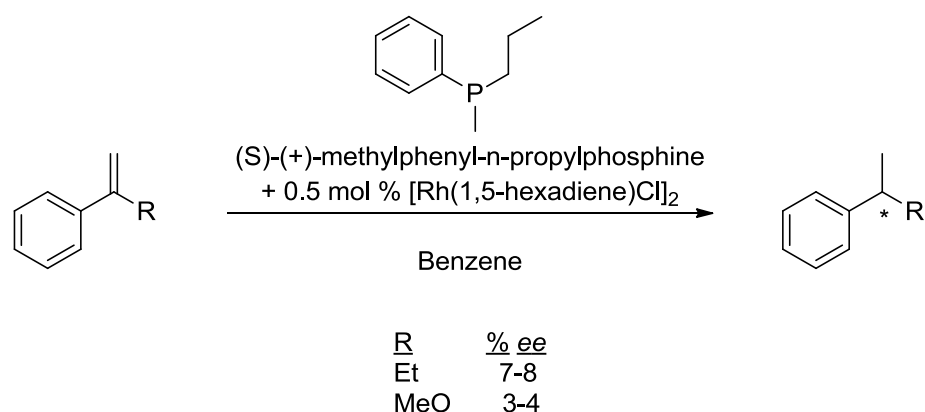
Scheme 1.2. One of the first successful examples of asymmetric hydrogenation reported by Hörner *et al.* [37]

9
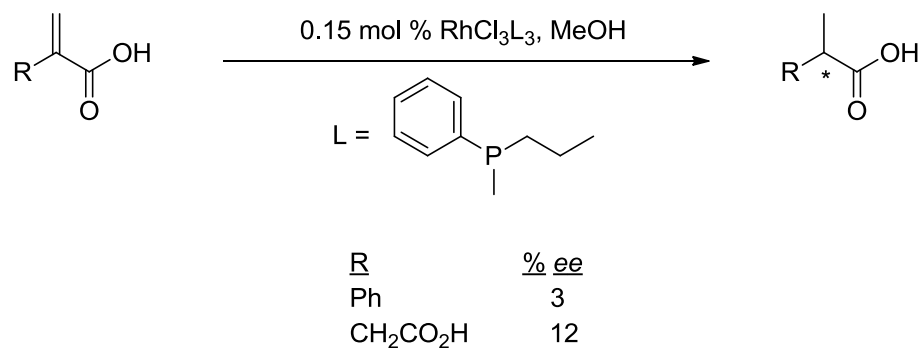
Scheme 1.3. One of the first successful examples of asymmetric hydrogenation by Knowles and Sabacky.[38]

1.7 – Asymmetric catalysis and the parameters which affect enantioselectivity

Asymmetric control in hydrogenation reactions results from the spatial arrangement of the substrate with the catalyst. However, this interaction between substrate and catalyst is not only affected by the properties and characteristics of the substrate and those of the catalyst, but also by the reaction conditions including hydrogen pressure, temperature, solvents, and reagents.[21]

1.7.1 – The substrate and its effect on enantioselectivity

Four structural features of a substrate that would affect the enantioselectivity of an asymmetric hydrogenation are the presence and strength

of a coordinating group, the proximity of the unsaturation of interest to the coordinating group, the type of unsaturation: C=C, C=O, and C=N double bonds, and lastly the steric hindrance or bulk present around the unsaturation.[14,21,31] Two major challenges with homogeneous asymmetric hydrogenations are the poor ability of some substrates to coordinate to the catalyst and the distance between the coordinating functional group and the prochiral centre of the substrate. The catalysis may be less effective if the functional group on the molecule is unable to strongly coordinate to the metal centre or if that functional group is far from the prochiral unsaturation that is to be hydrogenated.

1.7.1.1 – Coordinating ability

The coordinating ability of a molecule to a metal centre depends on several factors and properties of both the metal and the ligating functional group of that molecule. To determine whether a functional group will strongly or weakly coordinate to a metal, the following factors need to be taken into consideration: the Lewis basicity and π acidity of the ligating group; the coordination behaviour; the steric bulk of the ligand; the steric constraints on the metal; and the hard/softness of the metal and of the ligating group.[39]

The coordinating ability of a ligand is often discussed in terms of its Lewis basicity, yet the strength of ligand coordination is dependent on both its σ donating ability and its π accepting ability. General trends can thus be easily

11

observed. Strong σ donors and strong π acceptors are generally good ligands. One quantitative approach to discern strong ligands from weak ligands was carried out by Tsuchida, who gathered empirical evidence from regularities in UV/Vis absorbance spectra.[12,39,40] He observed an increase in the energy of the transitions as the ligands were varied in a complex, regardless of the metal centre. These ligands were arranged in a spectrochemical series (Figure 1.1) and from this series we can begin to relate the basicity of the ligand with how strong its interaction is with the metal centre. However, this spectrochemical series is in reference to the splitting of the d-orbital energies and is not the same as the binding strength of a ligand to a metal. In the spectrochemical series, NH_3 is lower in the list and a much weaker ligand than bipyridine, cyanide and carbon monoxide; however, NH_3 is much more basic. The reason is that these stronger ligands have the ability to accept π backdonation from the metal centre. They donate their electrons to the metal centre through σ-bonding. To relieve the build-up of negative charge on the metal, it can then π backdonate into the π* orbitals of the ligand.[12,39,40]

$I^- < Br^- < S^{2-} < SCN^- < Cl^-, NO_3^- < N_3^- < F^- < OH^- < C_2O_4^{2-} < H_2O <$

$NCS^- < CH_3CN < Py < NH_3 < en < bipy < NO^{2-} < PPh_3 < CN^- < CO$
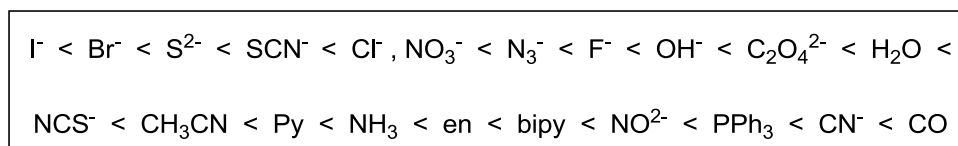
Figure 1.1. The spectrochemical series of ligands in order of increasing ability to split the d orbital energies.[12,39,40]

Another factor to consider is the effect of the ligand's charge. For example, Cl^- is shown as a weaker ligand than water in the spectrochemical series; however, this is not true. Cl^- is a strong ligand and this is because the metal is usually cationic. Therefore, displacing an anionic ligand, such as Cl^-, from a cationic metal is much harder than displacing a neutral ligand from a cationic metal.[12,39,40]

When considering the thermodynamics of ligand coordination, one must take into account the coordination mode of the ligand, with special attention to the chelate effect. Ligands can either be monodentate, meaning they only have one functional group that can bind to the metal centre, or multidentate, meaning the ligand has two or more functional groups that have the ability to bind to the metal centre. Multidentate ligands exhibit the phenomenon known as chelation, where the ligand can multiply bind to a single atom, in our case a metal ion. There is a higher affinity for chelating ligands to a metal centre than there is for monodentate ligands. This higher affinity and stability is known as the chelate effect. [12,39,40]

Lastly, the effects of hard/soft acids and bases, i.e. metals and ligands, are considered. When referring to hard and soft atoms, the atomic radius, the size of orbitals of that atom, and the extent of delocalization of electrons throughout those orbitals are examined. Heavy transition metals are soft acids due to their large and diffuse *d* orbitals and their large atomic radius. However,

when comparing nitrogen and phosphorus, both being Group 15 elements, amine ligands are hard bases, whereas the phosphines are soft bases. The reason amines are hard bases, yet phosphines are soft bases, is that nitrogen is a very small atom and therefore its valence atomic orbitals are small as well. The electrons are more localized because of its small size. Phosphines are softer bases due to the much larger valence atomic orbitals on phosphorus compared to those of nitrogen. As the valence orbitals are much larger, the electrons in these orbitals are therefore more delocalized. As such hard bases preferentially coordinate to hard acids and soft bases preferentially coordinate to soft acids.[12,39,40]

1.7.1.2 – Types of prochiral unsaturation

As mentioned above, the type of unsaturation, whether it is a C=C, C=O, or a C=N double bond, would affect the ability of the unsaturation to coordinate itself into the metal centre, along with its reactivity towards reduction. The exact ordering for these unsaturations depends on the reaction conditions, but an attempt to compare the relative activation barriers through kinetic control was made by Clayden *et al.* (Figure 1.2).[41] As the hydrogenation, or reduction, of the prochiral unsaturation becomes difficult to reduce, a more active catalyst is needed. Increasing the reactivity of the catalyst to hydrogenate these unsaturations would affect the control of the catalyst in terms of the chemoselectivity, regioselectivity, and stereoselectivity of the reaction.

14
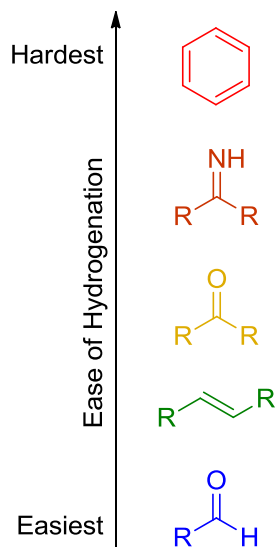
Figure 1.2. A rough arrangement of the easiest to the hardest unsaturation, C=C, C=O and C=N double bonds, to hydrogenate or reduce when only considering the type of unsaturation and kinetic control.[41]

1.7.1.3 – Proximity of the prochiral unsaturation to the metal coordinating group

The proximity of the prochiral unsaturation to the coordinating group may also affect the enantiomeric excess of the hydrogenation reactions (Figure 1.3). If the unsaturation is close to the coordinating group, such as A1, then the probability of the unsaturation to insert itself on a specific face is greater due to the constraints on the motion of the unsaturated portion of the substrate. However, in A2 the prochiral unsaturation is much further from the metal-binding

functional group, thus increasing the range of motion and therefore decreasing the probability of a specific facial selection. By this argument, it is postulated that as the length of the linker between the coordinating group and the prochiral unsaturation increases, the enantioselectivity of the hydrogenation should diminish. To our knowledge, there have been no deliberate studies of this effect.
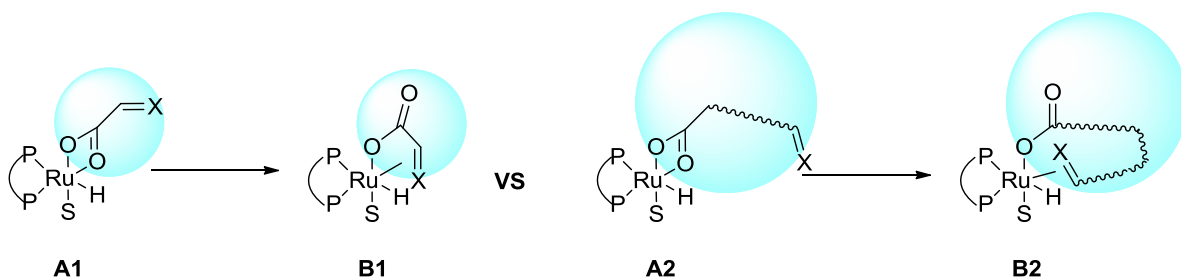
Figure 1.3. The proximity effect on facial selection between the prochiral unsaturation (where X = O, N or C) and the ruthenium centre. In the scenario to the left the prochiral unsaturation is in close proximity to the metal coordinating functional group while in the other scenario the prochiral unsaturation is far from the metal coordinating functional group.

1.7.1.4 – Steric effect of other functional groups

Asymmetric control in hydrogenation results from the spatial arrangement of the coordinated substrate with the catalyst. The chirality of the hydrogenated molecule is determined by the orientation of the unsaturated functionality when it coordinates to the metal centre of the catalyst. The olefin can bind to the metal centre via donation of the π electrons of the olefin into a vacant d orbital of the

metal to form a σ-type bond. The olefin can form this σ-type bond through either of its two faces (Figure 1.4). The d orbitals from the metal can then back-donate to the π anti-bonding orbitals of the olefin with the same symmetry to form a π-type of bond. This synergistic electron distribution activates the olefin by formally promoting π electrons into the π* orbital.[21]
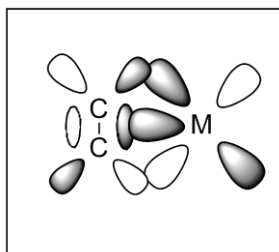
Figure 1.4. Facial interaction of the orbitals of an olefin with d orbitals of a metal centre.[21]

The faces on a prochiral unsaturated molecule are enantiotopic, so that substitution on either face, such as by hydrogenation, gives enantiomers. The face of the prochiral unsaturation that is hydrogenated is determined by which face binds to metal. Because the olefin can bind from either side of the double bond with no preferential facial selection, modifications to the design of the substrate and the catalyst are necessary to obtain some control over the facial selection of the olefin. At the simplest level, this is done by making the catalyst a chiral nonracemic compound itself; preferably a pure single enantiomer. Thus the binding of the unsaturated substrate by either face creates diastereomeric intermediates, so that the binding of the substrate on one face will be energetically or kinetically preferred over binding on the other face. However, this

17

is usually insufficient unless the catalyst and/or substrate are designed so as to maximize the difference in energies, and therefore rates. One way to do this is by covalently attaching to the prochiral unsaturation moiety, a functional group that has the ability to coordinate to the metal centre of the catalyst, as discussed in section 1.7.1.1. The coordination of the functional group to the metal centre reduces the ability of the prochiral unsaturation to bind at any angle. Additional control of the stereoselectivity can be introduced by functionalizing the catalyst or substrate, such that there is a preferential facial selection due to steric constraints between the ligand and the substrate (Figure 1.5). Introducing a chiral environment through the catalyst is one manner of control. This method uses steric effects to make the binding of one enantioface (prochiral face) preferred over the other. By having one larger group (R^1) and the other smaller (R^2) attached to the substrate, it can consequently promote one enantiofacial selection over the other due to an increase in steric interaction between the ligands bound to the metal centre and the larger group on the substrate.[21] This enantiofacial selection through steric interaction, i.e. the stability of the diasterotopic complexes formed, represents thermodynamic control; however it is also possible to proceed through kinetic control for the enantiofacial selection during the asymmetric hydrogenation as well. To explain thermodynamic enantiofacial control and kinetic enantiofacial control, we can look at a simplified subset of Noyori's ruthenium binap catalytic cycle for the hydrogenation of unsaturated carboxylic acids (Scheme 1.4).[21] The catalytic reaction would proceed through a sequence of reversible steps until the last step shown. For this

case, depending on the H_2 pressure, once the migratory insertion of the hydride occurs and complex **C** is formed, the last step, **C** to **D**, either occurs fast or slow. For example, if the H_2 pressure is low and thus the last step is slow, then the steps **A** to **B** and **B** to **C** have enough time to reach a pseudoequilibrium and complex **C** can equilibrate to the energetically most-stable diastereomer. In this case, thermodynamic enantiofacial selection can be obtained. However, if we consider the Curtin-Hammett principle, one case where the relative activation barrier of the most-stable diastereomer is too high in energy to proceed to the enantiomeric product then the diastereomer preequilibrium does not control the product ratio. Instead the reaction proceeds through kinetic control, i.e. the diastereomer that provides access to the lowest-energy transition state, which was demonstrated by Halpern.[42,43] On the other hand, if the H_2 pressure is high then the last step would be fast. Consequently, steps **A** to **B** and **B** to **C** would not have time to reach a pseudoequilibrium and the unsaturation would be hydrogenated with kinetic enantiofacial selection, as step **C** to **D** would occur as soon as the prochiral unsaturation binds to the metal centre. For each substrate the *ee* of the asymmetric hydrogenation can increase or decrease depending on which pathway is followed, i.e. kinetic control versus thermodynamic control.[21,44]

Version 1   Version 2

$$R_1 \neq R_2$$
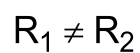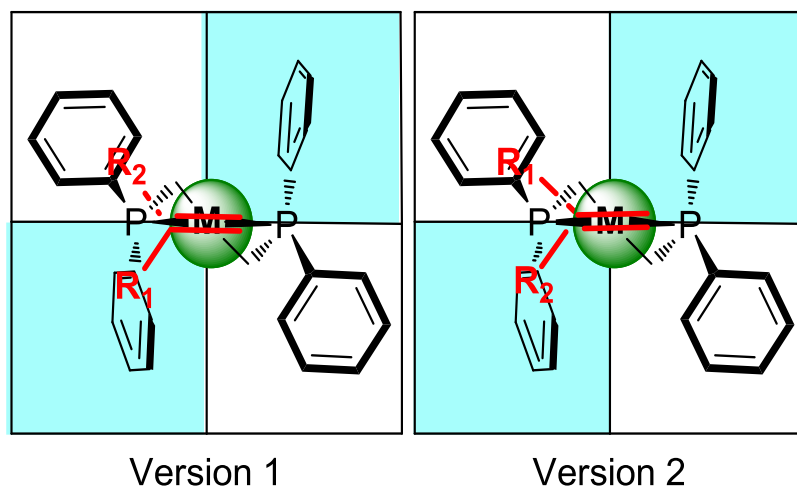
Figure 1.5. Enantiofacial selection of the prochiral unsaturation C=C double bond, where R^1 and R^2 can either be large or small functional groups. The blue and white boxes represent the spacial position of the ligands on the catalyst, where the blue boxes represent unoccupied areas by the substituents on the ligands and the white boxes occupied areas.
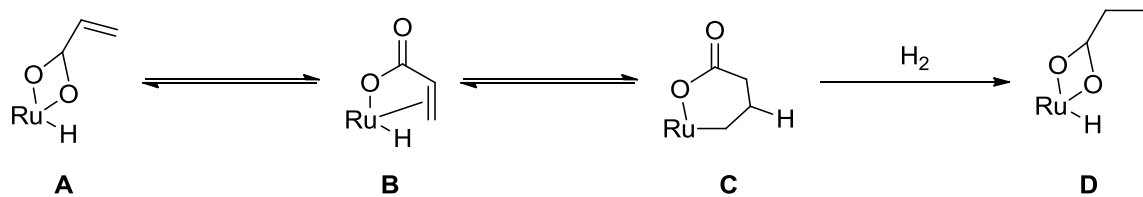
Scheme 1.4. Simplified subset of Noyori's ruthenium catalytic cycle, showing the steps between intermediates as reversible until the reaction with hydrogen gas.[21]

The asymmetric hydrogenation of tiglic acid and atropic acid with Ru-binap dicarboxylate illustrates the importance of kinetic versus thermodynamic facial selection. The two unsaturated acids need to be hydrogenated at different conditions—low versus high hydrogen pressure, respectively—to obtain high ee.[45,46] For atropic acid, kinetic enantiofacial selection produces higher ee than thermodynamic enantiofacial selection. Thus a high hydrogen pressure is used to ensure that the H_2 addition step is rapid and kinetic enantiofacial selection is obtained in the catalytic cycle. On the other hand, to obtain a high enantioselectivity with tiglic acid, one must utilize a low hydrogen pressure, as the thermodynamic enantiofacial selection is better. While it is clear that the substituents on the prochiral unsaturation determine the ee obtained by kinetic enantiofacial selection or thermodynamic enantiofacial selection, the structural effects are not well enough understood to allow predictions to be made.

Another report by Noyori *et al.*[21,47] demonstrated the effect of sterics on the enantioselectivity in the substrate. By solely changing R^2 from a methyl to an

iso-propyl (Figure 1.6) for the asymmetric redution of a ketone, the optical yield

decreases 25 %.[21,47]
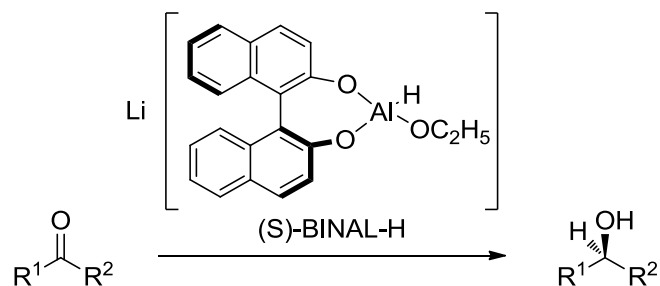
R^1	R^2	Optical yield
Ph	CH_3, alkyl	95-100
Ph	$(CH_3)_2CH$	71
Ph	$(CH_3)_3C$	44

Figure 1.6. The asymmetric reduction of similar substrates bearing a prochiral

ketone. This reaction demonstrates the effect of changing the substitutions (R^2)

on the enantioselective of the reaction.[21]

1.7.2 – The structure of the catalyst and its effect on enantioselectivity

Ligands, like substrates, contain the ability to coordinate to the metal through the same characteristics, factors and trends discussed in section 1.7.1.1. The same factors for the coordination of molecules are considered here for the coordination of the ligand: the Lewis basicity and π acidity of the ligating group; the coordination behavior; and the hard/softness of the metal and of the ligating group.[39,40] However, once the ligand is coordinated to the metal-centre, the characteristics of the resulting complex have a strong effect on the asymmetric hydrogenation of unsaturated substrates. These effects not only come from the chirality of the complex but also from the electron-donating and withdrawing character of the ligand, the bite angle of the ligand (if chelating), the steric hindrance of the ligand, and also the nature of the metal itself.[21,40]

1.7.2.1 – General catalytic cycle for homogeneous catalysts and for Noyori's ruthenium-binap complex

To fully understand the effects of the steric and electronic properties of the ligand, the metal, and from the external factors, one must first understand the catalytic mechanism. The prototypical catalytic hydrogenation cycle for the reduction of an olefin with Wilkinson's catalyst is shown in Scheme 1.5.[15] In most catalytic reactions, the transition metal complex employed is not the

catalytically active species, but instead a precatalyst or catalyst precursor. In the first step of the reaction, the complex undergoes ligand dissociation to form the catalytically active 14 electron species [step 1]. After the active catalyst has been formed, there is an oxidative addition of H_2 [step 2], followed by substrate coordination [step 3]. The hydrogen then reduces the unsaturated molecule by migratory insertion [step 4] and the final step of the catalytic cycle is reductive elimination [step 5], where the saturated product dissociates from the metal centre, and the active 14e complex is reformed.[15,21]
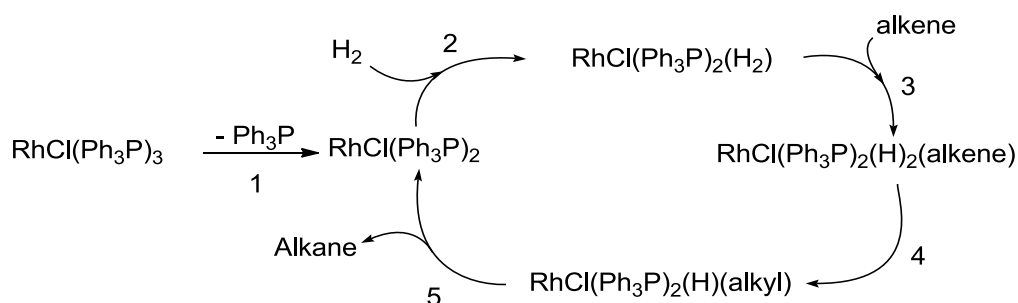
Scheme 1.5. Simplified hydrogenation reaction mechanism of an unfunctionalized olefin with Wilkinson's Catalyst. [15]

A well studied Ru-based chiral catalyst which demonstrates enantioselectivity is diacetato[(R)-(+)-2,2'-bis(diphenylphosphino)-1,1'-binapthyl]ruthenium(II), $Ru(OAc)_2[(R)-binap]$ (compound **38**, discussed in section 3.1). The proposed catalytic cycle for the hydrogenation of an

24

unsaturated carboxylic acid using Ru(OAc)$_2$[(R)-binap] is shown in Scheme 1.6. As Ru(OAc)$_2$[(R)-binap] is the precatalyst in the catalytic cycle, there is initial dissociation of one of the acetate ligands followed by substrate coordination through the carboxylate functionality as discussed above. There is structural evidence that the unsaturated substrate binds through this carboxylate moiety. After the addition of hydrogen and release of the other acetic acid ligand, the substrate undergoes an alkene insertion to form the Ru-alkyl intermediate. Within the catalytic cycle there are two possible routes by which this mechanism can proceed. The dominant route depends on the hydrogen pressure of the system. If the hydrogen pressure is high, the catalytic cycle will proceed through the route 1. As a result of the high pressure of hydrogen, there is an abundance of the gas in the reaction solution. Therefore the catalyst has a higher propensity to react quicker with an additional equivalent of hydrogen to proceed to the saturated substrate and resulting in alkyl dissociation. This is followed by subsequent ligand dissociation and thus, the catalyst is regenerated. If the system was under a low pressure of hydrogen, the catalytic cycle would proceed through route 2. Because the hydrogen pressure is lower, the overall concentration of hydrogen is not as high and thus this second route is dominant. Instead of addition of hydrogen to the catalyst, there is coordination of an additional equivalent of substrate and the hydrogen from the carboxylic acid is added to the alkyl. Then a mole of dihydrogen inserts and hydrogenates the substrate which is removed through ligand dissociation to regenerate the active catalyst.
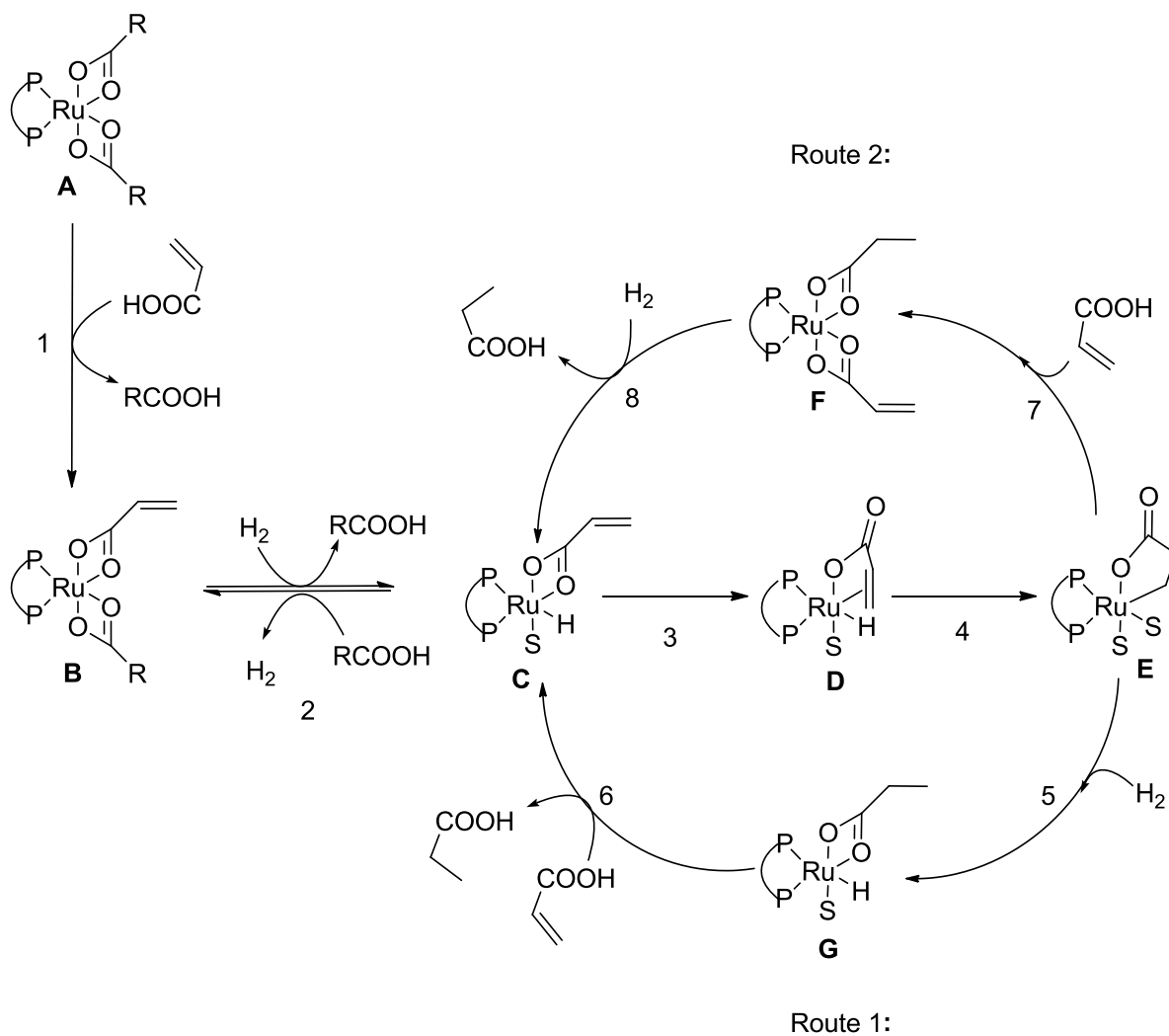
Scheme 1.6. Hydrogenation reaction mechanism of Ru[(OAc)$_2$[(R)-binap], **38**, proceeding at low hydrogen pressure (thermodynamic route) and at high pressure (kinetic route).[21]

1.7.2.2 – Effect of electron-donating and –withdrawing character of the ligand

Any ligand or substrate that coordinates to the metal centre of a complex can change the electron density at the metal through the electron-withdrawing or -donating character of the ligand.[13,40] The movement of electron density from, or to, the metal can affect the ability of the complex to proceed via oxidative addition or reductive elimination of the catalytic mechanism.[13,40] These electronic effects for PR_3 ligands were measured and quantified by Tolman[48] through measuring the symmetric stretching of vibration of CO bonded in $M(L)_m(CO)_n$ complexes.[13,40,48] Thus, if the ligands were particularly effective at donating electron density into the metal, then this would cause the metal to become more reactive toward oxidative addition, whereas if electron density was taken from the metal by the ligand, this would cause the metal to become less reactive towards oxidative addition, promoting reductive elimination instead. This electronic effect would in turn assist the kinetic or thermodynamic product to form, as the interaction with the unsaturated molecule has changed accordingly.

1.7.2.3 – Effects of the steric hindrance of the ligand and its bite angle

The ligands attached to the metal centre of the complex directly affect the enantioselectivity of the hydrogenation reaction of the substrate. For catalysis, each metal would only contain a limited amount of space and thus the size of the ligand attached is important simply because it limits the available space around

the metal. This space is referred to as a "reaction pocket" and if too much of the metal is occupied by coordinated ligands, the ability of the substrate to coordinate or insert itself into the reaction pocket of the metal is diminished.[13] This steric crowding of the metal centre is one of the main techniques that chemists have used to aid in controlling facial selection of a prochiral unsaturation (Figure 1.7). By increasing the steric bulk around the metal centre or the "reaction pocket", the manner in which the unsaturation inserts, i.e. facial selection of the unsaturation, becomes more restrictive. This is due to the steric interaction between the unsaturated substrate and the ligands.[13,21,44]
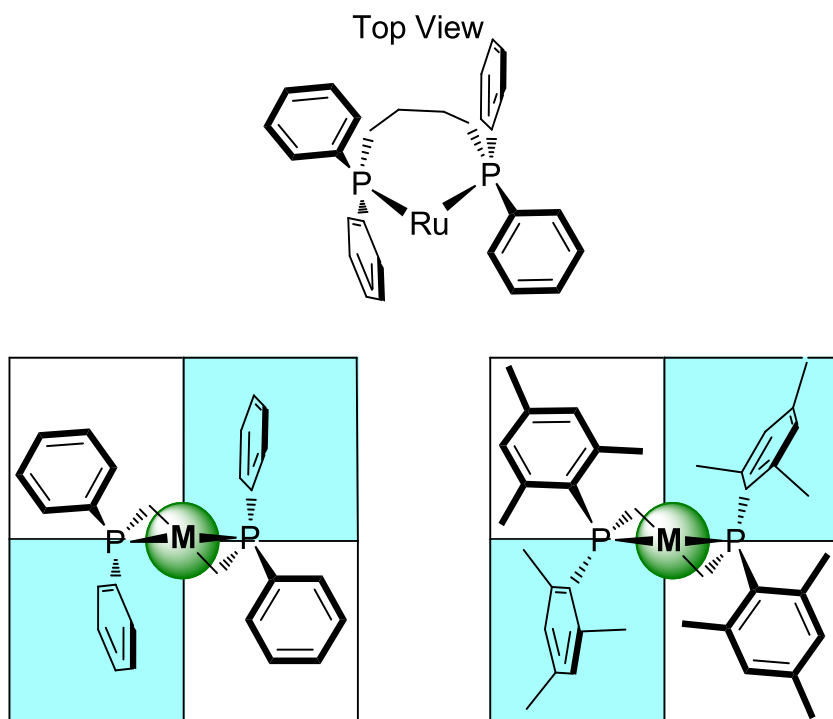
Figure 1.7. Quadrant diagrams demonstrating the effect of steric bulk of the ligands on the "reaction pocket" of the metal center restricting the manner in which an unsaturated substrate may insert into the complex. The blue and white boxes represent the spatial position of the ligands on the catalyst, where the blue boxes represent unoccupied areas by the substituents on the ligands and the white boxes occupied areas.

Another key concept related to the steric bulk of the ligand is the bite angle, α, of a chelating ligand. In general, as the α of the ligand increases, the more space the chelating ligand occupies, and as a result the large α causes the "reaction pocket" to decrease in size (Figure 1.8).[13,21,40,44]
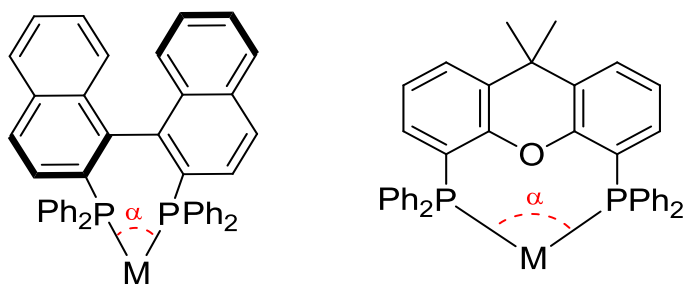
Figure 1.8. BINAP (α = 92 °) and Xantphos (α = 112 °) ligands bound to a transition metal, M, illustrating the effect of bite angles (shown in red) on relations to the space occupied by said ligand. (the difference in angles is exaggerated in the illustration)

1.7.2.4 – Effect of the metal

The effects of changing the transition metal in a complex can alter the properties of the complex itself, so much so that it is common to see research groups focusing on only one part of the periodic table, such as one group, throughout their careers. As one moves from the left to the right of the periodic table, the electronegativity of the metal increases. This dictates the ease of the catalyst towards their ability to form σ- and π- bonds with the ligands in the complex, and therefore, the stability of the complex itself.[40] Most importantly, the

electronegativity of the metal affects the electronics of the catalyst. It has been reported that the metal itself affects the enantioselectivity of the hydrogenation through electronic effects, specifically the electrostatic effects of the metal centre. The group of Cavallo has focused on the investigation of electrostatic effects, by studying the typographic electrostatic potentials of the metal. They have been applying this information towards improving asymmetric synthesis and have had success in demonstrating that the electrostatic effects can promote selectivity in asymmetric synthesis. This achievement was done by shaping the chiral reaction pocket of the catalyst through either steric or electrostatic effects.[49–51]

1.7.3 – External factors, conditions, reagents and their effects on enantioselectivity

As with the complex, its components (ligands, metal), and the substrate, external conditions and reagents of the asymmetric hydrogenation will affect the results in terms of the enantioselectivity of the reaction. The major contributors towards enantioselectivity, amongst external factors, are: hydrogen pressure, solvent, the presence of additives (acid or base), temperature, and time.

1.7.3.1 – Effect of hydrogen pressure

Hydrogen pressure can have a dramatic effect on the enantioselectivity of the asymmetric reaction (Scheme 1.6). While there is no concrete evidence to

which pressure produces the highest enantioselectivity, reports have shown that with the change in H_2 pressure, there is a shift between the facial selection of the unsaturation from hydrogenation from the thermodynamic controlled enantioface selection to the kinetically controlled enantioface or vice versa (Figure 1.9). Thus, at higher pressures of H_2, the enantiomeric excess of the resulting products, for some substrates, is generally different from that observed at lower pressures of H_2.[21]
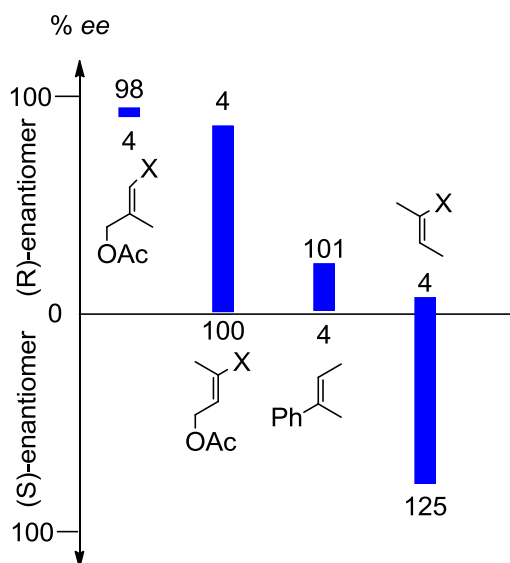
Figure 1.9. The relationship between the unsaturated substrate and the hydrogenation pressure for Ru(OAc)$_2$[(S)-binap] catalyst, where the enantioselectivity is directly affected by pressure. The x-axis is % *ee* of enantiomers R and S, whereas the numbers above and below the bars represent the H_2 pressure in bars utilized to obtain the % *ee*.[21]

Enantioselectivity is temperature dependent and this effect of temperature can be explained through the relationship between rate and $\Delta G^{\ddagger}$. There are two pathways to obtain R and S enantiomers and each pathway has different activation energies, $\Delta G^{\ddagger}_R$ and $\Delta G^{\ddagger}_S$, due to the diastereomeric intermediates. The ratio of R and S enantiomers obtained from a reaction is governed by the difference between the $\Delta G^{\ddagger}_R$ and $\Delta G^{\ddagger}_S$ activation energies, i.e. $\Delta\Delta G^{\ddagger}$. By rearranging the equilibrium equation with $\Delta\Delta G^{\ddagger}$ (Eq. 1) we obtain Eq. 2. If we assume $\Delta\Delta S^{\ddagger}$ is 0, then we only need to consider $\Delta\Delta H^{\ddagger}$. From this, we can see that as temperature increases, the enantioselectivity for the asymmetric hydrogenation would decrease. However, if $\Delta\Delta S^{\ddagger}$ is positive, then there will be a crossover temperature above which increases in temperature cause an increase in enantioselectivity.[44]

$$\Delta\Delta G^{\ddagger} = -RT\ln\frac{k_R}{k_S} \qquad\qquad \textbf{[1]}$$

$$\frac{k_S}{k_R} = e^{\frac{\Delta\Delta G^{\ddagger}}{RT}} = e^{\frac{\Delta\Delta H^{\ddagger}}{RT}} \times e^{\frac{-\Delta\Delta S^{\ddagger}}{R}} \qquad\qquad \textbf{[2]}$$

The enantioselectivity of asymmetric hydrogenation can also be affected by the solvent used in the system. Solvents can often become a crucial component for any chemical reaction in terms of selectivity and conversion.[43]

Most often it is the bulk properties—polarity, protic versus aprotic, dielectric constant, etc.—that are the main considerations when selecting a solvent. However, the optimal solvent must be established empirically, as there are no theoretical criteria for solvent selection.[15,44] It is also difficult to predict the optimal solvent, as the solvent may have multiple roles, such as dissolving the substrate and the catalyst, uptake of hydrogen gas, etc. Nevertheless, solvent does have a dramatic effect on the enantioselectivity, and one must investigate which is the optimal solvent for a specific reaction.[44,52]

Acidic or basic additives can assist the asymmetric hydrogenation by reacting with the substrate or the catalyst. The additive could transform the metal coordinating functional group of the substrate into a better coordinating group for the enantioselective reaction. The additive could react with an interfering functional group, to act as an *in situ* protecting or blocking group. Finally, the additive may also help temporarily stabilize the metal centre after the dissociation of a ligand, throughout the catalytic cycle.[21]

1.8 – Thesis Objective

The objectives of this project were to: 1. study the effect of the length of the linker between the prochiral unsaturation and the metal-binding coordinating group (MC) during asymmetric hydrogenation (Scheme 1.7) and 2. employ a reversible modification to change a poorly coordinating functional group into a strongly coordinating group, to allow for efficient catalysis (Scheme 1.8). In order to investigate the effect of the length of the linker, the study will focus on the asymmetric hydrogenation of alkenes or ketones bearing a carboxylic acid ligating group that is n atoms removed from the prochiral unsaturation. The test compounds were chosen to elucidate the effect of binding group proximity within the substrates. The conversion and enantioselectivity of the asymmetric hydrogenation of these chained substrates is studied. For the second objective, we will induce this reversible transformation utilizing CO_2 with allylamines, which will then be hydrogenated using known hydrogenation catalysts. Focus will be placed on the stereoselectivity and the rate of the hydrogenation reaction with respect to the effects of CO_2. As such, the methodology will be tested with several conditions and an extensive catalyst scope, in attempts to improve the conversion and enantioselectivity of the reaction.
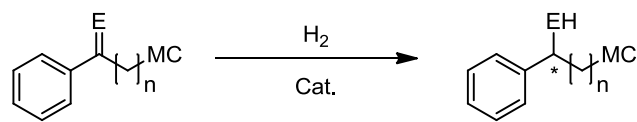
	E	n
7	CH_2	0
8	CH_2	2
9	CH_2	3
11	O	2
12	O	3

Scheme 1.7. Asymmetric hydrogenation mediated through a metal-binding

functional group.

$R^1 \neq H$ or CH_3

$R^2 = H$ or alkyl chain

$n = 1 - 10$
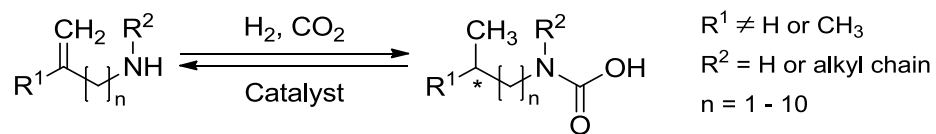
Scheme 1.8. Overall reaction for the asymmetric hydrogenation of an

unsaturated amine-containing substrate utilizing CO_2 reversibly.

Chapter 2 – Experimental Methods

2.1 – General

All reactions were conducted in the absence of oxygen and water under an inert atmosphere by use of standard Schlenk techniques, unless otherwise indicated. A manifold under an atmosphere of argon and a glovebag under an atmosphere of nitrogen were used for bench top manipulations of air sensitive materials. A Nexus One glovebox containing an atmosphere of nitrogen was also utilized for the preparation of high pressure reactions. All glassware and apparatus were dried in an oven at 130 °C and evacuated while hot before use. Reactions carried out at room temperature, RT, were done at 22 °C $\pm$ 2 °C. Solvents were dried by standard distillation procedures[53] before use or purchased from Drisolv® and then degassed by freeze, pump, thaw cycles. All reagents were purchased from chemical suppliers: Alfa Aesar, Sigma Aldrich, TCI America, and Acros Organics. All catalysts were purchased from Strem. Solvents, reagents and catalysts were used as received unless otherwise specified. All asymmetric hydrogenation experiments were done so in triplicate unless indicated. ^{1}H NMR and ^{13}C NMR spectra were recorded at 300 K on a Bruker AV-400 spectrometer operating at 400.3 and 100.7 MHz and/or AV-500 NMR spectrometer operating at 499.1 and 125.5 MHz, respectively, with chemical shifts (δ) expressed in parts per million, ppm, relative to SiMe$_4$ at 0

ppm, and referenced to the residual solvent peak of the deuterated solvent. Quantitative NMR spectroscopy was carried out using 1,3,5-trimethoxybenzene as the internal standard. Quantitative GC-FID analysis was performed on a PerkinElmer Clarus 680 gas chromatograph instrument equipped with a CP-Chirasil-DEX CB chiral column (25 m x 0.25 mm i.d., 0.25 mm film thickness) from Chrompak for the analysis of conversion and enantiomeric excess of the reactions. Low resolution mass spectrometry was done using the PerkinElmer Clarus 680 gas chromatograph paired with a Clarus 600T mass spectrometer equipped with an Elite-5MS column (25 m x 0.25 mm i.d., 0.25 mm film thickness) from PerkinElmer. Quantitative HPLC using Agilent Technologies 1260 Infinity with Chiralpak OJ-H, AD-H and IA chiral columns (25 cm x 0.46 cm i.d.) from Daicel were also used for the analysis of enantiomeric excess. High resolution mass spectra (HRMS) ESI and EI were obtained on a Qstar XL QqTOF from Applied Biosystems/MDS Sciex.

2.2 – Preparation of prochiral compounds

2.2.1 – Preparation of atropic acids
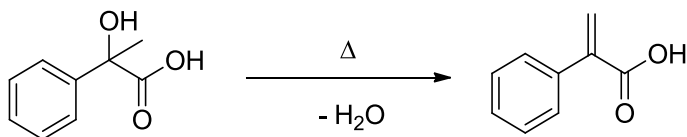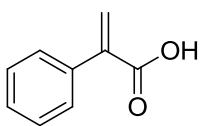
Atropic acid, 1, was synthesized by vacuum distillation of atrolactinic acid.[54] Atrolactinic acid (1.00 g, 0.571 mmol) was added to a Schlenk tube equipped with a condenser. The set-up was evacuated and then the white powder was heated with an open flame using a propane torch until a significant amount of white sublimate appeared in the condenser. The white solid collected in the condenser was dissolved in 100 mL of a 1:1 mixture of hot water:ethanol. An additional amount of hot water, 40-100 mL, was added to the solution and then the entire solution was subsequently cooled using an ice bath. Atropic acid crystallized and was collected by vacuum filtration. After washing the crystals with cold water, the product was left to air dry. ^{1}H NMR (400 MHz, CDCl$_3$): δ = 7.45 (m, 2H), δ 7.40-7.36 (m, 3H), δ 6.54 (s, 1H), δ 6.03 (s, 1H) ppm; ^{13}C NMR (100 MHz, CDCl$_3$): δ = 171.11, 140.52, 136.14, 129.26, 128.42, 128.36, 128.15 ppm. The ^{1}H and ^{13}C NMR spectra matched those reported in the literature.[55]

2.2.2 – General procedure for the synthesis of phenylalkenoic acids,[56,57] phenylethenylbenzoic acids and phenylprop-2-en-1-yl-1H-isoindole-2,3(2H)-dione
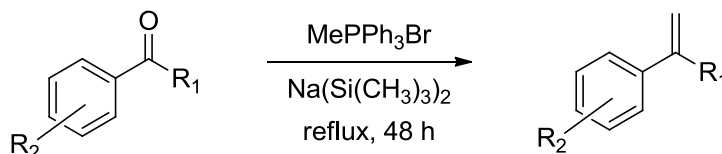
Methyltriphenylphosphonium bromide (5.6 mmol) was suspended in toluene, where it was subsequently cooled to 0 °C in an ice bath. Sodium bis(trimethylsilyl)amide (5.4 mmol) in a 1.0 M solution in THF was added drop-wise to the suspension and rapidly stirred for 1 h. The suspension was then cooled from 0 °C to ca. -78 °C using a dry ice/acetone bath, where 3-benzoylpropionic acid (5.2 mmol) was added to the solution. The reaction was then refluxed for 16-48 h until the reaction came to completion, which was monitored by GC-MS. Upon cooling, saturated ammonium chloride (80-100 mL) was added to the reaction flask and the resulting slurry was diluted with distilled water (100 mL). The product was extracted with ethyl acetate (3 x 100 mL), washed with brine, and dried with magnesium sulfate. The drying agent was removed by filtration, after which the product was concentrated under reduced pressure by rotary evaporation and purified by column chromatography on silica gel with 30 % ethyl acetate in hexane. Other unsaturated carboxylic acids were synthesized from the corresponding ketones in a similar manner.

2.2.2.1 – Analytical data for phenylalkenoic acids and derivatives

2
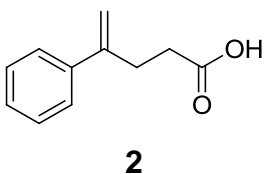
4-Phenyl-4-pentenoic acid, 2: The isolated yield was 48 % of a white solid. The ^{1}H and ^{13}C NMR spectra matched those reported in the literature.[56] ^{1}H NMR (400 MHz, CDCl$_3$): δ = 7.41 (m, 2H), 7.36-7.29 (m, 3H), 5.33 (s, 1H), 5.12 (s, 1H), 2.86 (t, 2H), 2.54 (t, 2H) ppm; ^{13}C NMR (100 MHz, CDCl$_3$): δ = 178.77, 146.57, 140.43, 128.42, 127.67, 126.08, 112.96, 32.87, 30.16 ppm.

3
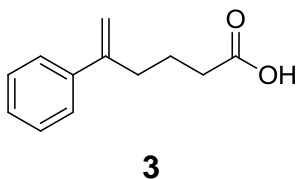
5-Phenyl-5-hexenoic acid, 3: The isolated yield was 77 % of a white solid. The ^{1}H and ^{13}C NMR spectra matched those reported in the literature.[58] ^{1}H NMR (400 MHz, CDCl$_3$): δ = 7.41-7.29 (m, 5H), 5.32 (s, 1H), 5.09 (s, 1H), 2.58 (t, 2H), 2.39 (t, 2H), 1.81 ppm (apparent quintet, 2H); ^{13}C NMR (100 MHz, CDCl$_3$): δ = 180.25, 147.24, 140.62, 128.25, 127.38, 125.99, 115.91, 34.32, 33.24, 22.92 ppm.

4
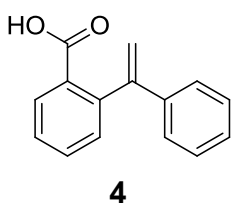
2-(1-phenylethenyl)benzoic acid, 4: The isolated yield was 24 % of a white solid. The ^{1}H spectrum matched those reported in the literature.[59,60] ^{1}H NMR (400 MHz, CDCl$_3$): δ = 7.94 (d, 1H), 7.57 (t, 1H), 7.44 (t, 1H), 7.38 (d, 1H), 7.25-7.22 (m, 5H), 5.69 (s, 1H), 5.24 (s, 1H) ppm; ^{13}C NMR (100 MHz, CDCl$_3$): δ = 171.73,

149.54, 143.62, 140.87, 132.39, 131.55, 130.65, 129.48, 128.09, 127.64, 127.50, 126.79, 114.36 ppm.
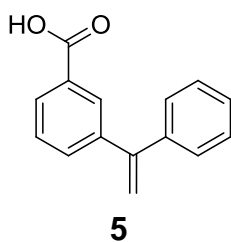
3-(1-phenylethenyl)benzoic acid, 5: The isolated yield was 55 % of a white solid. ^{1}H NMR (400 MHz, CDCl$_3$): δ = 8.12 (s, 1H), 8.07 (d, 1H), 7.58 (d, 1H), 7.46 (t, 1H), 7.37-7.32 (m, 5H), 5.56 (s, 1H), 5.53 (s, 1H) ppm; ^{13}C NMR (100 MHz, CDCl$_3$): δ = 172.08, 149.05, 142.03, 140.81, 133.65, 129.88, 129.45, 129.36, 128.40, 128.35, 128.12, 128.00, 115.37 ppm; ESI-HRMS [M-H]$^-$ calculated for C$_{15}$H$_{11}$O$_2$: 223.07645, found 223.07719.
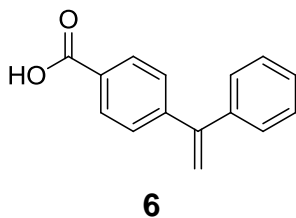
4-(1-phenylethenyl)benzoic acid, 6: The isolated yield was 53 % of a white solid. ^{1}H NMR (400 MHz, CDCl$_3$): δ = 8.08 (d, J = 8.2 Hz, 2H), 7.46 (d, J = 8.5 Hz, 2H), 7.37-7.32 (m, 5H), 5.58 (s, 1H), 5.57 (s, 1H) ppm; ^{13}C NMR (100 MHz, CDCl$_3$): δ = 171.62, 149.25, 146.98, 140.70, 130.19, 128.43, 128.34, 128.34, 128.21, 128.04, 116.14 ppm; ESI-HRMS [M-H]$^-$ calculated for C$_{15}$H$_{11}$O$_2$: 223.07645, found 223.07719.
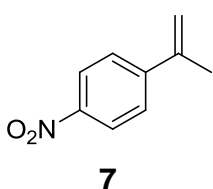
4-(propen-2-yl)nitrobenzene, 7: The isolated yield was 70 % of a yellow crystalline solid, which was purified by sublimation. The ^{1}H and ^{13}C spectra matched those reported in the literature.[61]

^{1}H NMR (500 MHz, CDCl$_3$): δ = 8.20 (d, 2H), 7.60 (d, 2H), 5.53 (s, 1H), 5.30 (s, 1H), 2.20 (s, 3H) ppm; ^{13}C NMR (125 MHz, CDCl$_3$): δ = 147.64, 147.00, 141.58, 126.22, 123.58, 116.35, 21.56 ppm.
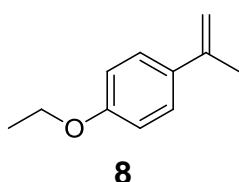
1-ethoxy-4-(prop-1-en-2-yl)benzene, 8: The isolated yield was 85 % of a clear yellow oil. ^{1}H NMR (400 MHz, CDCl$_3$): δ = 7.43-7.41 (dt, 2H), 6.88-6.86 (dt, 2H), 5.30 (s, 1H), 5.00 (t, 1H), 4.05 (q, 2H), 2.14 (s, 3H), 1.43 (t, 3H) ppm; ^{13}C NMR (100 MHz, CDCl$_3$): δ = 158.41, 142.54, 133.54, 126.53, 114.07, 110.50, 63.39, 21.86, 14.81 ppm; EI-HRMS [M$^-$] calculated for C$_{11}$H$_{14}$O:162.1050, found 162.1051.
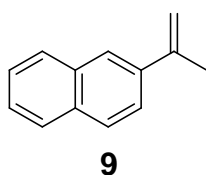
2-(prop-1-en-2-yl)naphthalene, 9: The isolated yield was 77 % of a white crystalline solid. The ^{1}H and ^{13}C spectra matched those reported in the literature.[62] ^{1}H NMR (400 MHz, CDCl$_3$): δ = 7.87-7.80 (m, 4H), 7.71-7.68 (m, 1H), 7.51-7.44 (m, 2H), 5.55 (s, 1H), 5.22 (t, 1H), 2.29 (s, 3H) ppm; ^{13}C NMR (100 MHz, CDCl$_3$): δ = 142.98, 138.32, 133.36, 132.78, 128.21, 127.66, 127.48, 126.08, 125.79, 124.24, 123.87, 112.99, 21.86 ppm.

10
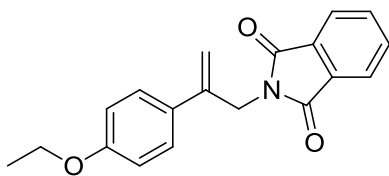
2-[2-(4-ethoxyphenyl)prop-2-en-1-yl]-1H-isoin-dole-1,3(2H)-dione, 10: The isolated yield was 74 % of white crystalline needle-like crystals. ^{1}H NMR (500 MHz, CDCl$_3$): δ = 7.85-7.83 (m, 2H), 7.71-7.69 (m, 2H), 7.43 (d, 2H), 6.86 (d, 2H), 5.37 (s, 1H), 5.08 (s, 1H), 4.68 (s, 2H), 4.03 (q, 2H), 1.40 (t, 3H) ppm; ^{13}C NMR (125 MHz, CDCl$_3$): δ = 167.93, 158.83, 141.70, 133.92, 131.99, 130.67, 127.45, 123.28, 114.23, 112.27, 63.35, 41.44, 14.75 ppm. EI-HRMS [M-] calcd for C$_{19}$H$_{17}$NO$_3$: 307.1213, found 307.1211.

11
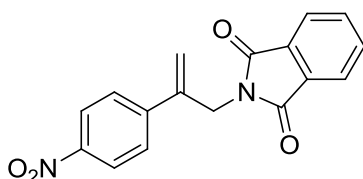
2-[2-(4-nitrophenyl)prop-2-en-1-yl]-1H-isoindole-1,3(2H)-dione, 11: The isolated yield was 13 % of a dark yellow powder; purity = 30 % by NMR. ^{1}H NMR (500 MHz, (CD$_3$)$_2$SO): δ = 8.22 (d, 2H), 7.89 (m, 2H), 7.85 (m, 2H), 7.81 (m, 2H), 5.71(s, 1H), 5.34 (s, 1H), 4.67 (s, 2H) ppm; ^{13}C NMR (125 MHz, (CD$_3$)$_2$SO): δ = 167.52, 146.96, 144.55, 140.51, 134.30, 131.44, 123.62, 123.25, 122.91, 117.07, 40.48 ppm; the carbon NMR peaks were determined using HSQC and HMBC. EI-HRMS [M+] calcd for C$_{17}$H$_{12}$N$_2$O$_4$:308.0791; found 308.0791.

2.2.3 – Preparation of α-(bromomethyl)styrene & derivatives
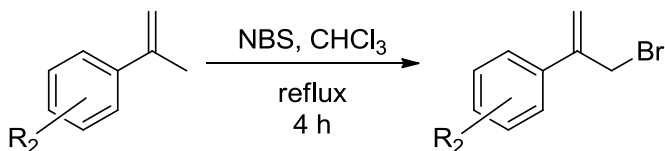
2.2.3.1 – Preparation of α-(bromomethyl)styrene

The synthesis of α-(bromomethyl)styrene, **12**, was adapted from the supporting information of Ohmura.[63] α-methylstyrene (25 mL, 192 mmol) was filtered through basic alumina to remove the inhibitor, p-*tert*-butylcatechol, and rinsed 3x with CHCl$_3$ (90 mL) into a round bottom flask. To the solution, N-bromosuccinimide (NBS, 39 g, 220 mmol) was added, the slurry was heated to reflux and a few drops of bromine were added. The reaction was monitored by GC-MS until completion, approximately 18 h. The reaction was cooled to room temperature and then the insoluble succinimide was removed by filtration. The filtrate was concentrated under reduced pressure and purified by column chromatography on silica gel with 15 % chloroform in hexane. The collected fractions containing product were combined and the solvent was removed by rotary evaporation to yield the pure product.

2.2.3.2 – Analytical data for α-(bromomethyl)styrene
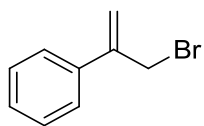
α-(bromomethyl)styrene, 12: The isolated yield was 65 %; clear colourless oil. The ^{1}H and ^{13}C NMR spectra matched those reported in the literature.[64] ^{1}H NMR (400 MHz, CDCl$_3$): δ = 7.52-7.50 (m, 2H), 7.42-7.33 (m, 3H), 5.58 (s, 1H), 5.51 (s, 1H), 4.40 (s, 2H) ppm; ^{13}C NMR (100 MHz, CDCl$_3$): δ = 144.24, 137.58, 128.49, 128.26, 126.08, 177.19, 34.18 ppm.

2.2.3.3 – Preparation of 2-(3-bromoprop-1-en-2-yl)naphthalene

The synthesis of 2-(3-bromoprop-1-en-2-yl)naphthalene, **13**, was adapted from the supporting information of Tripathi *et al.*[65] Under inert conditions, 2-(propen-2-yl)naphthalene (4.14 g, 24.6 mmol) was added to a schlenk rbf, where dry THF (100 mL) was cannula'd in to dissolve the starting material. To the solution, N-bromosuccinimide (NBS, 4.642 g, 26.1 mmol) and p-toluenesulfonic acid (TsOH, 0.474 g, 2.5 mmol) was added, the reaction mixture was heated to a vigorous reflux (100 °C) for *ca.* 4 h. The reaction was cooled to room temperature and then petroleum ether (50-100 mL) was added. The organic was collected and washed 3 x 100 mL of H$_2$O. The organic was then collected, dried with NaSO$_4$, filtered and concentrated under reduced pressure. Purification was done by column chromatography on silica gel using 100 % petroleum ether.
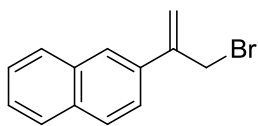
2-(3-bromoprop-1-en-2-yl)naphthalene, 13: The isolated yield was 56 %; clear yellow oil. ^{1}H NMR (400 MHz, CDCl$_3$): δ = 7.96 (s, 1H), 7.89-7.83 (m, 3H), 7.65-7.63 (m, 1H), 7.53-7.48 (m, 2H), 5.72 (s, 1H), 5.61 (s, 1H), 4.51 (s, 1H) ppm; ^{13}C NMR (100 MHz, CDCl$_3$): δ = 144.16, 134.79, 133.30, 133.17, 128.41, 128.22, 127.63, 126.41, 126.36, 125.29, 124.07, 117.66, 34.23 ppm; EI-HRMS [M$^-$] calcd for C$_{13}$H$_{11}$Br (Isotope 79): 246.0049, found 246.0044.

2.2.3.4 – Preparation of 2-bromo-1-(4-ethoxyphenyl)ethanone

The synthesis of 2-bromo-1-(4-ethoxyphenyl)ethanone, **14**, was adapted from the methods of Tripathi *et al.* [65] and Mohan Reddy *et al.*[66] To a round bottom flask equipped with a magnetic stir bar, 4'-ethoxyacetophenone (5.28 g, 32.1 mmol), *p*-toluenesulfonic acid (0.1 mol equivalents, 0.614 g, 3.21 mmol) and *ca.* 1/6th of the needed n-bromosuccinimide, NBS, (1.05 mol equivalents, 6.01 g, 33.7 mmol) was added. Methanol, 100 mL, was then added and the reaction was refluxed at 65 °C for 3 h. Each addition of NBS, a total of 6 additions, was added every 25-30 minutes. The methanol was removed by rotatory evaporation. Then to the product aqueous sodium thiosulfate was added, *ca.* 100 mL, and the product was extracted using CH$_2$Cl$_2$, 3 x 50 mL. The organic layers were collected and washed 3 x 100 mL with H$_2$O. The organic was then collected,

dried with Na_2SO_4, filtered and concentrated under reduced pressure. Purification was done by column chromatography on silica gel using 100 % CH_2Cl_2. The collected fractions containing product were combined and concentrated by rotary evaporation to yield the product.
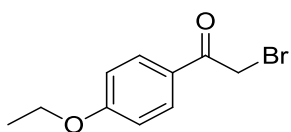
2-bromo-1-(4-ethoxyphenyl)ethanone, 14: The isolated yield was 88 %; white solid. ^{1}H NMR (400 MHz, CDCl$_3$): δ = 7.97 (d, 2H), 6.95 (d, 2H), 4.41 (s, 2H), 4.13 (q, 2H), 1.46 (t, 3H) ppm; ^{13}C NMR (100 MHz, CDCl$_3$): δ = 189.89, 163.56, 131.32, 126.69, 114.45, 63.87, 30.69, 14.60 ppm; EI-HRMS [M-] calcd for $C_{10}H_{11}BrO_2$ (Isotope 79): 241.9947, found 241.9949.

2.2.3.5 – Preparation of 2-[4-(trifluoromethyl)phenyl]prop-2-en-1-ol

The synthesis of 2-[4-(trifluoromethyl)phenyl]prop-2-en-1-ol, **15**, was adapted from the methods of Garzan *et al.*[67] and Duan *et al.*[68] To a round bottom flask equipped with a magnetic stir bar, Mg$_{(s)}$ (0.868 g, 35.7 mmol) was added and then the system was flame-dried and placed under inert conditions. Drisolv® diethyl ether, 64 mL, was added and then the system was cooled to 0 °C using an ice bath. The aryl bromide, 4-bromobenzotrifluoride (5.0 mL, 8.035 g, 35.7 mmol), was added slowly in a drop-wise fashion; once the addition was completed the reaction mixture was refluxed for 2.25 h, until all the magnesium

chunks visibly disappeared. The reaction was then cooled to room temperature, where copper (I) iodide (0.15 equivalents, 0.408 g, 2.14 mmol) was added and left to stir for 0.5 -0.75 h, until the solid copper (I) iodide was gone. Propargyl alcohol (0.4 equivalents, 0.83 mL, 0.801 g, 14.3 mmol) in 20 mL Drisolv® diethyl ether was then added slowly in a drop-wise manner to the solution. Once the addition was done the reaction was heated to reflux for 24 h. After cooling to room temperature, the solution was quenched using saturated $NH_4Cl_{(aq)}$ solution which was slowly added until the solution stopped reacting. The organic phase was separated from the aqueous phase, which was further extracted using diethyl ether (4-6 x 50-75 mL) until the aqueous phase went from brown to blue. The collected organic fractions were combined, washed with brine, and dried using anhydrous $MgSO_4$. The solvent was removed by rotary evaporation and the product purified by column chromatography using 10 % ethyl acetate in hexanes and slowly increasing the eluent to 15 % ethyl acetate in hexanes.

15
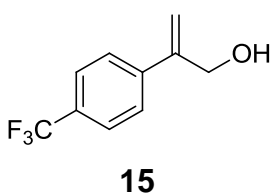
2-[4-(trifluoromethyl)phenyl]prop-2-en-1-ol, **15**: The isolated yield was 98 %; reddish orange oil . The ^{1}H and ^{13}C NMR spectra matched literature.[67] ^{1}H NMR (400 MHz, CDCl3): δ = 7.61 (d, 2H), 7.55 (d, 2H), 5.55 (s, 1H), 5.56 (d, 1H), 4.54 (s, 2H), 2.07 ppm (broad s, 1H); ^{13}C NMR (100 MHz, CDCl3): δ = 146.11, 142.08, 129.84 (q, J = 32.65 Hz), 126.37, 125.37 (q, J = 3.67 Hz), 124.10 (q, J = 271.8), 114.72, 64.69 ppm.

2.2.3.6 – Preparation of 1-(3-bromoprop-1-en-2-yl)-4-(trifluoromethyl)benzene

The synthesis of 1-(3-bromoprop-1-en-2-yl)-4-(trifluoromethyl)benzene, **16**, was adapted from the methods of Garzan *et al.*[67] and Baumgartner *et al.*[69] To a flame dried round bottom flask equipped with a magnetic stir bar, a solution of **15** (8.05 g, 39.8 mmol) in Drisolv® DCM, 75 mL, was prepared and cooled to 0 °C using an ice bath. Triphenylphosphine (1.2 equivalents, 12.5 g, 47.8 mmol) was first added and then CBr_4 (1.1 equivalents, 14.5 g, 43.8 mmol) was added slowly to the reaction mixture. The mixture was stirred at 0 °C for 1.25 h; the reaction was checked by GC-MS for completion. The solvent was removed by reduced pressure and the crude product was purified by column chromatography using 10 % ethyl acetate in hexane as the eluent.
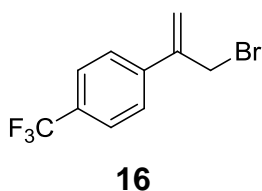
1-(3-bromoprop-1-en-2-yl)-4-(trifluoromethyl)benzene, 16: The isolated yield was 98 %; clear yellow liquid . The ^{1}H and ^{13}C NMR spectra matched literature.[67] ^{1}H NMR (400 MHz, CDCl$_3$): δ = 7.65 (d, 2H), 7.61 (d, 2H), 5.63 (s, 1H), 5.61 (s, 1H), 4.39 (s, 2H) ppm; ^{13}C NMR (100 MHz, CDCl$_3$): δ = 143.21, 141.15, 130.14 (q, J = 32.65 Hz), 126.45, 125.43 (q, J = 3.67 Hz), 124.06 (q, J = 271.8 Hz), 118.93, 33.41 ppm.

2.2.4 – Preparation of 2-phenyl-3-phthalimidopropene and derivatives by gabriel synthesis
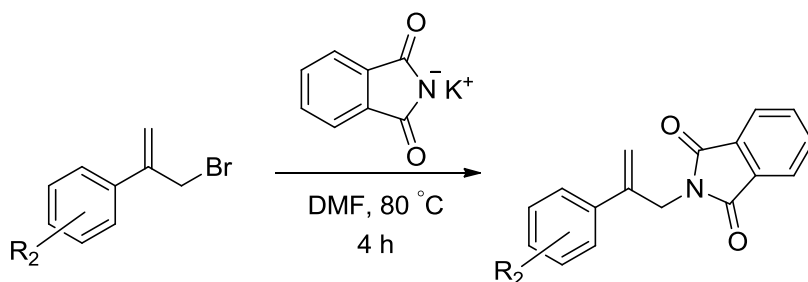
2.2.4.1 – Preparation of 2-phenyl-3-phthalimidopropene and derivatives by gabriel synthesis

The synthesis of 2-phenyl-3-phthalimidopropene and derivatives followed the synthesis by Dumas[70] with a slight variation. To a solution of α-(bromomethyl)styrene, **12**, (24.61 g, 124.9 mmol) dissolved in 100 mL of DMF, potassium phthalimide (1.11 equivalents, 25.71 g, 138.8 mmol) was added. The reaction mixture was heated to 82-83 °C and monitored by GC-MS until completion, *ca.* 1-19 h. Once the reaction had come to completion, the hot solution was poured onto ice and light yellow precipitate formed. The precipitate was collected by vacuum filtration and recrystallized using hot ethanol. White crystalline shards were collected by vacuum filtration and left to dry under vacuum for an hour.

2.2.4.2 – Analytical data for 2-phenyl-3-phthalimidopropene and derivative
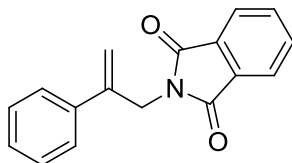
2-phenyl-3-phthalimidopropene, 17: Reaction time: 19 hours. The isolated yield was 87 %; white crystals. The ^{1}H and ^{13}C NMR spectra matched those reported in the literature.[71,72] ^{1}H NMR (400 MHz, CDCl$_3$): δ = 7.86-7.85 (m, 2H), 7.73-7.71 (m, 2H), 7.51 (d, 2H), 7.35 (t, 2H), 7.31-7.29 (m, 1H), 5.45 (s, 1H), 5.17 (s, 1H), 4.72(s 2H) ppm; ^{13}C NMR (100 MHz, CDCl$_3$): δ = 167.94, 142.41, 138.51, 133.99, 132.01, 128.39, 128.03, 126.38, 123.55, 113.87, 41.44 ppm.
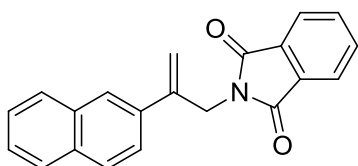
2-[2-(naphthalen-2-yl)prop-2-en-1-yl]-1*H*-isoind-ole-1,3(2*H*)-dione, 18: Reaction time: 3 hours. The isolated yield was 76 %; white fine crystalline shards. ^{1}H NMR (500 MHz, CDCl$_3$): δ = 7.97 (s, 1H), 7.87-7.80 (m, 5H), 7.71-7.69 (m, 2H), 7.66 (dd, 1H), 7.50-7.45 (m, 2H), 5.61 (s, 1H), 5.30 (s, 1H), 4.85 (s, 2H) ppm; ^{13}C NMR (125 MHz, CDCl$_3$): δ = 167.98, 142.24, 135.65, 133.98, 133.20, 132.99, 131.98, 128.30, 127.98, 127.50, 126.22, 126.11, 125.26, 124.56, 123.35, 144.59, 41.50 ppm; EI-HRMS [M⁻] calcd for C$_{21}$H$_{15}$NO$_2$: 313.1108, found 313.1109.

2.2.4.3 – Analytical data for 2-[2-(4-ethoxyphenyl)-2-oxoethyl]-1H-isoindole-1,3(2H)-dione

19
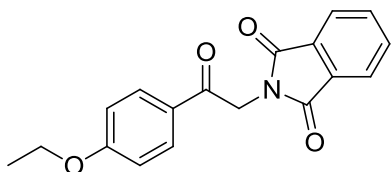
2-[2-(4-ethoxyphenyl)-2-oxoethyl]-1*H*-isoind-ole-1,3(2*H*)-dione, 19: Reaction time: 1 hours. The isolated yield was 70 %; white crystalline shards. ^{1}H NMR (500 MHz, CDCl$_3$): δ = 7.98 (d, 2H), 7.90-7.88 (m, 2H), 7.75-7.74 (m, 2H), 6.96 (d, 2H), 5.09 (s, 2H), 4.12 (q, 2H), 1.45 (t, 3H) ppm; ^{13}C NMR (125 MHz, CDCl$_3$): δ = 189.26, 167.93, 163.57, 134.01, 132.25, 130.41, 127.22, 123.45, 114.45, 63.83, 43.82, 14.58 ppm; EI-HRMS [M-] calcd for C$_{18}$H$_{15}$NO$_4$: 309.1007, found 309.1008.

20
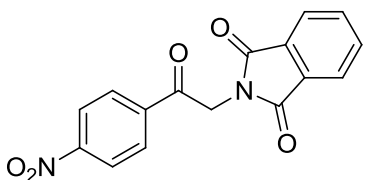
2-[2-(4-nitrophenyl)-2-oxoethyl]-1*H*-isoindole-1,3(2*H*)-dione, 20: Reaction time: 2 hours. The isolated yield was 24 %; extracted from the DMF:H$_2$O using ethyl acetate and recrystallized using hot THF, a orange solid was obtained. ^{1}H NMR (400 MHz, (CD$_3$)$_2$SO): δ = 8.39 (d, 2H), 8.34 (d, 2H), 7.94 (m, 4H), 5.35 (s, 2H) ppm; ^{13}C NMR (100 MHz, (CD$_3$)$_2$SO): δ = 192.08, 167.38, 150.52, 168.46, 134.87, 131.47, 129.83, 124.01, 123.44, 44.87 ppm; EI-HRMS [M-] calcd for C$_{16}$H$_{10}$N$_2$O$_5$: 310.0595, found 310.0596.
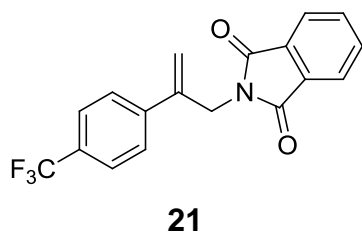
2-{2-[4-(trifluoromethyl)phenyl]prop-2-en-1-yl}-1H-isoindole-1,3(2H)-dione, 21: Reaction time: 0.5 hour. The isolated yield was 70 %; recrystallized using hot 95 % ethanol, white crystals were obtained. The ^{1}H and ^{13}C NMR matched literature.[67]

^{1}H NMR (400 MHz, CDCl$_3$): δ = 7.86 (m, 2H), 7.73 (m, 2H), 7.61 (m, 4H), 5.53 (s, 1H), 5.33 (s, 1H), 4.72 (s, 2H) ppm; ^{13}C NMR (100 MHz, CDCl$_3$): δ = 167.80, 141.97, 141.50, 134.05, 131.83, 129.94 (q, J = 32.6 Hz), 126.71, 125.32 (q, J = 3.67 Hz), 124.01 (q, J = 271.8 Hz), 123.35, 116.31, 41.17 ppm; EI-HRMS [M-] calcd for C$_{18}$H$_{12}$F$_3$NO$_2$: 331.0826, found 331.0828.

2.2.4.4 – Preparation of 2-phenylprop-2-en-1-amine and allylamine derivatives by deprotection
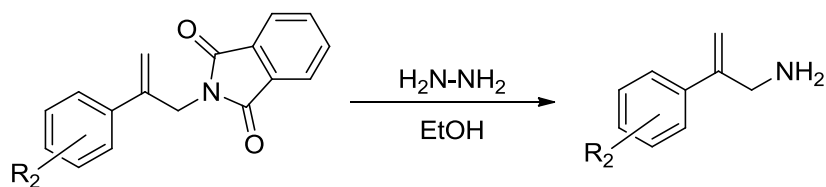
Modified from the preparation of Dumas,[70] to a slurry of 2-phenyl-3-pthalimidopropene, **17**, (24.71 g, 93.85 mmol) in 200 mL of ethanol was slowly added hydrazine hydrate (2 mol equivalence, 50-60 % solution, 14 mL) to the mixture at room temperature. The reaction mixture was placed in a hot oil bath

heated to 80 - 87 °C. The white solid in the slurry dissolved and the reaction mixture became a clear yellow solution. The resulting solution was refluxed for *ca.* 30 minutes and then cooled to room temperature. As the reaction cooled, white precipitate formed. Once cooled, 350 mL of 1 N HCl was added to the slurry and refluxed until the solution became clear or for *ca.* 5 minutes if the precipitate never re-dissolved. The reaction mixture was then cooled, and 2,3-dihydro-1,4-phthalazinedione precipitated and was removed by filtration and washed with a copious amount of H_2O. The filtrate was collected and the amine salt was obtained by rotary evaporation. The salt was purified by recrystallization in 2-propanol. The crystals were collected by vacuum filtration, re-dissolved in H_2O, and base treated with a concentrated solution of NaOH. Once the aqueous solution obtained a high pH, the 2-phenylprop-2-en-1-amine was extracted with *ca.* 200 mL $CHCl_3$, the combined organic fractions were dried with $MgSO_4$ and concentrated by rotary evaporation.

The reaction time varied depending on the size of the reaction, mg to g, and for the other substrates.

2.2.4.5 – Analytical data for 2-phenylprop-2-en-1-amine and its unsaturated allylamine derivatives
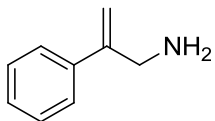
2-phenylprop-2-en-1-amine, 22: The isolated yield was 86 %; clear and colorless liquid. The ^{1}H and ^{13}C NMR spectra matched those reported in the literature.[67] ^{1}H NMR (400 MHz, CDCl$_3$): δ = 7.43 (d, 2H), 7.36, (t, 2H), 7.30 (m, 1H), 5.36 (s, 1H), 5.24 (s, 1H), 3.73 (s, 2H), 1.28 (s, 2H, NH) ppm; ^{13}C NMR (100 MHz, CDCl$_3$): δ = 149.73, 139.71, 128.39, 127.59, 126.04, 111.12, 46.06 ppm.
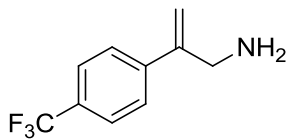
2-[4-(trifluoromethyl)phenyl]prop-2-en-1-amine, 23: The isolated yield was 35 %; clear colorless oil. ^{1}H NMR (500 MHz, CDCl$_3$): δ =7.61 (d, 2H), 7.53 (d, 2H), 5.44 (s, 1H), 5.36 (s, 1H), 3.75 (s, 2H), 1.31 (s, 2H, NH) ppm; ^{13}C NMR (100 MHz, CDCl$_3$): δ = 148.5, 143.4 (q, J = 1.2 Hz), 129.53 (q, J = 32.6 Hz), 126.34, 125.27 (q, J = 3.67 Hz), 124.08 (q, J = 271.8 Hz), 113.13, 45.83 ppm; the carbon NMR peaks were determined using Heteronuclear Single Quantum Coherence, HSQC, spectroscopy and Heteronuclear Multiple-bond Correlation, HMBC, spectroscopy. EI-HRMS [M+] calcd for C$_{10}$H$_{10}$F$_3$N: 201.0760, found 201.0761.
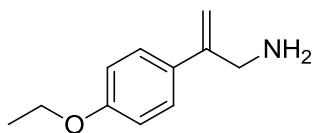
2-(4-ethoxyphenyl)prop-2-en-1-amine, 24: The isolated yield was 25 %; clear yellow oil. ^{1}H NMR (400 MHz, CDCl$_3$): δ = 7.37 (d, 2H), 6.90 (d, 2H), 5.30 (s, 1H), 5.16 (s, 1H), 4.07 (q, 2H), 3.71 (s, 2H), 1.44 (t, 3H), 1.49 (br. s, 2H, NH) ppm; ^{13}C NMR (100 MHz, CDCl$_3$): δ = 158.58, 148.94, 131.82, 127.09, 114.35, 109.60, 63.38, 46.05, 14.77 ppm; EI-HRMS [M-] calcd for C$_{11}$H$_{15}$NO: 177.1159, found 177.1159.
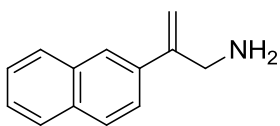
2-(naphthalen-2-yl)prop-2-en-1-amine, 25: The isolated yield was 76 %; whitish yellow solid. ^{1}H NMR (400 MHz, CDCl$_3$): δ = 7.86-7.82 (m, 4H), 7.60 (dd, 1H), 7.52-7.46 (m, 2H), 5.52 (s, 1H), 5.35 (s, 1H), 3.85 (s, 2H), 1.35 (br. s, 2H) ppm; ^{13}C NMR (100 MHz, CDCl$_3$): δ = 149.58, 136.95, 133.36, 132.89, 128.12, 128.05, 127.52, 126.19, 125.93, 124.65, 124.56, 111.80, 46.18 ppm; EI-HRMS [M-] calcd for C$_{13}$H$_{13}$N: 183.1053, found 183.1051.

2.3 – Hydrogenation procedures

2.3.1 – Non-enantioselective hydrogenation procedure

The unsaturated carboxylic acids, ketoacids, and allylamines were first hydrogenated with achiral catalysts in order to generate samples of the racemates for the development of instrumental methods capable of analyzing the mixture.

The non-enantioselective hydrogenations were developed from a procedure by Sajiki and Hirota.[73] The procedure below is the same for all substrates: phenylalkenoic acids, benzoylalkenoic acids and allylamines. Benzoylalkenoic acids were purified by recrystallization from hot ethyl ether before use. The heterogeneous catalyst, Pd(5%)/BaCO$_3$, was used for the hydrogenation of the unsaturated carboxylic acids in 1,4-dioxane at room temperature, whereas, Pd(20%)/vulcanized carbon or Pt(40%)/graphitized carbon were used for the hydrogenation of the ketoacids in THF at 50 °C. For the hydrogenation of the allylamines, Pd(5%)/CaCO$_3$ was used. The hydrogenation of 4-phenyl-4-pentenoic acid, 2, is presented below and can be regarded as a general protocol for the procedure regardless of minor changes in terms of the choice of catalyst, solvent and temperature for the different types of substrates.

To a test tube, equipped with a magnetic stir bar, 4-phenyl-4-pentenoic acid (10 mg, 0.06 mmol) and catalyst (0.5 wt % of the weight of the substrate, 2.1 mg) was added. The test tube was sealed with a rubber septum and then evacuated. Dioxane (1 mL) was added and then hydrogen was added via a syringe needle from a hydrogen-filled rubber balloon (1 atm). The reaction mixture was stirred at room temperature for 5-6 h. When the reaction had come to completion, the catalyst was removed by filtration through a diatomaceous earth plug, after which the product was isolated at reduced pressure by rotary evaporation.

2.3.2 – Asymmetric hydrogenation procedures

2.3.2.1 – Asymmetric hydrogenation procedure for phenylalkenoic acids and benzoylalkenoic acids

The following procedure was used to asymmetrically hydrogenate the phenylalkenoic acids and benzoylalkenoic acids. The benzoylalkenoic acids were purified by recrystallization from hot ethyl ether before use. The hydrogenation of atropic acid, **1**, with diaceto[(R)-(+)-2,2'-bis(diphenylphosphino)-1,1'-binapthyl]ruthenium(II) is presented below and can be regarded as a general procedure for the reaction.

In a 160 mL stainless steel autoclave, containing up to a dozen 1 dram glass vials, each containing a magnetic stir bar, atropic acid, 1, (10 mg, 0.1 mmol) and a catalyst, diaceto[(R)-(+)-2,2'-bis(diphenylphosphino)-1,1'-binapthyl]ruthenium(II) (1 mg, 0.0012 mmol) was added under a nitrogen atmosphere. Dry methanol (2 mL) was added to each vial and the autoclave was sealed. The vessel was flushed 3 times with hydrogen gas, pressurized to 100 bar H_2 gas, and stirred for 12-24 h at room temperature. Upon depressurization, a bright yellow solution was obtained, which was filtered through diatomaceous earth and an HPLC filter. The filtrate was concentrated by rotary evaporation. Characterization, conversion and enantiomeric excess were determined by GC-FID, HPLC and/or ^{1}H-NMR spectroscopy.

2.3.2.2 - Analytical data for phenylalkanoic and benzoylalkanoic acids

26
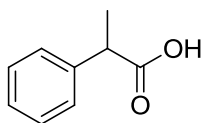
2-phenylpropanoic acid, 26: The NMR yield was > 95 % of a clear oil. The ^{1}H and ^{13}C NMR spectra matched those of the commercially available compound and those reported in the literature.[74] ^{1}H NMR (400 MHz, CDCl$_3$): δ = 7.38-7.28 (m, 5H), 3.77 (q, J = 7.2 Hz, 1H), 1.54 (d, J = 7.2 Hz, 3H) ppm; ^{13}C NMR (100 MHz, CDCl$_3$): δ = 181.14, 139.70, 128.64, 127.57, 127.35, 45.36, 18.02 ppm.
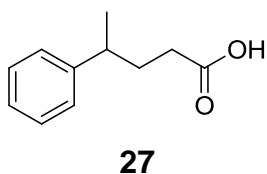
4-phenylpentanoic acid, 27: The NMR yield was > 95 % of a clear oil. The ^{1}H NMR spectrum matched that reported in the literature.[75,76] ^{1}H NMR (400 MHz, CDCl$_3$): δ = 10.14 (broad s, 1H), 7.30 (t, 2H), 7.22-7.17 (m, 3H), 2.74 (q, 1H), 2.23 (t, 2H), 1.92 (q, 2H), 1.28 (d, 3H) ppm; ^{13}C NMR (100 MHz, CDCl$_3$): δ = 179.65, 146.10, 128.48, 126.99, 126.25, 39.31, 33.01, 32.44, 22.13 ppm.
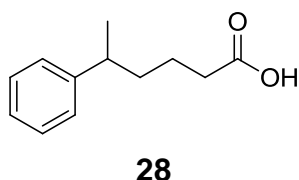
5-phenylhexanoic acid, 28: The NMR yield was > 95 % of a clear oil. The ^{1}H NMR spectrum matched that reported in the literature.[77] ^{1}H NMR (400 MHz, CDCl$_3$): δ = 7.30 (t, 2H), 7.20 (t, 3H), 2.70 (q, 1H), 2.32 (t, 2H), 1.65-1.49 (m, m, 4H) 1.26 (d, 3H) ppm; ^{13}C NMR (100 MHz, CDCl$_3$): δ = 178.96, 146.70, 128.49, 126.60, 126.05, 39.72, 37.00, 33.40, 22.84, 22.28 ppm.
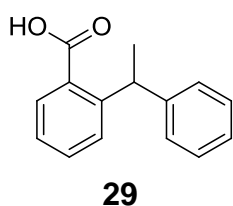
2-(1-phenylethyl)benzoic acid, 29: The NMR yield was > 95 % of a clear oil. The ^{1}H and ^{13}C NMR spectra matched those reported in the literature.[60] ^{1}H NMR (500 MHz, CDCl$_3$): δ = 7.96 (d, 1H), 7.49-7.44 (m, 1H), 7.29-7.25 (m, 6H), 7.20-7.17 (m, 1H), 5.32 (q, 1H), 1.66 (d, 3H) ppm; ^{13}C NMR (125 MHz, CDCl$_3$): δ = 172.81, 148.60, 145.90, 132.51, 130.85, 128.80, 128.68, 128.17, 127.93, 125.89, 125.82, 39.54, 21.96 ppm.
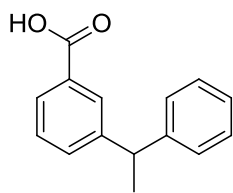
3-(1-phenylethyl)benzoic acid, 30: The NMR yield was > 95 % of a clear oil. ^{1}H NMR (500 MHz, CDCl$_3$): δ = 8.04 (s, 1H), 7.96 (d, J = 7.57 Hz, 1H), 7.47 (d, J = 7.57 Hz, 1H), 7.39 (t, J = 7.72 Hz, 1H), 7.33-7.30 (m, 2H), 7.25-.7.20 (m, 3H), 4.24 (q, J = 7.25 Hz, 1H), 1.69 (d, J = 7.25, 3H) ppm; ^{13}C NMR (100 MHz, CDCl$_3$): δ = 172.02, 146.87, 145.59, 133.20, 129.48, 129.17, 128.55, 128.50, 128.01, 127.55, 126.28, 44.60, 21.71 ppm. EI-HRMS [M-] calcd for C$_{15}$H$_{14}$O$_2$: 226.0999, found 226.0999.
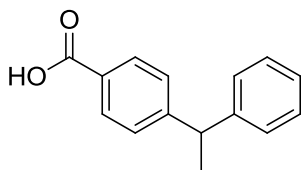
4-(1-phenylethyl)benzoic acid, 31: The NMR yield was > 95 % of a clear oil. ^{1}H NMR (500 MHz, CDCl$_3$): δ = 8.04 (d, J = 8.20 Hz, 2H), 7.34-7.30 (m, 4H), 7.23-7.21 (m, 3H) 4.23 (q, 1H), 1.68 (d, 3H) ppm; ^{13}C NMR (100 MHz, CDCl$_3$): δ = 171.63, 152.58, 145.32, 130.38, 128.55, 127.78, 127.62, 127.42, 126.39, 44.90, 21.57 ppm. EI-HRMS [M+] calcd for C$_{15}$H$_{14}$O$_2$: 226.0988, found 226.0989.
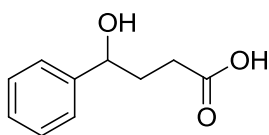
4-hydroxy-4-phenylbutanoic acid, **32**: The NMR yield was > 95 % of a clear oil. The ^{1}H NMR spectrum matched that reported in the literature.[78] ^{1}H NMR (400 MHz, CDCl$_3$): δ = 7.36 (d, 4H), 7.33-7.29 (m, 1H), 4.80 (t, 1H), 2.51 (t, 2H),

2.10 (q, 2H) ppm; ^{13}C NMR (100 MHz, CDCl$_3$): δ = 178.33, 143.78, 128.59, 127.81, 125.72, 73.51, 33.50, 30.22 ppm.

33
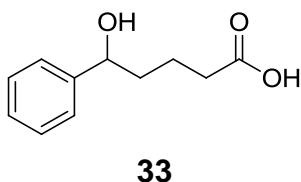
5-hydroxy-5-phenylpentanoic acid, 33: The NMR yield was 85 % of a clear oil. The ^{1}H NMR spectrum matched that reported in the literature.[79] ^{1}H NMR (400 MHz, CDCl$_3$): δ = 7.38-7.28 (m, 5H), 4.70 (t, 1H), 2.39 (t, 2H), 1.87-1.64 (m, m, 4H) ppm; ^{13}C NMR (100 MHz, CDCl$_3$): δ = 178.95, 144.30, 128.52, 127.66, 125.80, 74.15, 38.14, 33.67, 20.96 ppm.

2.3.2.3 – Asymmetric hydrogenation procedure for unsaturated allylamines

The following procedure was used to asymmetrically hydrogenate unsaturated allylamines. The study was completed with a variety of solvents (MeOH, IPA, and THF) with or without a non-chiral or chiral base (DBU, DMCA, DIPEA, (+)-cinchonine, (-)-cinchonidine, (+)-bis[(R)-1-phenylethyl]amine, and (-)-bis[(S)-1-phenylethyl]amine) with and without the presence of CO$_2$, and with multiple catalysts. The hydrogenation presented below of 2-phenylprop-2-en-1-amine, **22**, with (-)-4,5-bis[(2R,5R)-2,5-dimethylphospholanyl](1,2-dimethyl-1,2-dihydropyridazine-3,6-dione)(1,5-cyclooctadiene)rhodium(I) tetrafluoroborate can be regarded as a general procedure for the asymmetric hydrogenation study of prochiral unsaturated allylamines.

Stock solutions of the unsaturated allylamines, catalyst, and the optional base, were prepared in dry methanol the same day to ensure no decomposition of the chemicals occurred. In a 160 mL stainless steel autoclave, containing up to a dozen 1 dram glass vials, each containing a magnetic stir bar, 2-phenylprop-2-en-1-amine, **22**, (10 mg, 0.075 mmol), catalyst, (-)-4,5-bis[(2R,5R)-2,5-dimethylphospholanyl](1,2-dimethyl-1,2-dihydropyridazine-3,6-dione)(1,5-cyclooctadiene)rhodium(I) tetrafluoroborate, (1 mg, 0.0015 mmol) and, if desired, the optional base (*ca.* 0.075 mmol) was added under a nitrogen atmosphere. Additional dry methanol was added to each vial to obtain a total volume of 2 mL and then the autoclave was sealed. The vessel was flushed 3 times with hydrogen gas or carbon dioxide gas, and pressurized to either 100 bar H_2 gas, or if the presence of CO_2 is desired, 10 bar CO_2 gas and 90 bar H_2 gas and stirred for 6-12 h at room temperature. Once the reaction time was complete the autoclave was slowly depressurized, the solutions were filtered through diatomaceous earth, and concentrated by rotary evaporation. Enantiomer excess was determined by HPLC and yield was determined by ^{1}H-NMR spectroscopy using an internal standard, 1,3,5-trimethoxybenzene.

2.3.2.4 - Analytical data for phenylalkylamines
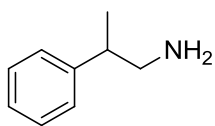
2-phenylpropan-1-amine, 34: The NMR yield was > 95 % of a yellow oil. The ^{1}H and ^{13}C NMR spectra matched the commercially available compound and those reported in the literature.[80] ^{1}H NMR (400 MHz, CDCl$_3$): δ = 7.35-7.31 (m, 2H), 7.24-7.21(m, 3H), 2.86 (d, J = 7.05 Hz, 2H), 2.76 (sextet, J = 6.92, 1 H), 1.27 (d, J = 6.8, 3H), 1.07 (br. s, 2H) ppm; ^{13}C NMR (100 MHz, CDCl$_3$): δ = 144.85, 128.28, 127.12, 126.09, 49.35, 43.36, 19.04 ppm.
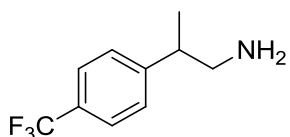
2-[4-(trifluoromethyl)phenyl]propan-1-amine, 35: The NMR yield was > 95 % of a yellow oil. ^{1}H NMR (500 MHz, CDCl$_3$): δ = 7.56 (d, J = 8 Hz, 2H), 7.32 (d, J = 8 Hz, 3H), 2.89 (dd, J = 12.1, 2.8 Hz, 1H), 2.85 (dd, J = 12.1, 2.4 Hz, 1H), 2.82 (sxt, J = 6.8 Hz, 1H), 1.26 (overlapping peaks, CH$_3$ = d, J = 6.6 Hz, NH$_2$ = br. s, 5H) ppm; ^{13}C NMR (125 MHz, CDCl$_3$): δ = 149.23, 128.61 (q, J = 32.1 Hz), 127.62, 125.36 (q, J = 3.8 Hz), 124.22 (q, J = 271.6 Hz), 49.17, 43.37, 18.95 ppm; ESI-HRMS [M+H]+ calcd for C$_{10}$H$_{13}$F$_3$N: 204.09946, found 204.09888.
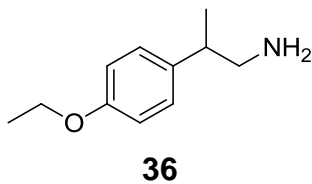
2-(4-ethoxyphenyl)propan-1-amine, 36: The NMR yield was > 95 % of a yellow oil. ^{1}H NMR (500 MHz, CDCl$_3$): δ = 7.12 (d, J = 8.5 Hz, 2H), 6.87 (d, J = 8.5 Hz, 2H), 4.03 (q, J = 6.9 Hz, 2H), 2.84 (dd, J = 12.45, 6.2 Hz, 1H), 2.79 (dd, J = 12.45, 8.2 Hz, 1H), 2.70 (sxt, J = 5 x 6.8 Hz, 1H), 1.41 (t, J = 6.9 Hz, 3H), 1.34 (NH, br. s, 2H), 1.23 (d, J = 6.8 Hz, 3H) ppm; ^{13}C NMR (125 MHz, CDCl$_3$): δ = 157.47, 136.89, 128.18, 114.51, 63.40, 49.66, 12.68, 19.43, 14.89 ppm; ESI-HRMS [M+H]+ calcd for C$_{11}$H$_{18}$NO: 180.13829, found 180.13757.
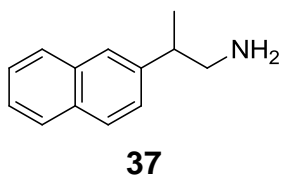
2-(naphthalene-2-yl)propan-1-amine, 37: The NMR yield was > 95 % of a yellow oil. ^{1}H NMR (500 MHz, CDCl$_3$): δ = 7.83-7.80 (m, 3H), 7.66 (s, 1H), 7.49-7.43 (m, 2H), 7.38 (dd, J = 8.5, 1.4 Hz, 1H), 2.97-2.90 (s, sxt, J = 8.35 Hz, 3H) 1.36 (overlapping peaks, CH$_3$ = d, NH$_2$ = br. s, 5H) ppm; ^{13}C NMR (125 MHz, CDCl$_3$): δ = 142.46, 133.57, 132.38, 128.22, 127.59, 127.56, 125.98, 125.88, 125.71, 125.33, 49.40, 43.73, 19.30 ppm; EI-HRMS [M-] calcd for C$_{13}$H$_{15}$N: 185.1209, found 185.1201.

2.3.3 – Analysis by gas chromatography with a flame ionization detector

The hydrogenated sample was filtered through diatomaceous earth and a 0.2 µm HPLC filter before it was used on the Clarus 680 chromatograph with a

Flame Ionization Detector (FID) from PerkinElmer. A CP-Chirasil-DEX CB chiral column, 25 m long, 0.25 μm thick, and with an internal diameter of 0.25 mm was used. The following methods, listed below, were used.

2.3.3.1 - Method 1 for gas chromatography analysis

The oven temperature started at 80 °C for 0 min and then temperature was increased at a rate of 5.0 °C/min up to 130 °C. Then the temperature continued to increase at a rate of 1.0 C/min up to 200 °C. Both the injector and detector temperature were held at 250 °C and helium was used as the carrier gas at a flow of 2 mL/min.

2.3.3.2 - Method 2 for gas chromatography analysis

The oven temperature started at 35 °C for 5.0 min and then temperature was increased at a rate of 1.0 °C/min up to 125 °C and held for 15 min. Then the temperature continued to increase at a rate of 10 °C/min up to 200 °C and held for 10 min. Both the injector and detector temperature were 250 °C and helium was used as the carrier gas at a flow of 1 mL/min.

2.3.3.3 - Method 3 for gas chromatography analysis

The oven temperature started at 30 °C for 0 min and then temperature was increased at a rate of 10.0 °C/min up to 190 °C and held for 10 min. Then the temperature continued to increase at a rate of 1.0 C/min up to 200 °C and again is held for 10 min. Both the injector and detector temperature were 250 °C and helium was used as the carrier gas at a flow of 1 mL/min.

2.3.4 – Analysis by gas chromatography with a mass spectrometry detector

As mentioned above, many reactions were monitored by GC-MS until completion had been reached. The reaction aliquot was diluted with HPLC MeOH and 1 µL was injected in the Clarus 660 chromatograph with a Clarus 600T Mass Spectrometer from PerlkinElmer. An Elite- 5MS column, 30 m long, 0.25 µm thick, with an internal diameter of 0.25 mm was used to analyze the sample. The oven temperature started at 100 °C for 0 min and then the temperature was increased at a rate of 20.0 °C/min up to 300 °C and held for 5 min. The injector was at 250 °C and the mass spectrometer was set with the inlet line at 200 °C and the source at 150 °C. The carrier gas was helium with a flow of 1 mL/min.

2.3.5 – Analysis by high pressure liquid chromatography

The hydrogenated samples were filtered through diatomaceous earth and a 0.2 μm HPLC filter before it was used on the Agilent technologies 1260 infinity HPLC equipped with either a Chiralpak OJ-H, AD-H or IA chiral columns (25 cm x 0.46 cm i.d.) from Daicel. The following methods, listed below, were used for the analysis of enantiomeric excess.

2.3.5.1 - Method 1 for HPLC analysis of phenylethylbenzoic acid substrates

The analysis of 2-(1-phenylethyl)benzoic acid, 3-(1-phenylethyl)benzoic acid, and 4-(1-phenylethyl)benzoic acid was done using the Chiralpak OJ-H chiral column (25 cm x 0.46 cm i.d.) from Daicel. The mobile phase was 97:3 n-hexane:*iso*-propanol with a flow of 0.4 mL/min.

2.3.5.2 - Method 2 for HPLC analysis of 2-phenylpropan-1-amine

The analysis of 2-phenylpropan-1-amine was done using a Chiralpak IA chiral column (25 cm x 0.46 cm i.d.) from Daicel. The mobile phase was 97:3 n-hexane:*iso*-propanol with an additive of 0.01 % ethylenediamine. The flow was 0.7 mL/min.

2.3.5.3 - Method 2 for HPLC analysis of 2-(naphthalene-2-yl)propan-1-amine, 2-(4-ethoxyphenyl)propan-1-amine, and 2-[4-trifluoromethyl)phenyl]propan-1-amine

The analysis of 2-(naphthalene-2-yl)propan-1-amine, 2-(4-ethoxyphenyl)propan-1-amine, and 2-[4-(trifluoromethyl)phenyl]propan-1-amine was done using a Chiralpak IA chiral column (25 cm x 0.46 cm i.d.) from Daicel. The mobile phase was 98.5-98.6 % n-hexane: 1.5-1.4 % *iso*-propanol with an additive of 0.01 % ethylenediamine. The flow was 0.6 mL/min.

Chapter 3 – Asymmetric Hydrogenation of Unsaturated Carboxylic Acids

The enantioselective reduction of C=C double bonds has been an important focus in asymmetric catalysis, which has played a significant role in drug design and development. Optically active compounds have been efficiently synthesized through the asymmetric hydrogenation of these functional groups, and after decades of research, we are still able to constantly improve the enantioselectivity of the homogeneous transition metal catalysts used today.[20,21,81,82]

One area of this field that has been extremely well studied is the enantioselective hydrogenation of functionalized olefins, i.e. C=C double bonds. These functionalized olefins usually have a polar moiety, in our case a carboxylic acid, which can easily coordinate to the metal-center of the catalyst. Furthermore, this metal ligation of the carboxylic acid helps with the efficiency of the catalyst to enantioselectively hydrogenate the olefin with high conversions and high enantiomeric excess.[21,22,83] These chiral products obtained from the asymmetric hydrogenation of unsaturated carboxylic acids are found in many pharmaceuticals and natural products (Figure 3.1).
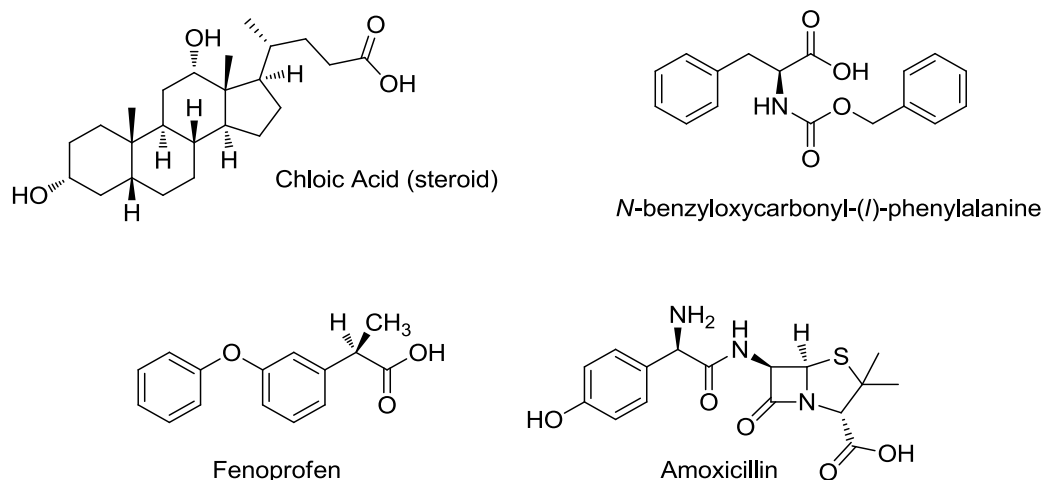
Figure 3.1. Natural and synthetic chiral pharmaceuticals with carboxylic acid functionalities.[24,187]

Ruthenium and rhodium catalysts have been well-studied and commonly used for the hydrogenation of α,β- and β,γ-unsaturated carboxylic acids.[20,21,84–86] Many pharmaceuticals and intermediates of pharmaceuticals were obtained with good enantioselectivities through the hydrogenation of α,β-unsaturated acid moieties utilizing many variations of these types of catalysts. Particular examples consist of the preparation of two anti-inflammatory drugs that are used in the treatment of headaches and arthritis: (S)-naproxen and (S)-ibuprofen (Scheme 3.1). These two pharmaceuticals were obtained through the asymmetric hydrogenation of an α,β-unsaturated acid with a ruthenium (II) binap catalyst.[20,21,45,87–89]
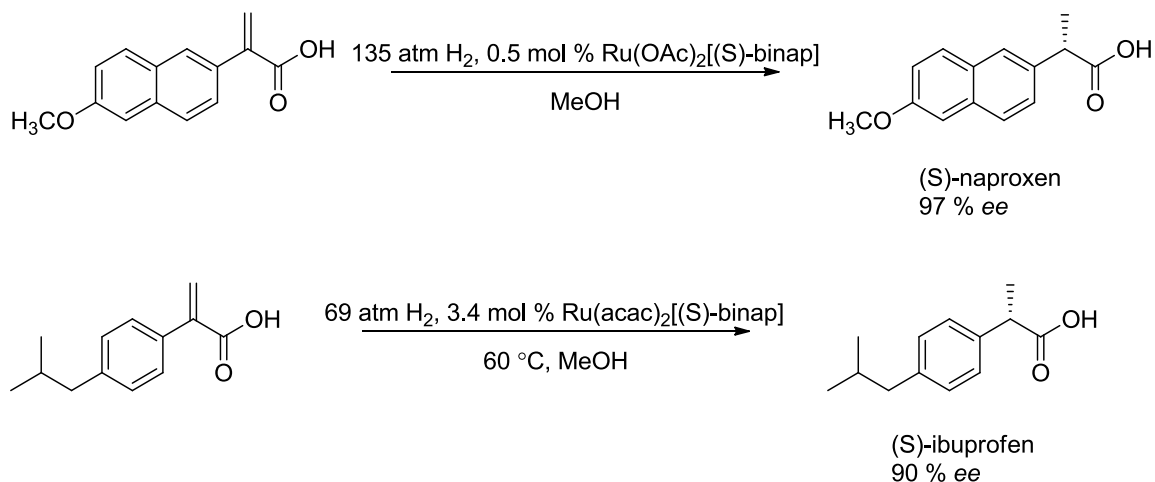
Scheme 3.1. Asymmetric hydrogenation examples utilizing Ru(OAc)$_2$[(S)-binap] and Ru(acac)$_2$[(S)-binap] for the synthesis of two pharmaceutical compounds, (S)-naproxen and (S)-ibuprofen, demonstrating high enantioselectivities.[45,89]

For several decades, research in the area of homogeneous asymmetric hydrogenation has focused on developing new homogeneous catalysts[22,90] and testing their hydrogenation activity and enantioselectivity on a limited scope of functionalized prochiral molecules.[90,91] While there has been some exciting work on the hydrogenation of alkenes containing no other functional group,[92–94] most of the substrates studied traditionally are prochiral compounds able to coordinate to the metal centre of the catalyst via a neighbouring carbonyl, carboxylate, or alkoxide functionality. Examples include dehydroamino acids, enamides, α,β-unsaturated carboxylic acids and esters, enol esters, α,β-unsaturated carbonates, and allylic alcohols.[82,95–101] Most compounds used for screening have prochirality α or, rarely, β to the coordinating functional group, with the most common coordinating group being a carboxylic acid group.[22] This strategy was

not explored for substrates in which the prochiral centre may be further away from the ligating functionality, until recently.

Published work has demonstrated that the limited scope of new prochiral substrates that one might use for the development of hydrogenation catalysts are still growing today. Song *et al.* developed an efficient chiral iridium catalyst bearing spiro phospine-oxazoline ligands in 2012, with which they successfully hydrogenated β,γ-unsaturated acids.[76] They demonstrated in 2013 the effectiveness of this catalyst in the successful asymmetric hydrogenation of 1,1-diarylethenes with high enantioselectivities.[60] Both of these substrates were the same compounds chosen for our study on the effect of length and rigid linkers on the asymmetric hydrogenation.

The focus of this chapter will be discussing the results of the hydrogenation of alkenes bearing a carboxylic acid group that is n atoms removed from the prochiral unsaturation of interest. The test compounds were chosen to elucidate the effect of binding group proximity to the unsaturation in terms of the rate and enantioselectivity of the asymmetric hydrogenation.

The unsaturated substrates chosen for this study are simple phenylalkenoic acids, Scheme 3.2, and phenylethenyl benzoic acids, Scheme 3.3. These substrates both contained a prochiral olefin as the unsaturation of interest and a carboxylic acid metal-binding functional group. The phenylalkenoic

acids only vary in the carbon chain length, n, whereas the phenylethenyl benzoic

acids vary in the positions around the benzoic acid moiety; ortho, meta, and para.
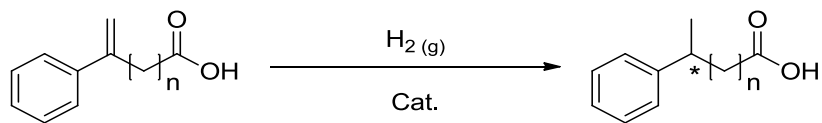
Substrate	n
1	0
2	2
3	3

Scheme 3.2. Asymmetric hydrogenation mediated through a

metal-binding carboxylic acid for phenylalkenoic acid substrates.
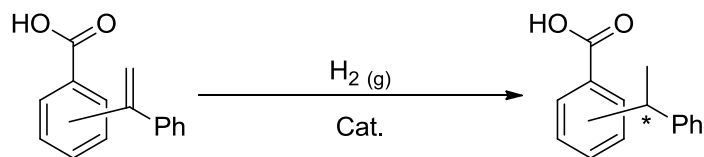
Substrate	Position
4	Ortho
5	Meta
6	Para

Scheme 3.3. Asymmetric hydrogenation mediated through a metal-

binding carboxylic acid for phenylethenyl benzoic acid substrates.

3.1 – The Selection of Chiral Catalysts

Six commercially available catalysts (Figure 3.2) were chosen to study the effect of chain length on the conversion and enantioselectivity of the asymmetric hydrogenation of prochiral unsaturated carboxylic acids.
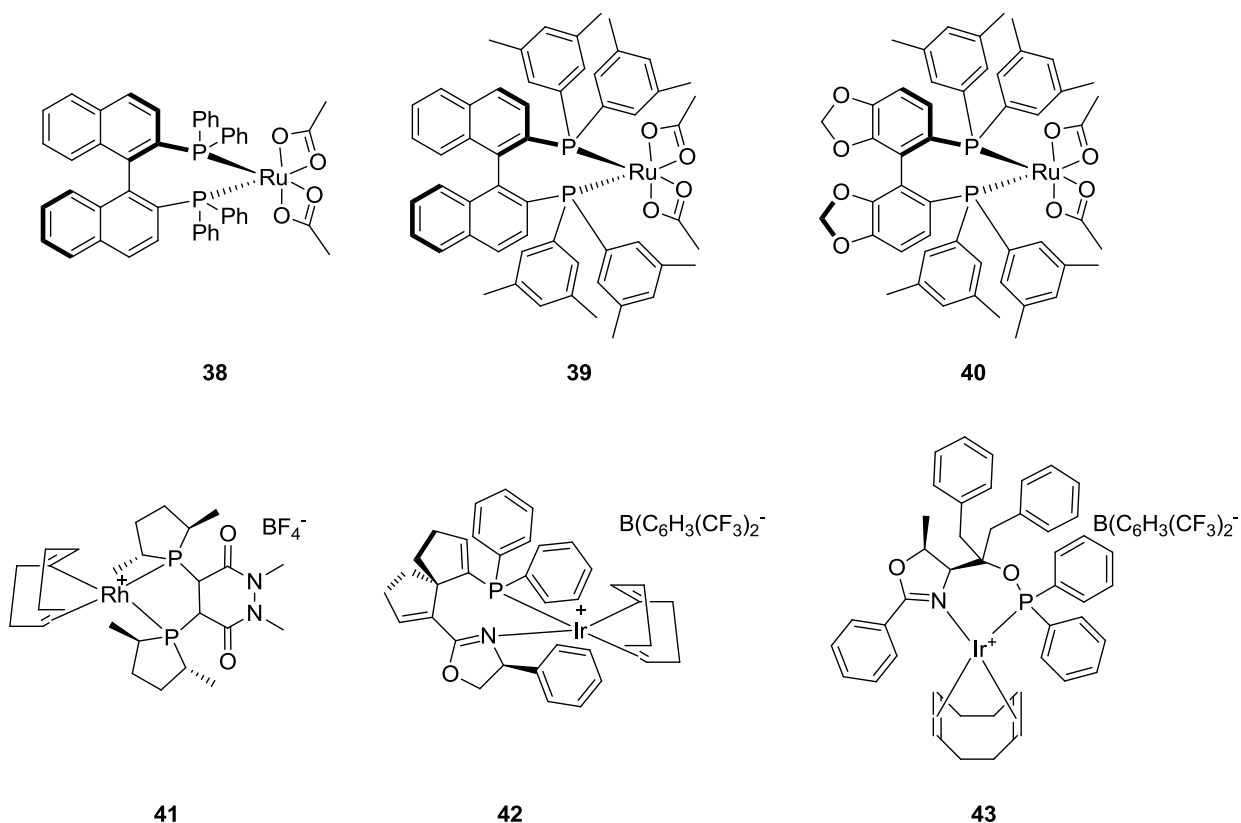
Figure 3.2. Catalysts employed in the asymmetric hydrogenations of alkenes mediated through carboxylic acids.

The first was Noyori's ruthenium catalyst, diacetato[(R)-(+)-2,2'-bis(diphenylphosphino)-1,1'-binaphthyl]ruthenium (II), **38**, as it is well-studied and

known to hydrogenate α,β-unsaturated carboxylic acids with high conversion and enantioselectivity.[21,46] The next two catalysts were variations of Noyori's catalyst: diacetato{(R)-(+)-2,2'-bis[di(3,5-xylyl)phosphino]-1,1'-binaphthyl}ruthenium(II), **39**, and diacetato{(R)-(+)-5,5'-bis[di(3,5-xylyl)phosphino]-4,4'-bi-1,3-benzodioxole}ruthenium(II), **40**. These two catalysts were chosen as they both have the bulky di(3,5-xylyl)phosphino groups, such that this facial steric hindrance might improve the facial selectivity of the olefinic group and increase the enantioselectivity of the reaction. Catalyst **40** was also chosen because of the benzodioxole group, as the oxygen atoms not only affect the electronics of the catalyst but also the steric bulk around the metal centre, which decreases the bite angle, further increasing the enantioselectivity of the catalyst.[102] The fourth catalyst was (-)-4,5-bis[(2R,5R)-2,5-dimethylphospholanyl](1,2-dimethyl-1,2'-dihydropyridazine-3,6-dione)(1,5-cyclooctadiene)rhodium(I) tetrafluoroborate, **41**, which was chosen because it is highly enantioselective for the hydrogenation of non-substituted itaconates at room temperature, along with the obvious change in the metal centre of the complex.[103] The last two catalyst chosen, 1,5-cyclooctadiene{(4S)-(-)-[(5R)-6-(diphenylphosphino)spiro[4.4]non-1.6-dien-1-yl]-4,5-dihydro-4-phenyloxazole}iridium(I) tetrakis(3,5-bistrifluoromethyl)phenylborate, **42**, and ((4S,5S)-(-)-O-[1-benzyl-1-(methyl-2-phenyl-4,5-dihydrooxazol-4-yl)-2-phenylethyl]-diphenylphosphinite)(1,5-cyclooctadiene)iridium(I) tetrakis(3,5-bistrifluoromethyl)phenylborate, **43**, are chiral mimics of Crabtree's catalyst.[104] Catalyst **42** was chosen because it is known to perform asymmetric

hydrogenations of α,β-unsaturated carboxylic acids with high yields and enantioselectivity.[105] Catalyst **43** has been reported to asymmetrically hydrogenate a number of alkenes without the need for a metal-coordinating functional group.[106] Catalyst **43** was chosen to see if the long chained unsaturated carboxylic acids, because the prochiral unsaturation is so far from the acid group, would best be hydrogenated by a catalyst that performs well without such a metal-binding functional group.

3.2 – Results and Discussion

3.2.1 – Synthesis of prochiral olefins containing carboxylic acids

For experimental procedure and general information see Chapter 2.

The preparations of 4-phenyl-4-pentenoic acid, **2**, 5-phenyl-5-hexenoic acid, **3**, 2-(1-phenylethenyl)benzoic acid, **4**, 3-(1-phenylethenyl)benzoic acid, **5**, and 4-(1-phenylethenyl)benzoic acid, **6**, were synthesized by following a procedure for the Wittig reaction written by Whitehead (Scheme 3.4).[56] Experimentally, the reaction proceeded under an inert atmosphere and to ensure the reaction would proceed, dry toluene had to be used.
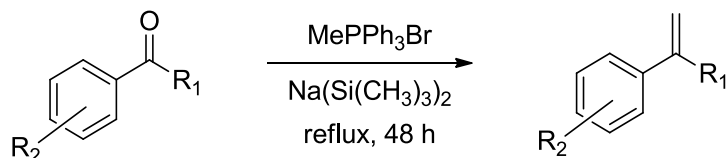
Scheme 3.4. Wittig reaction scheme for the synthesis of C=C double bonds from ketones.

The order of addition of reagents was crucial for the synthesis of these compounds. The ylide was prepared first by reacting the alkyltriphenylphosphine salt with a strong base, such as sodium bis(trimethylsilyl)amide, and then adding the ketoacid. If the ketoacid was added before the ylide was synthesized, the acid would react with the base, using it up and causing the reaction not to proceed. For the more bulky ketoacids: 2-(1-phenylethenyl)benzoic acid, **4**, 3-(1-phenylethenyl)benzoic acid, **5**, and 4-(1-phenylethenyl)benzoic acid, **6**, it was important to increase the reaction time from overnight 15 h to 48 h as the steric hindrance caused the reaction to slow down and the isolated yields to decrease.

3.2.2 - Asymmetric hydrogenation results and discussion for the phenylalkenoic acids in the study of the effects of length
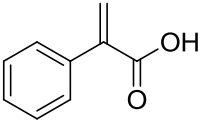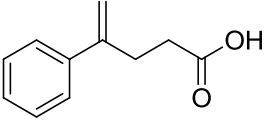
The concept of the project was to start with atropic acid, an α,β-unsaturated carboxylic acid, (compound **1**, n = 0) as its asymmetric hydrogenation has been extensively studied. It has been previously shown that high yields and enantioselectivities were obtained by using catalyst **38** at the following conditions: a temperature of 25 °C and a hydrogen pressure of 100 bar
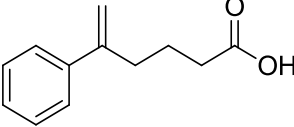
with dry methanol as the solvent (Table 3.1).[46] However, I have found that the hydrogenation not to be as facile with the other substrates containing longer chains.

For substrate **1**, it was found that all of the chosen Noyori ruthenium based catalysts, **38**, **39**, and **40,** were the same in terms of the yield of the reaction, > 99 % for each catalyst, and very similar in terms of the enantioselectivity of the reaction, 85, 84 and 82 % *ee*, respectively. Catalyst **41** also did very well in terms of the yield, > 99 %; however, the enantioselectivity of the reaction significantly decreased with the rhodium catalyst compared to the ruthenium catalysts, 25 %. The iridium catalysts **42** and **43** did not show favorable results at the conditions mentioned above. They both resulted in low yields and low enantioselectivities for the α,β-unsaturated acid. However, if the conditions were changed for catalyst **42** to 30 bar $H_{2\ (g),}$ 1 eq. triethylamine in methanol, the results of the hydrogenation significantly improved to an 88-89 % yield and an enantioselectivity of 88 % *ee*.[104,105]

Table 3.1. Asymmetric hydrogenation of prochiral unsaturated phenylalkenoic acids. [a]
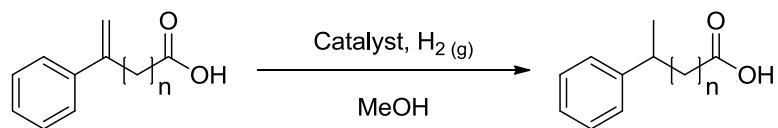
Substrates	Cat.	Temp. (°C)	Time (h)	Yield (%) [d]	ee (%) [d]
	38	25	14	> 99	85 ±3
	39	"	"	> 99	84 ±4
	40	"	"	> 99	82 ±1
	41	"	"	> 99	25 ±6
	42	"	15	15 ±6	10 ±7
1	**42** [c]	50	20	88-89 [g]	88 [g]
	43	25	15	35 ±7	4 ±1
	38 [b]	"	95	98 ±2	54 ±39
	39 [b]	"	"	97 ±2	53 ±13
	38	25	14	> 99	61 ±3
	39	"	"	> 99	68 ±1
	40	"	"	> 99	26 ±13
	41	"	"	> 99	11 ±7
	42	"	16	2 ±0.1	-
2	**42** [c]	50	20	2 ±0.1	-
	43	25	15	2 ±0.1	-
	38 [b]	"	95	2 ±1	17 ±4
	39 [b]	"	"	1.5 ±1	19±5

	Entry				
3	**38**	25	14	34 [e] ±4	-
	39	"	"	43 [e] ±11	-
	40	"	"	45 [e] ±2	-
	41	"	"	> 95 [e]	-
	42	"	16	12 [e] ±2	13 [f] ±2
	43	"	15	26 [e] ±9	2 [f] ±1
	38	50	24	69 [e]	28 [f]
	39	"	"	90 [e]	4 [f]
	40	"	"	66 [e]	10 [f]
	41	"	"	> 98 [e]	6 [f]
	42	"	"	41 [e]	16 [f]
	42 [c]	"	20	28 [e] ±4	5 [f] ±2
	43	"	24	97.2 [e]	13 [f]
	38 [b]	25	98	12 [e] ±5	47 [f] ±11
	39 [b]	"	"	29 [e] ±5	11 [f] ±2
	40 [b]	"	"	15 [e] ±4	58 [f] ±0.2
	41 [b]	"	"	6 [e] ±4	32 [f] ±0.2

[a] Experiments were all done in triplicate, except for the high pressure experiments with **3** at 50 °C, unless stated otherwise all standard deviation are 0. All % yields = % conv. Cat. = 0.7-2.3 mol %. *Reaction conditions:* 160 mL stainless steel pressure vessel, 100 bar $H_{2(g)}$, 2 mL methanol in a 1 dram vial. [b] *Reaction conditions:* 160 mL stainless steel pressure vessel, 10 bar $H_{2(g)}$, 2 mL methanol in a 1 dram vial. [c] *Reaction conditions:* 160 mL stainless steel pressure vessel, 30 bar $H_{2(g)}$, 1 eq. triethylamine, 2 mL methanol in a 1 dram vial. [d] GC-FID values, except where noted. [e] ^{1}H NMR yield. [f] Product was methylated before GC analysis. [g] Data from Zhang *et al.*[105]

Once it was determined which catalysts successfully hydrogenated atropic acid, I then evaluated the effect of chain length by increasing the number of carbon atoms, n, in the chain between the prochiral unsaturation and the metal-binding functional group, i.e. the carboxylic acid. The substrate where n = 1, or 3-phenyl-3-butanoic acid, **44**, Figure 3.3, was not studied due to its ability to decarboxylate, Scheme 3.5, producing carbon dioxide and prop-1-en-2-ylbenzene, i.e. resulting in decomposition products.[107,108]

44
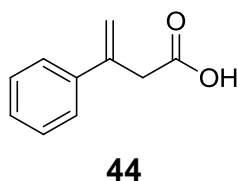
Figure 3.3. 3- Phenyl-3-butanoic acid with a link of n = 1.
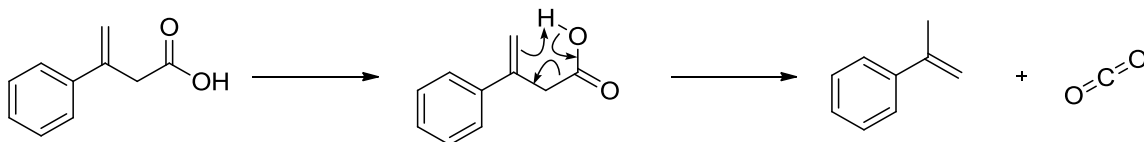
Scheme 3.5. Decarboxylation mechanism for 3-phenyl-3-butanoic acid.[107,108]

The asymmetric hydrogenation of the γ,δ-unsaturated acid, **2**, 4-phenyl-4-pentenoic acid, n = 2, did not decrease in activity in terms of the conversion of the reaction with the ruthenium catalysts **38**, **39**, and **40**, however there was a *ca.* 20 % decrease in the enantioselectivity of reaction for catalysts **38** and **39** and a *ca.* 60 % decrease for catalyst **40**. The rhodium catalyst **41** had comparable results to atropic acid, both obtaining poor *ee*, 11 – 20 %. For all catalysts used in Table 3.1 the same absolute configuration was produced for each substrate.

The best catalyst complexes continue to be **38** and **39** even with the longer chain length n = 3, the δ,ε-unsaturated carboxylic acid. 5-Phenyl-5-pentenoic acid, **3**, was hydrogenated with poor conversion and very poor enantioselectivity. The yield of the reaction could be increased, *ca.* 20-50 %, by increasing both the time to 24 h from 12 h, and the temperature to 50 °C from 22 °C, of the reaction. However, the enantioselectivity of the hydrogenation was at best 28 %.

For every substrate, the rhodium catalyst, **41**, gave very poor results in terms of enantioselectivity but gave high yields. Even though catalyst **41** was reported to work well with non-substituted itaconic acids and their derivatives,[103] it has been reported that the efficiency of ruthenium and rhodium catalysts are highly substrate-dependent.[109] Therefore, the slight change to a phenyl substituted unsaturated acid could have caused the significant drop in enantioselectivity for this study.

Both iridium catalysts **42** and **43** were used for all three unsaturated carboxylic acid substrates, **1**, **2**, and **3**, under the same conditions that were successful for catalyst **38** and atropic acid, **1**, for comparison. Catalyst **42** was found to result in poor yields and enantioselectivity at high pressure and room temperature for substrates **1**, **2** and **3**. When the reaction temperature was increased to 50 °C, the yield of substrate **3** was increased by ca. 20 %, but there was no improvement in terms of enantioselectivity. Catalyst **43** was also found to result in the same trend in terms of a poor yield and enantioselectivity for all three olefinic substrates. Using the conditions reported above[104,105] for catalyst **42** but with the lower hydrogen pressure, 30 bar instead of 100 bar, and an equivalent of triethylamine, it was found that substrates **2** and **3** were hydrogenated with poor yield and enantioselectivity.

Noyori reported that minor structural changes of the substrate could change the optimal reaction conditions required for successful hydrogenations in terms of pressure.[21,97] To verify that the conditions used in Table 3.1 at a high hydrogen pressure, 100 bar, were optimal for the unsaturated carboxylic acids, a set of reactions at a low hydrogen pressure, 10 bar, was completed. By inducing a low hydrogen pressure, the kinetics of the hydrogenation reaction had slowed down, increasing the overall reaction time to 96 h. Even with the dramatic increase in reaction time, the yield of the hydrogenation reactions was poor in comparison to the high pressure reactions. For two of the unsaturated carboxylic

acids, **1** and **2**, it was found that the enantioselectivity decreased significantly, from 85 to 54 % and 61 to 17 %, when using 10 bar of hydrogen pressure. For the δ,ε-unsaturated carboxylic acid, **3**, the yield of the low pressure reaction decreased; however, the enantioselectivity increased by ca. 20 %, for catalyst **38** and **39** and ca. 50 % for catalyst **40**.

Overall, the most promising catalysts for the asymmetric hydrogenation of the α,β- and β,γ-unsaturated carboxylic acids were **38** and **39**. Both catalysts demonstrated complete conversion, > 99 %, for the hydrogenation reactions and comparable *ee* of 85 and 84 % for **1** and 61 and 68 % for **2** respectively for **38** and **39**. The reason proposed for the improved enantioselectivity for catalyst **39** over the other catalysts for the asymmetric hydrogenation of the β,γ-unsaturated carboxylic acid, n = 2, was the steric hindrance around the metal-centre of the catalyst. The steric bulk in catalyst **39** would potentially cause the selection of the enantioface to become more restricted, such that the unsaturated C=C double bond must come in a more specific manner than the other catalysts examined. Nonetheless, the more sterically-hindered catalyst did not work once the linker of the unsaturated carboxylic acids were increased to n = 3. With asymmetric hydrogenations, the bound unsaturated substrate must come into the catalyst with the correct direction and face towards the metal centre for the chirality of the catalyst to be imposed into the substrate. As the carbon chain is increased from n = 0 to n = 3, the probability of the unsaturation to insert itself into the metal-centre with the correct face decreases exponentially. Thus, for the

γ,ε-unsaturated carboxylic acid the carbon linker has become too long for the catalyst to efficiently restrict the enantioface selection of the olefin.[21] Interestingly, once the conditions of the hydrogenation were changed from a high pressure of H_2, 100 bar, to the lower pressure of 10 bar the *ee* of catalyst **40** increased to 58 %, for the γ,ε-unsaturated carboxylic acid, **3**, yet the yield was poor, 15 %. The increase in enantioselectivity for the lower pressure of hydrogen was due to the different possible reaction pathways for the Ru-catalyzed hydrogenation of unsaturated carboxylic acids, (Scheme 1.6). Because of the lower hydrogen pressure, the kinetics of the hydrogenation reaction slows down, allowing for the olefin of the unsaturated acid to fall back off and re-insert itself to the metal-centre until the thermodynamic complex is achieved. This allows the enantioface selection between the substrate and metal complex to arrange itself in the most favourable conformation, i.e. producing the higher enantiomeric excess. On the other hand, this affects the turnover of the catalyst as the kinetics have slowed down. To improve the conversion of the hydrogenation of the γ,ε-unsaturated carboxylic acid, one would have to increase the reaction time longer than four days, which is undesirable for an industrial application.

To improve the enantioselectivity and the yield of the asymmetric hydrogenation reaction, as mentioned above, one could manipulate the reaction conditions, solvents and further variations in the catalysts. However, this was not pursued as during my project, Song *et al.*[76] reported a newly developed iridium

complex that hydrogenated the β,γ-unsaturated carboxylic acid substrate, **2**, with high yields and enantioselectivity.

3.2.3 - Asymmetric hydrogenation results and discussion for the phenylethenyl benzoic acids in the study of rigidity and bulk

Because many pharmaceuticals and natural products can contain rigid or semi-rigid moieties, a more rigid linker was developed to study the effects on the asymmetric hydrogenation of olefins mediated through carboxylic acid functionalities. The substrates synthesized for the study were 2-(1-phenylethenyl)benzoic acid, **4**, 3-(1-phenylethenyl)benzoic acid, **5**, and 4-(1-phenylethenyl)benzoic acid, **6**. In this system, the unsaturation of interest moves around the benzoic acid moiety, in the ortho-, meta-, and para-position. The effect on the enantioselective hydrogenation, caused by these changes in position, was examined for the conversion and enantioselectivity of the reaction (Scheme 3.6).
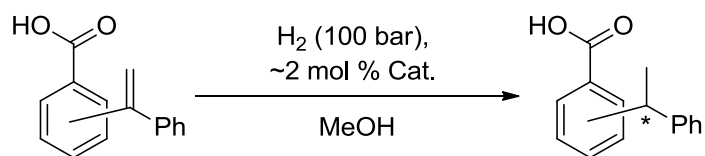
Scheme 3.6. Hydrogention of the phenylethenylbenzoic acids; 2-(1-phenylethenyl)benzoic acid, **4**, 3-(1-phenylethenyl)benzoic acid, **5**, and 4-(1-phenylethenyl)benzoic acid, **6**.

For the asymmetric hydrogenation of the phenylethenylbenzoic acid substrates, there are two possible pathways: intramolecular and intermolecular. If the catalytic mechanism follows the intramolecular pathway, first the carboxylic acid group will coordinate to the metal centre, followed by the C=C double bond wrapping around to coordinate next. In the intermolecular pathway the carboxylic acid group does not participate in the mechanism and only the C=C double bond coordinates to the metal centre of the catalyst. In the asymmetric hydrogenation of the ortho-substrate, 2-(1-phenylethenyl)benzoic acid, **4**, we hypothesized that the reaction would proceed through an intramolecular pathway, resulting in high conversions and high enantioselectivity, due to the prochiral unsaturation being close in proximity to the metal-binding functionality, the carboxylic acid. We expect the conversion and enantioselectivity to be greatly affected by the different stabilities of the transition states for the ortho-, meta-, and para-phenylethenyl benzoic acid substrates. Of the three positions around the benzoic

moiety, the ortho-position would most likely follow the intramolecular mechanism as it would form the least strained transition state (Scheme 3.7). Moving from the ortho-substrate to the meta-substrate we expect that the intramolecular mechanism becomes more unlikely as the catalytic transition state would become too strained in the case of 3-(1-phenylethenyl)benzoic acid. This would in turn result in lower yield and enantioselectivity for the asymmetric hydrogenation. For the para-substrate, it is predicted to exhibit the worst enantioselectivity and yield of the three substrates if the intramolecular pathway if followed. If the mechanism proceeds through an intramolecular route then the aromaticity of 4-(1-phenylethenyl)benzoic acid, **6**, would be interrupted due to the bending of the ring in the transition state of the catalytic cycle when the unsaturation comes into the metal centre (Scheme 3.8), which is highly unlikely. Thus the intermolecular mechanism would take over, and the carboxylic acid would not coordinate to the metal centre (Scheme 3.9). For both the meta- and especially the para-substrate the intermolecular mechanism is more likely to occur, where the alkene is inserted without binding of the carboxylic acid to the metal. However, if the reactivity of the carboxylic acid group is too strong, this interaction would interfere with the intermolecular pathway by binding to the catalyst and thereby blocking the active site necessary to perform the asymmetric hydrogenation.
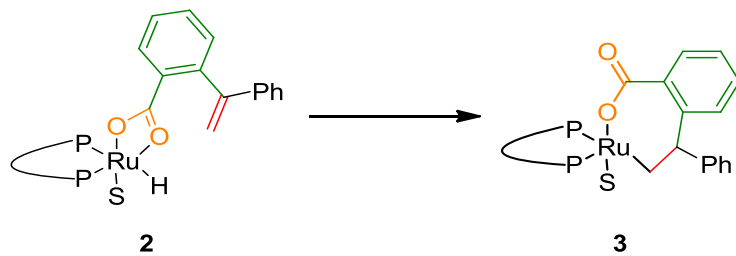
Scheme 3.7. Intramolecular reaction for the asymmetric hydrogenation of 2-(1-phenylethenyl)benzoic acid, **4**, with catalyst **38**, where s is a solvent molecule.
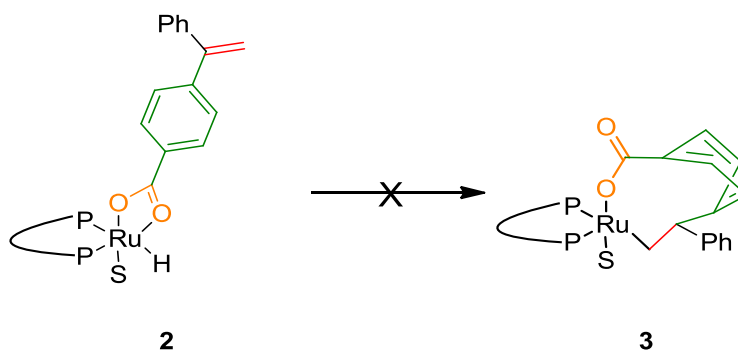
Scheme 3.8. Intramolecular reaction for the asymmetric hydrogenation of 4-(1-phenylethenyl)benzoic acid, **6**, with catalyst **38**, where s is a solvent molecule.
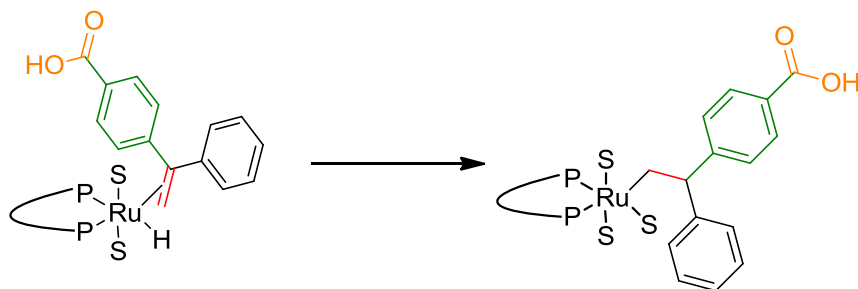
Scheme 3.9. Intermolecular reaction for the asymmetric hydrogenation of 4-(1-phenylethenyl)benzoic acid, **6**, with catalyst **38**, where s is a solvent molecule.

Computational energy calculations were done by a coworker, Gurpaul Kochhar, to calculate and support the theory of the increase in strain within the transition state of the intramolecular pathway as the prochiral unsaturation moved from the ortho, to the meta, or para position of the benzoic acid. All calculations were performed using density functional theory with the B3LYP exchange-correlation functional. The Ru atom was treated with the LANL2DZ effective core potential basis set. All other atoms (C, H, P, and O) were treated with the 6-31G(d,p) basis set. Geometry optimizations and frequency calculations were performed in single-point energy calculations were performed in methanol. The resulting energies of the complexes from the computations were plotted against one another to evaluate their stabilities (Figure 3.4). These relative energies allow us to look at the intermediates (point 3 in the figure) and whether it is realistic for them to form. These computational results were interesting as they suggested that the meta-substrate 3-(1-phenylethenyl)benzoic acid, **5**, in its

intermediate complex, should be more stable than the complex formed with the ortho-substrate 2-(1-phenylethenyl)benzoic acid, **4**. This was not in accordance with our expectations, as mentioned above. As expected, the calculations predicted that the transition state for the para-substrate in the intramolecular pathway had the highest energy, *ca.* 60 kJ/mol in both the gas-phase and in MeOH.
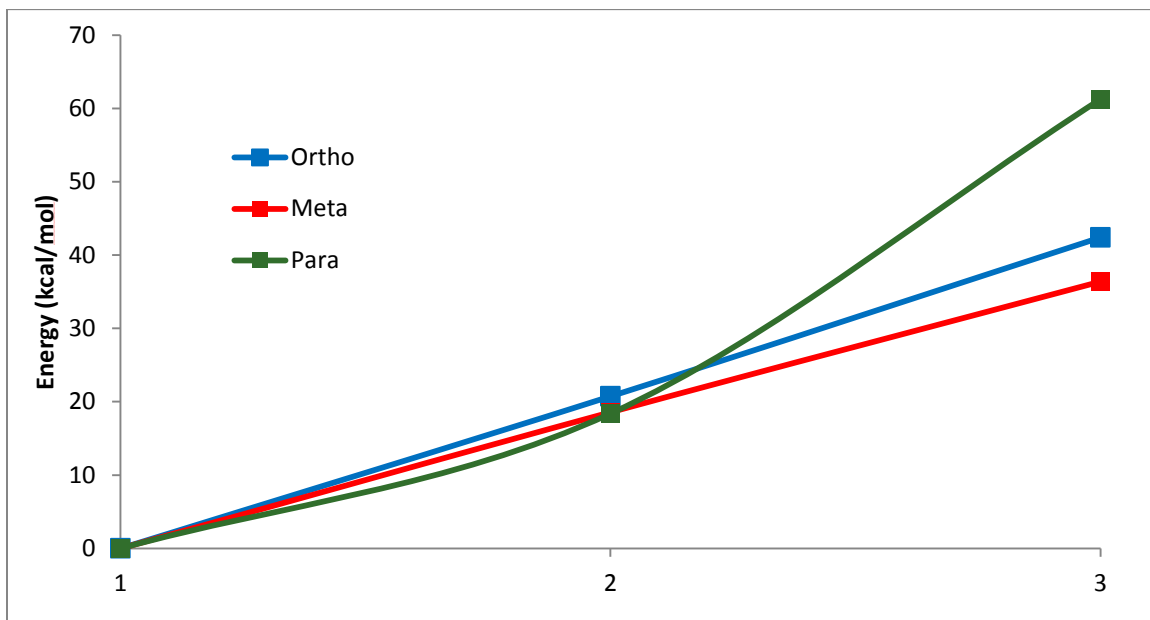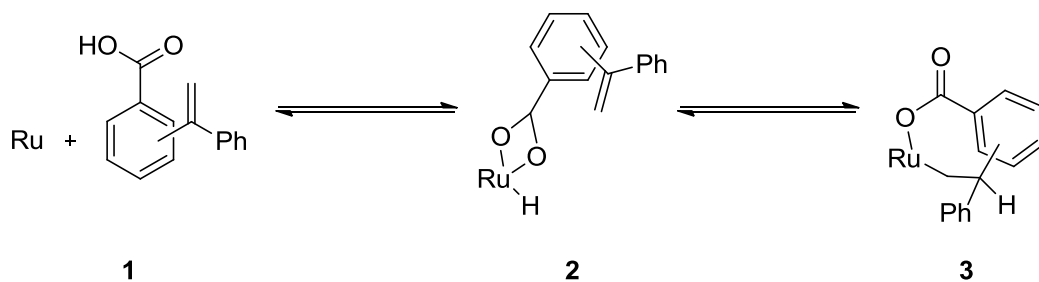
Figure 3.4. Computational results for the catalytic complexes for the intramolecular pathway for 2-(1-phenylethenyl)benzoic acid, **4**, 3-(1-phenylethenyl)benzoic acid, **5**, and 4-(1-phenylethenyl)benzoic acid, **6**, in the gas-phase and in methanol. The relative energies represent that of the complex themselves without the activation barriers of the reaction. Catalyst **38** is represented by 1, catalytic complexes 2 represents the bound substrate, ortho, meta or para, through the carboxylate and complexes 3 are those where the olefin has inserted into the metal.

With the exception of the para-substrate, the computational work established that the experimental results from the asymmetric hydrogenation could be promising (Table 3.2). The chosen catalysts were **38** and **40**, from the list of previously used catalysts (Figure 3.2) as they were the best catalysts in terms of the enantioselectivity and yield for the unsaturated carboxylic acids. In addition, a new catalyst was also employed in the asymmetric hydrogenation of the more rigid substrates: dichloro[(S)-(-)-2,2'-bis(diphenylphosphino)-1,1'-binaphthyl]ruthenium, **45**, (Figure 3.5). Catalyst **45** was added to the list of studied catalysts as we wanted to see the effect of a chloro-ligand versus the acetato-ligand.
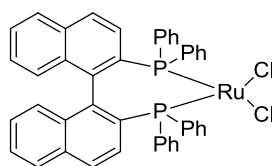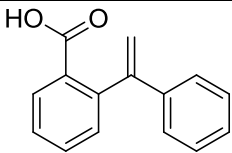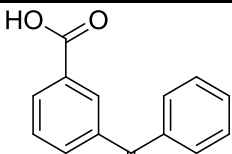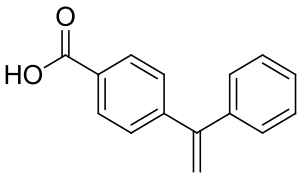
45
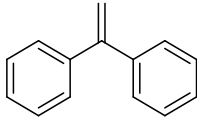
Figure 3.5. Simplified structure of an additional catalyst, [RuCl$_2$((S)-binap)]$_n$, employed for the asymmetric hydrogenation of 2-(1-phenylethenyl)benzoic acid, **4**, 3-(1-phenylethenyl)benzoic acid, **5**, and 4-(1-phenylethenyl)benzoic acid, **6**.

The hydrogenation results of 2-(1-phenylethenyl)benzoic acid, **4**, matched the results we expected, with a high conversion for both catalysts **38** and **40** and good enantioselectivities, 91 and 97 %, respectively. Surprisingly, neither the

meta- nor para-substrates resulted in good conversion and enantioselectivity. Both substrates had a large decrease in conversion, *ca.* 80 % and *ca.* 90 % drop in value and a decrease in enantiomeric excess, *ca.* 90 % decrease, relative to the ortho substrate.

Table 3.2. Results of the asymmetric hydrogenation reaction of for 2-(1-phenylethenyl)benzoic acid, **4**, 3-(1-phenylethenyl)benzoic acid, **5**, and 4-(1-phenylethenyl)benzoic acid, **6**.[a]

Substrate	Cat.	Temp. (°C)	Time (h)	% Yield [b]	% ee [b]
4	**38**	25	48	> 99.8	91
	45	"	"	16.9	94
	40	"	"	> 99.9	97
5	**38**	"	"	8	6
	45	"	"	3	5
	40	"	"	21	12
6	**38**	"	"	7	8
	45	"	"	5	7
	40	"	"	22	6

Without Benzoic acid	**38**	"	45	3 [c]	n/a
With Benzoic acid **46**	**38**	"	"	4 [c]	n/a

[a] *Reaction conditions:* 160 mL stainless steel pressure vessel, 100 bar $H_{2\,(g)}$, *ca.* 2 mol % catalyst, 2 mL methanol in a 1 dram vial. [b] Values were obtained by HPLC. All experiments were done in triplicate. [c] Values obtained by ^{1}H NMR.

Accounting for the poor yields for the meta- and the para-substrates, it was hypothesize that the carboxylic acid group was binding non-productively to the metal, effectively preventing the metal from catalyzing the hydrogenation by the intermolecular pathway. The failure of the intramolecular pathway is most likely to the energy requirements for the bending and disruption of the aromaticity of the benzene ring in the transition state for this pathway. The binding of the carboxylic acid to the metal potentially blocked the intermolecular pathway, thus blocking the active site of the catalyst needed for the hydrogenation to occur. To test this, we first hydrogenated 1,1-diphenylethylene, **46**, with catalyst **38** to see if, in the absence of the carboxylic acid group, the intermolecular pathway could proceed (Table 3.2). We also attempted to hydrogenate 1,1-diphenylethylene in the presence of benzoic acid to see if the carboxylic acid would block the

intermolecular pathway and thereby impede the production of the desired hydrogenation product. However, according to the results in Table 3.2 neither conditions, with and without benzoic acid, for the hydrogenation of 1,1-diphenylethylene worked. We conclude that the intermolecular pathway may not proceed due to the steric bulk of the phenyl rings on the substrates.

It is possible that the computational results did not match the experimental as we only investigated the stability of the complexes themselves and compared these relative energies to one another. We believe that the activation barriers to proceed from complexes 2 to 3 (from Figure 3.4) are realistically too high for the meta- and para- complexes; thus, the reaction did not proceed.

Instead of focusing on catalyst development to improve the reactivity of the meta and para unsaturated benzoic acid substrates, **5** and **6**, we instead discontinued the project because a recent publication by Song *et al.*[60] successfully hydrogenated the ortho substrate, **4**, and derivatives with high yields and enantioselectivities (Scheme 3.10).
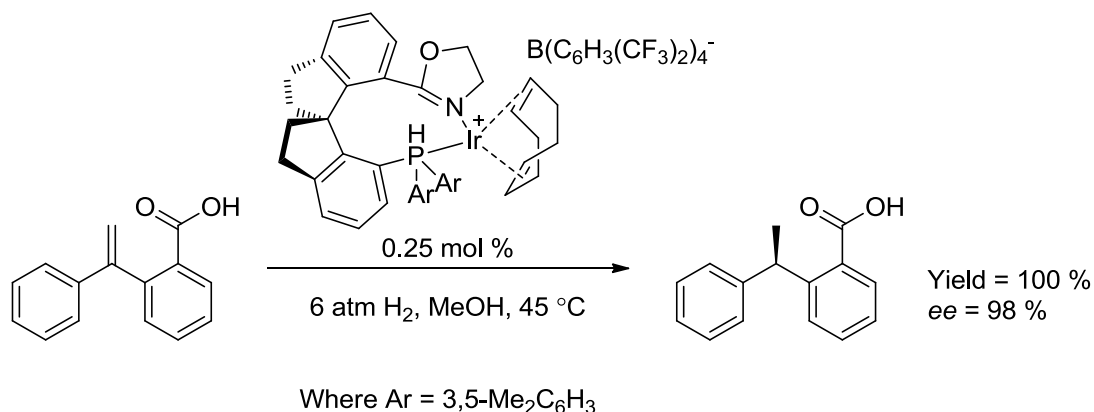
Scheme 3.10. Asymmetric hydrogenation of prochira lphenylethenyl benzoic acid with an iridium catalyst bearing a spiro phosphine-oxazoline ligand.

3.3 – Conclusion

3.3.1 – Conclusion for the prochiral unsaturated carboxylic acids

Overall, it can be concluded that the yield and enantioselectivity of asymmetric hydrogenation reactions are strongly affected by the distance between the prochiral unsaturation and the carboxylic acid group. Increasing the chain length, n, between the metal-binding functional group and the unsaturation causes the hydrogenation reaction to become slower and less enantioselective. For the unsaturated carboxylic acids, the maximum number of carbon atoms in the chain between the metal-binding functional group and the unsaturation is 2. Once the carbon chain is increased to three carbons or more, there is a dramatic

decrease in conversion. By increasing reaction time and temperature, we can increase the yield of the hydrogenation of the δ,ε-unsaturated acid, but this does not improve the enantioselectivity of the product; a nearly racemic mixture is achieved, *ca.* 4-28 % yield depending on the catalyst used. By decreasing the hydrogen pressure of the reaction, we were able to slightly increase the enantioselectivity of the desired product at the cost of a diminishing yield even with a longer reaction time.

Catalysts **38** and **39** produced the best results for the prochiral unsaturated carboxylic acids. The rhodium catalyst, **41**, gave very poor enantioselectivity but high yields for all the substrates, **4, 5,** and **6**.

3.3.2 - Conclusions for the prochiral phenylethenyl benzoic acids.

For the hydrogenation of the rigid substrates it was found that only the ortho-substrate, 2-(1-phenylethenyl)benzoic acid, **4**, was successfully hydrogenated in terms of high conversion and high enantioselectivity. When catalysts **38** and **40** were used for the hydrogenation they gave the best results, with HPLC yields > 99 % and the best enantioselectivity result of 98 %. Catalyst **45** did not work well with these rigid prochiral phenylethenyl benzoic acid substrates. The yield resulted in poor results, > 20 %, however the enantiomeric excess for the ortho-substrate, **4**, was good, 94 %, when catalyst **45** was used.

According to the computational analysis, the hydrogenation of the meta-substrate, 3-(1-phenylethenyl)benzoic acid, **5**, should have yielded successful results as well. However, experimentally successful results were not achieved. Both the conversion and enantioselectivity of the asymmetric hydrogenation was diminished when the meta- and the para-substrates were investigated. What was interesting, however, was that even though the hydrogenation of the meta- and the para-substrates did not work as well as the hydrogenation of the ortho-substrate, they resulted in approximately the same yields and enantioselectivity.

Chapter 4 – Asymmetric Hydrogenation of Unsaturated Ketoacids
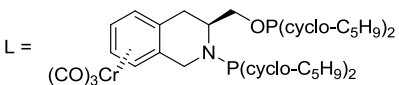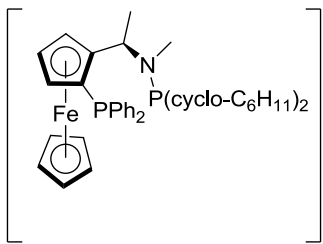
Chiral alcohols are important and valuable chiral building blocks for industrially relevant compounds, such as pharmaceuticals,[20,82,110–112] as well as for their use as resolving agents.[113] Focusing on only a specific subcategory of these chiral alcohols, significant research has been done on the methodology for obtaining α- & β-hydroxy acids and their derivatives. The constant need for these enantiomerically pure α-hydroxy acids and β-hydroxy acids as pharmaceuticals or for building blocks in pharmaceuticals has driven research into the asymmetric hydrogenation of α-ketoesters over the last few years.[31,111,114,115] Synthetically, these compounds can be obtained by metal-catalyzed asymmetric hydrogenation, enzymatic or biomimetic methods,[116–118] Cannizzaro reactions,[119–121] Friedel-Crafts reactions,[122–124] Aldol reactions,[125] as well as through the use of chiral titanium-carbohydrate complexes,[126] and tin(II) reagents.[127] Of these, the metal-catalyzed asymmetric hydrogenation of α- & β-ketoesters has shown to be efficient and economically feasible for the preparation of the corresponding chiral hydroxy acids.[20,21,83,98,128]

The asymmetric hydrogenation of α-ketoesters has been explored with various metal catalysts, the most studied being ruthenium and rhodium

based.[20,83] Initially, it was found that the homogeneous hydrogenations of ketone substrates were difficult compared to the reaction with olefinic substrates as they proceed more slowly and with lower stereoselectivity.[21] However, through extensive investigations a number of catalytic systems have been found to achieve high enantioselectivities (Table 4.1); the most effective of these contain either a ruthenium or a rhodium metal centre with chiral phosphine ligands (Scheme 4.1). The highest % *ee* in Table 4.1 result from the use of either [Ru(S)SunPhos(benzene)Cl]Cl or $RuCl_2$[(S)-C4-Tunephos]$Cl_2(DMF)_n$, at 96 and 97 %, respectively. The best result for a Rh containing catalyst came from the use of (S)-Cy,Cy-oxoProNOP-Rh, at 95 % *ee*.[20,81,82]

Table 4.1. Recent examples of asymmetric homogeneous hydrogenations of α-ketoesters using Ru and Rh catalysts.[a]

R¹	R²	Catalyst	Reaction Conditions	% ee (Config.)	Reference
Ph	Et	[Ru((S)-SunPhos)(benzene)Cl]Cl⁻	EtOH, 70 °C, 50 atm H_2, 20 h, $CeCl_3 \cdot 7\,H_2O$	96 (S)	[129]
Ph	Me	$RuCl_2$[(S)-C4-Tunephos](DMF)	MeOH, rt, 5 atm H_2, 20 h	97 (S)	[130]
Me	Et	4,4'-RuBr₂-(R)-*diam*Binap	H_2O, 50 °C, 40 atm H_2, 15 h	95	[131]
Ph	Me	[RuBnCl₂-(R)-tetrahydroxy-Binap]	MeOH, 50 °C, 40 atm H_2, 24 h	92 (R)	[111]
Me	Et	$Rh(CF_3CO_2)\{(anti)\text{-}L\}]_2$ L = (structure)	MeOH, 25 °C, 50 atm H_2, 6 h	95	[132]
Me	Et	(ferrocenyl Rh structure)	THF, rt, 20 atm H_2, 6 h	91 (R)	[133]
Me	Me	(2S,4S)-MCCPM-Rh	THF, 20 °C, 20 atm H_2	87 (R)	[134]
Me	Et	(S)-Cy,Cy-oxoProNOP-Rh	toluene, 20 °C, 50 atm H_2	95 (R)	[135]

a) All examples above demonstrated complete conversion for all catalytic hydrogenations listed.

(S)-Cₙ-TunePhos
n = 1 -6

4,4'-(R)-*diam*BINAP

(R)-TetrahydroxyBINAP

(2S,4S)-MCCPM

(S)-CY,Cy-oxoProNOP

(R)-SpiroPAP: Ar = 3,5-(^{t}Bu)$_2$Ph
X = H, 3-Me, 4-^{t}Bu,
6-Me, 6-Et

(R)-SEGPHOS

TangPhos

ClickFerrophos

tetraMe-BITIOP

(S)-SunPhos
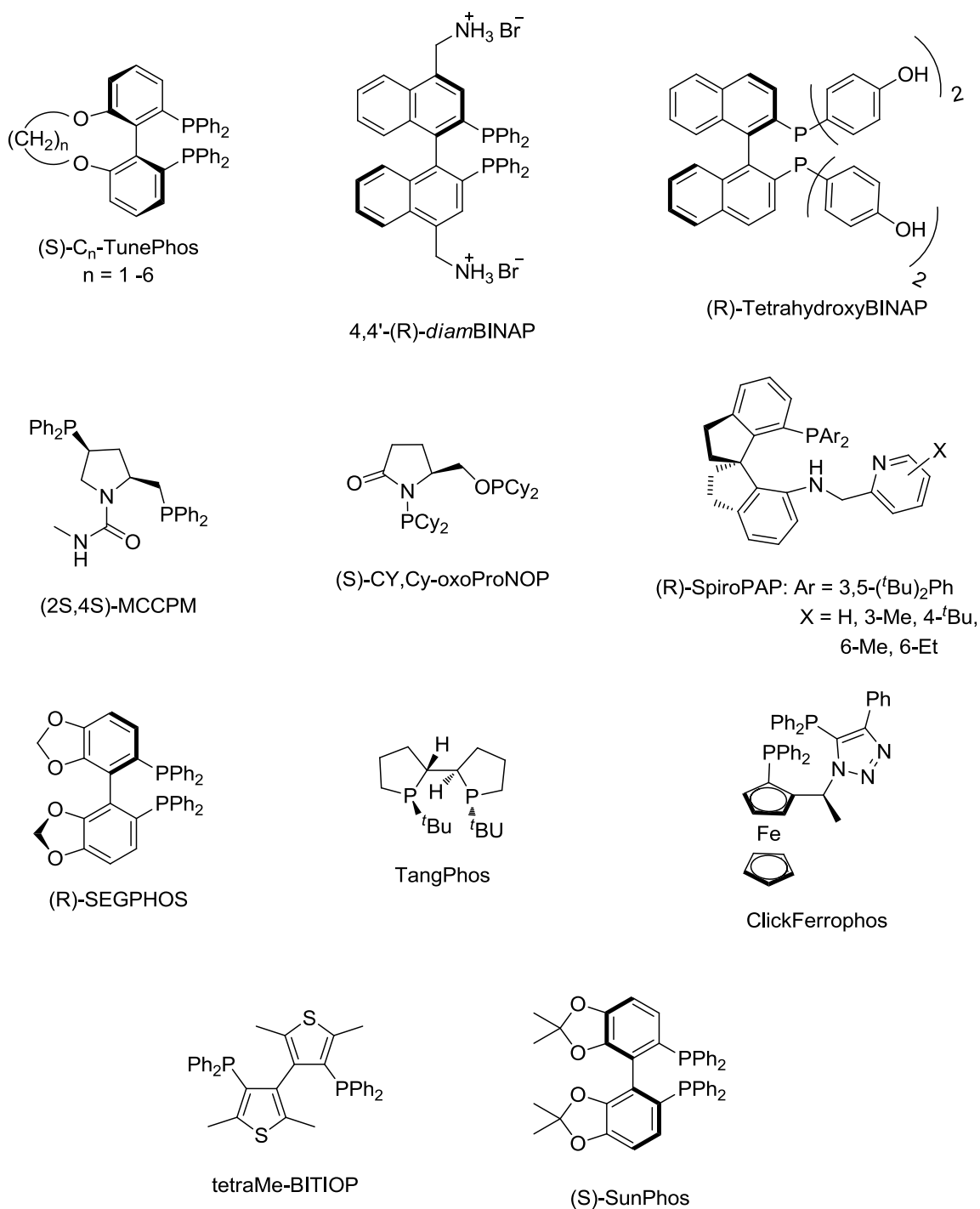
Scheme 4.1. Chiral phosphine ligands utilized in selected examples from literature for the asymmetric hydrogenation of α- and β- keto esters and acids.

The asymmetric hydrogenation of β-ketoesters has also been studied in great detail utilizing ruthenium based catalysts[20] and more recently with iridium based catalysts.[136–138] These catalysts have demonstrated their effectiveness and their ability to yield high enantioselectivities for a variety of *beta*-ketoesters (Table 4.2). To date, there are no examples of rhodium based catalysts hydrogenating *beta*-ketoesters in the literature. For the Ru based catalysts, the use of $RuBr_2$[P,P-clickFerroPhos], $[NH_2Me_2][\{RuCl[(R)\text{-}SEGPHOS]\}(\mu\text{-}Cl)_3]$, and $RuCl_2$[(S,S,R,R)-TangPhos](DMF)n all resulted in enantioselectivities > 97 %. For the Ir based catalysts, complexes containing the tridentate spiro pyridine-aminophosphine ligand, SpiroPap, resulted in enantioselectivities > 98 %.

Table 4.2. Recent examples of asymmetric homogeneous hydrogenations of β-ketoesters utilizing Ru and Ir chiral catalysts.[a)]
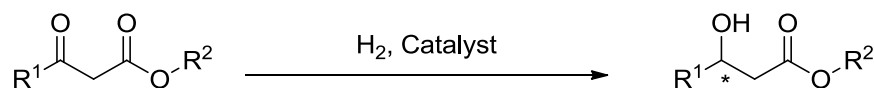
R[1]	R[2]	Catalyst	Reaction Conditions	% ee (Config.)	Reference
Ph	Et	RuBr$_2$[P,P-clickFerroPhos]	EtOH, 50 °C, 10 atm H$_2$	98 (S)	[139]
"	Me	[NH$_2$Me$_2$][{RuCl[(R)-SEGPHOS]}(μ-Cl)$_3$]	MeOH, 80 °C, 30 atm H$_2$	97.6 (S)	[102]
Me	Et	RuCl$_2$[(S,S,R,R)-TangPhos](DMF)n	MeOH/H$_2$O, 50 °C, 5 atm H$_2$	99.8 (R)	[140]
Ph	Et		5 equiv HCO$_2$H, H$_2$O, rt, 24 h, pH 8.0	95	[137]
"	"	[{Ir(cod)Cl}$_2$]/(R)-SpiroPAP	EtOH, rt, 8 atm H$_2$, KO^{t}Bu	98	[138]
m-Me-Ph	"	Ir-(R)-SpiroPAP	"	99	[136]
o-Me-Ph	"	"	"	99.8	"

a) All examples above demonstrated complete conversion for all catalytic hydrogenations listed.

Unlike α- and β-keto esters, there are fewer examples reported for the asymmetric hydrogenation of γ-ketoesters. One recent example was published for the preparation of enantiomerically pure γ-lactones by implementing the

asymmetric hydrogenation of γ-ketoesters. This hydrogenation demonstrated high enantioselectivity with multiple γ-ketoesters using (-)-(R)-(tetraMe-BITIOP)Ru(CF$_3$COO)$_2$ as the chiral catalyst (Scheme 4.2).[141]

R^1 = Me; R^2 = H; R^3 = Et; % *ee* = 98 %
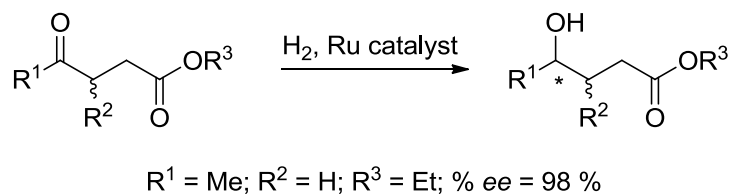
Scheme 4.2. An example for the asymmetric hydrogenation of an γ-ketoester using (-)-(R)-(tetraMe-BITIOP)Ru(CF$_3$COO)$_2$ as the catalyst.[141]

Unlike ketoesters, ketoacids have not been as well-studied as substrates in asymmetric hydrogenation reactions. In literature, it is believed that the carboxylic acid functional group of the substrate could preferentially coordinate to the metal centre of the catalyst, leading to deactivation as well as diminishing the enantioselectivity of the reaction.[112] One of the most successful attempts at hydrogenating a ketoacid involved (*E*)-2-oxo-4-arylbut-3-enoic acid and 2-oxo-4-arylbutanoic acid as the substrates. Zhu *et al.*[142,143] employed a ruthenium catalyst, [RuCl(benzene)(S)-SunPhos]Cl, to hydrogenate 2-oxo-4-phenylbut-3-enoate (Scheme 4.3) and (*E*)-2-oxo-4-arylbut-3-enoic acid (Scheme 4.4) to the corresponding alcohol with *ee* values of 88.4~92.6 % and 85.4~91.8 %, respectively (conversion > 99 %).[142,143] Yan *et al.* have successfully

hydrogenated α-aryl-α-ketoacids and α-alkyl-α-ketoacids using an iridium catalyst, Ir/SpiroPap-(R), yielding the corresponding chiral α-hydroxy acids with high enantioselectivity and high conversion (Scheme 4.5).[112] The high *ee* values were attributed to the tridentate ligand, which is proposed to be a more stable and active catalyst by preventing formation of the inactive iridium dihydride complex, which readily forms when the bidentate SpiroAP ligand is employed.[144,145]
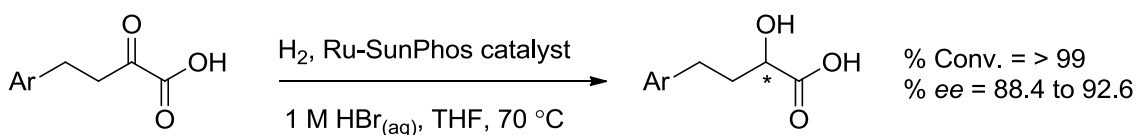
Scheme 4.3. Asymmetric hydrogenation of 2-oxo-4-phenylbut-3-enoate using [RuCl(benzene)(S)-SunPhos]Cl by Zhu *et al.*[142]
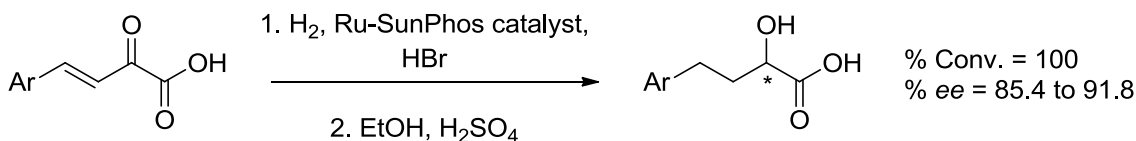
Scheme 4.4. Asymmetric hydrogenation of (*E*)-2-oxo-4-arylbut-3-enoic acid using [RuCl(benzene)(S)-SunPhos]Cl by Zhu *et al.*[143]
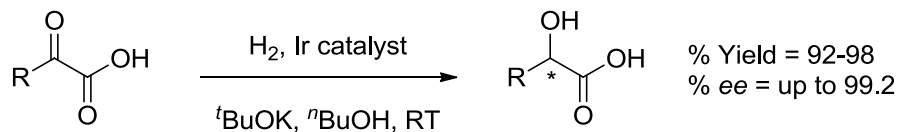
Scheme 4.5. Asymmetric hydrogenation of α-aryl-α-ketoacids and α-alkyl-α-ketoacids using Ir/SpiroPap-(R) as the catalyst by Yan *et al.*[112]

To the best of our knowledge, the asymmetric hydrogenation of β-ketoacids has only been studied in two reports. The more recent account is by Flowers *et al.*,[110] where simple ketones first proceed through carboxylation and then an asymmetric hydrogenation to produce the desired β-hydroxy acid (Table 4.3). The second known report is by Genêt *et al.*[146] where a single example of a successful asymmetric hydrogenation of a β-ketoacid was reported using RuCl$_2$(binap), RuBr$_2$(binap), etc. The lack of published work on the asymmetric hydrogenation of β-ketoacids could be due to the inherent instability of most of these acids, which can undergo a decarboxylation reaction, similar to the mechanism reported earlier in chapter 2 for 3-phenyl-3-butanoic acid, **44** (Scheme 3.5).[110]

Table 4.3. Asymmetric homogeneous hydrogenations of β-ketoacids utilizing Ru catalysts.

$$R^1 \overset{O \quad O}{\underset{R^2 \ R^3}{\diagup}} OH \quad \xrightarrow{\text{H}_2, \text{ Catalyst}} \quad R^1 \overset{OH \quad O}{\underset{R^2 \ R^3}{*}} OH$$
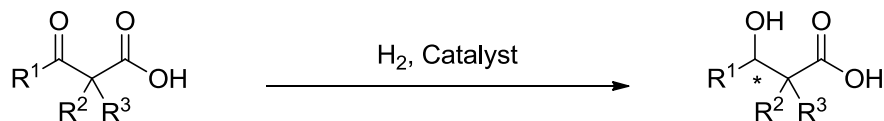
R¹	R²	R³	Catalyst	Reaction Conditions	% Yield	% ee (dr)	Reference
Ph	H	H	RuCl₂[(S)-Binap]	MeOH, 25 °C, 70 bar H₂	85	>99	[110]
"	Me	H	"	MeOH, 25 °C, 70 bar H₂	91	10 (1:6.6)	[110]
"	Me	Me	"	MeOH, 25 °C, 80 bar H₂	75	97	[110]
Me	H	H	RuBr₂[(R)-Binap]	MeOH, 80 °C, 10 atm H₂	100	98	[146]
"	"	"	RuBr₂[(S)-Binap]	MeOH, 40 °C, 20 atm H₂	100	>99	[146]
Et	"	"	RuBr₂[(R)-Binap]	MeOH, 40 °C, 20 atm H₂	100	>99	[146]

There are two possible pathways for the hydrogenation of ketoacids to occur (Scheme 4.6). Based on the report from Flowers *et al.*[110] the initial complex formed is from the carboxylate moiety binding to the Ru(II) catalyst.[21,45] From this initial metal complex the mechanism can then proceed through either a

keto and/or enol hydrogenation. However, the concentration of keto:enol complexes cannot be predicted due to the dramatic change the coordination of the substrate to the metal can have on the keto/enol ratio relative to their ratios when uncoordinated and in solution. Nonetheless, the enolization is not necessary for the hydrogenation to proceed, which was demonstrated by replacing the two hydrogen atoms with two methyl groups, see Table 4.3. Therefore, the keto pathway is a possible catalytic cycle; however, the enol pathway may still be dominate when possible.[110]
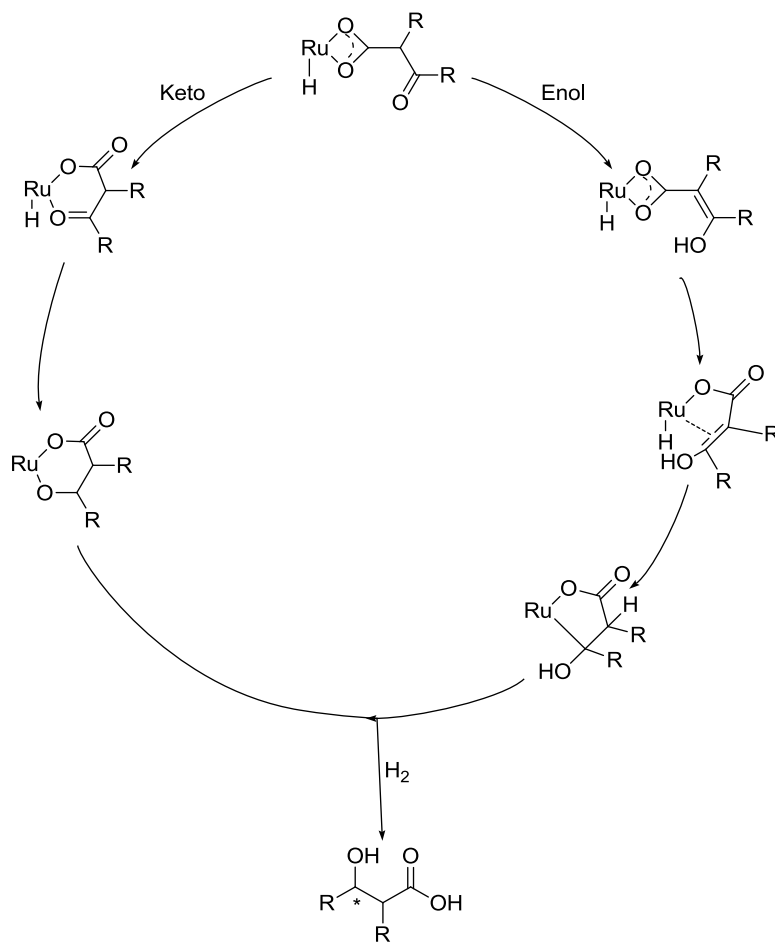
Scheme 4.6. Two possible hydrogenation pathways for β-ketoacids.

4.1 – Results and Discussion

4.1.1 – Asymmetric homogeneous hydrogenation of *alpha*- to *delta*-ketoacids

Since α-ketoacids have been studied with successful yields, > 99 %, and enantioselectivities, > 90 %, as with β-ketoacids with enantioselectivities > 95 %, which were also studied by Flowers *et al.*, a previous Jessop group member, we decided to extend the previous work done by Flowers. The study investigated the effects on enantioselectivity and conversion as the linker, n, is increased between the carboxylic acid function group and the prochiral unsaturation.

The five catalysts described in Chapter 3, **38**, **39**, **40**, **41,** and **45** (Figure 4.1) used in the asymmetric hydrogenation of unsaturated carboxylic acids were also employed initially for the hydrogenation of 3-benzoylpropionic acid, **47** (Figure 4.2). This γ-ketoacid was chosen as a test substrate because the linker between the metal-binding functional group and the unsaturation for the analogous compounds having linker lengths of n = 0 and 1 had already been studied. It was found that the first 4 catalysts applied (**38**, **39**, **40**, **41**) did not result in high yields or good enantioselectivities for the final product compared to those obtained for 4-phenyl-4-butanoic acid, **2** (Table 4.4). For the four catalysts, the yield of the reaction for the γ-ketoacid, **47**, was low for catalysts **38**, **40**, and **41**, respectively. The enantioselectivity was also low for the same 3 catalysts,

resulting in 32, 3, and 20 % *ee*, respectively. Surprisingly, the yield and enantioselectivity for the hydrogenation achieved with catalyst **39** were twice as high as the other catalysts. The yield obtain for **39** was 64 % whereas catalyst **40** only obtained a yield of 30 %. The enantioselectivity of catalyst **39** was also 64 %, which was double that of catalyst **38**, which only obtained an *ee* of 32 %. One reason for better yield and enantioselectivity obtained with catalyst **39** could be the increase in steric hindrance around the metal centre of catalyst **39** as well as the narrower bite angle due to the segphos ligand compared to that of catalysts **38** and **39** with their binap backbones.[147]
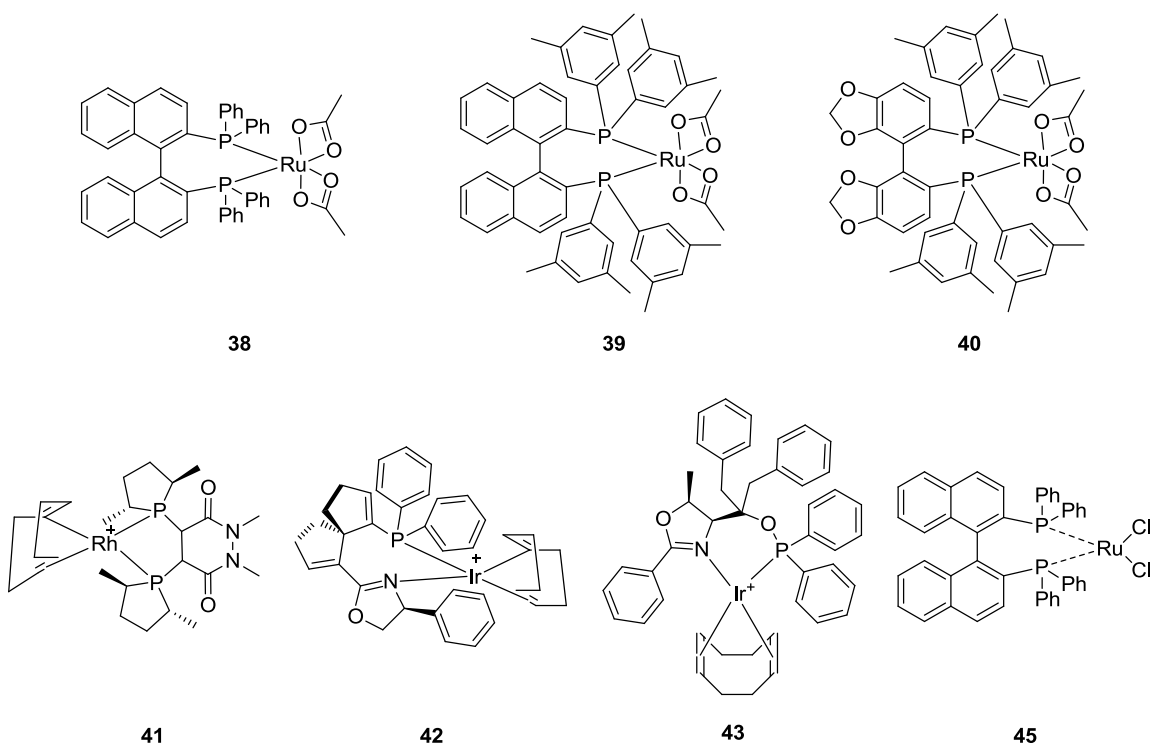
Figure 4.1. Previous catalysts employed in Chapter 3 for the asymmetric hydrogenation of unsaturated carboxylic acids.

47
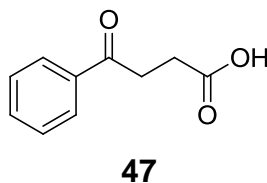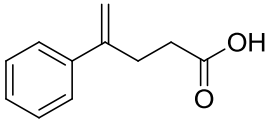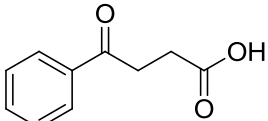
Figure 4.2. γ-Ketoacid, 3-benzoylpropionic acid.

Even though catalyst **39** performed the best of all 4 of the ruthenium catalysts, there was still a much lower yield for the hydrogenation of the ketoacid than for the analogous unsaturated acid. Surprisingly, the enantioselectivity achieved with catalyst **39** for the ketoacid was comparable to that obtained with the unsaturated acid, even though the conversion of the reaction did decrease by *ca.* 35 %. Catalyst **39** produced similar *ee* values for both the olefin and ketone unsaturation, where the 4-phenyl-4-butanoic acid, **2**, resulted in 68 % *ee* and 3-benzoylpropionic acid, **47**, resulted in 64 % *ee.*

The asymmetric hydrogenation of ketoacids requires different catalysts than those initially tested. The above four catalysts for the asymmetric hydrogenation of unsaturated carboxylic acids were poor for the hydrogenation of the ketoacids (Table 4.4). However, Flowers *et al*. showed earlier that the related complex, **45** (Figure 3.5 and Figure 4.1), RuCl$_2$[(S)-BINAP] could obtain conversions approaching 85 % and ee's above 99 % for benzoylacetic acid, a β-ketoacid, **48** (Figure 4.3).[110]

Table 4.4. Comparison of the asymmetric hydrogenation of 4-phenylbutenoic acid, **2**, and 3-benzoylpropionic acid, **47**, for the ruthenium catalysts, **38**, **39**, **40** and the rhodium catalyst, **41**.

Substrate	Cat.	Temp. (°C)	Time (h)	% Yield [a]	% ee [a]
	38	25	14	> 99	61
2	**39**	"	"	> 99	68
	40	"	"	> 99	26
	41	"	"	> 99	11
	38	"	24	8	32
47	**39**	"	"	64	64
	40	"	"	29	3
	41	"	"	17	20

[a] GC-FID values, except where noted.

48
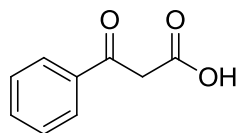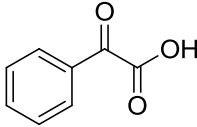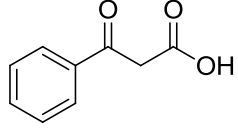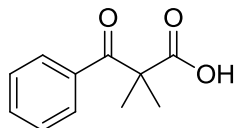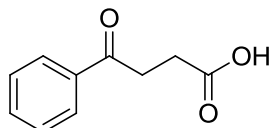
Figure 4.3. β-Ketoacid, benzoylacetic acid, used for the the asymmetric hydrogenation.
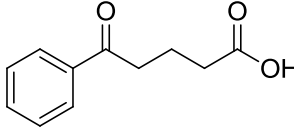
Catalyst 38 was developed by the Noyori group and was the first of many to demonstrate the ability to hydrogenate ketoacids in high yields; however, catalyst 38 gave poor enantioselectivities.[21] Phenylglyoxylic acid, n = 0, was hydrogenated with a yield of 93 % and an enantioselectivity of 45 %.[128] More recently in literature,[110] catalyst 45 demonstrated a high yield and enantioselectivity for the asymmetric hydrogenation of β-ketoacids, n = 1 Table 4.5). For benzoylacetic acid, 48, it was found that a hydrogen pressure of 70 bar gave a good yield and enantioselectivity after 25 h, 84 and > 99 %, respectively. When 2 methyl groups replaced the two hydrogen atoms on the carbon atom in the linker in benzoylacetic acid, the conversion of the ketoacid decreased, presumably due to suppression of enolization. However, with a longer reaction time, a decent yield and a high enantioselectivity were obtained, 75 and 97 %, respectively.[102]

Catalyst **45** was then used for 3-benzoylpropionic acid, **47**. This increase in the length of the carbon linker from n=1 to n=2, γ-ketoacid, **47**, resulted in increased yield compared to that of benzoylacetic acid but somewhat decreased enantioselectivity, 95 and 81 %, respectively. Using catalyst **45** improved both the conversion and enantioselectivity when compared to the catalysts listed in Table 4.4. Comparing the best catalyst, **45**, the yield of the reaction increased *ca.* 30 % and the % *ee* increased *ca.* 20 %.

Table 4.5. Asymmetric hydrogenation of prochiral unsaturated ketoacids.[a) i)]
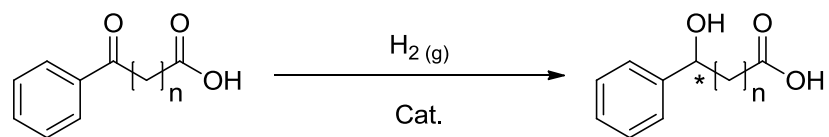
Substrate	Cat.	Temp. (°C)	Time (h)	% Yield [f)]	% ee [f)]
c)	**38**	60	20	93	45
d) **48**	**45**	25	25	84 [g)]	> 99 [g)]
e)	**45**	"	72	75 [g)]	97 [g)]
47	**38**	"	24	20 ±2	15 ±1
	39	"	"	57 ±3	67 ±1
	40	"	"	30 ±5	5 ±1
	41	"	"	10 ±1	19 ±4
	45	"	"	96 ±1	81 ±4

	38	"	"	0 [h]	-
	45	"	"	0 [h]	-
	38	"	48	0 [h]	-
	45	"	"	0 [h]	-
	45 [b]	"	98	49 [h],[f]	24 [f]

49

[a] *Reaction conditions:* 160 mL stainless steel pressure vessel, 100 bar $H_{2(g)}$, methanol in a 1 dram vial. [b] *Reaction conditions:* 160 mL stainless steel pressure vessel, 10 bar $H_{2(g)}$, 2 mL methanol in a 1 dram vial. [c] Data from Noyori *et al.*[128] *Conditions:* 50 atm H_2, toluene. [d] Data from Flowers *et al.*[110] *Conditions:* 70 bar H_2, 3 mL methanol. [e] Data from Flowers *et al.*[110] *Conditions:* 80 bar H_2, 4 mL methanol. [f] GC-FID values, except where noted. [g] Determined by SFC. [h] ^1H NMR yield. [i] Experiments were done in duplicate for **47** and in triplicate for **48** except for the 98 h experiment. Unless stated otherwise all standard deviation are 0. All % yields = % conv and cat. = 0.7-2.3 mol %.

After optimizing the reaction conditions for the γ-ketoacid, the number of carbons in between the carboxylic acid group and the ketone of interest was increased to n = 3. However, neither catalysts **38** or **45** were successful in the enantioselective hydrogenation of 4-benzoylbutyric acid, **49**, under the same conditions. Furthermore, increasing the reaction time to *ca.* four days resulted in only marginal product formation and a low % *ee*, *ca.* 24 %.

With this, we do believe that further improvements for the enantioselectivity of the hydrogenation of 4-benzoylbutyric acid, **49**, are a possibility. Such improvements would have the focus of the study change to the catalysts. By implementing changes in the structure of the catalyst, such as developing bulkier ligands that do not impede the "reaction pocket" of the catalyst, or by changing the metal centre of the catalysts, the enantioselectivity would possibly increase.

4.2 – Conclusions

It can be concluded that the yield and enantioselectivity of the asymmetric hydrogenation of the ketoacids are strongly affected by the change in the unsaturation of interest, olefin to ketone, as well as by the distance between the unsaturation and the carboxylic acid group. Asymmetric hydrogenation of the ketoacid becomes more difficult upon increasing the chain length, n, between the metal-binding functional group and the unsaturation until, at $n = 3$, and the conversion and enantioselectivity are disappointingly low. Increasing the time for the δ-ketoacid ($n = 3$), **49**, did not affect the yield until the reaction was left to stir for four days. Even though some product was obtained from the reaction, the enantioselectivity was poor, only obtaining a % *ee* of 24 %. For both the unsaturated carboxylic acid and the ketoacids, it seems that the maximum number of carbon atoms between the metal-binding functional group and the unsaturation is 2. However, the unsaturated carboxylic acid substrate with a

linker of n = 2, 4-phenyl-4-butenoic acid, **2**, was hydrogenated with high conversion, however there was an enantioselectivity of 68 %. On the other hand, the γ-ketoacid, 3-benzoylpropionic acid, **47**, worked just as well as the β-ketoacid, benzoylacetic acid, **48**, n = 1, with a yield of 96 % and an enantioselectivity of 81 %, whereas the β-ketoacid obtained a yield of 84 % and a % *ee* of > 99 %. Overall, these catalysts work well until we increase the chain length or number of carbon atoms past 2.

Chapter 5 – Asymmetric Hydrogenation of Allylamines

5.1 – Introduction

5.1.1 – Literature reports of asymmetric hydrogenation of related substrates

Optically active amines and their derivatives are found in many drugs, as well as natural and bioactive products; accordingly, it is not surprising these chiral building blocks are used for pharmaceuticals, agrochemicals and as resolving agents or chiral auxiliaries.[20,148–152] Many efforts have been directed towards the enantioselective hydrogenation of C=C and C=N double bonds, as it could afford an efficient and convenient route to desired chiral amine substrates.[20,85,149,150,153–158] The asymmetric hydrogenation of unsaturated C=C double bonds, i.e. olefins, containing N-acyl and carbamate functional groups, was first described by Knowles *et al.*[34,38] in 1968, and by Kagan *et al.*[159] in 1975. Since then, the variety of these unsaturated substrates has expanded alongside the homogeneous asymmetric hydrogenation catalysts used to make them. The unsaturated amine-containing substrates studied today are α- and β-amino acids,[20,21,91,150,154,156,157] imines,[22,82,151,160–162] and unsaturated olefins

containing protected amino groups, which include N-acyl,[20,153,163] carbamates,[149] and others.[152,164,165]

The most studied unsaturated amine-containing substrates used to evaluate catalysts for asymmetric hydrogenation are α- and β-amino acids, specifically α- and β-dehydroamino acids.[20–22,82] Even though Ru, Rh, and Ir based catalysts have been used successfully (i.e. complete conversion and *ee* > 90 %) Rh-based catalysts with phosphine ligands have been demonstrated to be the most effective for the asymmetric hydrogenation of α,β-dehydroamino acids (Figure 5.1).[20] The most commonly studied α-dehydroamino acids for the asymmetric hydrogenation reaction are (Z)-2-(acetamido)cinnamic acid, 1-(acetamido)acrylic acid, and their methyl esters, (Table 5.1).[20] A number of Rh complexes achieved both high conversions and enantioselectivities for the asymmetric hydrogenation of these α-dehydroamino acids. It was found that [((S,S)-Ph-Quinox)Rh(COD)]BF$_4$ exhibited high activity and selectivity in the asymmetric hydrogenation of olefins which resulted in an *ee* of 99.9 %. Also, when a more versatile ligand was used, such as the "ClickFerroPhos", the Rh complex readily hydrogenated the prochiral dehydroamino acids resulting in an *ee* of 96 % when a 1:1 ratio of MeOH and toluene was used.

(R,R)-Me-BPE

(R,R)-DUPHOS

TangPhos

SIAPhos

3,3'-substituted phosphoramidites

ClickFerrophos

(S,S)-Ph-Quinox

(R,R)-Ph-BPM

4-amino-4,5-dihydro-3H-dinaphtho[2,1-c;1',2'-e]phosphepine
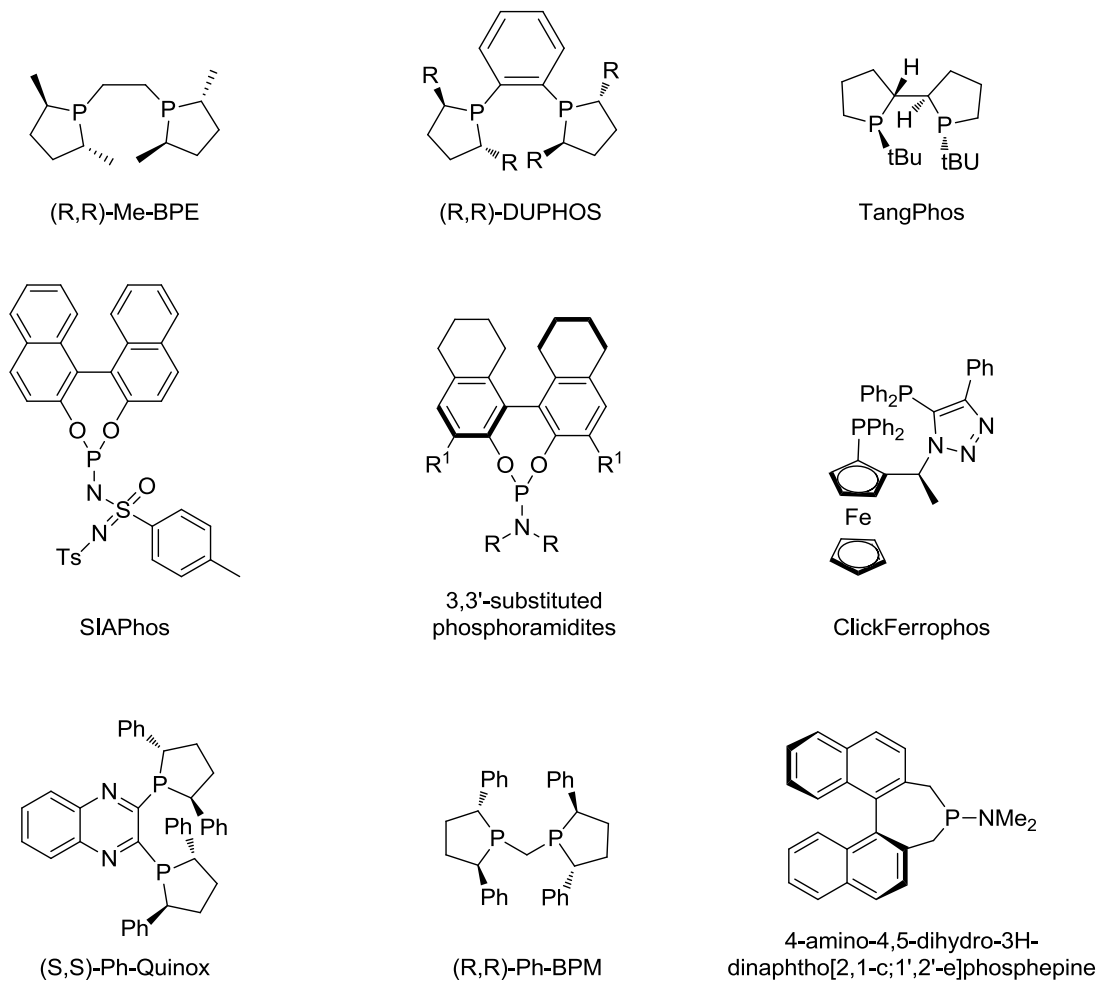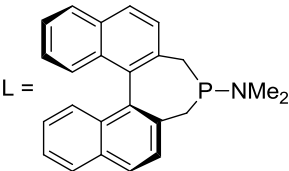
Figure 5.1. Chiral phospine ligands utilized in literature for the asymmetric hydrogenation of α-dehydroamino acids, enamides and one carbamate ester.

Table 5.1. Asymmetric hydrogenation of protected α-dehydroamino acids using rhodium-based phosphine catalysts.[a]
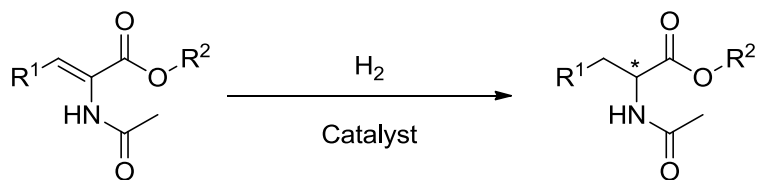
R¹	R²	Catalyst	Reaction Conditions	% ee (Config.)	Reference
H	H	[((R,R)-Ph-BPM)Rh(COD)]BF$_4$	MeOH, 30 °C, 6 bar	> 99 (S)	[166]
H	Me	[((S,S)-Ph-Quinox)Rh(COD)]BF$_4$	MeOH, 25 °C, 10 bar	99.9 (R)	[167]
H	Me	[Rh(nbd)$_2$]BF$_4$/ClickFerro-Phos complex	MeOH/toluene 1:1, 1 atm	99.3 (R)	[139]
Ph	H	[Rh(nbd)$_2$]BF$_4$/ClickFerro-Phos complex	MeOH/toluene 1:1, 1 atm	99 (R)	[139]
Ph	Me	[Rh(COD)L$_2$]BF$_4$ L =	toluene/ sodium dodecylsulfate, 25 °C, 1 bar	96 (R)	[156]

a) All examples above demonstrated complete conversion for all catalytic hydrogenations listed.

Currently, to obtain chiral amines through asymmetric hydrogenation of allylamines, one must use good metal-binding functional groups or sterically

bulky substrates containing unfunctionalized amines. One method in particular that is utilized in asymmetric hydrogenation of olefins is an amide functional group, such as the N-acetyl group, rather than an amine. Once the enantioselective hydrogenation is completed the N-acetyl group can be transformed into the desired amine substrate by treatment with base.[41] The other method frequently employed is to have a second functional group in the molecule, such as a carboxylic acid or the methylester derivative, neighbouring the unsaturation to aid in the metal coordination.

The asymmetric hydrogenation with the presence of an N-acetyl group has been demonstrated with a few examples of enamides. Nonetheless, the chiral amines obtained from the hydrogenation of prochiral enamines are an important class of substrate that are frequently employed as building blocks in pharmaceuticals and resolving agents or chiral auxiliaries.[20] As with the hydrogenation of dehydroamino acids, most examples for the asymmetric hydrogenation of enamides involve Rh-phosphine complexes with some recent examples utilizing ruthenium and iridium-based complexes (Table 5.2).[20,149,153,163,168–170] The Rh-based phosphine catalysts demonstrated high enantioselectivity and complete conversion for the hydrogenation of prochiral enamides. For example, the asymmetric catalysts (R,R)-Me-BPE-Rh and TangPhos-Rh were successfully used in the hydrogenation of an α-arylalkylenamide resulting in an *ee* of 95 and > 99 %, respectively. However, when the same α-arylalkylenamide was hydrogenated by an iridium-complex with

the 3,3'-substituted phosphoramidite ligand the best *ee* achieved was 84 %. One example of a carbamate ester was asymmetric hydrogenated using a Ru catalyst with complete conversion, however, only a 77 % *ee* was obtained for such substrates.

Table 5.2. Highlighted examples of asymmetric hydrogenation of various enamides and one carbamate ester demonstrating very good enantioselectivities for Rh-based complexes and decent enantioselectivities for new Ru- and Ir complexes.[a]
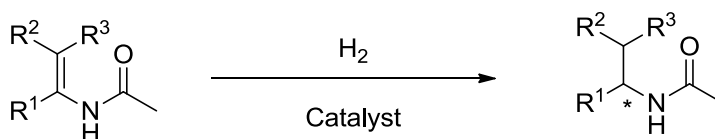
Substrate	Catalyst	Reaction Conditions	% ee (Config.)	Reference
	(R,R)-Me-BPE-Rh	MeOH, 22 °C, 60 bar, 15 h	95.2 (R)	[153]
	[Ir(cod)Cl]$_2$/2L L = 3,3'-substituted phosphoramidites	toluene, 10 °C, 10 bar, 16 h	84 (S)	[170]
	TangPhos-Rh	MeOH, RT, 20 PSI, 12 h	> 99	[171]
	(S,S)-Me-DuPHOS-Rh	MeOH, 22 °C, 60 bar, 15 h	96.6 (S)	[153]
	(SIAPhos)-Ir	CH$_2$Cl$_2$, RT, 50 bar, 18 h	70	[168]
	(S,S)-Et-DuPHOS-Ru	MeOH, 50 °C, 100 bar, 20 h	77	[149]

a) All examples above demonstrated complete conversion for all catalytic hydrogenations listed.

As previously mentioned above, there is a demand for chiral amines for pharmaceuticals and natural products. In 2005, the American Chemical Society Green Chemistry Institute brought together several leading pharmaceutical companies and created a list of chemical transformations that, if made more sustainable would allow for a cleaner synthetic approach to many pharmaceuticals.[90] One reaction near the top of that list is the asymmetric hydrogenation of unfunctionalized olefins, enamines, imines and similar molecules.[90] However, it would be more efficient to asymmetrically hydrogenate these prochiral enamines as their prochiral primary amine derivatives. To the best of our knowledge, the direct asymmetric hydrogenations with prochiral allylamines have not been studied to obtain the desired chiral products. Below we discuss a new methodology and its development, with the objective to hydrogenate a prochiral allylamine, 2-phenylprop-2-en-1-amine, **22**, with high conversions and good enantiomeric excess.
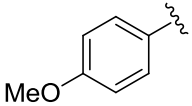
5.1.2 – A strategy for asymmetric hydrogenation of unprotected allylamines

The strategic plan for the asymmetric hydrogenation of prochiral allylamines involved developing a methodology that would overcome two major challenges common to homogeneous asymmetric hydrogenation: the lack of or poor ability to coordinate to the metal, and the distance between the coordinating functional group and the prochiral centre of the substrate, which was shown in

Chapters 3 and 4 to work with a maximum length of 2 atoms. The most important aspect to consider is the poor ability of some substrates to coordinate to the catalyst's metal centre that would be detrimental to the catalytic transformation in terms of enantiomeric excess. In current literature, unfunctionalized and functionalized prochiral amine containing compounds are usually the two types of amine substrates commonly studied with hydrogenations. As discussed above, these functionalized prochiral amine containing compounds are dehydroamino acids and enamines. To overcome the poor coordinating ability, Pfatlz *et al.* demonstrated significant results toward the hydrogenation of unfunctionalized tertiary amines by using sterically hindered substrates and iridium catalysts (Table 5.3).[152] They have also demonstrated the hydrogenation of functionalized allylamines, resulting in higher stereoselectivity. These functionalized allylamines usually have a much stronger coordinating group attached to the amine functionality, such as an N-acetyl group,[93] or a second functional group that is strongly coordinating elsewhere in the substrate, such as those found in dehydroamino acids.[20,21]

Table 5.3. Asymmetric hydrogenation of unfunctionalized enamines using an Iridium-P,N catalysts.[152]
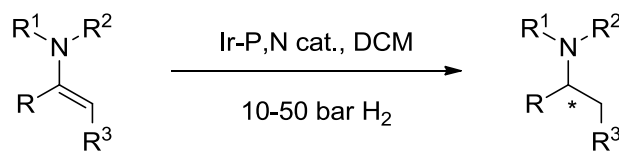
R	R^1	R^2	R^3	Conv. (%)	ee (%)
Ph	Me	Ph	H	98	91 (+)
"	"	Bn	"	> 99	78 (+)
MeO-C6H4 (structure)	"	"	"	> 99	56 (+)
Ph	Et	Et	"	> 99	18 (+)

We desired a different route that was more direct, potentially greener, and could use already developed and well-known catalysts. Recently, a method had been developed that utilized $CO_{2(g)}$ along with amine containing substrates to form either carbamic acids or carbamate salts, which allows aqueous and organic solvents to become miscible, or better known as switchable polarity solvents.[172–177] Many applications developed from this reaction took advantage of its reversibility (Scheme 5.1).[172–177] We felt that this strategy could be an advantage with our amine substrates for asymmetric hydrogenations. There were

also two reports by Chatterjee *et al.*[178] and Xie *et al.*[179] where they implemented $CO_{2(g)}$ in the hydrogenation of nitriles and imines. They suggested that the formation of the carbamic acid, through the reaction of $CO_{2(g)}$ with an amine, could act as a protecting group during the hydrogenation, improving selectivity of the reaction and preventing catalyst deactivation.[178,179] We hypothesized that if $CO_{2(g)}$ could act as a protecting group and functionalize the amine into a stronger metal-coordinating group, then it could replace the N-acetyl group that is currently used for asymmetric hydrogenation. Converting the amine into a carbamate or carbamic acid during the hydrogenation reaction would circumvent separate amine protection and deprotection steps, making this a potentially greener route to the desired product as less material is used and the potential byproducts eliminated.[180,181] Therefore, the objective is to employ an *in situ* reversible modification to temporarily change a poorly coordinating functional group into a strongly coordinating group, and allow for efficient catalysis (Scheme 5.2). In order to induce this reversible transformation, $CO_{2(g)}$ and a base will be employed to convert 1° and 2° amines to carbamate salts or carbamic acids,[172] which will then be hydrogenated using previously studied transition metal based hydrogenation catalysts. After hydrogenation, the substrate will be exposed to heat or argon to liberate $CO_{2(g)}$ and thus yield an amine with a chiral centre. This method can only be employed for 1° and 2° amines and not 3°, since a proton must be available on the amine functionality to form the carbamic acid and sequentially a carbamate salt using $CO_{2(g)}$.
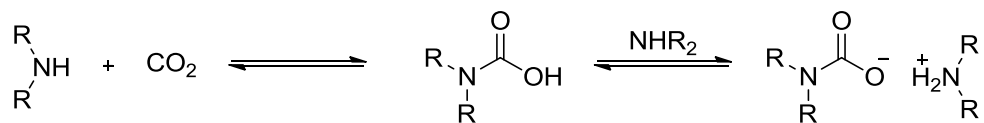
Scheme 5.1. Secondary amine reacting with $CO_{2(g)}$ to produce a carbamic acid. A subsequent reaction occurs with another equivalent of the amine, or another base, to result in the carbamate salt.[172]
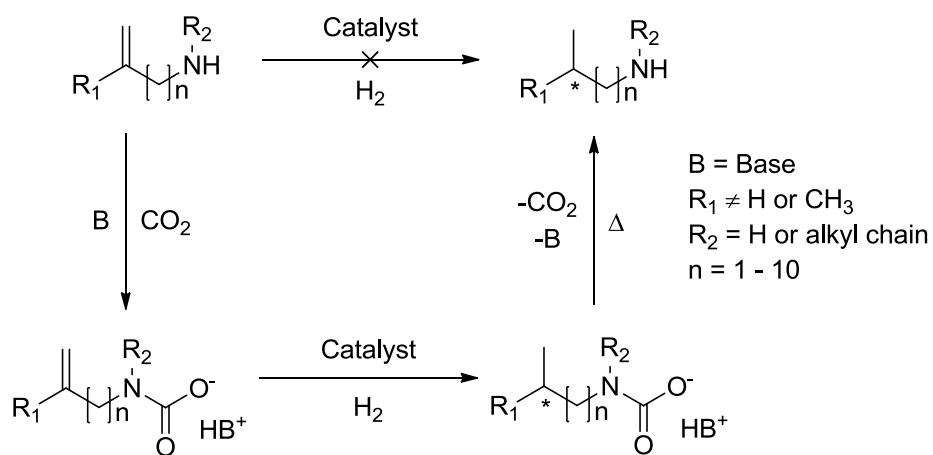
Scheme 5.2. New hydrogenation route for allylamines implementing a reversible modification with CO_2. Where the x implies the reaction without CO_2 produces poor results.

5.2 – Results and Discussion

The objective of this project was to develop a new asymmetric hydrogenation methodology utilizing $CO_{2 (g)}$ to obtain chiral substrates from solely unfunctionalized primary or secondary amines. Before the details of the proposed methodology is discussed, it is necessary to pick an appropriate substrate to develop the methodology with.

5.2.1 –Substrate Selection

In the first step of the reaction, the amine substrate will react with the available $CO_{2 (g)}$ to change the amine, a poor metal-binding functional group, into a carbamic acid, a good metal-binding functional group (Scheme 5.3). That means the number of atoms between the olefin and the metal is increased by 2 for that substrate, i.e. the total number of atoms is 4. As discussed in sections 3.2.2 and 4.1.1, the enantioselectivity and conversion of the reaction diminishes if the number of atoms between the unsaturation and the metal is longer than 4. Therefore, the substrates that could be employed in the study can be either 1-phenylethenamine, where the prochiral unsaturation would be 3 atoms away from the metal centre of the catalyst during the hydrogenation, or 2-phenylprop-2-en-1-amine, **22**, where the prochiral unsaturation would be 4 atoms away from the metal centre during the hydrogenation. Out of the two choices, 2-phenylprop-2-en-1-amine, **22** was selected for the asymmetric hydrogenation as we could

directly compare the effects of the length of the linker to 4-phenyl-4-pentenoic acid, **2**, and 3-benzoylpropionic acid, **47**, which both contain 4 atoms between the unsaturation and the metal centre during the hydrogenation. We also did not study 1-phenylethenamine, as we wanted to avoid the possibility of an amine/imine tautomerization occurring during the hydrogenation.
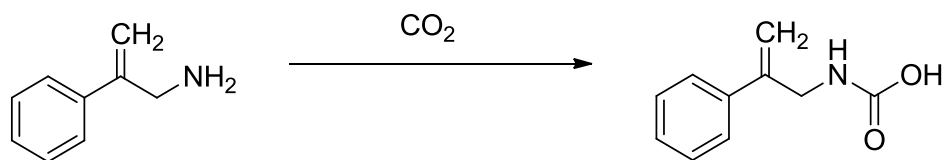
Scheme 5.3. Reaction of CO_2 with 2-phenylprop-2-en-1-amine, **22**.

5.2.2 – Synthesis of prochiral allylamines

For experimental procedure and general information see Chapter 2.

5.2.2.1 – Synthesis of 2-phenylprop-2-en-1-amine, 22

The synthesis of 2-phenylprop-2-en-1-amine, **22**, (Scheme 5.4) was developed from previous methods; see Sections 2.2.3.1, 2.2.4.1, and 2.2.4.4. The initial attempt was to first synthesize an alkenyl bromide, followed by a Gabriel synthesis and then a deprotection of the phthalimide (Scheme 5.4). This synthesis of 2-phenylprop-2-en-1-amine was successful; however, initial yields were low, < 10 %, for two of the three steps of the reactions.

Step 1:

12

Step 2:

17

Step 3:

22
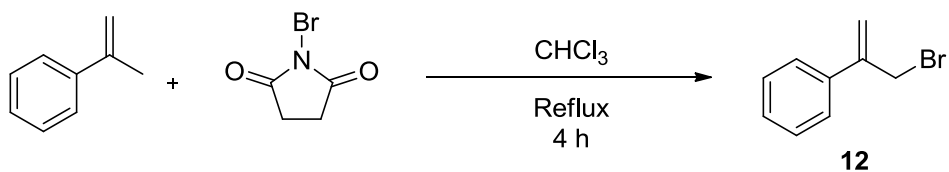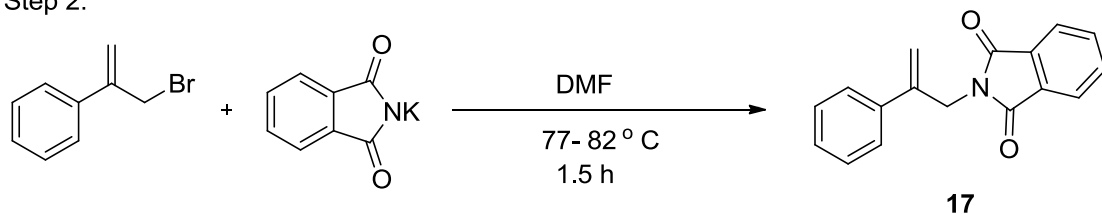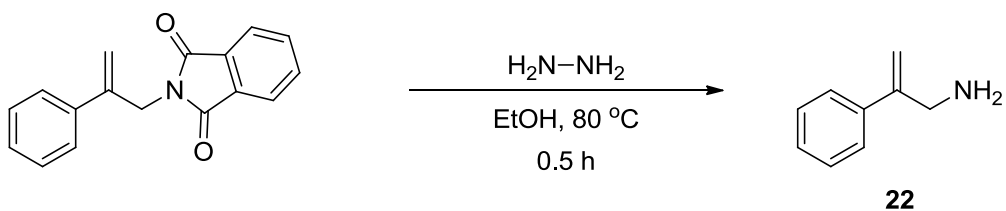
Scheme 5.4. Overall synthetic design for the preparation of 2-phenylprop-2-en-1-amine.

One problem encountered during the bromination of α-methylstyrene was that the outcome of the reaction was dependent on the purity of the NBS (Scheme 5.4). For the bromination step to work, it was necessary to have ppm amounts of bromine in the NBS to initiate the reaction. That is, the older the NBS, which led to some decomposition, the better the reaction outcome. A few drops of bromine were added to the reaction to compromise the purity of NBS; that led

to an increase in yield, 46 %, of the desired product, α-(bromomethyl)styrene, **12**. To improve the reaction yield further, up to 76 %, it was found that the removal of the inhibitor, p-*tert*-butylcatechol, was necessary; this was achieved by running the starting material, α-methylstyrene, through a glass fritted funnel containing a basic alumina plug beforehand.

The synthesis of 2-phenyl-3-phthalimidopropene, **17**, proceeded according to literature[70] in a yield of 87 %. The removal of the phthalimide functional group, i.e. deprotection of the amine, yielded not only the allylamine, but the hydrazine hydrate also reduced the target alkene of the substrate. It was necessary to add *ca.* 2 mol % hydrazine hydrate to the slurry of reactants at room temperature with vigorous stirring. We found if *ca.* 3 mol % or more was added, we obtained undesired hydrogenated product. If a smaller amount was added, *ca.* 1.2 mol %, the reaction time had to be increased, which caused the reaction to become incomplete while still obtaining the undesired reduced product. We also found the scale of the reaction, mg to g, affected the amount of time required for the reaction to occur, potentially due to mass transfer of the hydrazine hydrate. It was absolutely necessary to monitor the reaction for the formation of the new precipitate as the reaction needed to be removed from the heat once a significant amount of precipitate was visible in the solution to avoid formation of the reduced product. The desired 2-phenylprop-2-en-1-amine, **22**, was obtained with a yield of 86 %.

5.2.2.2 – Synthesis of the other allylamine derivatives

The methodology used to synthesize **22** (Scheme 5.4) was modified, *vide infra*, and was adopted in the synthesis of the allylamine derivatives: 2-[4-(trifluoromethyl)phenyl]prop-2-en-1-amine, **23**, 2-(4-ethoxyphenyl)prop-2-en-1-amine, **24**, 2-(naphthalene-2-yl)prop-2-en-1-amine, **25**, and 2-(4-nitrophenyl)prop-2-en-1-amine.

5.2.2.2.1 – Synthesis towards 2-[4-(trifluoromethyl)phenyl]prop-2-en-1-amine, 23, through bromination of 2-[4-(trifluoromethyl)phenyl]prop-2-en-1-ol, 15

The synthesis of 1-(3-bromoprop-1-en-2-yl)-4-(trifluoromethyl)benzene, **16**, was broken into two steps, 1a and 1b, (Scheme 5.5) as described in sections 2.2.3.5 and 2.2.3.6. It was found that the two step procedure worked better in terms of obtaining the desired brominated product for the fluorinated substrate. From Scheme 5.5, 1-(3-bromoprop-1-en-2-yl)-4-(trifluoromethyl)benzene, **16**, could be obtained by first synthesizing 2-[4-(trifluoromethyl)phenyl]prop-2-en-1-ol, **15**, via a cuprate catalyzed Grignard reaction, 1a. Once the alcohol was synthesized, the hydroxyl group was exchanged for a bromide atom by the reaction with phosphorus tribromide, 1b.

Step 1a:
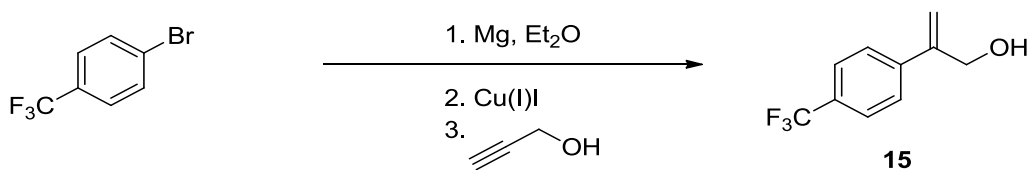
Step 1b:
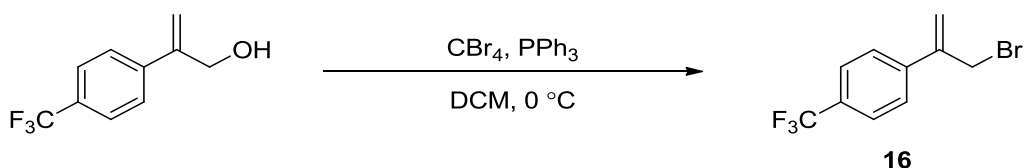
Scheme 5.5. Synthetic route to obtain alkenyl bromine derivative, 1-(3-bromoprop-1-en-2-yl)-4-(trifluoromethyl)benzene, **16**, through a cuprate-catalyzed Grignard reaction followed by a bromination.

5.2.2.2.2 – Synthesis of 2-(4-ethoxyphenyl)prop-2-en-1-amine, 24, through bromination of 4'-ethoxyacetophenone and a Wittig reaction

Initially, 4'-ethoxyacetophenone was converted into 1-ethoxy-4-(prop-1-en-2-yl)benzene, **8**, through a Wittig reaction (Scheme 5.6) obtaining an isolated yield of 85 %. Following the synthesis of the α-methylstyrene derivative, **8**, the synthetic steps in Scheme 5.6 were applied for the preparation of 1-(3-bromoprop-1-en-2-yl)-4-ethoxybenzene. As with the synthesis of the other derivatives, step one involving bromination became an issue. During the bromination step the desired monobrominated product was formed, 1-(3-

bromoprop-1-en-2-yl)-4-ethoxybenzene; however, multiple dibrominated products were recovered as well (Scheme 5.7). Column chromatography was challenging to isolate the desired product causing excessive losses.
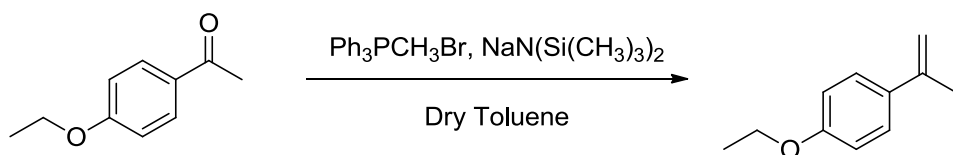
Scheme 5.6. Wittig reaction of 4'-ethoxyacetophenone to prepare 1-ethoxy-4-(pro-1-en-2-yl)benzene, **8**.
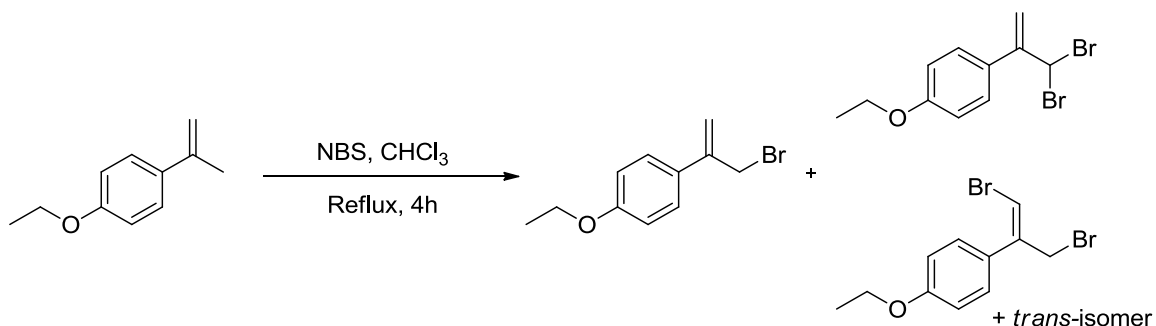
Scheme 5.7. Resulting products from following the bromination procedure for α-methylstyrene in discussed in sections 2.2.3.1 and 5.1.1.1 applied to 4'-ethoxyacetophenone.

Alternatively, 4'-ethoxyacetophenone was monobrominated by a modified procedure (step 1, Scheme 5.8), as described in section 2.2.3.4.[65,66]   Once formed, the brominated ketone was reacted with potassium phthalimide to form 2-[2-(4-ethoxyphenyl)-2-oxoethyl]-1*H*-isoindole-1,3(2*H*)-dione, **19**, as described in section 2.2.4.1. Performing the Gabriel synthesis before the Wittig reaction removed the possibility of a polymerization with during the Wittig reaction. This was then followed by a Wittig reaction, step 3 (Scheme 5.8), to produce the desired olefin (as described in section 2.2.2). The last step of the synthetic route in Scheme 5.8 followed the general deprotection step previously discussed for 2-phenylprop-2-en-1-amine, **22**, to obtain the desired product **24**.

Step 1:
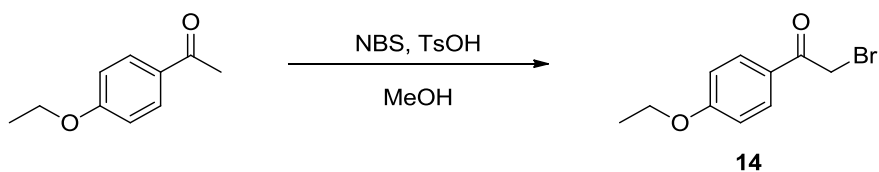
Step 2:
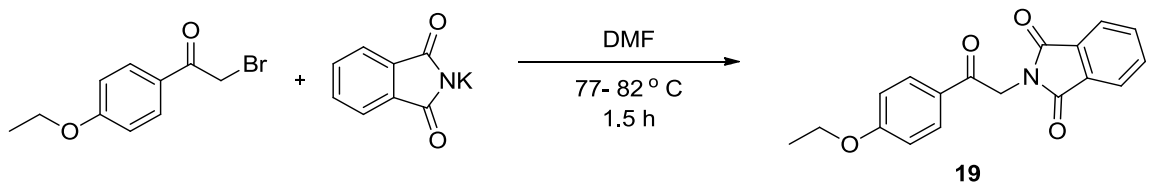
Step 3:
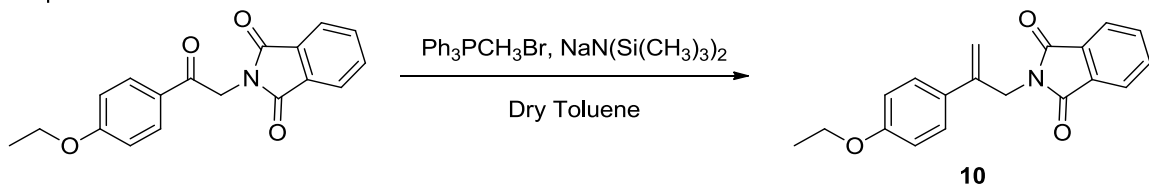
Step 4:
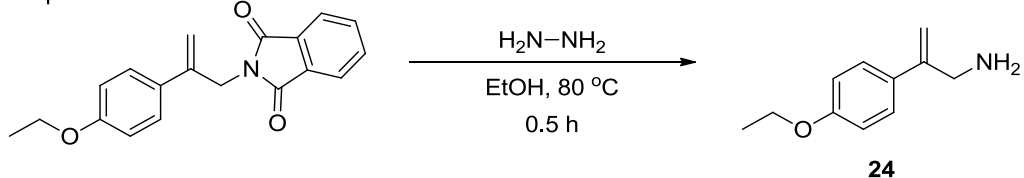
Scheme 5.8. The preparation of 2-(4-ethoxyphenyl)prop-2-en-1-amine, **24**.

5.2.2.2.3 – Synthesis towards 2-(naphthalene-2-yl)prop-2-en-1-amine, 25

The synthesis of 2-(naphthalene-2-yl)prop-2-en-1-amine, **25**, was adapted from the synthetic route discussed above for 2-phenylprop-2-en-1-amine, **22**, in Scheme 5.4. Initially, a Wittig reaction on 2-acetonaphthone produced 2-(prop-1-en-2-yl)naphthalene, **9**, followed by bromination. Chloroform instead of THF was

142

used for the synthesis of 2-(3-bromoprop-1-en-2-yl)naphthalene, and the reaction was done under inert conditions. The last two steps in Scheme 5.4 were followed without change, producing **25** in 76 % yield.

5.2.2.2.4 – Synthesis of 2-(4-nitrophenyl)prop-2-en-1-amine

2-(4-Nitrophenyl)prop-2-en-1-amine, **50**, was chosen to study the effects that electron-withdrawing substituents would have on the asymmetric hydrogenation of an unsaturated prochiral amine containing substrate. The synthetic strategy designed for the synthesis of 2-(4-nitrophenyl)prop-2-en-1-amine (Scheme 5.9) was similar to that of **22**. The commercially available 2-bromo-4'-nitroacetophenone reacted to form 2-[2-(4-nitrophenyl)-2-oxoethyl]-1*H*-*iso*indolde-1,3(2*H*)-dione, **20**, through a Gabriel synthesis. However, **20** did not precipitate appreciably but instead stayed in the DMF:H_2O solution mixture (see sections 2.2.4.1 and 2.2.4.3). The product 2-[2-(4-nitrophenyl)-2-oxoethyl]-1*H*-*iso*indolde-1,3(2*H*)-dione, **20**, was extracted from the DMF:H_2O solution mixture using ethyl acetate. Once the solvent was removed by rotatory evaporation, the solid was recrystallized from hot THF. After multiple extractions, and a copious amount of ethyl acetate, *ca.* 4 L, the isolated yield was low, 24 %. Following the synthetic route below shown in Scheme 5.9, the next step was a Wittig reaction to form the desired alkene. It is believed that the low solubility of **20** in most organic solvents cause the reaction to be low yielding at 13 %. As a result of the

poor yields and insolubility issues, the synthesis of 2-(4-nitrophenyl)prop-2-en-1-amine was not continued.

Step 1:
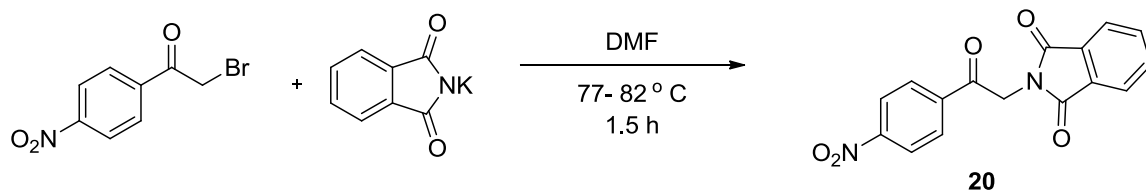
Step 2:
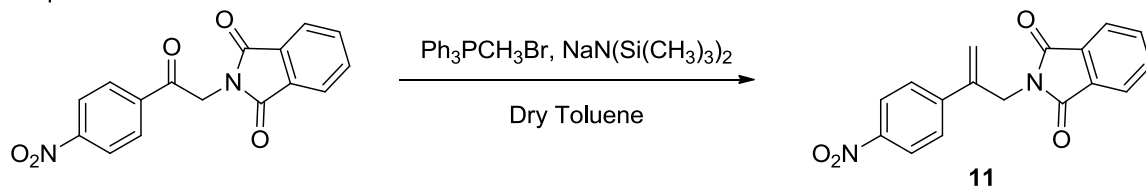
Step 3:
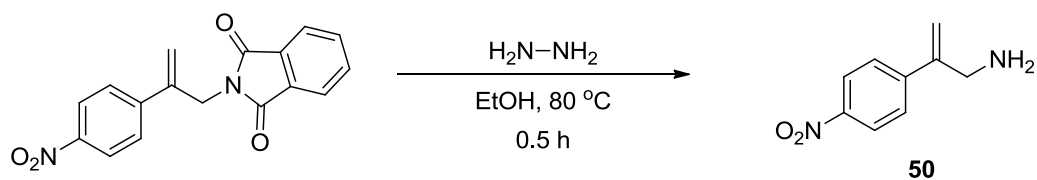
Scheme 5.9. Synthetic route to 2-(4-nitrophenyl)prop-2-en-1-amine, **50**, from

2-bromo-4'-nitroacetophenone.

5.2.3 – Asymmetric homogeneous hydrogenation methodology development for 2-phenylprop-2-en-1-amine

As an extension to the previous studies on the effects of alkyl chain length, the five catalysts described above (**38**, **39**, **40**, **41**, and **45**) were employed in the asymmetric hydrogenation of unsaturated allylamines. Four different conditions were investigated for the hydrogenation of 2-phenylprop-2-en-1-amine, **22**; each catalyst listed above was tested with a) only $H_{2(g)}$, b) $H_{2(g)}$ and base, c) $H_{2(g)}$ and $CO_{2(g)}$, and lastly d) $H_{2(g)}$, $CO_{2(g)}$ and base. It was necessary to select a base that would preferably not form a carbamic acid and have a high enough basicity, to deprotonate the substrate to form the carbamate; thus, 1,8-diazabicyclo[5.4.0]undec-7-ene, DBU, was selected (Scheme 5.10).[172]
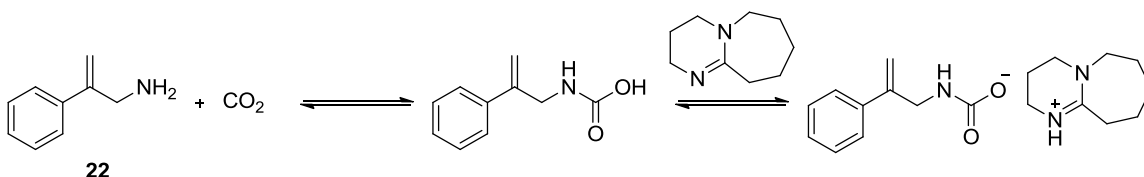
Scheme 5.10. Hypothesis for the interaction of the unsaturated allylamine, **22**, with DBU and $CO_{2(g)}$.

Initial experiments were conducted for 24 h in order to maximize the chances that at least one catalyst would be able to give a significant yield in the asymmetric hydrogenation of 2-phenylprop-2-en-1-amine, **22** (Table 5.4). With solely $H_{2(g)}$, all catalysts produced low to moderate yields and *ee*s of 2-phenylpropan-1-amine, **34**, during the hydrogenation. Using catalysts, **39**, **40**, **41**

and **45** resulted in conversions between 29 ~ 38 %. However, with catalyst **38**, 2-phenylpropan-1-amine, **34**, was produced in a yield of 72 %. In regards to the enantioselectivities with only $H_{2(g)}$ present, low *ee*s, ca. 30 %, for catalysts **38** and **45** were obtained. The *ee* was increased to 48 % and 60 % when the catalyst was changed to **39** and **40**, respectively, with this increase most likely due to the steric bulk of the mesitylenes found on the binap ligand. The high *ee* seen when catalyst **40** was used in comparison to **39** is most likely due to the electronics of the dm-segphos backbone in catalyst **40**. The use of catalyst **41** resulted in the highest enantioselectivity, 74 %.

When the conditions were changed to include DBU with $H_{2(g)}$ (Table 5.4), the yield of **34** did not change significantly for catalysts **45**, **39**, and **40**, 38 ~ 48 %. The conversion for catalyst **38**, however, decreased by *ca.* 50 %, and increased by *ca.* 20 % for catalyst **41**. Once $CO_{2(g)}$ was added to the asymmetric hydrogenation, with and without base, an increase in both the conversion and the enantioselectivity of the reaction was observed. By adding $CO_{2(g)}$ with the base, the conversions of catalysts **45**, **39**, **40**, and **41**, all increased *ca.* 50, 10, 20, and 30 %, respectively. However, the conversion for catalyst **38** was not affected by the addition of $CO_{2(g)}$ remaining constant within error, 64 %. The enantioselectivity of the hydrogenation of **22** was not affected by the addition of only $CO_{2(g)}$. When $CO_{2(g)}$ and DBU were present in the hydrogenation the yield increased but the enantioselectivity remained constant.

Table 5.4. Initial asymmetric hydrogenation for 2-phenylprop-2-en-1-amine, **22**, testing four different conditions: only $H_{2(g)}$; $H_{2(g)}$ and DBU; $H_{2\ g)}$ and $CO_{2(g)}$; and $H_{2(g)}$, $CO_{2(g)}$ and DBU.[a]

$$\mathbf{22} \xrightarrow[\textbf{CAT.}, \text{24 h, DBU, MeOH}]{\text{90 bar } H_2, \text{ 10 bar } CO_2} \mathbf{34}$$

Catalyst Screening	Cat.	H_2 [b]		H_2 + DBU [c]		H_2 + CO_2 [d]		H_2 + CO_2 + DBU [e]	
		% yield[f]	% ee[g]	% yield[f]	% ee[g]	% yield[f]	% ee[g]	% yield[f]	% ee[g]
	38	72	33	21	50	64	26	68	25
24 h	**45**	32	30	38	52	85	26	96	31
High	**39**	35	48	38	49	45	36	64	31
Pressure	**40**	38	60	48	49	56	41	50	40
	41	29	74	54	31	64	77	96	75

a) Experiments were done in triplicate and at RT. Conversions for all reactions above was > 95 % and the experimental errors for % yield and % *ee* were ±10 and ±4, respectively. b) *Reaction conditions:* 160 mL stainless steel pressure vessel, 10 mg **22**, 100 bar $H_{2(g)}$, 2 mL methanol in a 1 dram vial. c) *Reaction conditions:* 160 mL stainless steel pressure vessel, 10 mg **22**, 100 bar $H_{2(g)}$, 1 eq. DBU, 2 mL methanol in a 1 dram vial. d) *Reaction conditions:* 160 mL stainless steel pressure vessel, 10 mg **22**, 90:10 bar $H_{2(g)}$:$CO_{2(g)}$, 2 mL methanol in a 1 dram vial. e) *Reaction conditions:* 160 mL stainless steel pressure vessel, 10 mg **22**, 90:10 bar $H_{2(g)}$:$CO_{2(g)}$, 1 eq. DBU, 2 mL methanol in a 1 dram vial. f) ^{1}H NMR values, internal standard used: 1,3,5-trimethoxybenzene. g) Determined by HPLC.

Following the positive results for the asymmetric hydrogenation at 24 h, the reaction time was investigated (Table 5.5). By decreasing the time for all four conditions, we found an increase in conversion for all catalysts. However, there were no differences in enantioselectivities with any of the catalysts. Even so, catalyst **41** demonstrated the best results of all the catalysts for the asymmetric hydrogenation of 2-phenylprop-2-en-1-amine, **22**. When $CO_{2(g)}$ was present, the conversion without base was 84 % and increased with the presence of base to 94 %.

Table 5.5. Asymmetric hydrogenation of 2-phenylprop-2-en-1-amine, **22**, testing a shorter reaction time, overnight 14-15 h.[a]

Catalyst Screening	Cat.	H_2 [b]		H_2 + DBU [c]		H_2 + CO_2 [d]		H_2 + CO_2 + DBU [e]	
		% yield[f]	% ee[g]	% yield[f]	% ee[g]	% yield[f]	% ee[g]	% yield[f]	% ee[g]
	38	79	33	48	45	70	23	73	25
14 - 15 h	**45**	72	31	60	46	72	25	92	25
High	**39**	66	39	52	42	82	36	69	36
Pressure	**40**	67	57	58	48	84	37	62	49
	41	57	68	50	26	84	75	94	73

[a] Experiments were done in triplicate and at RT. Conversions for all reactions above was > 95 % and the experimental errors for % yield and % *ee* were ±10 and ±4, respectively. [b] *Reaction conditions:* 160 mL stainless steel pressure vessel, 10 mg **22**, 100 bar $H_{2(g)}$, 2 mL methanol in a 1 dram vial. [c] *Reaction conditions:* 160 mL stainless steel pressure vessel, 10 mg **22**, 100 bar $H_{2(g)}$, 1 eq. DBU, 2 mL methanol in a 1 dram vial. [d] *Reaction conditions:* 160 mL stainless steel pressure vessel, 10 mg **22**, 90:10 bar $H_{2(g)}$:$CO_{2(g)}$, 2 mL methanol in a 1 dram vial. [e] *Reaction conditions:* 160 mL stainless steel pressure vessel, 10 mg **22**, 90:10 bar $H_{2(g)}$:$CO_{2(g)}$, 1 eq. DBU, 2 mL methanol in a 1 dram vial. [f] ^{1}H NMR values, internal standard used: 1,3,5-trimethoxybenzene. [g] Determined by HPLC.

It was concluded from Table 5.4 and Table 5.5 that Rh-based catalysts may be more suitable for the asymmetric hydrogenation of 2-phenylprop-2-en-1-amine, **22**, as catalyst **41** yielded higher conversions and enantioselectivities. As a result, two more Rh based catalysts were chosen from the catASium® family of catalysts (Figure 5.2). The catalysts were chosen only to have minor changes in structure compared to the original catalyst **41**. The first, (R,R)-Me-DUPHOS was chosen as it had a more rigid backbone due to the phenyl ring, the second was (R,R)-Me-BPE-Rh, **52**, which was chosen as it would be more flexible with very little electronic effects present in the ligand. Furthermore, both of these catalysts have been reported to be extremely effective in the enantioselective hydrogenation of α-arylenamides, a prochiral unsaturated substrate with N-acetal functional groups.[153] When catalysts **51** and **52** were employed in the hydrogenation of **22** (Table 5.6) with the same conditions used above, it was found that catalyst **51** resulted in comparable conversions and enantioselectivities as **41**. However, once DBU was added with $H_{2(g)}$ the conversion and enantioselectivity increased to 71 % and 69 %, respectively. The hydrogenation of **22** using catalyst **51** resulted in similar values for the first Rh-based catalyst, **41**. Once $CO_{2(g)}$ and DBU were utilized with the $H_{2(g)}$, again we found no change in either the yield nor the enantioselectivity for catalyst **51**, whereas there was a significant increase, *ca.* 40 %, when these conditions were

applied to the hydrogenations with catalyst **41**. It was found that for catalyst **52** the yields and enantioselectivities for all four conditions resulted in low values.
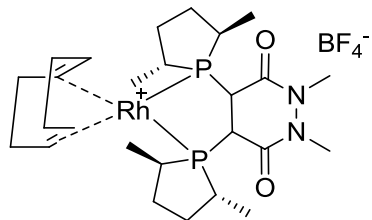
41 ; catASium® MNN(R)Rh
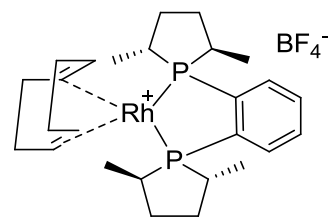
51 ; (R,R)-Me-DUPHOS-Rh
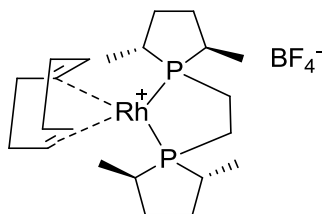
52 ; (R,R)-Me-BPE-Rh

Figure 5.2. Two new rhodium (I) catASium® catalysts, **50** and **51**, applied to the asymmetric hydrogenation of 2-phenylprop-2-en-1-amine, **22**.

Table 5.6. Asymmetric hydrogenation results for 2-phenylprop-2-en-1-amine, **22**, studying two new rhodium(I) catASium® catalysts, (R,R)-Me-Duphos-Rh, **51**, and (R,R)-Me-BPE-Rh, **52**, at high pressure and low pressure of $H_{2(g)}$, and $CO_{2(g)}$.[a]

Catalyst Screening	Cat.	H_2 [b]		H_2 + DBU [c]		H_2 + CO_2 [d]		H_2 + CO_2 + DBU [e]	
		% yield[f] (% conv.)	% ee[g]	% yield[f] (% conv.)	% ee[g]	% yield[f] (% conv.)	% ee[g]	% yield[f] (% conv.)	% ee[g]
14 h High Pressure $H_{2(g)}$:$CO_{2(g)}$ 90:10 bar	**41**	57 (>95)	68	50 (>95)	26	84 (>95)	75	94 (>95)	73
	51	66 (>95)	61	71 (>95)	69	54 (>95)	65	72 (>95)	69
	52	47 (>95)	24	48 (>95)	20	57 (>95)	23	49 (>95)	22
24 h Low Pressure $H_{2(g)}$:$CO_{2(g)}$ 10:10 bar	**41**	79 (>95)	63	56 (>95)	33	88 (>95)	61	76 (>95)	66
	51	79 (>95)	70	79 (>95)	54	79 (>95)	72	71 (>95)	69
	52	74 (>95)	39	67 (>95)	2	72 (>95)	42	58 (>95)	43

[a] Experiments were done in triplicate and at RT. The experimental errors for % yield and % ee were ±10 and ±4, respectively. [b] *Reaction conditions:* 160 mL stainless steel pressure vessel, 10 mg **22**, 100 or 10 bar $H_{2(g)}$, 2 mL methanol in a 1 dram vial. [c] *Reaction conditions:* 160 mL stainless steel pressure vessel, 10 mg **22**, 100 or 10 bar $H_{2(g)}$, 1 eq. DBU, 2 mL methanol in a 1 dram vial. [d] *Reaction conditions:* 160 mL stainless steel pressure vessel, 10 mg **22**, 90 or 10:10 bar $H_{2(g)}$:$CO_{2(g)}$, 2 mL methanol in a 1 dram vial. [e] *Reaction conditions:* 160 mL stainless steel pressure vessel, 10 mg **22**, 90 or 10:10 bar $H_{2(g)}$:$CO_{2(g)}$, 1 eq. DBU, 2 mL methanol in a 1 dram vial. [f] ^{1}H NMR values, internal standard used: 1,3,5-trimethoxybenzene. [g] Determined by HPLC.

As mentioned in section 1.7.3.1, the enantioselectivity of asymmetric hydrogenation reactions is greatly affected by the structure of the substrate and the hydrogen pressure.[21] As catalyst **52** resulted in such low yields and enantiomeric excess for the high pressure reactions, it was postulated that this could be one example where the asymmetric hydrogenation requires low $H_{2(g)}$ pressure rather than high pressure for the best enantioselectivity. The conditions of the asymmetric hydrogenation with rhodium based catalysts **41**, **51**, and **52** were changed such that only 10 bar of $H_{2(g)}$ was used rather than 100 bar and the pressure of $CO_{2(g)}$ remained at 10 bar (Table 5.6). To accommodate the lower $H_{2(g)}$ pressure, the reaction time was increased since the rate of reaction would be affected. The change in $H_{2(g)}$ pressure positively affected the enantioselectivity of the hydrogenation with catalyst **52** increasing to *ca.* 40 % from *ca.* 20 % and the conversion to *ca.* 70 % from *ca.* 50 %. The hydrogenations in the presence of DBU resulted in a decrease of 10-20 % in the conversion with and without $CO_{2(g)}$ present. However, when the base was used without $CO_{2(g)}$, the enantioselectivity of the hydrogenation resulted in a racemic mixture. When $CO_{2(g)}$ was present the enantioselectivity remained the same with and without base in the reaction, *ca.* 40 %. Even though the asymmetric hydrogenation of **22**, at a low pressure of $H_{2(g)}$ resulted in improved conversions and enantiomeric excess for catalyst **52**, the ee did not result as high of values as the other two rhodium based catalysts, **45** and **51**, at a high pressure. Because of this, improvements to this new methodology were continued with only catalysts **41** and **51**.

To improve the enantioselectivity and conversion of the asymmetric hydrogenation for **22**, the effect of solvent on the reaction was examined (Table 5.7). For catalyst **51** it was reported that the best solvents for the asymmetric hydrogenations of α-aminomethylacrylates,[154] ene-carbonates,[149] β-acylamido acrylates,[150] and enamides[153] were IPA, MeOH and THF. For this reason, the asymmetric hydrogenation of 2-phenylprop-2-en-1-amine in the presence of $CO_{2(g)}$ was tested with these solvents for catalysts **41** and **51**. When the reaction was performed in THF with no $CO_{2(g)}$, the yield of the reaction remained the same as when the experiments had been completed in methanol. However, the enantioselectivity of the reaction was diminished and an essentially racemic mixture was obtained, with an *ee* between 1-7 %. Once $CO_{2(g)}$ was added to the system there was *ca.* 10 % decrease in the yield of the reaction. The enantioselectivities for catalyst **41** increased *ca.* 20 % when DBU and $CO_{2(g)}$ were present, whereas with catalyst **51** the enantioselectivity only increased when DBU was not present with the $CO_{2(g)}$, *ca.* 30 %. Changing the solvent to IPA from MeOH, an increase in enantioselectivity, *ca.* 20 %, was observed when only $H_{2(g)}$ was utilized with **41**; however, the yield of the reaction remained constant. Even though the enantioselectivity improved for catalyst **41**, this was not the case when DBU was present with and without $CO_{2(g)}$.

For catalyst **51**, using IPA as the reaction solvent improved the yield and enantioselectivity when $CO_{2(g)}$ and DBU were present; a *ca.* 10 % increase for

both. Using an aprotic solvent such as THF causes a significant decrease in the enantioselectivity. It was concluded that the best solvents were protic and more specifically for catalyst **41** MeOH, as it produced the highest enantiomeric excess whereas catalyst **51** worked best with IPA.

Table 5.7. The effect of solvent on conversion and enantioselectivity on the asymmetric hydrogenation of 2-phenylprop-2-en-1-amine, **22**.[a]
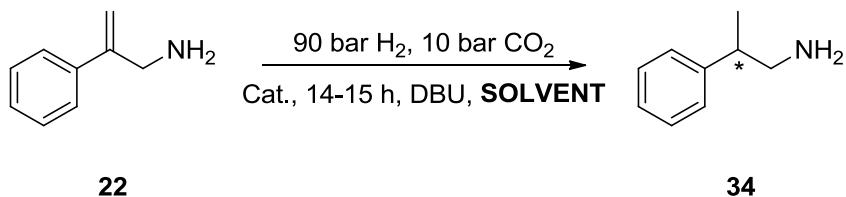
Solvent	Cat.	H_2 [b]		H_2 + DBU [c]		H_2 + CO_2 [d]		H_2 + CO_2 + DBU [e]	
		% yield[f] (% conv.)	% ee[g]	% yield[f] (% conv.)	% ee[g]	% yield[f] (% conv.)	% ee[g]	% yield[f] (% conv.)	% ee[g]
MeOH	41	57 (>95)	68	50 (>95)	26	84 (>95)	75	94 (>95)	73
	51	66 (>95)	61	71 (>95)	69	54 (>95)	65	72 (>95)	69
THF	41	52 (93)	3	69 (>95)	4	40 (74)	14	36 (70)	22
	51	52 (>95)	7	58 (>95)	1	46 (>95)	43	31 (76)	6
IPA	41	57 (>95)	93	73 (>95)	17	74 (>95)	62	96 (>95)	50
	51	62 (>95)	59	71 (>95)	25	81 (>95)	67	80 (>95)	70

[a] Experiments were done in triplicate and at RT. The experimental errors for % yield and % ee were ±10 and ±4, respectively. [b] *Reaction conditions:* 160 mL stainless steel pressure vessel, 10 mg **22**, 100 bar $H_{2(g)}$, 2 mL methanol in a 1 dram vial. [c] *Reaction conditions:* 160 mL stainless steel pressure vessel, 10 mg **22**, 100 bar $H_{2(g)}$, 1 eq. DBU, 2 mL methanol in a 1 dram vial. [d] *Reaction conditions:* 160 mL stainless steel pressure vessel, 10 mg **22**, 90:10 bar $H_{2(g)}$:$CO_{2(g)}$, 2 mL methanol in a 1 dram vial. [e] *Reaction conditions:* 160 mL stainless steel pressure vessel, 10 mg **22**, 90:10 bar $H_{2(g)}$:$CO_{2(g)}$, 1 eq. DBU, 2 mL methanol in a 1 dram vial. [f] ^{1}H NMR values, internal standard used: 1,3,5-trimethoxybenzene. [g] Determined by HPLC.

Throughout the analysis of the ^{1}H NMR spectra of **34**, we observed that during the asymmetric hydrogenation, the substrate 2-phenylprop-2-en-1-amine, **22**, was completely consumed each timed during the reaction. However, either low yields or unknown peaks in the ^{1}H NMR spectra were obtained along with the product. It was postulated that the use of DBU as the base may be leading to or assisting the decomposition of starting material or product. However, the overall yields were higher with the presence of DBU. Accordingly, we investigated the presence of other bases in the asymmetric hydrogenation reaction (Table 5.8). Selecting bases that could not react with $CO_{2(g)}$, it was necessary to pick a tertiary amine, and we desired ones with lower basicity than that of DBU. To satisfy these criteria, N,N-dimethylcyclohexylamine, $CyNMe_2$, and N,N-diisopropylethylamine, i-Pr_2NEt, were selected to test with catalyst **41** in MeOH and IPA, whereas these bases were tested with catalyst **51** in solely IPA as the solvent, as they are known to work with previous switchable systems. The best results, conversion and enantioselectivity, for catalyst **41** was found to be in the presence of $H_{2(g)}$, $CO_{2(g)}$, MeOH and $CyNMe_2$, producing the cleanest ^{1}H NMR spectra and highest enantioselectivity. For catalyst **51**, we found that $H_{2(g)}$, $CO_{2(g)}$, IPA and i-Pr_2NEt resulted in the highest yield and *ee*, 83 % and 72 %, respectively. These bases were carried forward with their respective catalysts for further asymmetric hydrogenations.

Table 5.8. The effects of different bases on the conversion and enantioselectivity on the asymmetric hydrogenation of 2-phenylprop-2-en-1-amine, **22**.[a]

Base Effect	Cat.	H_2 [b]		H_2 + Base [c]		$H_2 + CO_2$ [d]		$H_2 + CO_2 +$ Base [e]	
		% yield[f] (% conv.)	% ee[g]	% yield[f] (% conv.)	% ee[g]	% yield[f] (% conv.)	% ee[g]	% yield[f] (% conv.)	% ee[g]
DBU in MeOH	41	57 (>95)	68	50 (>95)	26	84 (>95)	75	94 (>95)	73
	51	66 (>95)	61	71 (>95)	69	54 (>95)	65	72 (>95)	69
CyNMe$_2$ in MeOH	41	60 (>95)	67	58 (>95)	64	71 (>95)	71	77 (>95)	71
i-Pr$_2$NEt in MeOH	41	66 (>95)	61	66 (>95)	59	95 (>95)	65	> 99 (>95)	69
DBU in IPA	41	57 (>95)	63	73 (>95)	17	74 (>95)	62	96 (>95)	50
	51	62 (>95)	59	71 (>95)	25	81 (>95)	67	80 (>95)	70
CyNMe$_2$ in IPA	41	65 (>95)	57	62 (>95)	44	71 (>95)	54	80 (>95)	55
	51	62 (>95)	67	60 (>95)	63	81 (>95)	72	78 (>95)	72
i-Pr$_2$NEt in IPA	41	46 (>95)	63	56 (>95)	64	91 (89)	64	75 (>95)	72
	51	42 (>95)	65	48 (>95)	65	62 (87)	70	83 (83)	72

[a] Experiments were done in triplicate and at RT. The experimental errors for % yield and % *ee* were ±10 and ±4, respectively. [b] *Reaction conditions:* 160 mL stainless steel pressure vessel, 10

158

mg **22**, 100 bar $H_{2(g)}$, 2 mL methanol in a 1 dram vial. [c] *Reaction conditions:* 160 mL stainless steel pressure vessel, 10 mg **22**, 100 bar $H_{2(g)}$, 1 eq. base, 2 mL methanol in a 1 dram vial. [d] *Reaction conditions:* 160 mL stainless steel pressure vessel, 10 mg **22**, 90:10 bar $H_{2(g)}:CO_{2(g)}$, 2 mL methanol in a 1 dram vial. [e] *Reaction conditions:* 160 mL stainless steel pressure vessel, 10 mg **22**, 90:10 bar $H_{2(g)}:CO_{2(g)}$, 1 eq. base, 2 mL methanol in a 1 dram vial. [f] ^1H NMR values, internal standard used: 1,3,5-trimethoxybenzene. [g] Determined by HPLC.

As previously observed in Table 5.4 and Table 5.5, reducing the reaction time to 15 h for the asymmetric hydrogenation of 2-phenylprop-2-en-1-amine improved the yield of the reaction. To investigate this trend, the reaction times were shortened further. As a result, the asymmetric hydrogenations were performed at 3 h and 6 h, the results of which were then compared to those obtained with a 15 h reaction time (Table 5.9). The reaction conditions that excluded $CO_{2(g)}$ were eliminated from the investigation on the asymmetric hydrogenation of **22** as we concluded that the presence of $CO_{2(g)}$ positively assisted the yield of these reactions. It was determined that a reaction time of 6 h was necessary when catalyst **41** was employed as the conversion was only *ca.* 70 % after 3 hours. A yield increase of *ca.* 20 % without base and an increase of *ca.* 10 % with base were observed with catalyst **41** with a 6 h reaction compared to the 3 h and 15 h reaction times, respectively.

The enantioselectivity of the reaction also increased with the increase of reaction time for catalyst **41**. Even though the reaction was complete after six

hours, the enantioselectivity of the reaction improved as time increased further. We believe that catalyst **41** may also be performing a kinetic resolution, as the enantioselectivity of the reaction improved by *ca.* 20 % by changing the reaction time from 6 h to 15 h. Yet the yield of the reaction decreased *ca.* 10 to 20 % between the 6 and 15 h reaction times. There is a decrease for both enantiomers; however, the major enantiomer is decreased by only 5 % while the minor enantiomer is decreased by half of its concentration. This trend occurred in all experiments, which were repeated in triplicate. In contrast for catalyst **51**, the reaction was complete in 3 h, but the enantioselectivity and conversion of the asymmetric hydrogenation was not affected by additional reaction time.

Table 5.9. The effects of time on the conversion and enantioselectivity on the asymmetric hydrogenation of 2-phenylprop-2-en-1-amine, **22**.[a]
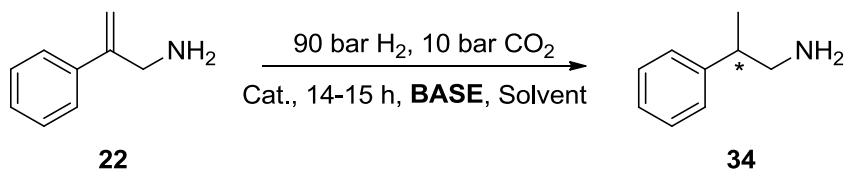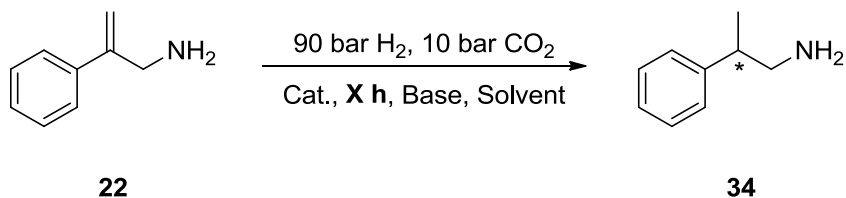

Time Effect	Cat.	$H_2 + CO_2$ [b]		$H_2 + CO_2 +$ Base [c]	
		% yield[d] (% conv.)	% ee[e]	% yield[d] (% conv.)	% ee[e]
3 h	**41**	58 (81)	47	74 (84)	49
	51	78 (>95)	70	76 (>95)	69
6 h	**41**	84 (95)	53	85 (95)	51
	51	75 (>95)	71	82 (>95)	70
15 h	**41**	71 (>95)	71	69 (>95)	71
	51	62 (>95)	70	83 (>95)	72

[a] Experiments were done in triplicate and at RT. The experimental errors for % yield and % *ee* were ±10 and ±4, respectively. [b] *Reaction conditions:* 160 mL stainless steel pressure vessel, 10 mg **22**, 90:10 bar $H_{2(g)}:CO_{2(g)}$, 2 mL methanol in a 1 dram vial. [c] *Reaction conditions:* 160 mL stainless steel pressure vessel, 10 mg **22**, 90:10 bar $H_{2(g)}:CO_{2(g)}$, 1 eq. base (catalyst **41**: $CyNMe_2$+ MeOH, and catalyst **51**: *i*-Pr_2NEt + *i*-PrOH), 2 mL methanol in a 1 dram vial. [d] ^{1}H NMR values, internal standard used: 1,3,5-trimethoxybenzene. [e] Determined by HPLC.

Two out of the three catASium® rhodium based catalysts had shown positive results for the asymmetric hydrogenation of **22** in terms of good conversions, *ca.* 80-90 % and the best enantioselectivity demonstrated thus far, *ca.* 70 %. As such, another catalyst from this family was tested for the asymmetric hydrogenation of 2-phenylprop-2-en-1-amine. Catalyst **53** (Figure 5.3) was chosen because the electronic effect of the ligand was expected to be different than the other catalysts and has a bite angle that is slightly larger than the other catalysts: **53** = 86.1 °, **41** = 85 °, **51** = 83.6 °, **52** = 83.9 °.[150,182,183] The results of the asymmetric hydrogenation of 2-phenylprop-2-en-1-amine with catalyst **53** are shown below in Table 5.10. For the hydrogenations using catalyst **53** all four conditions were investigated: with only $H_{2(g)}$; $H_{2(g)}$ and base; $H_{2(g)}$ and $CO_{2(g)}$; and lastly $H_{2(g)}$, $CO_{2(g)}$ and base. The reaction was also explored with the three bases previously tested: DBU, $CyNMe_2$, and *i*-Pr_2NEt. In general, the asymmetric hydrogenation resulted in much higher yields and the best results were *ca.* 30 % higher when $CO_{2(g)}$ was utilized in the reaction. However, as observed with catalysts **41** and **51**, the addition of $CO_{2(g)}$ to the reaction did not affect the enantioselectivity of the asymmetric hydrogenation reactions completed with **53**. When DBU was employed in the hydrogenation we found the yield of the reaction decreased from 90 to 69 %, however, the enantioselectivity was slightly increased by *ca.* 6 %, whereas the use of $CyNMe_2$ in the reaction the yield increased by 5 % and the enantioselectivity was unchanged.

53
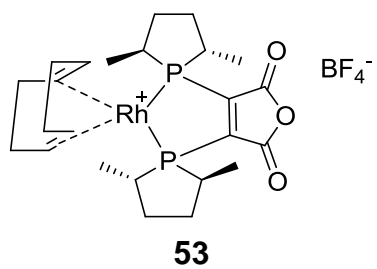
Figure 5.3. New rhodium (I) catASium® catalyst for the asymmetric

hydrogenation of 2-phenylprop-2-en-1-amine, **22**.

Table 5.10. Asymmetric hydrogenation of 2-phenylprop-2-en-1-amine, **22**, using catalyst **53**, catAsium® M(S)Rh.[a]

$$\text{22} \quad \xrightarrow[\text{Cat. }\textbf{52}\text{, 6 h, Base, Solvent}]{\text{90 bar H}_2\text{, 10 bar CO}_2} \quad \text{34}$$

Base Effect	Cat.	H$_2$ [b]		H$_2$ + Base [c]		H$_2$ + CO$_2$ [d]		H$_2$ + CO$_2$ + Base [e]	
		% yield[f]	% ee[g]	% yield[f]	% ee[g]	% yield[f]	% ee[g]	% yield[f]	% ee[g]
DBU	**53**	54	71	52	36	90	70	69	76
CyNMe$_2$	**53**	54	71	60	71	90	70	95	71
i-Pr$_2$NEt	**53**	54	71	66	74	90	70	85	73

[a] Experiments were done in triplicate and at RT. Conversions for all reactions above was > 95 % and the experimental errors for % yield and % *ee* were ±10 and ±4, respectively. [b] *Reaction conditions:* 160 mL stainless steel pressure vessel, 10 mg **22**, 100 bar H$_{2(g)}$, 2 mL methanol in a 1 dram vial. [c] *Reaction conditions:* 160 mL stainless steel pressure vessel, 10 mg **22**, 100 bar H$_{2(g)}$, 1 eq. base, 2 mL methanol in a 1 dram vial. [d] *Reaction conditions:* 160 mL stainless steel pressure vessel, 10 mg **22**, 90:10 bar H$_{2(g)}$:CO$_{2(g)}$, 2 mL methanol in a 1 dram vial. [e] *Reaction conditions:* 160 mL stainless steel pressure vessel, 10 mg **22**, 90:10 bar H$_{2(g)}$:CO$_{2(g)}$, 1 eq. base, 2 mL methanol in a 1 dram vial. [f] ^{1}H NMR values, internal standard used: 1,3,5-trimethoxybenzene. [g] Determined by HPLC.

In an attempt to improve the enantioselectivity, we decided to apply a chiral environment to the reaction by selecting a chiral base.[184] Natural bases, (+)-cinchonine and (-)-cinchonidine, and a bulky secondary base known not to form carbamates with $CO_{2(g)}$, (+)-bis[(R)-1-phenylethyl]amine and (-)-bis[(S)-1-phenylethyl]amine, (Figure 5.4) were selected to induce a chiral environment during the asymmetric hydrogenation (Table 5.11).[185] The natural bases did not increase the enantioselectivity with any of the ruthenium based catalysts **41**, **51** and **53**. However, the employment of the secondary chiral bases improved the enantioselectivity for the hydrogenation using catalyst **51** to 77 %. Furthermore, the enantioselectivity was not affected by the chirality of base, whereas if the chirality had affected the catalysis, one would have expected one enantiomer to improve the enantioselectivity and the other to diminish it. We believe that the (+)-bis[(R)-1-phenylethyl]amine and (-)-bis[(S)-1-phenylethyl]amine were a better choice for the base in terms of forming the carbamate salt. Given that all three ruthenium base catalysts **41**, **51**, and **53** were cationic, we propose that the chiral bases, in their cationic form, were not close enough to the catalysts to induce a chiral environment as their positive charges would have repelled one another. Therefore, we propose that the best base for the asymmetric hydrogenation is a weak base, rather than whether it's chiral.
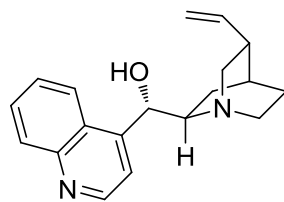
(+)-cinchonine
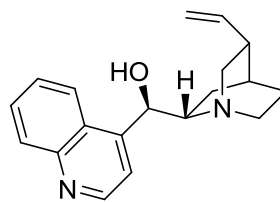
(-)-cinchonidine
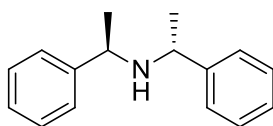
(+)-bis[(R)-1-phenylethyl]amine
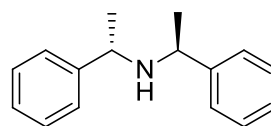
(-)-bis[(S)-1-phenylethyl]amine

Figure 5.4. Chiral bases used in the asymmetric hydrogenation of 2-phenylprop-2-en-1-amine, **22**.

Table 5.11. The effects of chiral bases on the conversion and enantioselectivity on the asymmetric hydrogenation of 2-phenylprop-2-en-1-amine, **22**.[a]
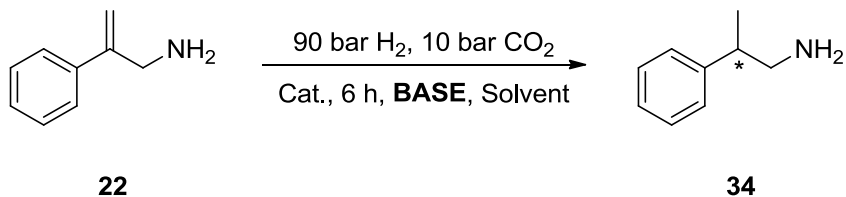
Chiral Base Effect	Cat.	$H_2 + CO_2 +$ (+)-cinchonine [b]		$H_2 + CO_2 +$ (-)-cinchonidine [b]		$H_2 + CO_2 +$ (+)-Bis[(R)-1-phenylethyl]-amine [b]		$H_2 + CO_2 +$ (-)-Bis[(S)-1-phenylethyl]-amine [b]	
		% yield[c]	% ee[d]	% yield[c]	% ee[d]	% yield[c]	% ee[d]	% yield[c]	% ee[d]
MeOH	**41**	n/a	49	n/a	51	84	65	84	64
IPA	**51**	n/a	75	n/a	75	90	77	88	76
MeOH	**53**	n/a	n/a	n/a	n/a	94	74	96	71

[a] Experiments were done in triplicate and at RT. Conversions for all reactions above was > 95 % and the experimental errors for % yield and % ee were ±10 and ±4, respectively. [b] *Reaction conditions:* 160 mL stainless steel pressure vessel, 10 mg **22**, 90:10 bar $H_{2(g)}:CO_{2(g)}$, 1 eq. base, 2 mL methanol in a 1 dram vial. [c] ^{1}H NMR values, internal standard used: 1,3,5-trimethoxybenzene. [d] Determined by HPLC.

5.2.4 – Proposed mechanism for the asymmetric homogeneous hydrogenation of 2-phenylprop-2-en-1-amine and its derivatives

While the mechanism of the hydrogenation is not yet known, we can offer the following speculation based upon some of the observations. For the asymmetric hydrogenation of 2-phenylprop-2-en-1-amine, **22**, we needed to find a mechanism of the reaction that could explain why the carbon dioxide had no effect or very little effect on the enantioselectivity of the hydrogenation.

Scheme 5.11 shows two proposed mechanisms for the asymmetric hydrogenation in the absence of $CO_{2(g)}$, where the amine coordinates to the metal center in mechanism **A** but mechanism **B** follows a route where the amine group does not participate in the mechanism and only the C=C double bond coordinates to the metal center of the catalyst. In mechanism **A**, after the substrate coordinates to the metal by the amine group, the C=C double bond wraps around and binds, at which point the chirality is imposed onto the substrate. This would then be followed (or potentially preceded) by an oxidative addition of H_2 to generate a dihydride. An insertion followed by a reductive elimination completes the cycle. Mechanism **B** is somewhat analogous to the previously discussed mechanism for Wilkinson's catalyst, involving (in either order) an oxidative addition of hydrogen and the coordination of the unsupported C=C double bond. Again, insertion and reductive elimination complete the cycle.

While the scheme shows dihydride mechanisms, monohydride pathways are also possible.

When deciding between several possible mechanisms, one must consider the experimental results obtained to get some clues which is the correct mechanism. When DBU was added to the system without $CO_{2(g)}$, we found that the enantioselectivity and the yield of the reaction both decreased; however, when weaker bases were used the enantioselectivity and yield remain the same as was observed without added base within experimental error. However, the trend with the weaker bases can support both mechanisms **A** and **B** equally, therefore, we cannot identify the correct mechanism from only studying the hydrogenations without $CO_{2(g)}$.
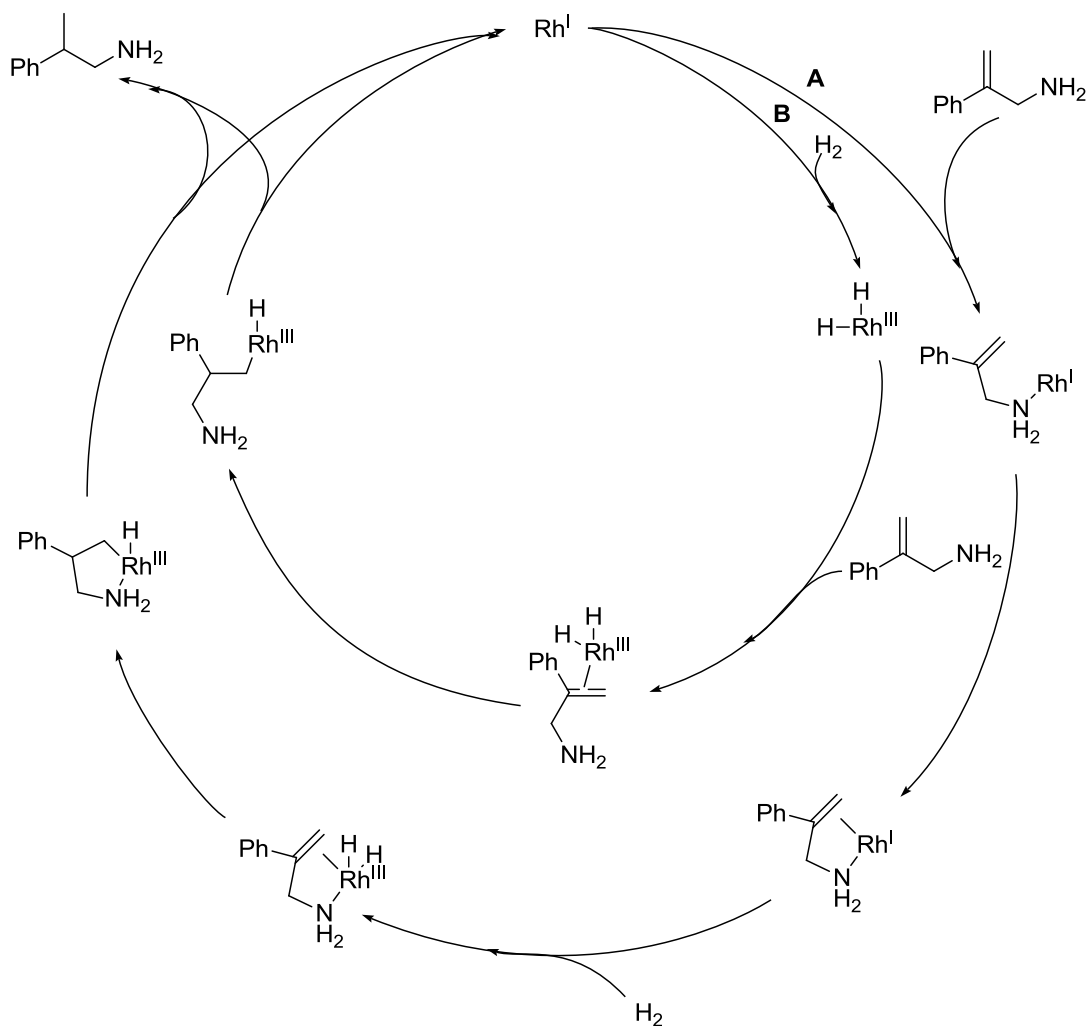
Scheme 5.11. Two proposed catalytic mechanisms for the asymmetric hydrogenation of 2-phenylprop-2-en-1-amine without $CO_{2(g)}$. In mechanism **A** the amine group coordinates to the metal while in mechanism **B** the amine does not bind at all throughout the mechanism.

For the asymmetric hydrogenation of 2-phenylprop-2-en-1-amine, **22**, in the presence of $CO_{2(g)}$, we propose three possible catalytic mechanisms; **C**, **D** and **E**, that the reaction could follow (Scheme 5.12). Mechanism **C** is analogous to the catalytic cycle shown in mechanism **B** (Scheme 5.11), where the mechanism involves an oxidative addition of hydrogen and the coordination of the unsupported C=C double bond, in either order. Again, insertion and reductive elimination complete the cycle. The difference between the two mechanisms is that instead of a free amine group, the substrate contains a free carbamic acid/anion that never binds to the catalyst. In mechanism **D** the initial step involves coordination of the carbamic anion to the metal center though the nitrogen and possibly also an oxygen atom. After this, the C=C double bond wraps around and coordinates to the metal center, and once again the chirality is imposed onto the substrate at this point. This step would then be followed (or potentially preceded) by an oxidative addition of H_2 to generate a dihydride. An insertion followed by a reductive elimination completes the cycle. Mechanism **E** is analogous to mechanism **D** and follows the same catalytic cycle with few differences. The initial step involves the coordination of the carbamic acid/anion to the metal centre of the catalyst through one or both oxygen atoms of the carbamic acid/anion group rather the nitrogen as seen in **D**. The C=C double bond then wraps around and coordinates to the metal center. The mechanism would then have an oxidative addition of H_2 to generate the dihydride. At this point, the hydride follows a migratory insertion, either forming a 6- or 7-membered ring intermediate, and then a reductive elimination completes the

cycle. Comparing Scheme 5.11 to the proposed mechanism where $CO_{2(g)}$ forms the carbamate salt *in situ* before the oxidative insertion (Scheme 5.12), It is proposed that the two hydrogenations, with and without $CO_{2(g)}$, follow the same pathway and form the same or similar 5-membered ring intermediate (routes **A** and **D**) regardless of whether $CO_{2(g)}$ was present during the hydrogenation. We believe that this could be a possibility due to the enantioselectivity of the two asymmetric hydrogenation systems resulting in the same *ee*, which suggests that these two mechanisms should form the same 5-membered ring intermediate, as this is where the chirality of the catalyst is imposed into the substrate. However, it is also possible that instead of a 5-membered ring intermediate, the mechanism could follow route **E** where a 6- or 7-membered ring intermediate is formed. However, if that were the case then the $CO_{2(g)}$ should have affected the enantioselectivity of the reaction. If the mechanism in the presence of $CO_{2(g)}$ is significantly different from that in the absence of $CO_{2(g)}$ (e.g. mechanisms **A** and **D**), then the fact that the *ee* was the same must have been due to a coincidence. From my work described in Chapters 3 and 4, the hydrogenation of 4-phenyl-4-pentenoic acid, **2**, and 3-benzoylpropionic acid, **47**, were successful in terms of high conversions, > 99 and 96 % respectively, and had somewhat similar enantioselectivities, 68 and 81 %, respectively. The catalytic mechanism for theses substrates proceed through either 6- or 7-membered Ru intermediates similar to those proposed in mechanism **E**. Therefore it is possible that the catalytic mechanism for the hydrogenation of **22** in the presence of $CO_{2(g)}$ proceeds through similar 6- or 7-membered Rh intermediates. However, the

enantiofacial selection of the C=C double bond must be the same for mechanism **A** as it is for mechanism **E**. We believe this because the experimental results obtained for the asymmetric hydrogenations with and without the presence of CO_2 gave roughly the same *ee* values.
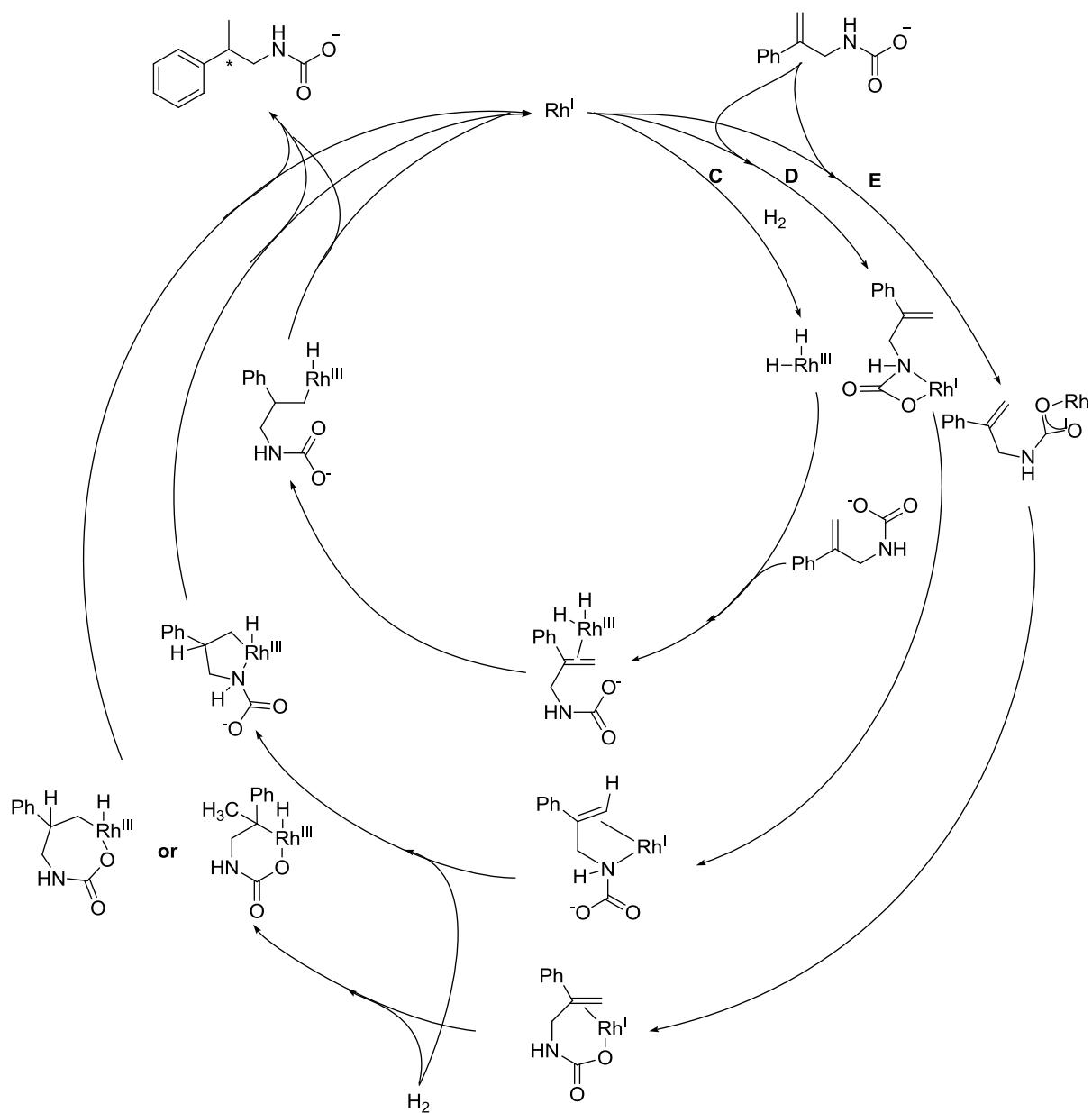
Scheme 5.12. The proposed mechanisms for the asymmetric hydrogenation of **22** in the presence of $CO_{2(g)}$, where route C follows a coordination through the C=C double bond without coordination of the carbamate group, whereas route D follows a 5-membered ring transition complex, and route E follows a 6- or 7-membered ring transition complex.

The most significant effect the addition of $CO_{2(g)}$ had on the asymmetric hydrogenation of 2-phenylprop-2-en-1-amine was the disappearance of byproduct. We propose that the presence of $CO_{2(g)}$ suppressed an unwanted side reactions such as dehydroamination, although currently we are unable to identify the byproducts. However, the ^{1}H NMR spectra clearly reveal that the addition of $CO_{2(g)}$ does affects the asymmetric hydrogenation of **22** in terms of preventing the side reactions and the formation of side product (Figure 5.5).

I.S.

I.S.

CDCl₃

b

b

P

a

P

b

c

No CO$_{2(g)}$

P

2

With CO$_{2(g)}$

1

| 7.5 | 7.0 | 6.5 | 6.0 | 5.5 | 5.0 | 4.5 | 4.0 | 3.5 | 3.0 | 2.5 | 2.0 | 1.5 | 1.0 | 0.5 |

Chemical Shift (ppm)
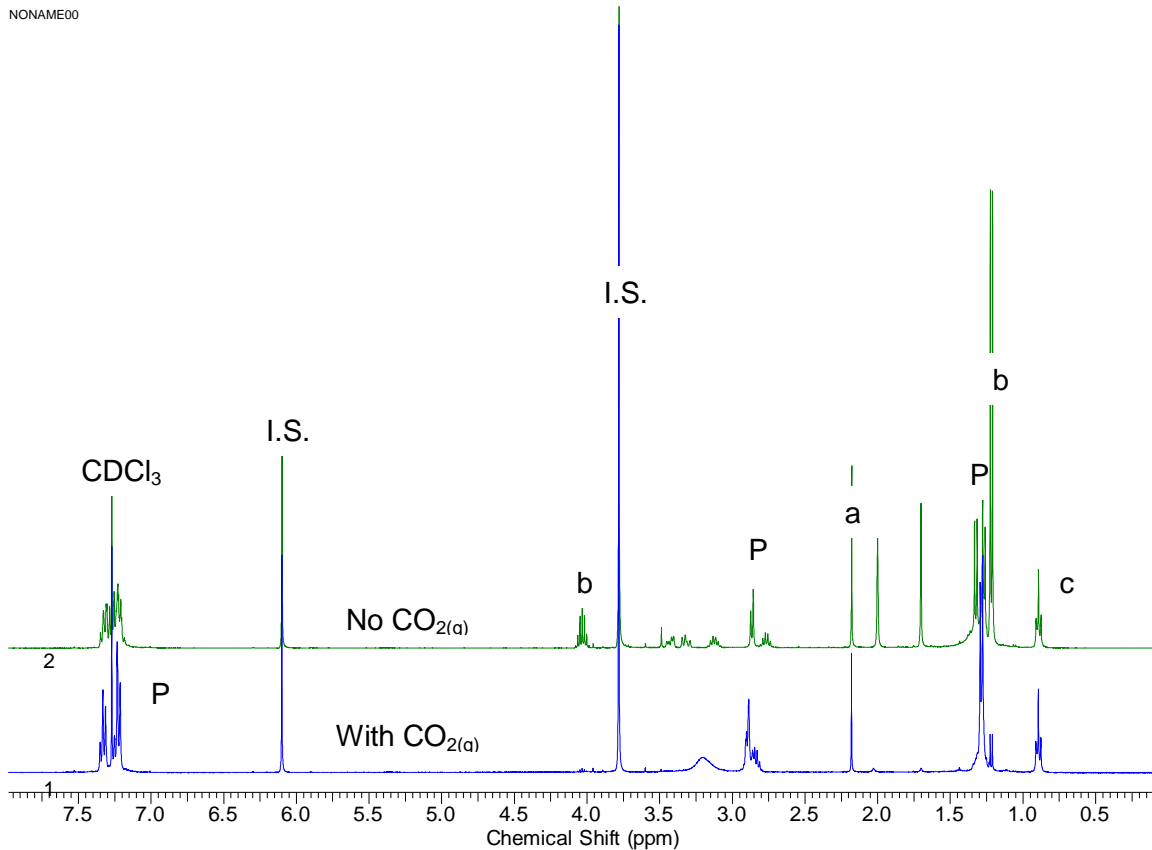
Figure 5.5. ^{1}H NMR spectra of 2-phenylpropan-1-amine (P) after the asymmetric hydrogenation without base and 1,3,5-trimethoxybenzene as the NMR internal standard (I.S.) (acetone = a, isopropanol = b, hexane = c). The green spectrum represents the hydrogenation without CO$_{2(g)}$ and the blue spectrum represents the hydrogenation with CO$_{2(g)}$.

5.2.5 – Asymmetric homogeneous hydrogenation of 2-phenylprop-2-en-1-amine and its derivatives.

Once an efficient methodology had been developed for the asymmetric hydrogenation of unsaturated allylamines, this method was tested with the corresponding catalysts: **41**, **51** and **53** and their best conditions on the derivatives of 2-phenylprop-2-en-1-amine (Table 5.12). For **41** the asymmetric hydrogenation was performed with $CO_{2\,(g)}$ and $CyNMe_2$, whereas catalyst **51** was utilized with $CO_{2\,(g)}$ and (-)-bis[(S)-1-phenylethyl]amine, (-)-bis-(S)-1-PEA. For **53** both set of conditions used for **41** and **51** were equally as successful in terms of asymmetrically hydrogenating 2-phenylprop-2-en-1-amine with high yield and enantioselectivity.

To study the effect of a bigger, more rigid substrate on the hydrogenation, the phenyl ring was changed into a naphthylene in compound **37**. The conversion of the hydrogenation for 2-(naphthalene-2-yl)prop-2-en-1-amine, **37**, was good, 77-85 %, however, compared to 2-phenylprop-2-en-1-amine the conversion decreased *ca.* 10 %. Furthermore, the enantioselectivity for the reaction also decreased an average of 10 % when applied to the larger **37**.

Next the effects of an electron-donating group and an electron-withdrawing group on the ring were studied. Therefore, the methodology for the

asymmetric hydrogenation of **22** was applied to 2-(4-ethoxyphenyl)prop-2-en-1-amine, **36**, and 2-[4-(trifluoromethyl) phenyl]prop-2-en-1-amine, **35**, where an ethoxy and a trifluoro group were placed para in the ring to the unsaturation. Catalyst **51** and **53**, with CyNMe$_2$ as the base, both worked the best in the presence of the electron-rich substrate, **36**, resulting in conversions of 93 and 88 %, respectively, and similar *ee* values of 82 and 81 %, respectively. Both catalysts **51** and **53** produced better enantioselectivities for the ethoxy-substrate than for the original **22**.

For the electron-withdrawing substrate, **35**, the opposite effect occurred than that for the electron-donating. Both yields and enantioselectivity significantly decreased; nonetheless the ^{1}H NMR spectrum of the reaction mixture after the reaction appeared clean and showed that the reaction was incomplete after 6 h. Therefore, the amount of product might improve if the reaction time were longer for the hydrogenation of **35**.

Table 5.12. Asymmetric hydrogenation of **22** and its derivatives: 2-(naphthalene-2-yl)prop-2-en-1-amine, **37**, 2-(4-ethoxyphenyl)prop-2-en-1-amine, **36**, and 2-[4-(trifluoromethyl) phenyl]prop-2-en-1-amine, **35**, utilizing catalysts **41**, **51**, and **53** and employing the best conditions for each.[a]
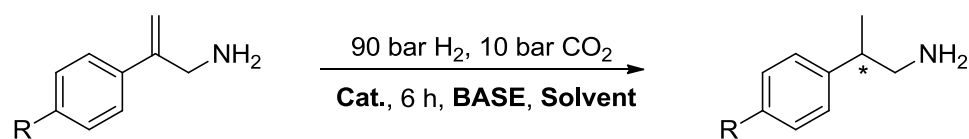
Catalyst (base + solvent)[b]	2-(naphthalene-2-yl)prop-2-en-1-amine		2-(4-ethoxyphenyl) prop-2-en-1-amine		2-[4-(trifluoro-methyl)phenyl] prop-2-en-1-amine		2-phenylprop-2-en-1-amine	
	% yield[c]	% ee[d]	% yield[c]	% ee[d]	% yield[c]	% ee[d]	% yield[c]	% ee[d]
41 (CyNMe$_2$ + MeOH)	84	51	74 (93)	70	57 (90)	28	94	73
51 ((-)-bis-(S)-1-PEA + IPA)	80	67	93	82	41 (92)	30	88	76
53 (CyNMe$_2$ + MeOH)	77	62	88	81	48 (91)	27	95	71
53 ((-)-bis-(S)-1-PEA + MeOH)	85	66	82	77	43 (91)	18	96	71

[a] Experiments were done in triplicate and at RT. Conversions for all reactions above were > 95 %, except for those listed in brackets and the experimental errors for % yield and % ee were ±10 and ±4, respectively. [b] *Reaction conditions:* 160 mL stainless steel pressure vessel, 10 mg of allylamine derivative, 90:10 bar H$_2$ (g):CO$_2$ (g), 1 eq. base, 2 mL solvent in a 1 dram vial. [c] ^{1}H NMR values, internal standard used: 1,3,5-trimethoxybenzene. [d] Determined by HPLC.

5.3 – Conclusion

In conclusion, a new methodology has been developed for the asymmetric hydrogenation of unsaturated olefins containing primary amines. It was found that the Rh-based catASium® catalysts resulted in higher conversion and enantiomeric excess values than the Ru-binap based catalysts. Furthermore, by employing CO_2 in the asymmetric hydrogenation of 2-phenylprop-2-en-1-amine, a clean reaction was produced due to the carbon dioxide acting as a protecting group for the amine functionality, increasing the yield of the reaction up to 94-96 %. Nonetheless, the enantioselectivity of the reaction was not affected by the addition of CO_2 but instead the *ee* increased when the base was changed into a weaker secondary amine, bis(1-phenylethyl)amine. When this base was used as a chiral auxiliary it was found that the chirality of the base did not affect the enantioselectivity of the hydrogenation. This could have been due to the repulsion of the positive charges on the metal center of the catalyst and the cationic protonated base.

The derivatives of 2-phenylprop-2-en-1-amine were then asymmetrically hydrogenated with the best catalysts from the above study at their preferred reaction conditions. It was found that 2-(naphthalene-2-yl)prop-2-en-1-amine, and 2-(4-ethoxyphenyl)prop-2-en-1-amine were enantioselectively hydrogenated with the best conversions being *ca.* 85 and 90 %, respectively. The enantioselectivity of 2-(naphthalene-2-yl)prop-2-en-1-amine result in an *ee* of

67 %, which had decreased compared to the *ee* of 2-phenylprop-2-en-1-amine, 77 %. The addition of an electron-donating group in 2-(4-ethoxyphenyl)prop-2-en-1-amine had a positive effect on the enantioselectivity of the enantioselective hydrogenation resulting in an *ee* of 82 %. In comparison, the asymmetric hydrogenation of 2-[4-(trifluoromethyl)phenyl]prop-2-en-1-amine was not as successful due to the electron-withdrawing effects of the trifluoromethyl group on the phenyl ring, resulting in a decrease in both conversion, 57 %, and the *ee*, 28 %.

These results demonstrate that a direct asymmetric hydrogenation of prochiral allylamines, without prior derivatization, is a viable strategy for preparing chiral amines. Further optimization of the catalyst and the conditions, including the beneficial effect of CO_2, should be able to bring the enantioselectivity to industrially viable levels.

Chapter 6 – Conclusion & Future Work

6.1 –Summary of Key Results

Although conclusions have been discussed within each chapter, some significant points and future work are summarized here.

In this thesis, a study was conducted where the effect of the length of the linker, between the prochiral unsaturation, an olefin, and the metal coordinating functional group, was investigated (described in chapter 3). The resulting conversion and enantioselectivity of the asymmetric hydrogenation was examined as the length of the linker in the substrates was increased. It was found that as the number of carbons in the linker increased the enantioselectivity for the asymmetric hydrogenation decreased. However, once the number of carbons in the linker was increased to 3, it was found that both the enantioselectivity and the conversion of the reaction diminished. This trend was evident for the Ru-binap and derivative catalysts, as well as the Ir-based catalysts. Interestingly, the Rh-based catalyst always resulted in very low enantiomeric excess; however, a complete conversion for the reaction was obtained each time regardless of the length of the linker.

The same catalysts were then applied to more bulky substrates, described in Chapter 3, where the prochiral unsaturation moves along the positions of a phenyl ring. Computational analysis was performed to rationalize the results obtained. It was found that both the computed reactions' trajectories agreed with the experimental data; the asymmetric hydrogenation of the ortho substrate, 2-(1-phenylethenyl)benzoic acid resulted in complete conversion and a high enantioselectivity. However, once the prochiral double bond changed positions to the meta and para, the enantioselectivity and conversion of the reaction were once again lost.

The asymmetric hydrogenations of prochiral ketoacids and the effect of the length of the linker were then investigated in Chapter 4. During the study it was found that an increase in linker length from 1 carbon atom to 2 affected the enantioselectivity, resulting in a 20% decrease, for the hydrogenation. When the linker was increased to 3 atoms, both the conversion and enantioselectivity of the reaction was diminished, as previously demonstrated with the asymmetric hydrogenation of the olefins.

As described in Chapter 5, the information obtained from the asymmetric hydrogenation of the unsaturated substrates, ketoacids and unsaturated carboxylic acids, and the effect of the linker, was utilized to develop a new methodology for the asymmetric hydrogenation of unsaturated amine-containing substrates, i.e. the linker should preferably not be over 4 atoms between the

prochiral unsaturation and the metal center. In this methodology, carbon dioxide was implemented in the asymmetric hydrogenation to modify the amine functionality reversibly into a carbamic acid or carbamate salt. It was anticipated that the CO_2 would improve the *ee* of the hydrogenation; however, we did not see this effect. Instead the presence of CO_2 improved the chemoselectivity of the hydrogenation reaction. We propose that the CO_2 acted as protecting group against possible decomposition of the substrate and product. With an extensive investigation of catalysts, additives and conditions (time, solvent, pressure) the asymmetric hydrogenation of 2-phenylprop-2-en-1-amine resulted in complete conversion (or close to complete) and moderate enantioselectivity. This new method is the first example of asymmetric hydrogenation of allylamines. It has been reported that CO_2 will act as a protecting group for the hydrogenation of nitriles and imines but as of yet it has not been reported in asymmetric hydrogenation. Once the best conditions were obtained for the asymmetric hydrogenation of 2-phenylprop-2-en-1-amine, we synthesized its derivatives: 2-(naphthalene-2-yl)prop-2-en-1-amine, 2-(4-ethoxyphenyl)prop-2-en-1-amine and 2-[4-(trifluoromethyl)phenyl]prop-2-en-1-amine to investigate the effects of an electron-donating and –withdrawing groups, as well as a larger substituent on the asymmetric hydrogenation reaction. We found that the electron-donating group helped with the asymmetric hydrogenation, increasing the conversion and the *ee* for the reaction; however, the electron-withdrawing group had the opposite effect on the reaction, with a significant decrease in both the conversion and enantioselectivity. The larger substituent, naphthalene, caused a slight decrease

in both the conversion and enantioselectivity; however, it did not affect the asymmetric hydrogenation as poorly as the electron-withdrawing group.

6.2 – Future Work

The asymmetric hydrogenation of prochiral unsaturated substrates (unsaturated carboxylic acids, ketoacids, and allylamines) produced exciting results and they are very promising for future development. From this, we believe it is possible to continue the work for all three types of substrates. Future work with chapters 3 and 4 may entail testing a much wider range of ligands and catalysts for the asymmetric hydrogenation of these unsaturated carboxylic acids and ketoacids. Also, we could investigate the degree of substitution along the other chains, n = 2 and n = 3, as there was an increase in yield and enantioselectivity when 2 methyl groups were substituted on benzoylacetic acid.

For the allylamine substrates, future work would entail investigating a larger variety of catalysts, in terms of different metal centres and larger more sterically hindered ligands. Applying the information gathered from the catalysts thus far, it is possible to begin catalyst development for this methodology. We can begin to fine tune our best catalyst by synthesizing ligands with different bite angles, more sterically hindered groups on the phosphine atoms, as well as looking into electron donating groups rather than electron withdrawing ones. We

can also begin to move from Rh-based catalysts, and begin to investigate other metals, such as harder metal like Fe, which should improve the coordination of the allylamine. It is also possible to continue investigating the reaction conditions, testing other secondary and tertiary bases that will not interact with CO_2 but rather act as the counter-part in the carbamate salt, as weaker bases may be most promising. A better understanding of the catalytic cycle would help in improving this methodology, whether it is by changing the catalyst, substrate or conditions. Thus, experimental and computational work can be done to investigate this mechanism. In particular, we need to fully understand the role of CO_2 in the reaction and how it is interacting. It would be to our advantage to study how the CO_2 is blocking undesirable reactions, what those are and identifying the byproducts formed during the asymmetric hydrogenation.

We also propose that one of the Rh-catalysts was not only asymmetrically hydrogenating 2-phenylprop-2-en-1-amine but also performing kinetic resolution. It's not clear at this point what is occurring in the reaction for the yield to decrease with time and the enantiomeric excess to increase but we believe it is worth investigating.

Chapter 7– References

[1]   D. R. Lide, Ed. , *CRC Handbook of Chemistry and Physics*, 80th ed., CRC Press, Florida, **1999**, p. 4-14 - 4-15.

[2]   M. Appl, in *Ullmann's Encycl. Ind. Chem.*, Wiley-VCH Verlag GmbH & Co. KGaA, Weinheim, Germany, **2011**.

[3]   Peak Scientific, "Using Hydrogen as a Carrier Gas for GC," can be found under http://www.peakscientific.com/page/489-using-hydrogen-as-a-carrier-gas-for-gc/#.VTU3_NzF9Bk, **2015**.

[4]   "U.S. Department of Energy; U.S. Energy Information Administration: Independent Statistics & Analysis," **2008**.

[5]   R. E. Kirk, *Kirk-Othmer Encycl. Chem. Technol.* **2004**, 1–24.

[6]   W. Keim, in *Transit. Met. Org. Synth.* (Eds.: M. Beller, C. Bolm), Wiley-VCH Verlag GmbH, Weinheim, Germany, **2004**, p. 17.

[7]   G. W. Parshall, R. E. Putscher, *J. Chem. Educ.* **1986**, *63*, 189–189.

[8]   G. V. Smith, F. Notheisz, *Heterogeneous Catalysis in Organic Chemistry*, Academic Press, Inc, Dan Diego, California, **1999**.

[9]   B. Trost, *Science (80-.).* **1991**, *254*, 1471–1477.

[10]   B. Elvers, *Ullmann's Encyclopedia of Industrial Chemistry*, Wiley-VCH Verlag GmbH & Co. KGaA, Weinheim, Germany, **2000**.

[11]   J. M. J. Lambert, *Chim. Oggi – Chem. Today* **2013**, *31*, 4–9.

[12]   C. E. Housecroft, A. G. Sharpe, Pearson Education Limited, Essex, England, **2001**, pp. 452–487.

[13]   G. Rothenberg, *Catalysis*, Wiley-VCH Verlag GmbH & Co. KGaA, Weinheim, Germany, **2008**.

[14]   G.-Q. Lin, L. Yue-Ming, A. S. C. Chan, *Principles and Applications of Asymmetric Synthesis*, Wiley-Interscience, **2001**.

[15]   B. R. James, *Homogeneous Hydrogenation*, John Wiley & Sons, Inc., Toronto, Canada, **1973**.

[16]   P. N. Rylander, *Catalytic Hydrogenation in Organic Syntheses*, Academic Press, Inc, New York, NY, **1979**.

[17]   M. Beller, C. Bolm, Eds. , *Transition Metals for Organic Synthesis*, Wiley-VCH Verlag GmbH, Weinheim, Germany, **2004**.

[18]   "Asymmetric Catalysis," can be found under http://www.nature.com/subjects/asymmetric-catalysis, **2016**.

[19]   B. M. Trost, *Proc. Natl. Acad. Sci.* **2004**, *101*, 5348–5355.

[20]   I. Ojima, Ed. , *Catalytic Asymmetric Synthesis*, John Wiley & Sons, Inc., New Jersey, **2010**.

[21]   R. Noyori, *Asymmetric Catalysis in Organic Synthesis*, John Wiley & Sons, Inc., New York, NY, **1994**.

[22]   D. J. Ager, in *Handb. Homog. Hydrog.* (Eds.: J.G. de Vries, C.J. Elsevier), Wiley-VCH, Weinheim, Germany, **2007**, pp. 745–772.

[23]   C. K. Ralph, O. M. Akotsi, S. H. Bergens, *Organometallics* **2004**, *23*, 1484–1486.

[24]   S. C. Stinson, *Chem. Eng. News* **2000**, *78*, 55–78.

[25]   S. C. Stinson, *Chem. Eng. News* **1997**, *75*, 38–70.

[26]   S. C. Stinson, *Chem. Eng. News* **1995**, *73*, 44–54.

[27]   S. C. Stinson, *Chem. Eng. News* **1994**, *72*, 38–50.

[28]   S. C. Stinson, *Chem. Eng. News* **1993**, *71*, 38–65.

[29]   S. C. Stinson, *Chem. Eng. News* **1992**, *70*, 46–79.

[30]   T. Ito, H. Ando, T. Suzuki, T. Ogura, K. Hotta, Y. Imamura, Y. Yamaguchi, H. Handa, *Science (80-.).* **2010**, *327*, 1345–1350.

[31]   G. Shang, W. Li, X. Zhang, in *Catal. Asymmetric Synth.* (Ed.: I. Ojima), John Wiley & Sons, Inc., New York, NY, **2010**, p. 343.

[32]   G. O. Spessard, G. L. Miessler, *Organometallic Chemistry*, Prentice-Hall, Inc., **1997**.

[33]   J. A. Osborn, F. H. Jardine, J. F. Young, G. Wilkinson, *J. Chem. Soc. A Inorganic, Phys. Theor.* **1966**, 1711–1732.

[34]   W. S. Knowles, M. J. Sabacky, B. D. Vineyard, *J. Chem. Soc. Chem. Commun.* **1972**, 10.

[35]   W. S. Knowles, M. J. Sabacky, B. D. Vineyard, in *Adv. Chem. Ser.*, **1974**, pp. 274–282.

[36]   J. D. Morrison, W. F. Masler, M. K. Neuberg, *Adv. Catal.* **1976**, *25*, 81–124.

[37]   L. Horner, H. Siegel, H. Büthe, *Angew. Chem. Int. Ed. Engl.* **1968**, *7*, 942–942.

[38]   W. S. Knowles, M. J. Sabacky, *Chem. Commun.* **1968**, 1445–1446.

[39]   D. Shriver, P. Atkins, W. H. Freeman And Company, New York, NY, **1999**, pp. 459–524.

[40]   R. H. Crabtree, *The Organometallic Chemistry of the Transition Metals*, John Wiley & Sons, Inc., New Jersey, **2005**.

[41]   J. Clayden, N. Greeves, S. Warren, P. Wothers, *Organic Chemistry*, Oxford University Press, New York, NY, **2000**.

[42]   J. Halpern, *Science (80-.).* **1982**, *217*, 401–407.

[43]   F. A. Carey, R. J. Sundberg, *Advanced Organic Chemistry Part A: Structure and Mechanisms*, Springer, New York, NY, **2007**.

[44]   P. J. Walsh, M. C. Kolzlowski, *Fundamentals of Asymmetric Catalysis*, University Science Books, United States, **2009**.

[45]   T. Ohta, H. Takaya, M. Kitamura, K. Nagai, R. Noyori, *J. Org. Chem.* **1987**, *52*, 3174–3176.

[46]   P. G. Jessop, R. R. Stanley, R. A. Brown, C. A. Eckert, C. L. Liotta, T. T. Ngo, P. Pollet, *Green Chem.* **2003**, *5*, 123–128.

[47]   R. Noyori, *Pure Appl. Chem.* **1981**, *53*, 2315–2322.

[48]   C. A. Tolman, *Chem. Rev.* **1977**, *77*, 313–348.

[49]   A. Poater, F. Ragone, R. Mariz, R. Dorta, L. Cavallo, *Chem. - A Eur. J.* **2010**, *16*, 14348–14353.

[50]   C. Costabile, L. Cavallo, *J. Am. Chem. Soc.* **2004**, *126*, 9592–9600.

[51]   F. Ragone, A. Poater, L. Cavallo, *J. Am. Chem. Soc.* **2010**, *132*, 4249–4258.

[52]   P. G. Jessop, T. Ikariya, R. Noyori, *Chem. Rev.* **1995**, *95*, 259–272.

[53]   W. I. F. Armaego, C. L. Chai, *Purification of Laboratory Chemicals*, Elsevier Ltd, Burlington, MA, **2003**.

[54]   A. McKenzie, J. K. Wood, *J. Chem. Soc. Trans.* **1919**, *115*, 828–840.

[55]   V. D. Vitnik, M. D. Ivanović, Ž. J. Vitnik, J. B. Đorđević, Ž. S. Žižak, Z. D. Juranić, I. O. Juranić, *Synth. Commun.* **2009**, *39*, 1457–1471.

[56]   D. C. Whitehead, R. Yousefi, A. Jaganathan, B. Borhan, *J. Am. Chem. Soc.* **2010**, *132*, 3298–300.

[57]   D. C. Braddock, G. Cansell, S. A. Hermitage, *Chem. Commun.* **2006**, 2483–2485.

[58]   G. E. Veitch, E. N. Jacobsen, *Angew. Chem. Int. Ed.* **2010**, *49*, 7332–5.

[59]   S. Nicolai, S. Erard, D. F. González, J. Waser, *Org. Lett.* **2010**, *12*, 384–7.

[60]   S. Song, S.-F. Zhu, Y.-B. Yu, Q.-L. Zhou, *Angew. Chem. Int. Ed.* **2013**, *52*, 1556–1559.

[61]   H. Lebel, M. Davi, S. Díez-Gonzalez, S. P. Nolan, *J. Org. Chem.* **2007**, *72*, 144–149.

[62]   Z. Liang, L. Ju, Y. Xie, L. Huang, Y. Zhang, *Chemistry* **2012**, *18*, 15816–21.

[63]   T. Ohmura, K. Masuda, I. Takase, M. Suginome, *J. Am. Chem. Soc.* **2009**, *131*, 16624–5.

[64]   Z. Ni, L. Giordano, A. Tenaglia, *Chemistry* **2014**, *20*, 11703–6.

[65]   C. B. Tripathi, S. Mukherjee, *Angew. Chem. Int. Ed.* **2013**, *52*, 8450–3.

[66]   B. Mohan Reddy, V. Venkata Ramana Kumar, N. Chinna Gangi Reddy, S. Mahender Rao, *Chin. Chemi. Lett.* **2014**, *25*, 179–182.

[67]   A. Garzan, A. Jaganathan, N. Salehi Marzijarani, R. Yousefi, D. C. Whitehead, J. E. Jackson, B. Borhan, *Chemistry* **2013**, *19*, 9015–21.

[68]   Z.-C. Duan, X.-P. Hu, C. Zhang, D.-Y. Wang, S.-B. Yu, Z. Zheng, *J. Org. Chem.* **2009**, *74*, 9191–4.

[69]   C. Baumgartner, C. Eberle, F. Diederich, S. Lauw, F. Rohdich, W. Eisenreich, A. Bacher, *Helv. Chim. Acta* **2007**, *90*, 1043–1068.

[70]   D. J. Dumas, *J. Org. Chem.* **1988**, *53*, 4650–4653.

[71]   D. A. Fort, T. J. Woltering, M. Nettekoven, H. Knust, T. Bach, *Chem. Commun.* **2013**, *49*, 2989–91.

[72]   J. P. Holland, P. J. Barnard, S. R. Bayly, H. M. Betts, G. C. Churchill, J. R. Dilworth, R. Edge, J. C. Green, R. Hueting, *Eur. J. Inorg. Chem.* **2008**, *2008*, 1985–1993.

[73]   K. Hattori, H. Sajiki, K. Hirota, *Tetrahedron* **2000**, *56*, 8433–8441.

[74]   T. León, A. Correa, R. Martin, *J. Am. Chem. Soc.* **2013**, *135*, 1221–4.

[75]   J. I. Brauman, A. J. Pandell, *J. Am. Chem. Soc.* **1967**, *89*, 5421–5424.

[76]   S. Song, S.-F. Zhu, S. Yang, S. Li, Q.-L. Zhou, *Angew. Chem. Int. Ed.* **2012**, *51*, 2708–11.

[77]   T. D. Hoffman, D. J. Cram, *J. Am. Chem. Soc.* **1969**, *91*, 1000–1008.

[78]   D. J. Abraham, D. M. Gazze, P. E. Kennedy, M. Mokotoff, *J. Med. Chem.* **1984**, *27*, 1549–1559.

[79]   J.-J. Bourguignon, M. Maitre, E. Klotz, M. Schmitt, S. Gobaille, J.-P. Macher, *Derivatives of 4-hydroxybutanoic Acid and of Its Higher Homologue as Ligands of γ-hydroxybutyrate (GHB) Receptors, Pharmaceutical Compositions Containing Same and Pharmaceutical Uses*, **2002**, WO 2002042250.

[80]   M. Szostak, B. Sautier, M. Spain, D. J. Procter, *Org. Lett.* **2014**, *16*, 1092–5.

[81]   J. G. de Vries, C. J. Elsevier, Eds. , *The Handbook of Homogeneous Hydrogenation*, Wiley-VCH Verlag GmbH, Weinheim, Germany, **2006**.

[82]   E. N. Jacobsen, A. Pfaltz, H. Yamamoto, Eds. , *Comprehensive Asymmetric Catalysis: Supplement 1*, Springer Berlin Heidelberg, Germany, **1999**.

[83]   J. G. de Vries, C. J. Elsevier, Eds. , *The Handbook of Homogeneous Hydrogenation*, Wiley-VCH Verlag GmbH, Weinheim, Germany, **2007**.

[84]   J. Halpern, J. F. Harrod, B. R. James, *J. Am. Chem. Soc.* **1961**, *83*, 753–754.

[85]   D. Evans, J. A. Osborn, F. H. Jardine, G. Wilkinson, *Nature* **1965**, *208*, 1203–1204.

[86]   M. A. Bennett, T. W. Matheson, in *Compr. Organomet. Chem.* (Eds.: G. Wilkinson, F.G.A. Stone, E.W. Abel), Pergamon Press, Oxford, **1982**.

[87]   Cerner Multum Inc, "Naproxen," can be found under http://www.drugs.com/naproxen.html, **2013**.

[88]   Cerner Multum Inc, "Ibuprofen," can be found under http://www.drugs.com/ibuprofen.html, **2015**.

[89]   T. Manimaran, T. C. Wu, W. D. Klobucar, C. H. Kolich, G. P. Stahly, F. R. Fronczek, S. E. Watkins, *Organometallics* **1993**, *12*, 1467–1470.

[90]   D. J. C. Constable, P. J. Dunn, J. D. Hayler, G. R. Humphrey, J. L. Leazer, Jr., R. J. Linderman, K. Lorenz, J. Manley, B. A. Pearlman, A. Wells, et al., *Green Chem.* **2007**, *9*, 411.

[91]   T. L. Church, P. G. Andersson, *Coord. Chem. Rev.* **2008**, *252*, 513–531.

[92]   Y. Zhu, K. Burgess, *Acc. Chem. Res.* **2012**, *45*, 1623–36.

[93]   D. H. Woodmansee, A. Pfaltz, in *Top. Organomet. Chem. Iridium Catal.* (Ed.: P.G. Andersson), Springer Berlin Heidelberg, Berlin, Heidelberg, **2011**, pp. 31–76.

[94]   X. Quan, V. S. Parihar, M. Bera, P. G. Andersson, *European J. Org. Chem.* **2014**, *2014*, 140–146.

[95]   S. Gruber, A. Pfaltz, *Angew. Chem. Int. Ed.* **2014**, *53*, 1896–900.

[96]   W. S. Knowles, *Angew. Chem. Int. Ed. English* **2002**, *41*, 1999–2007.

[97]   R. Noyori, *Angew. Chem. Int. Ed. Engl.* **2002**, *41*, 2008–2022.

[98]   J. Halpern, D. Morrison, James, Eds. , *Asymmetric Synthesis: Chiral Catalysis*, Academic Press, Inc, Orlando, Florida, **2006**.

[99]   C. J. A. Daley, J. A. Wiles, S. H. Bergens, *Inorganica Chim. Acta* **2006**, *359*, 2760–2770.

[100]   M. T. Ashby, J. Halpern, *J. Am. Chem. Soc.* **1991**, *113*, 589–594.

[101]   I. D. Gridnev, T. Imamoto, *Acc. Chem. Res.* **2004**, *37*, 633–44.

[102]   T. Saito, T. Yokozawa, T. Ishizaki, T. Moroi, N. Sayo, T. Miura, H. Kumobayashi, *Adv. Synth. Catal.* **2001**, *343*, 264–267.

[103]   J. Almena, A. Monsees, R. Kadyrov, T. H. Riermeier, B. Gotov, J. Holz, A. Börner, *Adv. Synth. Catal.* **2004**, *346*, 1263–1266.

[104]   J. J. Verendel, O. Pàmies, M. Diéguez, P. G. Andersson, *Chem. Rev.* **2014**, *114*, 2130–69.

[105]   Y. Zhang, Z. Han, F. Li, K. Ding, A. Zhang, *Chem. Commun.* **2010**, *46*, 156–8.

[106]   F. Menges, A. Pfaltz, *ChemInform* **2010**, *33*, 40–44.

[107]   E. T. Denisov, T. S. Pokidova, *Russ. J. Phys. Chem. B* **2010**, *4*, 557–565.

[108]   T. W. G. Solomons, C. B. Fryhle, S. A. Snyder, *Organic Chemistry - Decarboxylation*, John Wiley & Sons, Inc., Hoboken, NJ, **2014**.

[109]   Q.-L. Zhou, Ed. , *Privileged Chiral Ligands and Catalysts*, Wiley-VCH, Weinheim, Germany, **2011**.

[110]   B. J. Flowers, R. Gautreau-Service, P. G. Jessop, *Adv. Synth. Catal.* **2008**, *350*, 2947–2958.

[111]   M. Jahjah, M. Alame, S. Pellet-Rostaing, M. Lemaire, *Tetrahedron: Asymmetry* **2007**, *18*, 2305–2312.

[112]   P.-C. Yan, J.-H. Xie, X.-D. Zhang, K. Chen, Y.-Q. Li, Q.-L. Zhou, D.-Q. Che, *Chem. Commun.* **2014**, *50*, 15987–15990.

[113]   K. Kinbara, *Synlett* **2005**, 0732–0743.

[114]   K. Koh, R. N. Ben, T. Durst, *Tetrahedron Lett.* **1993**, *34*, 4473–4476.

[115]   G. Jian-Xin, L. Zu-Yi, L. Guo-Qiang, *Tetrahedron* **1993**, *49*, 5805–5816.

[116]   G. A. Applegate, R. W. Cheloha, D. L. Nelson, D. B. Berkowitz, *Chem. Commun.* **2011**, *47*, 2420–2422.

[117]   M. Landwehr, L. Hochrein, C. R. Otey, A. Kasrayan, J.-E. Bäckvall, F. H. Arnold, *J. Am. Chem. Soc.* **2006**, *128*, 6058–6059.

[118]   D. Zhu, Y. Yang, L. Hua, *J. Org. Chem.* **2006**, *71*, 4202–4205.

[119]   W. Wu, X. Liu, Y. Zhang, J. Ji, T. Huang, L. Lin, X. Feng, *Chem. Commun.* **2015**,

51, 11646–11649.

[120]   E. Schmitt, I. Schiffers, C. Bolm, *Tetrahedron Lett.* **2009**, *50*, 3185–3188.

[121]   P. Wang, W.-J. Tao, X.-L. Sun, S. Liao, Y. Tang, *J. Am. Chem. Soc.* **2013**, *135*, 16849–16852.

[122]   Y. Yamamoto, T. Shirai, N. Miyaura, *Chem. Commun.* **2012**, *48*, 2803.

[123]   J. Majer, P. Kwiatkowski, J. Jurczak, *Org. Lett.* **2008**, *10*, 2955–2958.

[124]   J. Majer, P. Kwiatkowski, J. Jurczak, *Org. Lett.* **2009**, *11*, 4636–4639.

[125]   K. Sisido, K. Kumazawa, H. Nozaki, *J. Am. Chem. Soc.* **1960**, *82*, 125–129.

[126]   K. Oertle, H. Beyeler, R. O. Duthaler, W. Lottenbach, M. Riediker, E. Steiner, *Helv. Chim. Acta* **1990**, *73*, 353–358.

[127]   S. Kobayashi, T. Sano, T. Mukaiyama, *Chem. Lett.* **1989**, 1319–1322.

[128]   N. Sayo, H. Kumobayashi, S. Akutagawa, R. Noyori, H. TAKAYA, *Process of Preparing Optically Active Alcohol.*, **1988**, EP0295890.

[129]   Y. Sun, X. Wan, J. Wang, Q. Meng, H. Zhang, L. Jiang, Z. Zhang, *Org. Lett.* **2005**, *7*, 5425–7.

[130]   C.-J. Wang, X. Sun, X. Zhang, *Synlett* **2006**, *2006*, 1169–1172.

[131]   M. Berthod, J.-M. Joerger, G. Mignani, M. Vaultier, M. Lemaire, *Tetrahedron: Asymmetry* **2004**, *15*, 2219–2221.

[132]   M. G. Vinogradov, E. V Starodubtseva, O. V Turova, *Russ. Chem. Rev.* **2008**, *77*, 725–737.

[133]   N. W. Boaz, S. D. Debenham, E. B. Mackenzie, S. E. Large, *Org. Lett.* **2002**, *4*, 2421–2424.

[134]   K. Inoguchi, S. Sakuraba, K. Achiwa, *Synlett* **1992**, *1992*, 169–178.

[135] J. Carpentier, A. Mortreux, *Tetrahedron: Asymmetry* **1997**, *8*, 1083–1099.

[136] X.-H. Yang, J.-H. Xie, Q.-L. Zhou, *Org. Chem. Front.* **2014**, *1*, 190.

[137] M. A. Ariger, E. M. Carreira, *Org. Lett.* **2012**, *14*, 4522–4524.

[138] J.-H. Xie, X.-Y. Liu, X.-H. Yang, J.-B. Xie, L.-X. Wang, Q.-L. Zhou, *Angew. Chem. Int. Ed.* **2012**, *51*, 201–203.

[139] S. Fukuzawa, H. Oki, M. Hosaka, J. Sugasawa, S. Kikuchi, *Org. Lett.* **2007**, *9*, 5557–5560.

[140] C.-J. Wang, H. Tao, X. Zhang, *Tetrahedron Lett.* **2006**, *47*, 1901–1903.

[141] T. Benincori, S. Rizzo, T. Pilati, A. Ponti, M. Sada, E. Pagliarini, S. Ratti, C. Giuseppe, L. de Ferra, F. Sannicolò, *Tetrahedron: Asymmetry* **2004**, *15*, 2289–2297.

[142] L. Zhu, H. Chen, Q. Meng, W. Fan, X. Xie, Z. Zhang, *Tetrahedron* **2011**, *67*, 6186–6190.

[143] L. Zhu, Q. Meng, W. Fan, X. Xie, Z. Zhang, *J. Org. Chem.* **2010**, *75*, 6027–6030.

[144] J.-H. Xie, X.-Y. Liu, J.-B. Xie, L.-X. Wang, Q.-L. Zhou, *Angew. Chem. Int. Ed.* **2011**, *50*, 7329–7332.

[145] J.-B. Xie, J.-H. Xie, X.-Y. Liu, Q.-Q. Zhang, Q.-L. Zhou, *Asian J. Chem.* **2011**, *6*, 899–908.

[146] J. P. Genêt, C. Pinel, V. Ratovelomanana-Vidal, S. Mallart, X. Pfister, L. Bischof, M. C. C. De Andrade, S. Darses, C. Galopin, J. A. Laffitte, *Tetrahedron: Asymmetry* **1994**, *5*, 675–690.

[147] R. D. Larsen, Ed. , *Organometallics in Process Chemistry*, Springer, New York, NY, **2004**.

[148] A. P. Green, N. J. Turner, E. O'Reilly, *Angew. Chem. Int. Ed.* **2014**, *53*, 10714–10717.

[149] P. Dupau, A.-E. Hay, C. Bruneau, P. H. Dixneuf, *Tetrahedron: Asymmetry* **2001**,

12, 863–867.

[150] J. Holz, A. Monsees, H. Jiao, J. You, I. V. Komarov, C. Fischer, K. Drauz, A. Börner, *J. Org. Chem.* **2003**, *68,* 1701–1707.

[151] X. Dai, D. Cahard, *Adv. Synth. Catal.* **2014**, *356*, 1317–1328.

[152] A. Baeza, A. Pfaltz, *Chem. - A Eur. J.* **2009**, *15*, 2266–2269.

[153] M. J. Burk, Y. M. Wang, J. R. Lee, *J. Am. Chem. Soc.* **1996**, *118*, 5152–5143.

[154] L. Qiu, M. Prashad, B. Hu, K. Prasad, O. Repic, T. J. Blacklock, F. Y. Kwong, S. H. L. Kok, H. W. Lee, A. S. C. Chan, *Proc. Natl. Acad. Sci.* **2007**, *104*, 16787–16792.

[155] J. Almena, A. Monsees, R. Kadyrov, T. H. Riermeier, B. Gotov, J. Holz, A. Börner, *Adv. Synth. Catal.* **2004**, *346*, 1263–1266.

[156] K. Junge, G. Oehme, A. Monsees, T. Riermeier, U. Dingerdissen, M. Beller, *J. Organomet. Chem.* **2003**, *675*, 91–96.

[157] G. P. Aguado, A. G. Moglioni, E. García-Expósito, V. Branchadell, R. M. Ortuño, *J. Org. Chem.* **2004**, *69*, 7971–8.

[158] S. Enthaler, G. Erre, K. Junge, D. Michalik, A. Spannenberg, F. Marras, S. Gladiali, M. Beller, *Tetrahedron: Asymmetry* **2007**, *18*, 1288–1298.

[159] H. B. Kagan, N. Langlois, T. P. Dang, *J. Organomet. Chem.* **1975**, *90*, 353–365.

[160] Z.-P. Chen, M.-W. Chen, R.-N. Guo, Y.-G. Zhou, *Org. Lett.* **2014**, *16*, 1406–1409.

[161] K. H. Hopmann, A. Bayer, *Organometallics* **2011**, *30*, 2483–2497.

[162] Q. Zhao, J. Wen, R. Tan, K. Huang, P. Metola, R. Wang, E. V. Anslyn, X. Zhang, *Angew. Chem. Int. Ed.* **2014**, *53*, 8467–8470.

[163] M. Zhou, T.-L. Liu, M. Cao, Z. Xue, H. Lv, X. Zhang, *Org. Lett.* **2014**, *16*, 3484–3487.

[164]   P. Cheruku, T. L. Church, A. Trifonova, T. Wartmann, P. G. Andersson, *Tetrahedron Lett.* **2008**, *49*, 7290–7293.

[165]   X.-F. Cai, R.-N. Guo, M.-W. Chen, L. Shi, Y.-G. Zhou, *Chem. - A Eur. J.* **2014**, *20*, 7245–7248.

[166]   M. Jackson, I. C. Lennon, *Tetrahedron Lett.* **2007**, *48*, 1831–1834.

[167]   M. E. Fox, M. Jackson, I. C. Lennon, J. Klosin, K. A. Abboud, *J. Org. Chem.* **2008**, *73*, 775–784.

[168]   F. W. Patureau, C. Worch, M. A. Siegler, A. L. Spek, C. Bolm, J. N. H. Reek, *Adv. Synth. Catal.* **2012**, *354*, 59–64.

[169]   W.-J. Lu, X.-L. Hou, *Adv. Synth. Catal.* **2009**, *351*, 1224–1228.

[170]   G. Erre, S. Enthaler, K. Junge, D. Addis, M. Beller, *Adv. Synth. Catal.* **2009**, *351*, 1437–1441.

[171]   W. Tang, X. Zhang, *Angew. Chem. Int. Ed.* **2002**, *41*, 1612–1614.

[172]   L. Phan, H. Brown, J. White, A. Hodgson, P. G. Jessop, *Green Chem.* **2009**, *11*, 53–59.

[173]   P. G. Jessop, D. J. Heldebrant, X. Li, C. A. Eckert, C. L. Liotta, *Nature* **2005**, *436*, 1102–1102.

[174]   L. Phan, J. R. Andreatta, L. K. Horvey, C. F. Edie, A.-L. Luco, A. Mirchandani, D. J. Darensbourg, P. G. Jessop, *J. Org. Chem.* **2008**, *73*, 127–132.

[175]   T. Yu, R. Cristiano, R. G. Weiss, *Chem. Soc. Rev.* **2010**, *39*, 1435–1447.

[176]   T. Yamada, P. J. Lukac, M. George, R. G. Weiss, *Chem. Mater.* **2007**, *19*, 967–969.

[177]   T. Yu, T. Yamada, G. C. Gaviola, R. G. Weiss, *Chem. Mater.* **2008**, *20*, 5337–5344.

[178]   M. Chatterjee, H. Kawanami, M. Sato, T. Ishizaka, T. Yokoyama, T. Suzuki, *Green Chem.* **2010**, *12*, 87–93.

[179]   X. Xie, C. L. Liotta, C. A. Eckert, *Ind. Eng. Chem. Res.* **2004**, *43*, 7907–7911.

[180]   ACS, "12 Principles of Green Chemistry," can be found under http://www.acs.org/content/acs/en/greenchemistry/what-is-green-chemistry/principles/12-principles-of-green-chemistry.html, **2015**.

[181]   ACS, "Green Chemistry Definition," can be found under http://www.acs.org/content/acs/en/greenchemistry/what-is-green-chemistry/definition.html, **2015**.

[182]   S. Schulz, C. Fischer, H.-J. Drexler, D. Heller, *Acta Crystallogr. Sect. E Struct. Reports Online* **2010**, *66*, 1370–1370.

[183]   J. Holz, O. Zayas, H. Jiao, W. Baumann, A. Spannenberg, A. Monsees, T. H. Riermeier, J. Almena, R. Kadyrov, A. Börner, *Chem. - A Eur. J.* **2006**, *12*, 5001–5013.

[184]   D. Chen, B. Sundararaju, R. Krause, J. Klankermayer, P. Dixneuf, W. Leitner, *ChemCatChem* **2010**, *2*, 55–57.

[185]   R. Guzmán-Mejía, G. Reyes-Rangel, E. Juaristi, *Nat. Protoc.* **2007**, *2*, 2759–2766.

[186]   V. Kogan, Z. Aizenshtat, R. Neumann, *New J. Chem.* **2002**, *26*, 272–274.

[187]   G.-Q. Lin, Q.-D. You, J.-F. Cheng, Eds. , *Chiral Drugs-Chemistry and Biological Action*, John Wiley & Sons, Inc., Hoboken, NJ, **2011**.

Appendix A: Selected Spectra
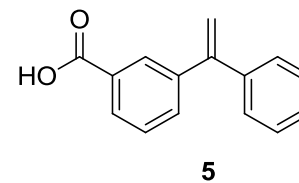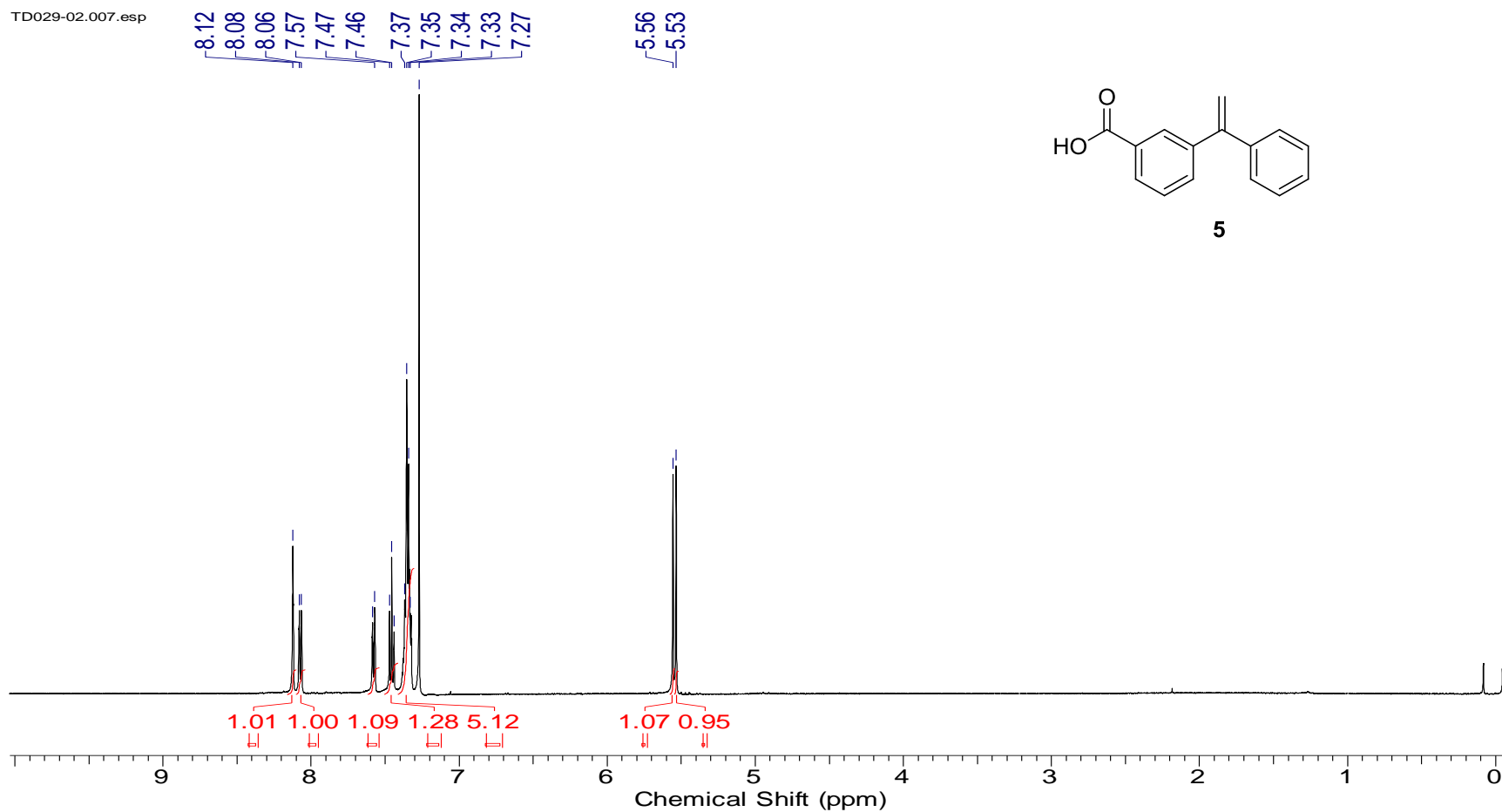
Figure AA 1. ^{1}H NMR spectrum of 3-(1-phenylethenyl)benzoic acid, 4 (400 MHz, CDCl$_3$).
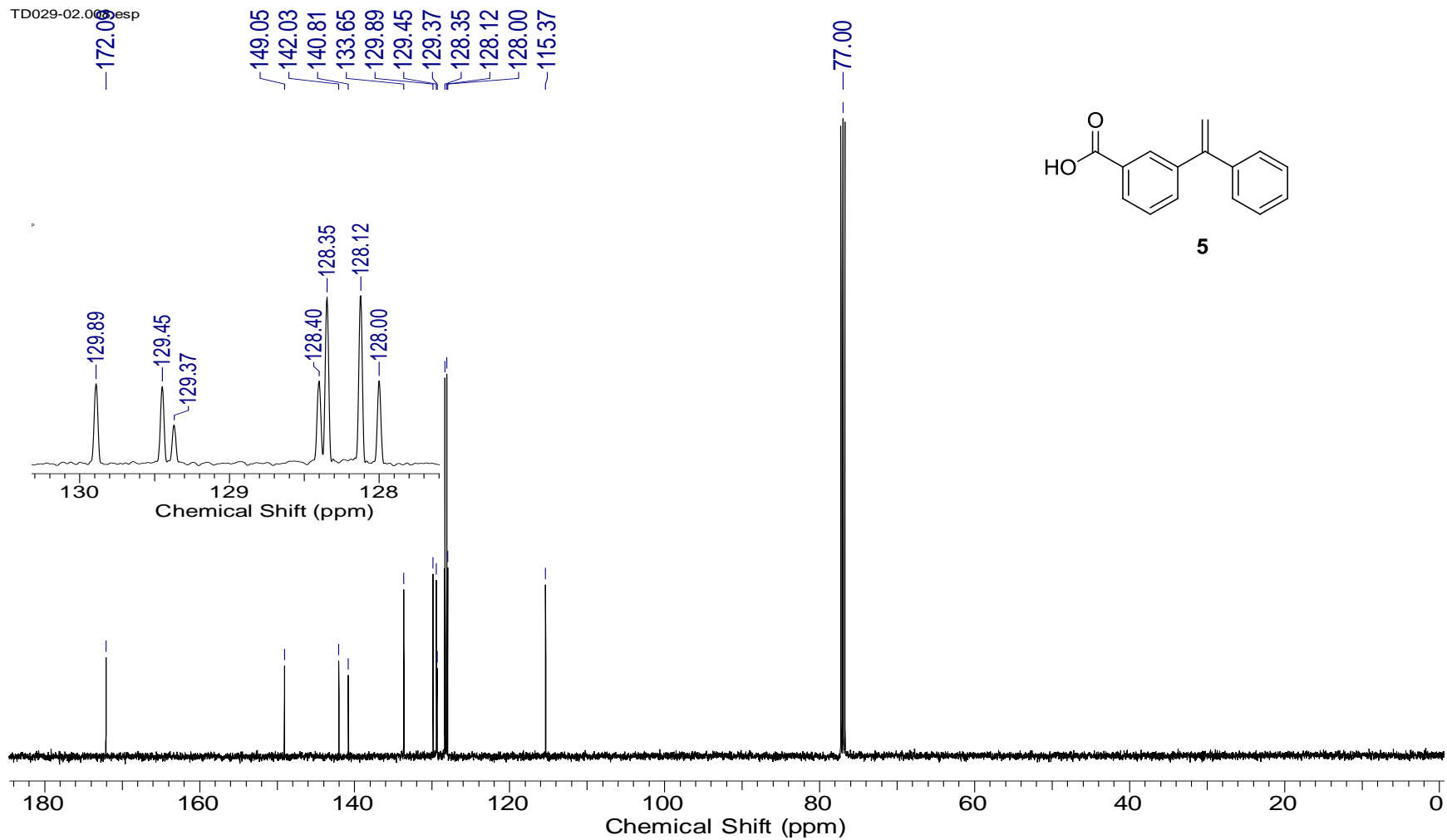
Figure AA 2. ^{13}C NMR spectrum of 3-(1-phenylethenyl)benzoic acid, 4 (100 MHz, CDCl$_3$).
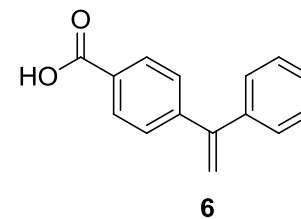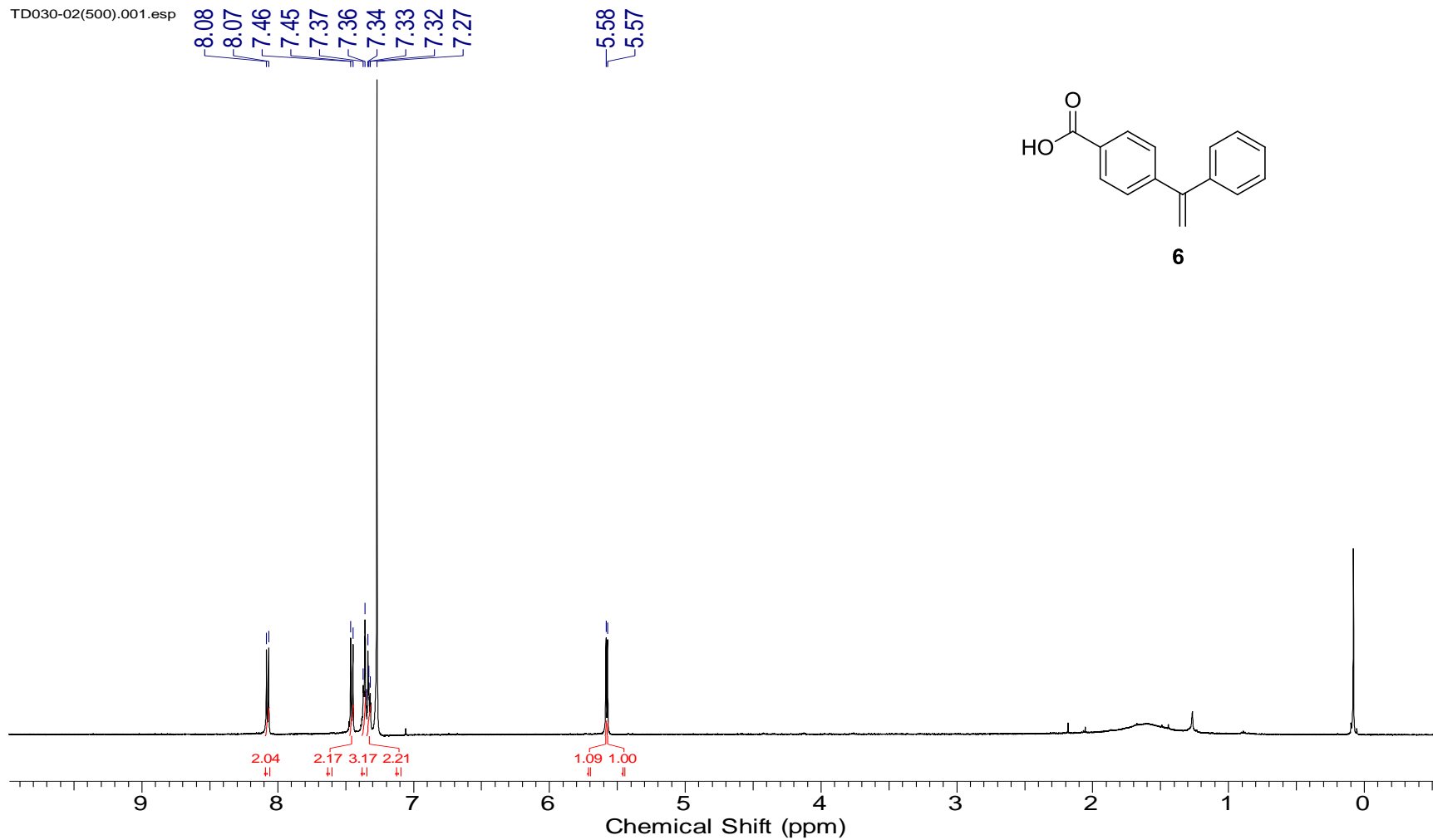
Figure AA 3. ^{1}H NMR spectrum of 4-(1-phenylethenyl)benzoic acid, 6 (400 MHz, CDCl$_3$).

3
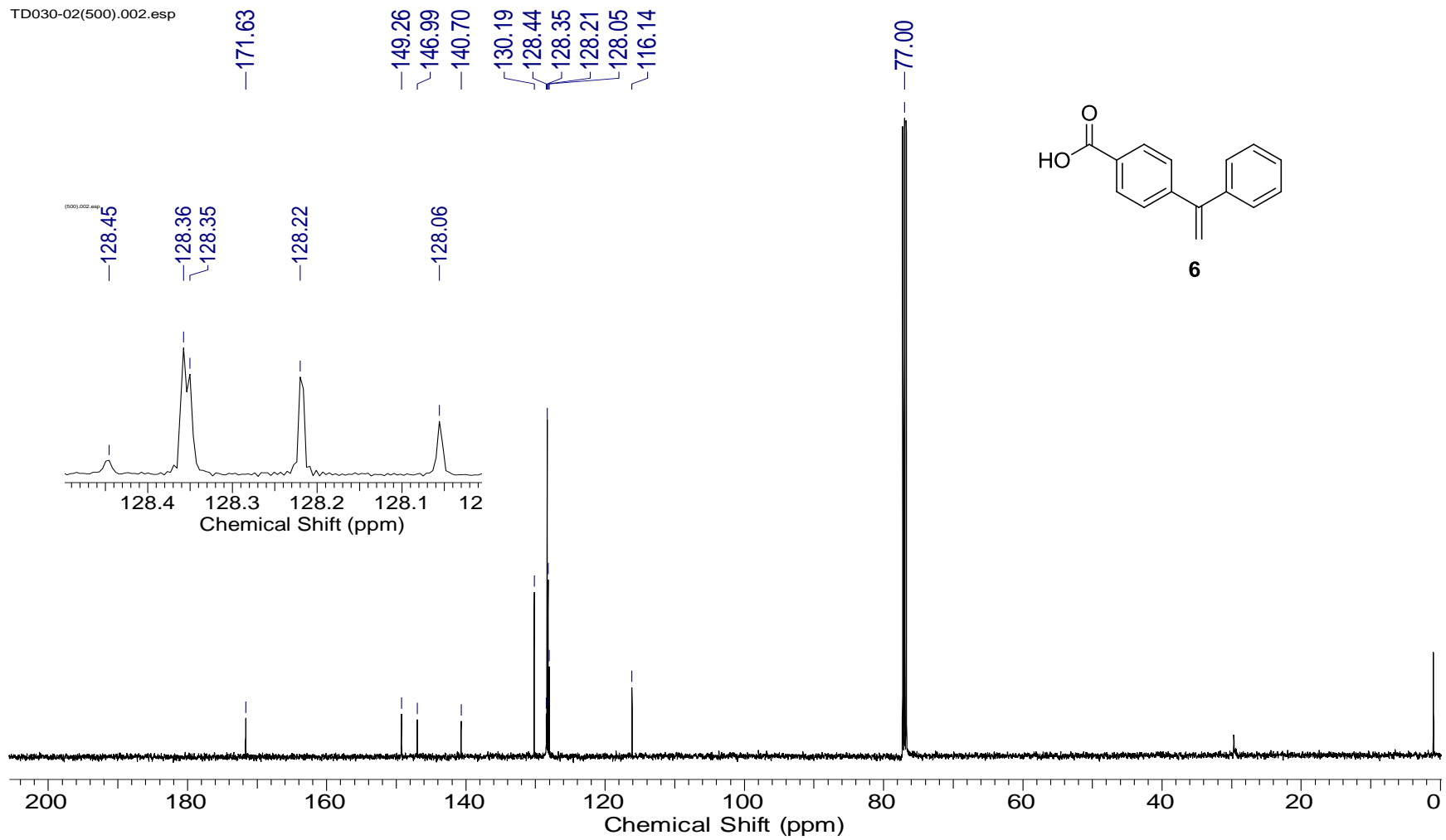
Figure AA 4. ^{13}C NMR spectrum of 4-(1-phenylethenyl)benzoic acid, 6 (100 MHz, CDCl$_3$).

7.43
7.41
7.27
6.88
6.85
5.30
5.00
4.08
4.06
4.05
4.03
2.14
1.56
1.45
1.43
1.41

8

2.00 1.99 1.06 1.04 2.09 3.13 3.17

9 8 7 6 5 4 3 2 1
Chemical Shift (ppm)
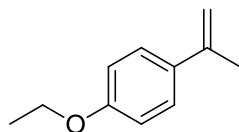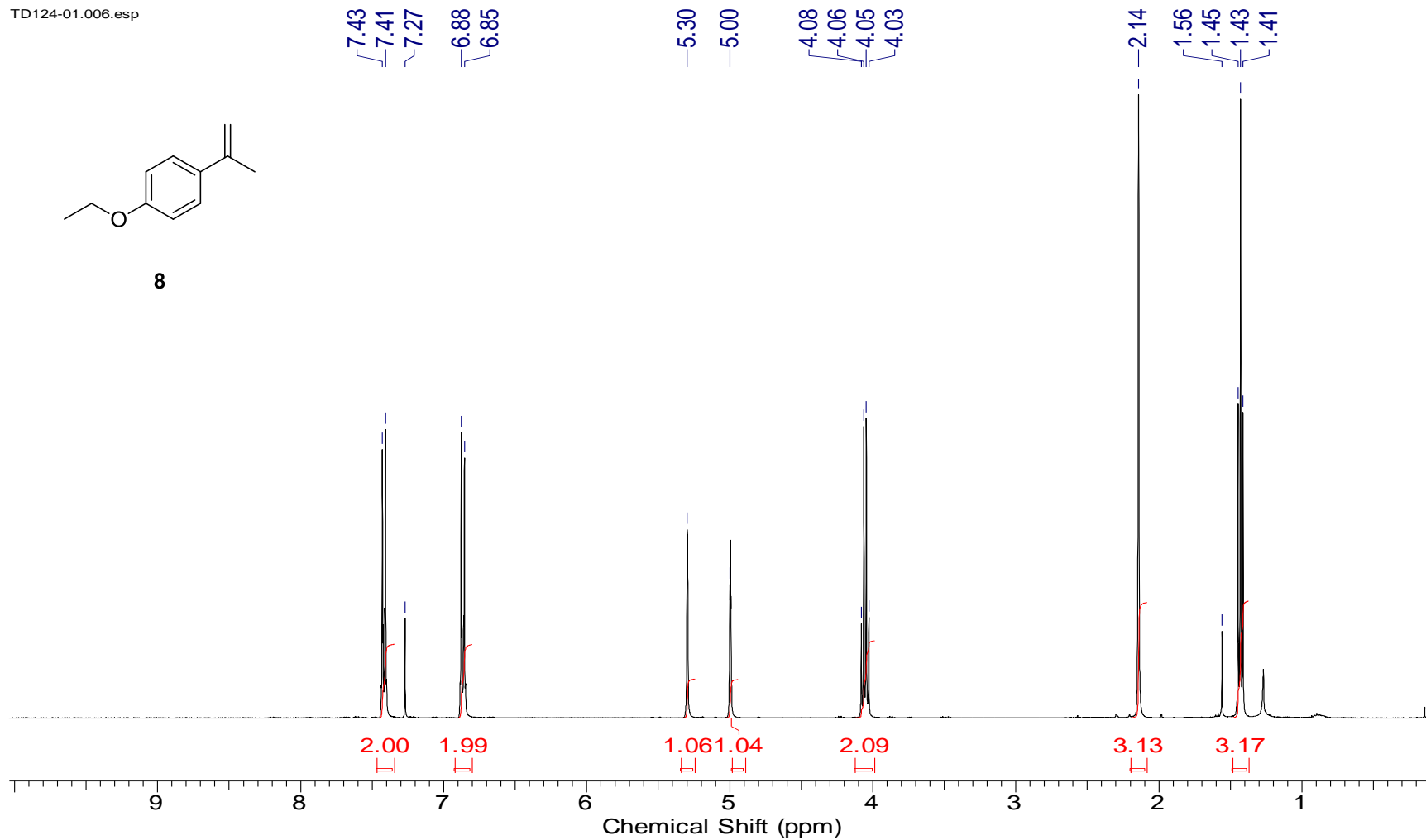
Figure AA 5. ^{1}H NMR spectrum of 1-ethoxy-4-(prop-1-en-2-yl) benzene, 8 (400 MHz, CDCl$_3$).
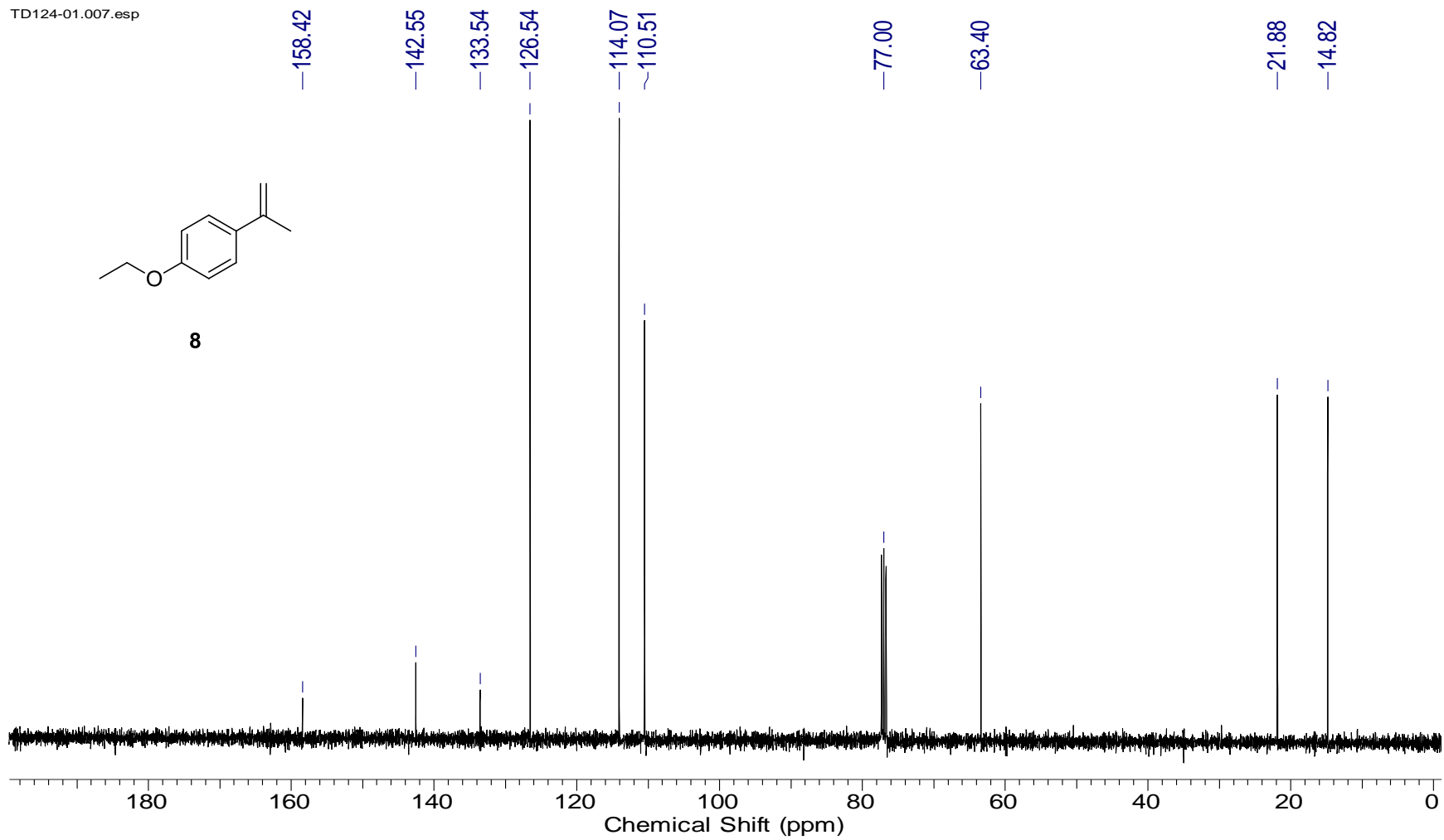
Figure AA 6. ^{13}C NMR spectrum of 1-ethoxy-4-(prop-1-en-2-yl) benzene, 8 (100 MHz, CDCl$_3$).
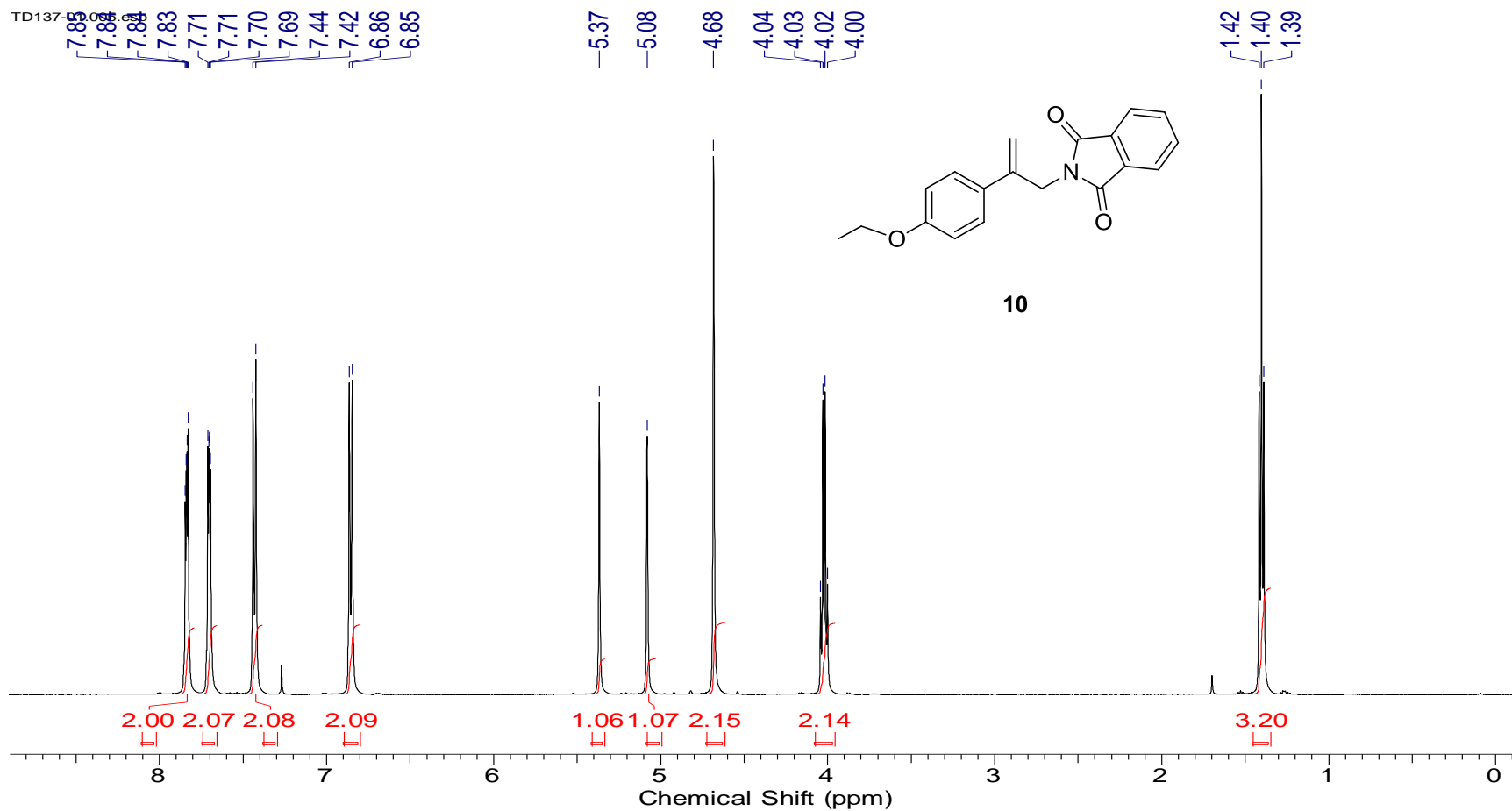
Figure AA 7. ^{1}H NMR spectrum of 2-[2-(4-ethoxyphenyl)prop-2-en-1-yl]-1*H*-isoindole-1,3(2*H*)-dione, 10 (500 MHz, CDCl$_3$).
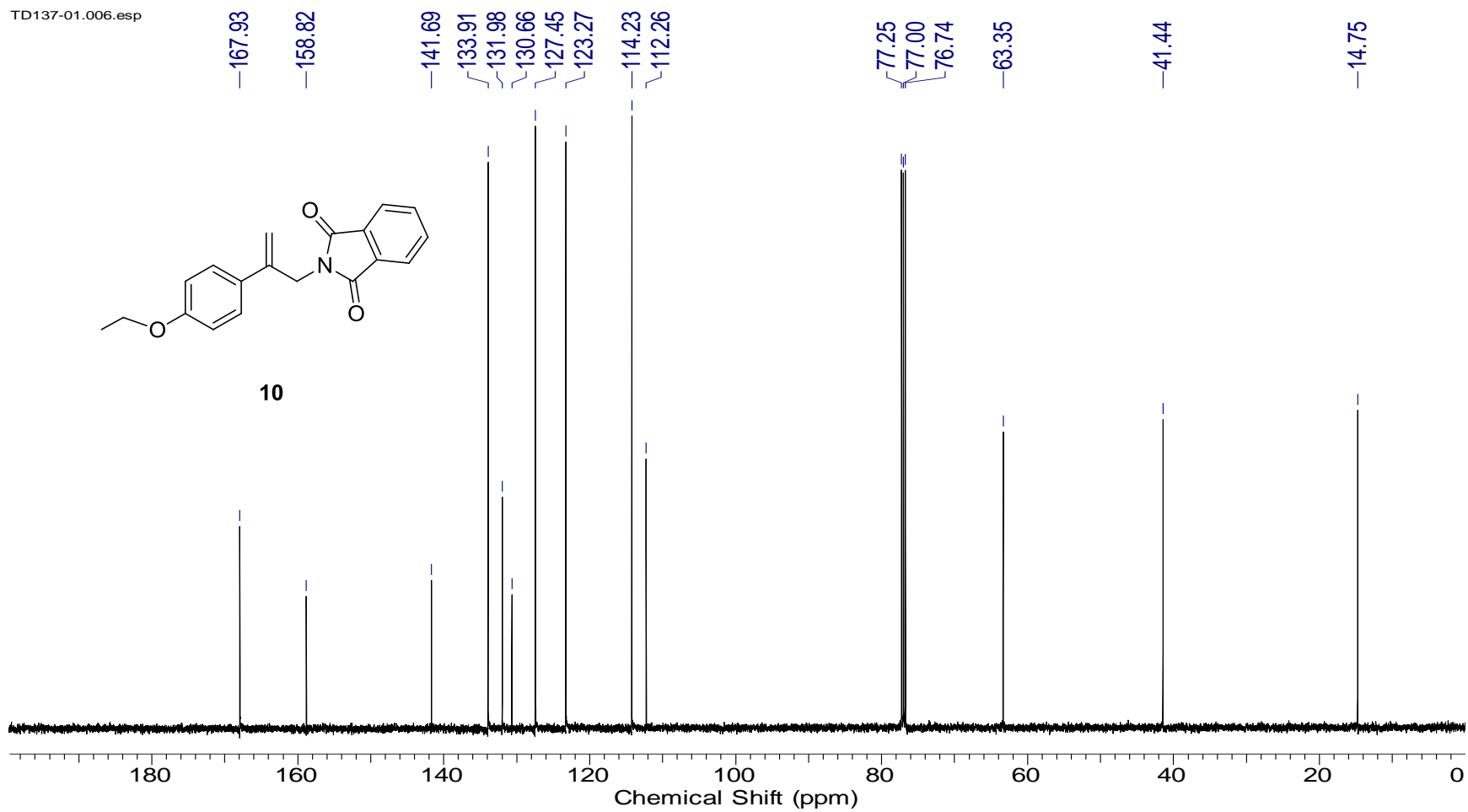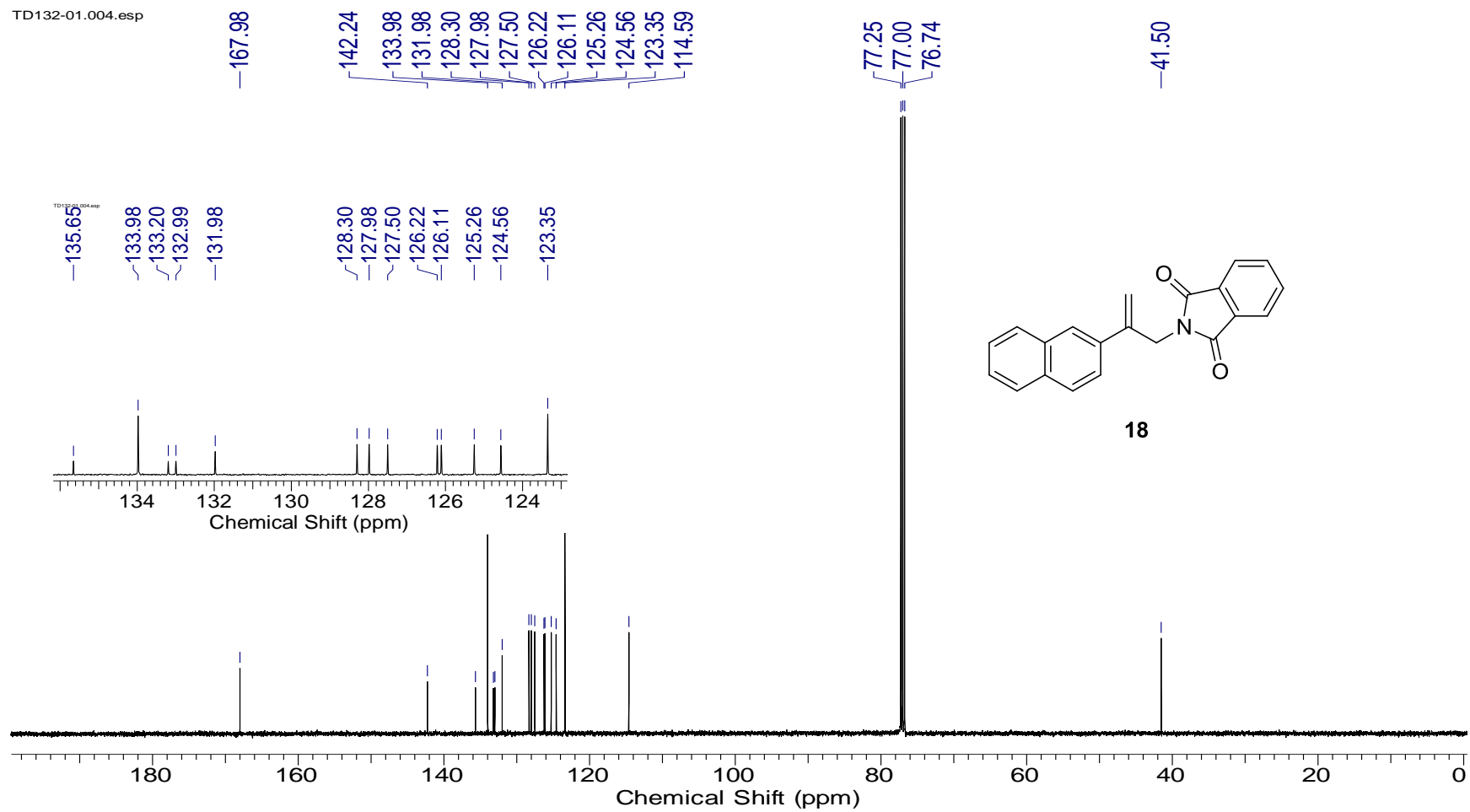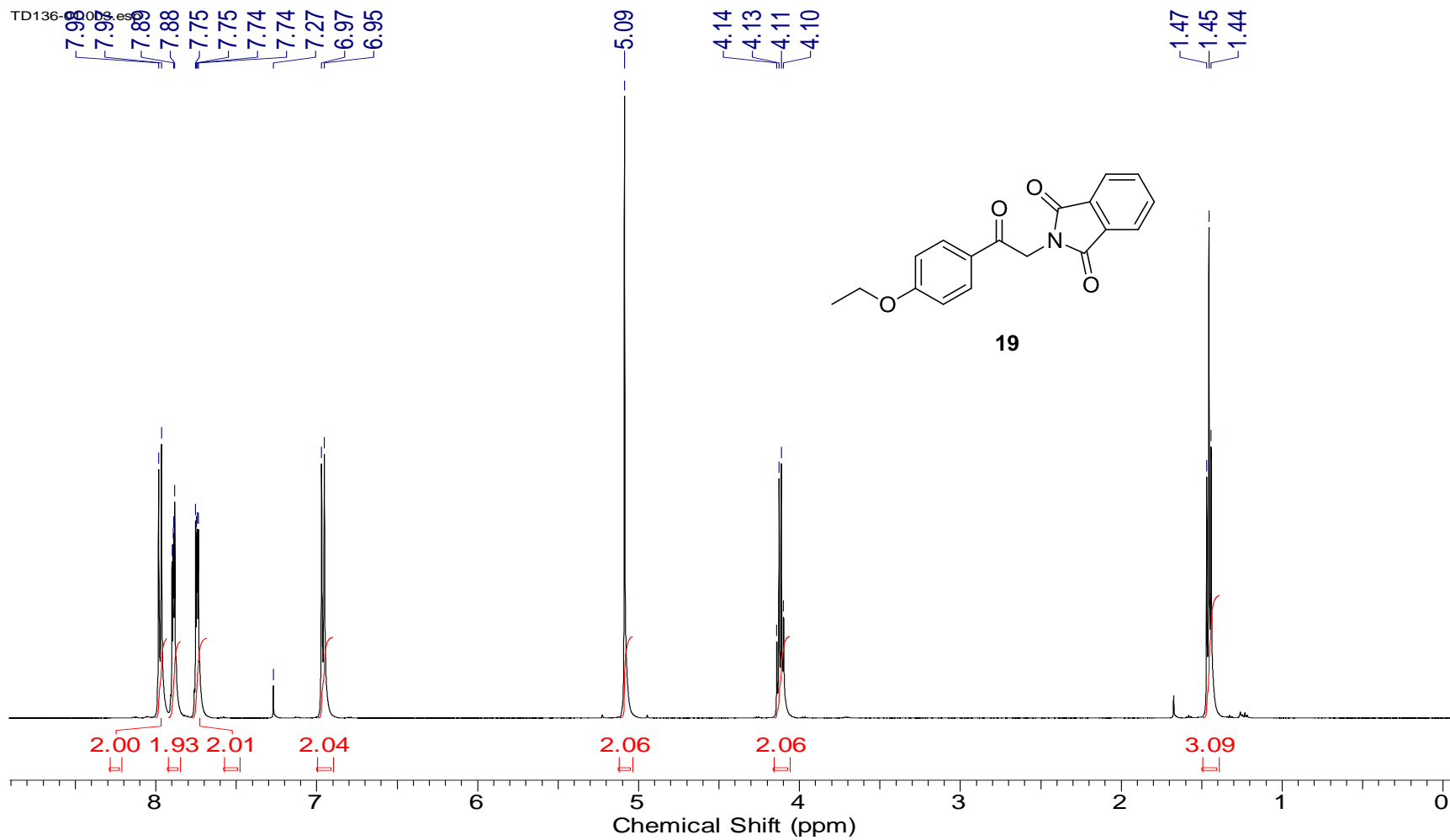
Figure AA 8. ^{13}C NMR spectrum of 2-[2-(4-ethoxyphenyl)prop-2-en-1-yl]-1*H*-isoindole-1,3(2*H*)-dione, 10 (125 MHz, CDCl$_3$).
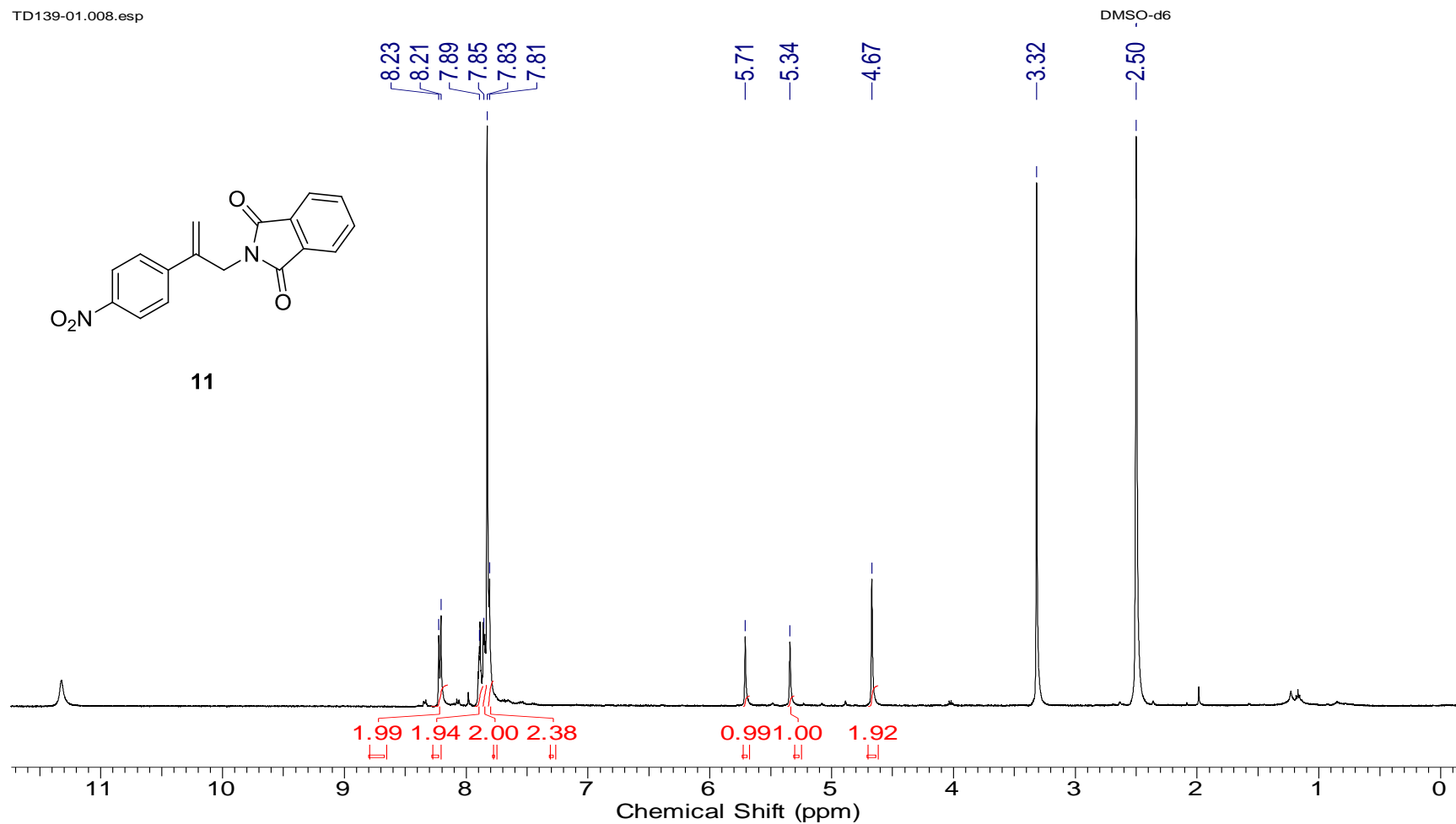
Figure AA 9. ^{1}H NMR spectrum of 2-[2-(4-nitrophenyl)prop-2-en-1-yl]-1*H*-isoindole-1,3(2*H*)-dione, 11 (500 MHz, DMSO-d6, 13 % pure).
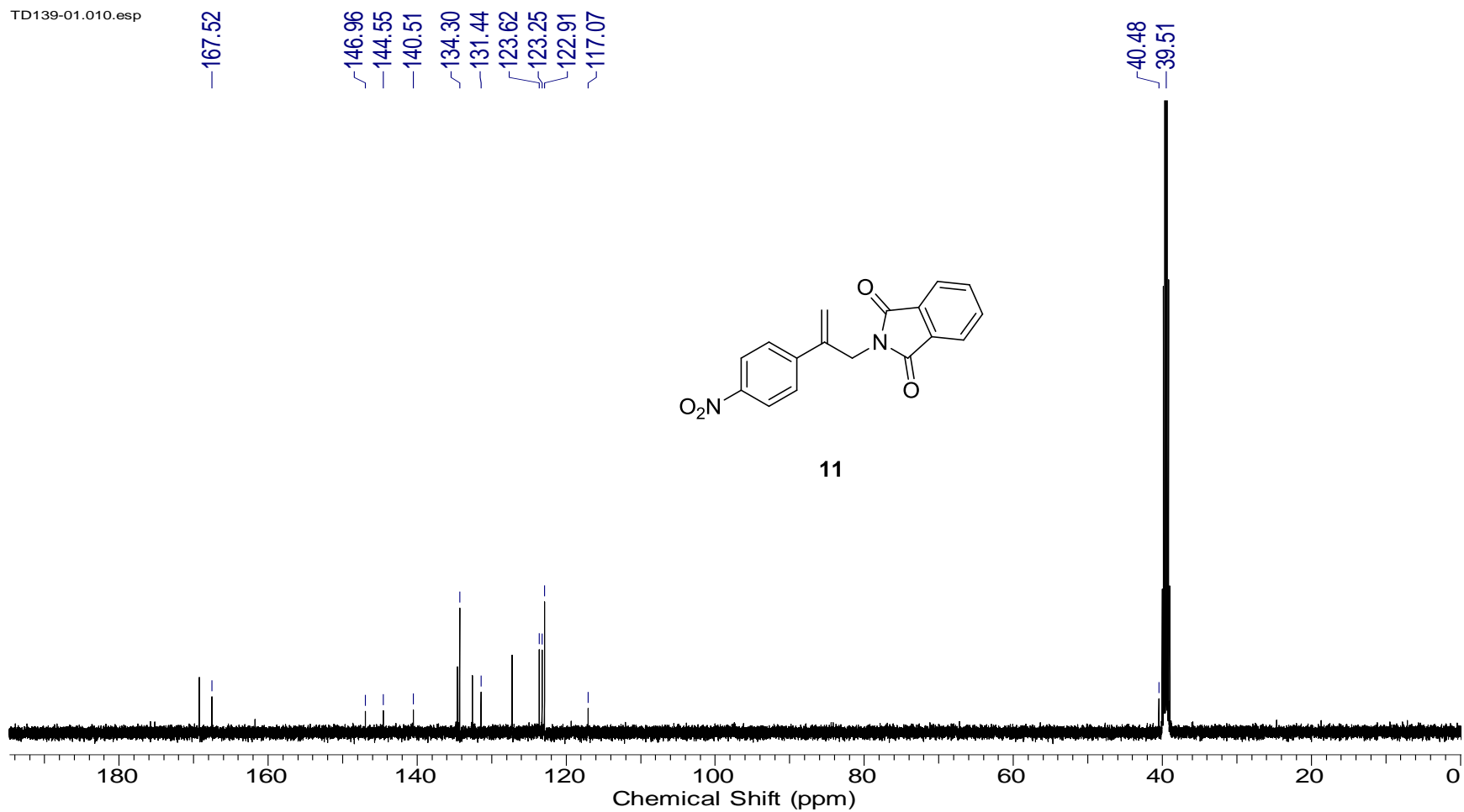
Figure AA 10. ^{13}C NMR spectrum of 2-[2-(4-nitrophenyl)prop-2-en-1-yl]-1*H*-isoindole-1,3(2*H*)-dione, 11 (125 MHz, DMSO-d6, 13 % pure).
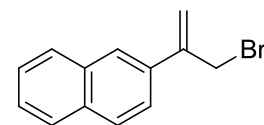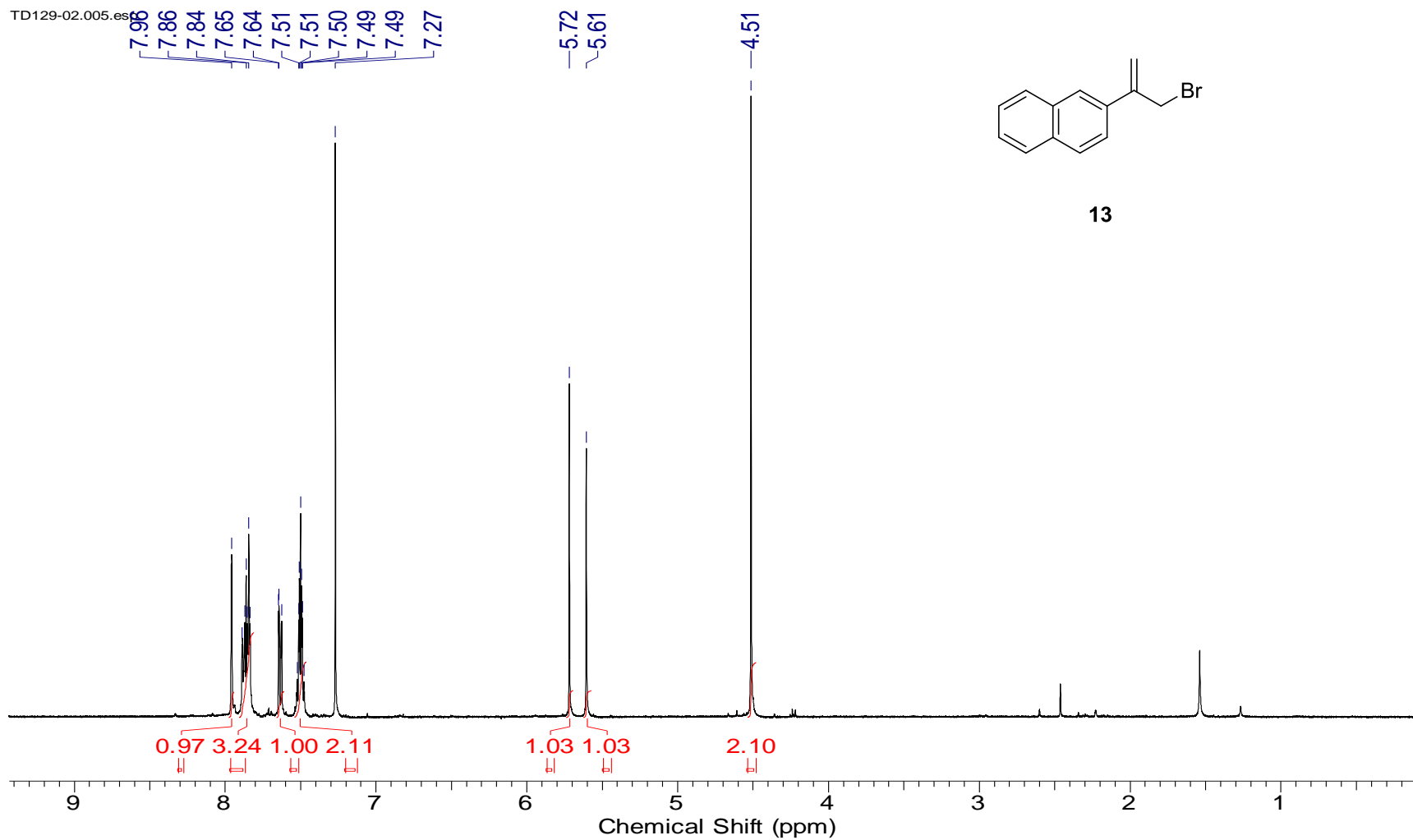
Figure AA 11. ^{1}H NMR spectrum of 2-(3-bromoprop-1-en-2-yl)naphthalene, 13 (400 MHz, CDCl$_3$).

144.08
134.71
133.21
133.08
128.32
128.13
127.55
126.27
125.20
123.98
117.58

77.26
77.00
76.74

34.14

13

180   160   140   120   100   80   60   40   20   0
Chemical Shift (ppm)
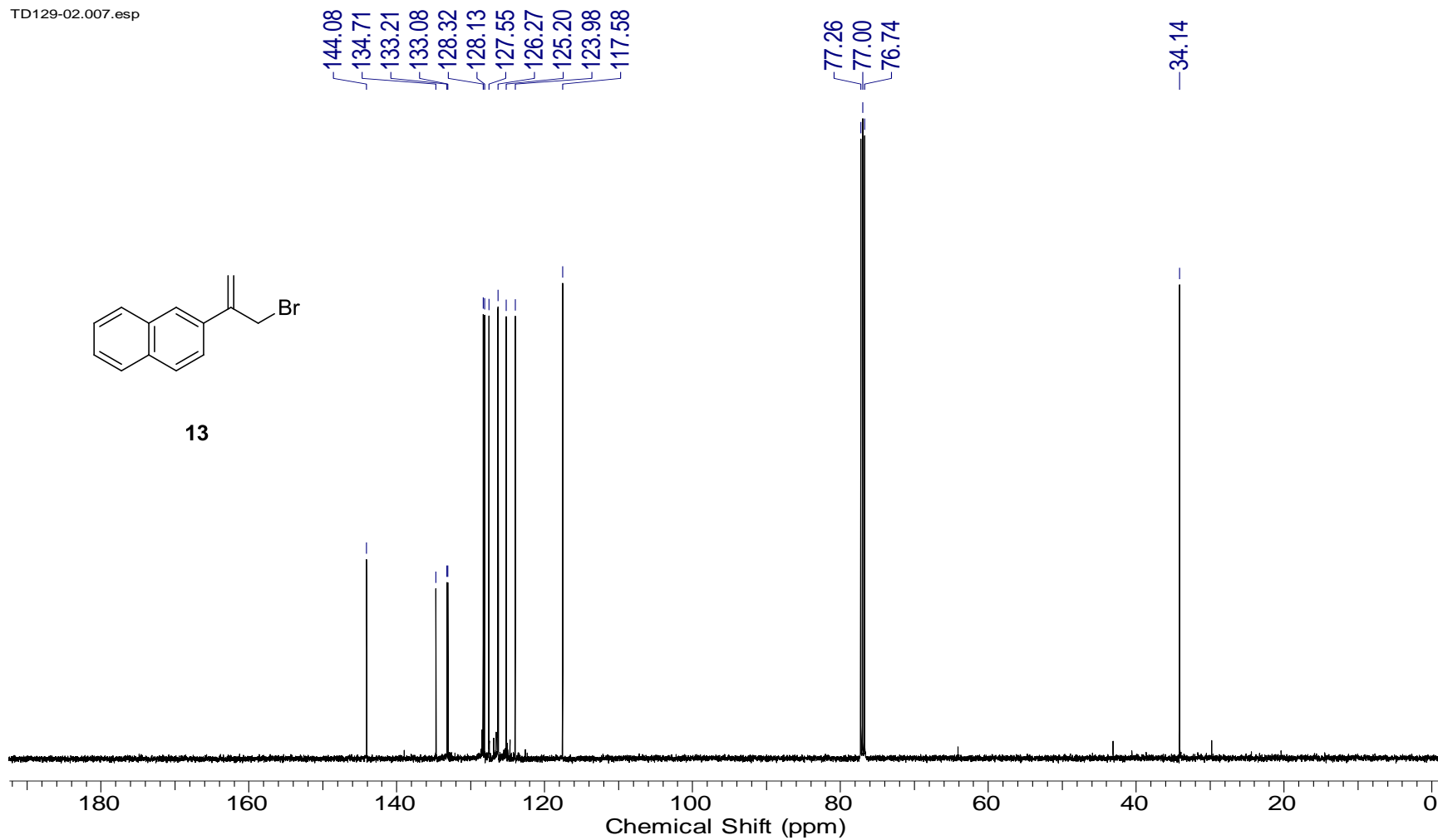
Figure AA 12. ^{13}C NMR spectrum of 2-(3-bromoprop-1-en-2-yl)naphthalene, 13 (100 MHz, CDCl$_3$).
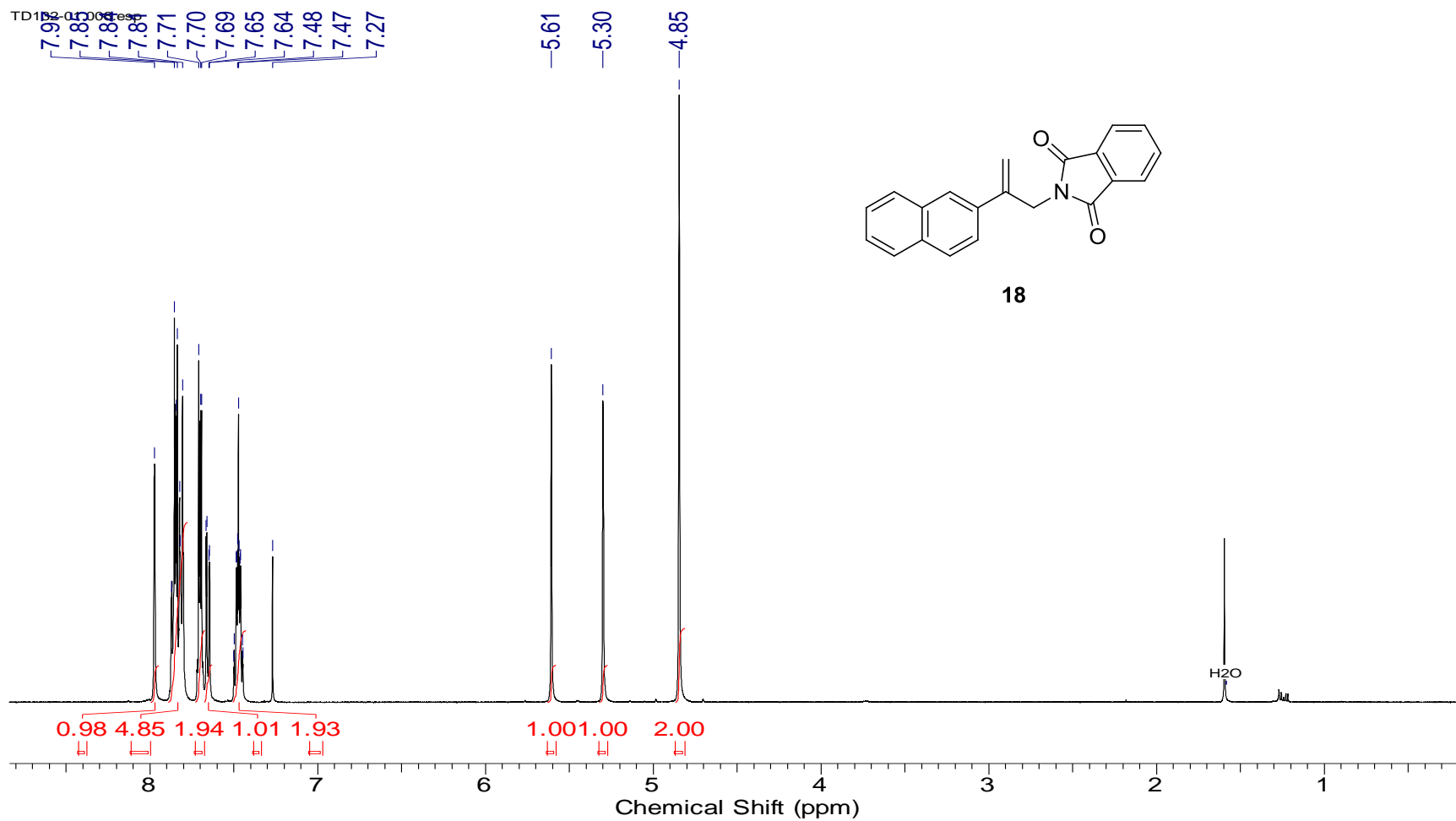
Figure AA 13. ^{1}H NMR spectrum of 2-[2-(naphthalen-2-yl)prop-2-en-1-yl]-1*H*-isoindole-1,3(2*H*)-dione, 18 (500 MHz, CDCl$_3$).

Figure AA 14. ^{13}C NMR spectrum of 2-[2-(naphthalen-2-yl)prop-2-en-1-yl]-1*H*-isoindole-1,3(2*H*)-dione, 18 (125 MHz, CDCl$_3$).

14

Figure AA 15. ^{1}H NMR spectrum of 2-[2-(4-ethoxyphenyl)-2-oxoethyl]-1*H*-isoindole-1,3(2*H*)-dione, 19 (500 MHz, CDCl$_3$).
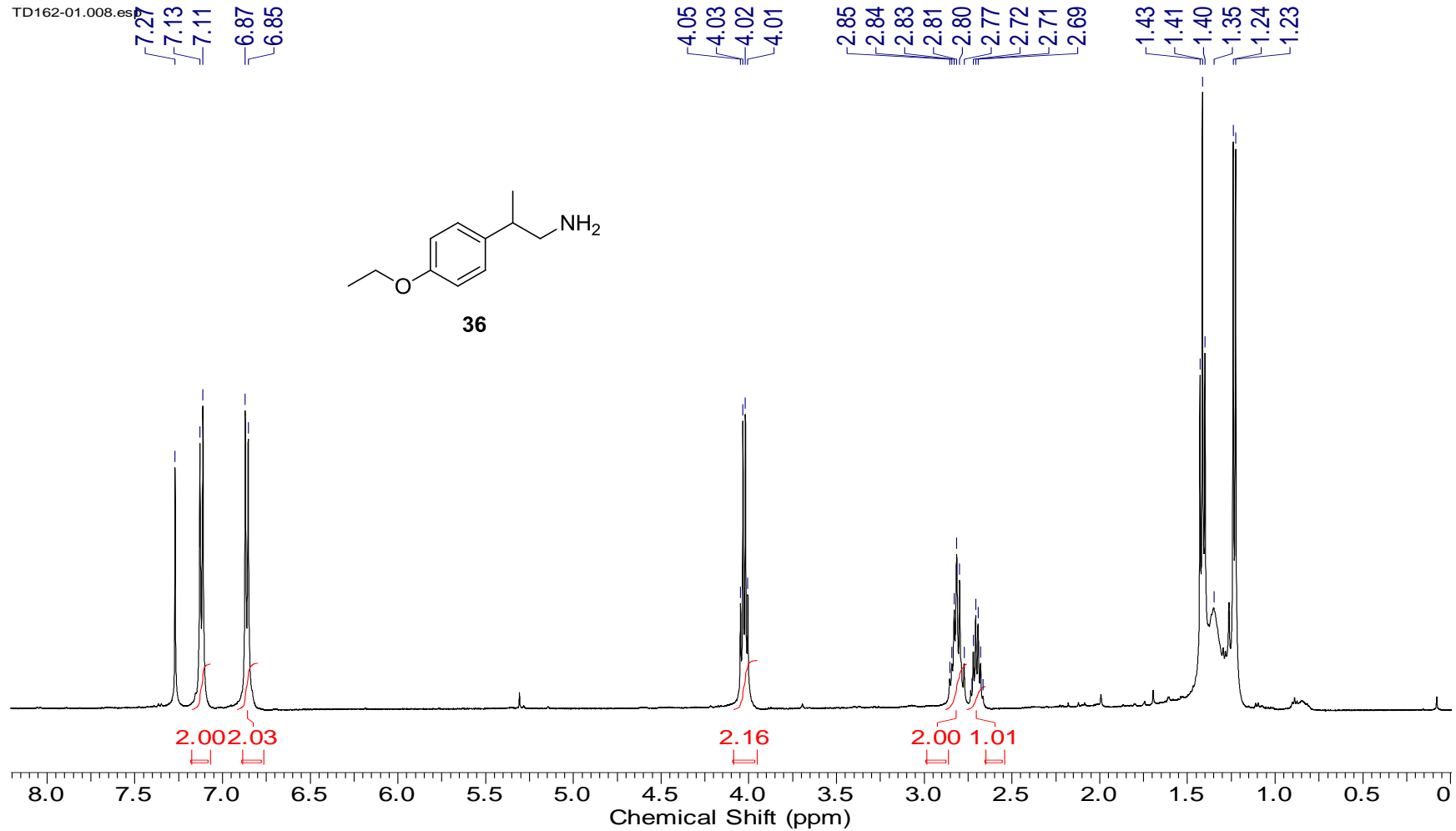
TD136-01.004.esp

189.24
167.93
163.56
134.01
132.25
130.40
127.22
123.45
114.45
77.26
77.00
76.74
63.83
43.83
14.58

19

Chemical Shift (ppm)
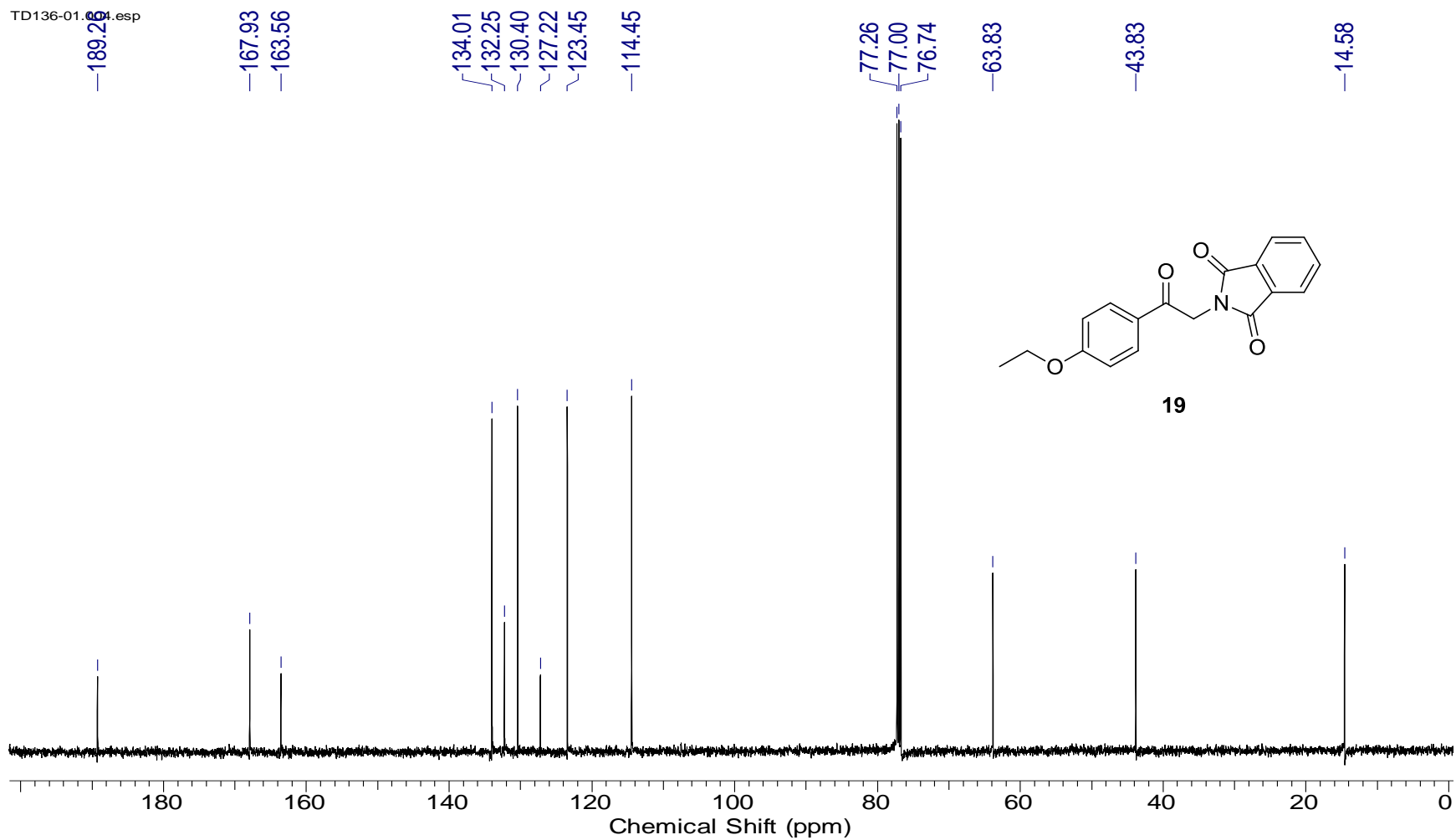
Figure AA 16. ^{13}C NMR spectrum of 2-[2-(4-ethoxyphenyl)-2-oxoethyl]-1*H*-isoindole-1,3(2*H*)-dione, 19 (125 MHz,

CDCl$_3$).

16

Figure AA 17. ^{1}H NMR spectrum of 2-(4-ethoxyphenyl)propan-1-amine, 36 (500 MHz, CDCl₃).

17
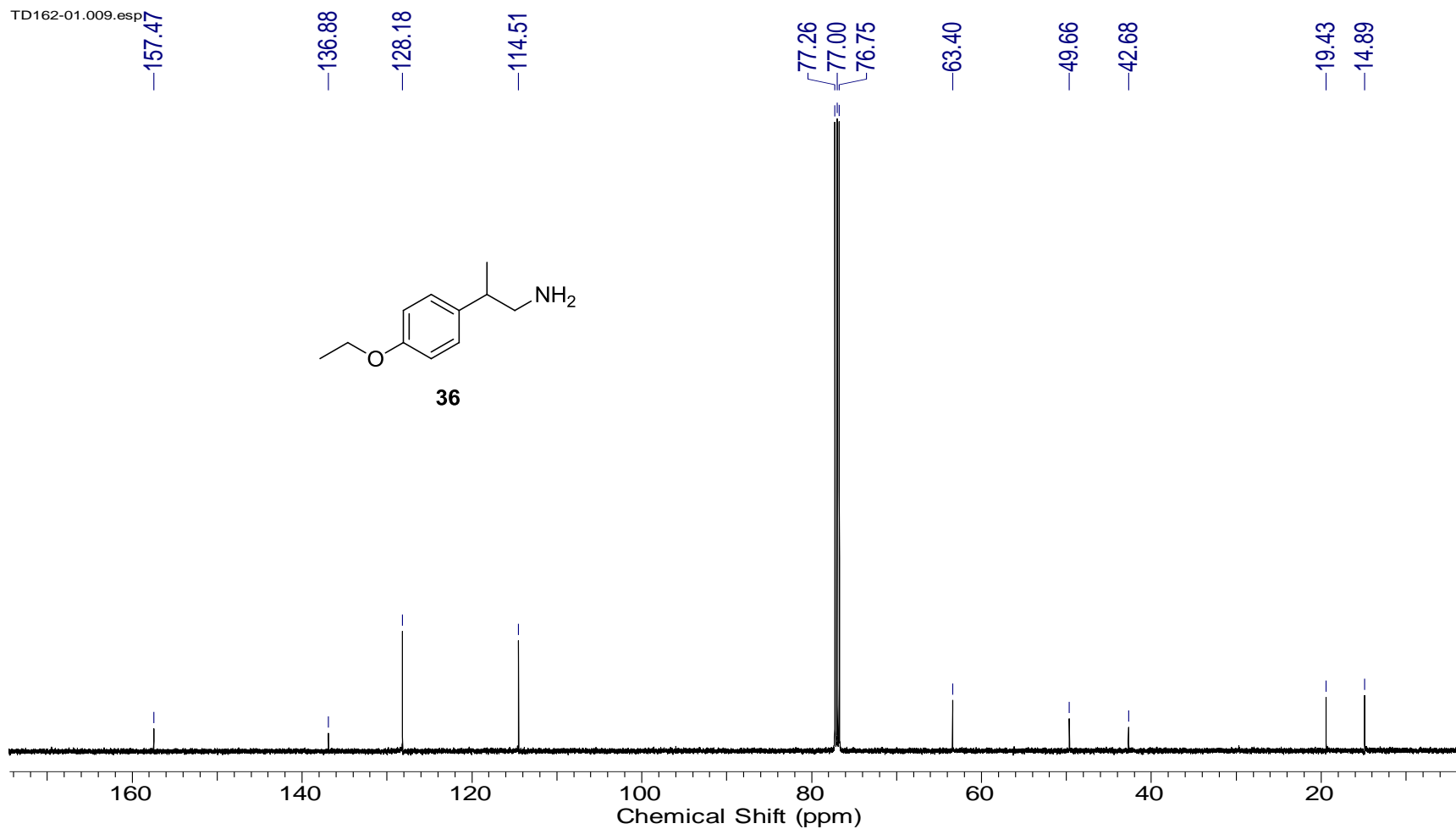
Figure AA 18. ^{13}C NMR spectrum of 2-(4-ethoxyphenyl)propan-1-amine, 36 (125 MHz, CDCl$_3$).
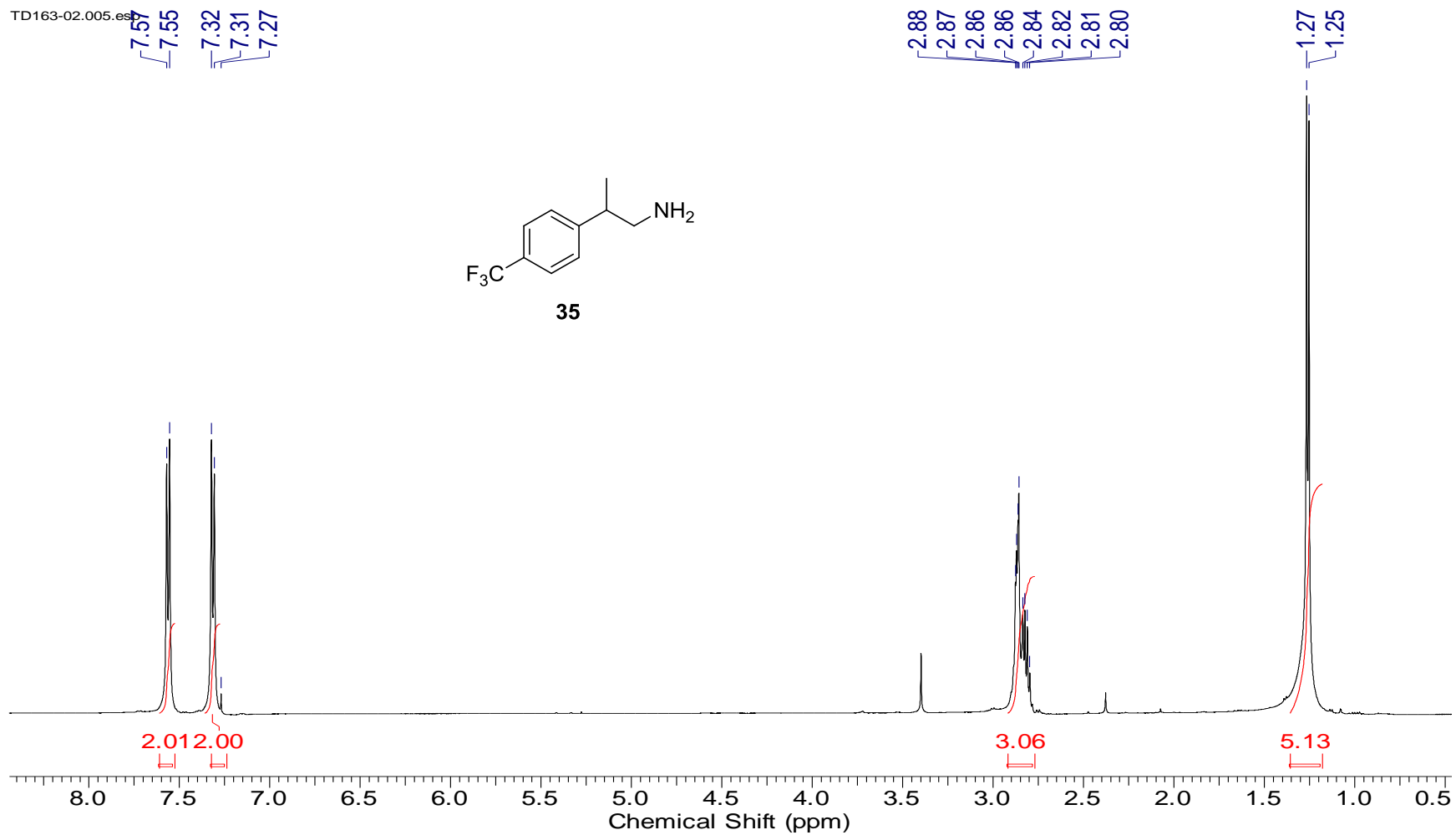
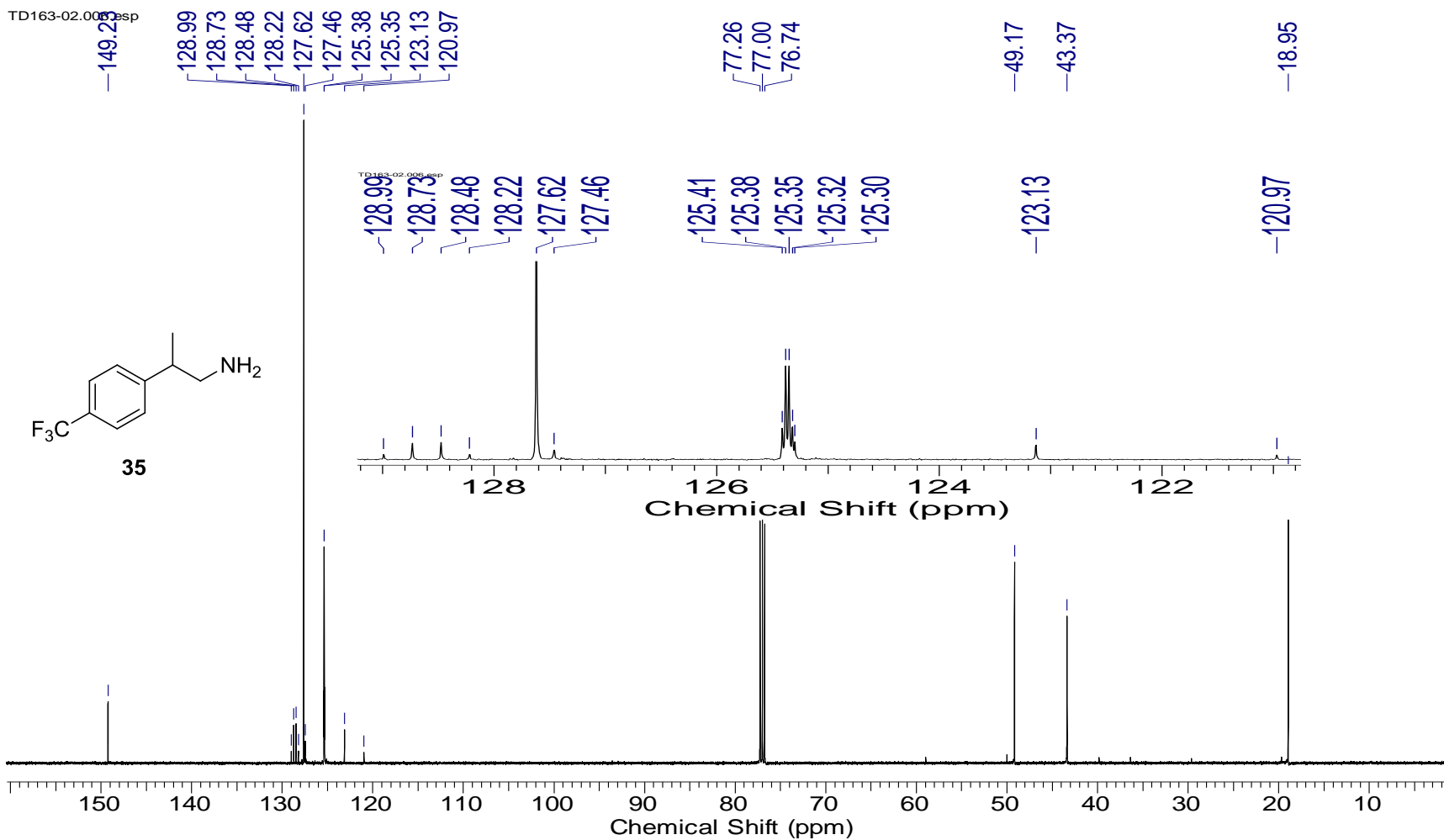**Figure AA 19.** ^{1}H NMR spectrum of 2-[4-(trifluoromethyl)pheny])propan-1-amine, **35** (500 MHz, CDCl$_3$).

Figure AA 20. ^{13}C NMR spectrum of 2-[4-(trifluoromethyl)pheny])propan-1-amine, 35 (125 MHz, CDCl$_3$).
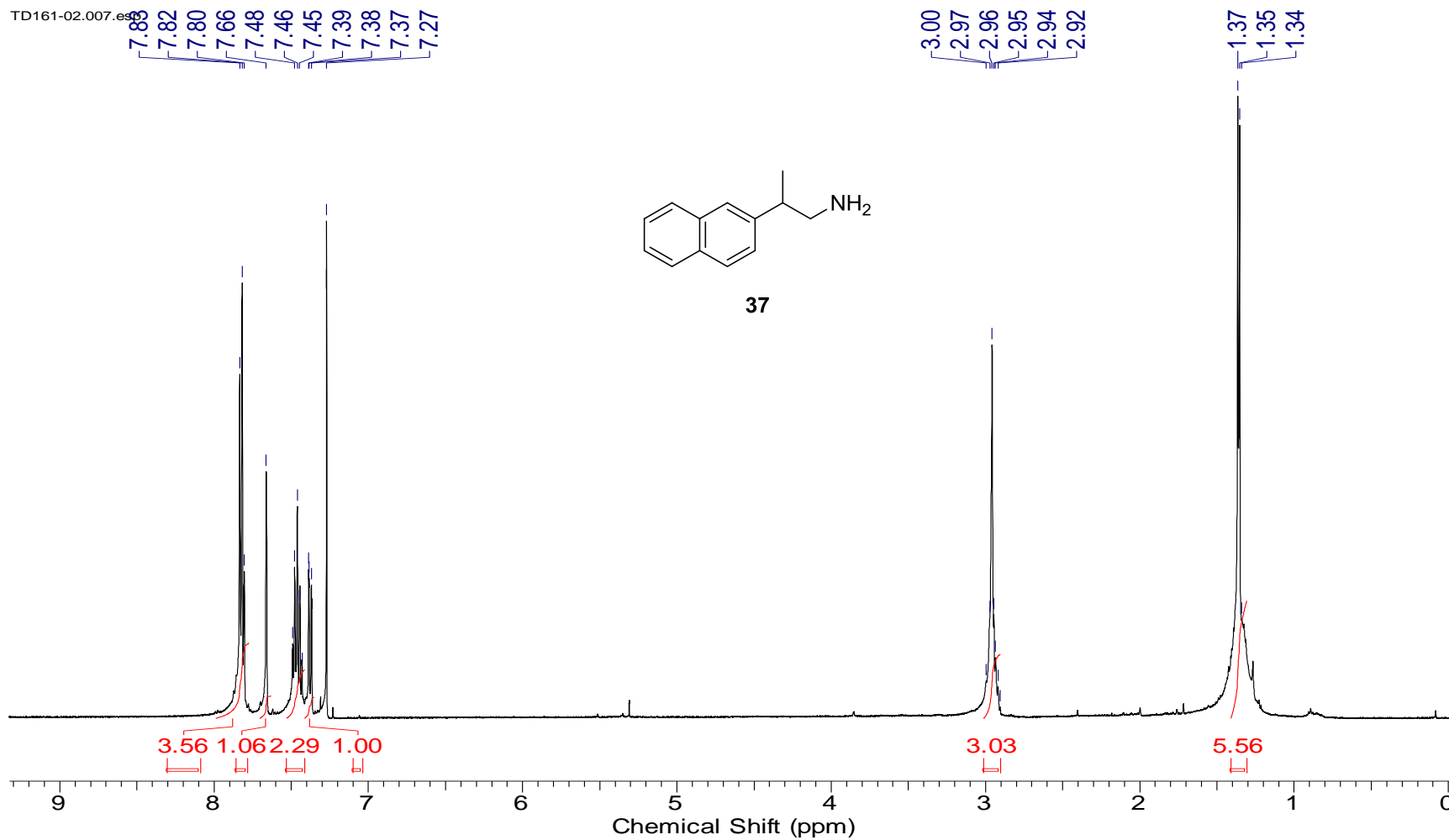
Figure AA 21. ^{1}H NMR spectrum of 2-(naphthalen-2-yl)propan-1-amine, 37 (500 MHz, CDCl$_3$).
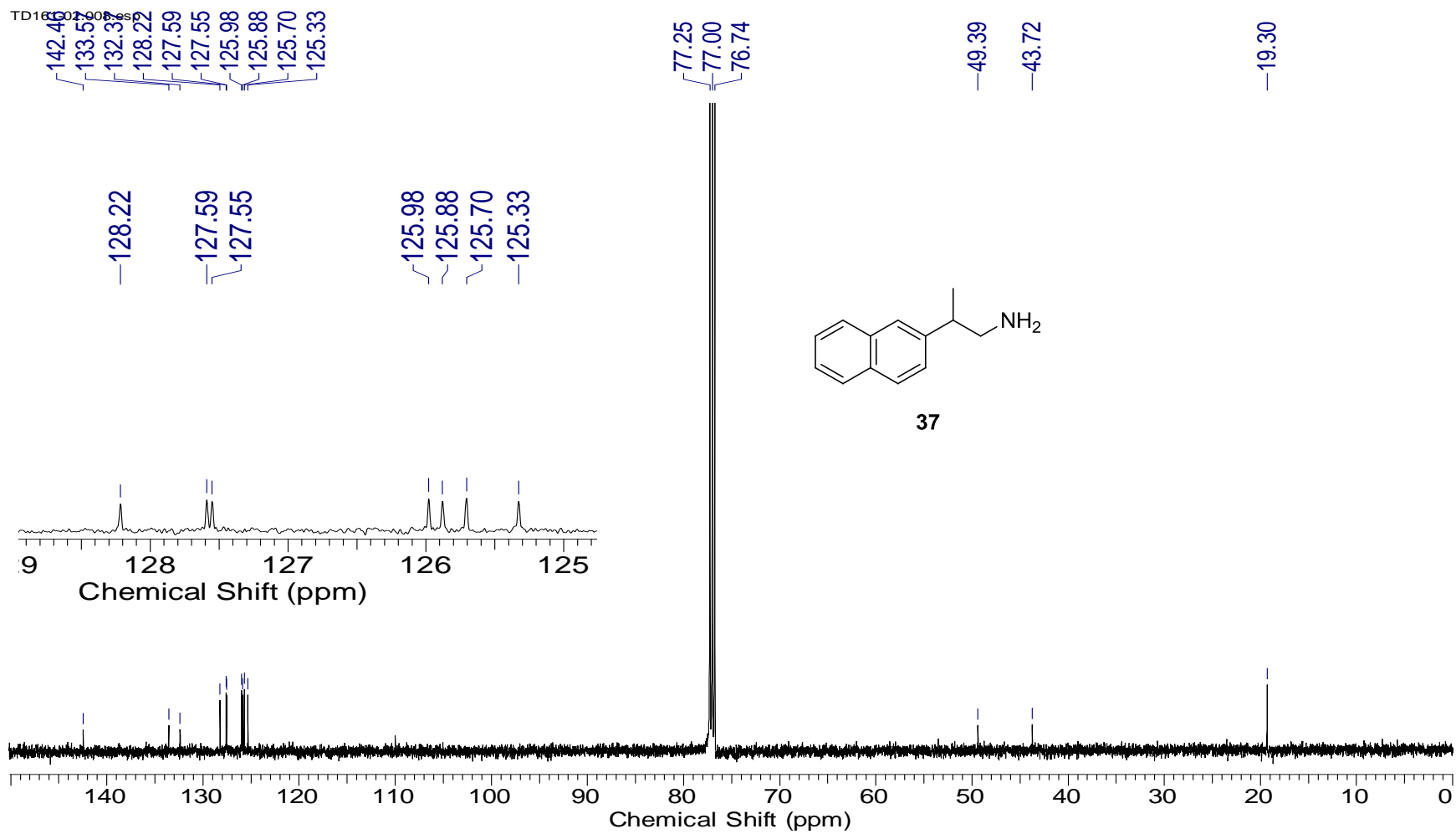
Figure AA 22. ^{13}C NMR spectrum of 2-(naphthalen-2-yl)propan-1-amine, 37 (125 MHz, CDCl$_3$).